0031-6997/04/5604-439–513$7.00
PHARMACOLOGICAL REVIEWS
Vol. 56, No. 4
40403/1185176
Pharmacol Rev 56:439–513, 2004
Printed in U.S.A

Pharmacological Modulation of Sarcoplasmic Reticulum Function in Smooth Muscle

RÉGENT LAPORTE, ADRIAN HUI, AND ISMAIL LAHER

Ferring Research Institute, Inc., Ferring Pharmaceuticals, San Diego, California (R.L.); and Department of Pharmacology and Therapeutics, University of British Columbia, Vancouver, Canada (A.H., I.L.)

Address correspondence to: Ismail Laher, Department of Pharmacology and Therapeutics, University of British Columbia, 2176 Health Sciences Mall, Vancouver, British Columbia, Canada V6T 1Z3. E-mail: ilaher@interchange.ubc.ca

Article, publication date, and citation information can be found at http://pharmrev.aspetjournals.org.
doi:10.1124/pr.56.4.1.

***Abstract*——The sarco/endoplasmic reticulum (SR/ER) is the primary storage and release site of intracellular calcium (Ca^{2+}) in many excitable cells. The SR is a tubular network, which in smooth muscle (SM) cells distributes close to cellular periphery (superficial SR) and in deeper aspects of the cell (deep SR). Recent attention has focused on the regulation of cell function by the superficial SR, which can act as a buffer and also as a regulator of membrane channels and transporters. Ca^{2+} is released from the SR via two types of ionic channels [ryanodine- and inositol 1,4,5-trisphosphate-gated], whereas accumulation from the**

cytoplasm occurs exclusively by an energy-dependent sarco-endoplasmic reticulum Ca^{2+}-ATPase pump (SERCA). Within the SR, Ca^{2+} is bound to various storage proteins. Emerging evidence also suggests that the perinuclear portion of the SR may play an important role in nuclear transcription. In this review, we detail the pharmacology of agents that alter the functions of Ca^{2+} release channels and of SERCA. We describe their use and selectivity and indicate the concentrations used in investigating various SM preparations. Important aspects of cell regulation and excitation-contractile activity coupling in SM have been uncovered through the use of such activators and inhibitors of processes that determine SR function. Likewise, they were instrumental in the recent finding of an interaction of the SR with other cellular organelles such as mitochondria. Thus, an appreciation of the pharmacology and selectivity of agents that interfere with SR function in SM has greatly assisted in unveiling the multifaceted nature of the SR.

I. Smooth Muscle Cell Ca^{2+} Handling and Role of the Sarcoplasmic Reticulum

A. Ca^{2+} Handling

The most abundant cation in the vertebrate body is calcium (Ca^{2+}), where in humans it amounts to 20 to 30 g/kg body weight. There are large reservoirs of Ca^{2+} in the form of depots in bone, which are available to the body for cellular processes. Despite the availability of such a large, extracellular source of Ca^{2+}, cells have an organized internal store of Ca^{2+} that is readily available for rapid release as needed upon membrane excitation. The identification and universal acceptance of the SR[1] as a Ca^{2+} store and sink is a relatively late event in smooth muscle research and begs the question of its utility in establishing a maintained cellular response in the face of a very large, inwardly facing gradient of accessible Ca^{2+} that is of infinite abundance relative to enzymatic requirements.

As Pozzan et al. (1994) and others have argued, the diffusion of Ca^{2+} within the cell is not an unimpeded process, so the presence of various immobile binding sites for Ca^{2+} imposes severe constraints on its ability to reach a rapid and useful cellular concentration at critical sites within the cell, especially in the case of cells with relatively large volumes. The intracellular diffusion coefficient for Ca^{2+} in water is 7×10^{-6} cm^2/s, which is more than 10 times that in cytoplasmic extracts containing intracellular Ca^{2+} buffers (Allbritton et al., 1992). This impediment to the movement of Ca^{2+}, coupled with the presence of intracellular structures close to the plasma membrane, ensures local areas of high Ca^{2+} concentrations, which in turn may lead to a regenerative release of Ca^{2+} from the SR. In careful mathematical modeling of Ca^{2+} movement in cells using physiological constraints, Kargacin (1994) calculated that the concentration of Ca^{2+} below the plasma membrane reaches ~8 μM during the Ca^{2+}-induced Ca^{2+} release (CICR) process.

The release of Ca^{2+} from internal stores ensures a more diffuse and timely increase in cytoplasmic Ca^{2+} that is coordinated with the ensuing entry of extracellular Ca^{2+}. Through such an intricate dependence of the timely movement of Ca^{2+} from within the cell and from extracellular sources, the cell is able to initiate Ca^{2+} oscillators that act as regional "switches" and "relays" within cytoplasmic domains (Bootman et al., 2002). For instance, in the smooth muscle cell, Ca^{2+}-mediated contractile regulation by extracellular Ca^{2+} influx and/or SR Ca^{2+} release could take place principally by two mechanisms. The first is by direct activation of the contractile apparatus through global cytoplasmic free Ca^{2+} concentration ($[Ca^{2+}]_{cyt}$) increase throughout the cytoplasm (Sanders, 2001). A second pathway is via indirect regulation of plasma membrane excitability by an increase in $[Ca^{2+}]_{cyt}$ spatially localized to a narrow gap (20–40 nm in depth) between the plasma membrane and the superficially located SR, termed the plasma membrane-SR junctional space (Lee et al., 2002a) (see *Section I.A.*) (Fig. 1). $[Ca^{2+}]_{cyt}$ increase in this junctional space may also be the source of cell-wide $[Ca^{2+}]_{cyt}$ oscillations and waves coupled either to contractile activity or relaxation (Pabelick et al., 2001b; Lee et al., 2002a).

[1]Abbreviations: SR, sarcoplasmic reticulum; $[Ca^{2+}]_{cyt}$, concentration of cytoplasmic free Ca^{2+}; ER, endoplasmic reticulum; SERCA, sarco/endoplasmic reticulum Ca^{2+}-ATPase(s); $InsP_3$, inositol 1,4,5-triphosphate; $InsP_3R$, $InsP_3$-gated Ca^{2+} channel/$InsP_3$ receptor; ER, endoplasmic reticulum; PM, plasma membrane; RyR, Ca^{2+}-gated channel/ryanodine receptor(s); PMCA, plasma membrane Ca^{2+}-ATPase pump(s); HEK, human embryonic kidney; CICR, Ca^{2+}-induced Ca^{2+} release; SBB, superficial buffer barrier; IICR, inositol 1,4,5-trisphophate-induced Ca^{2+} release; $InsP_3R$, $InsP_3$-gated Ca^{2+} channel/$InsP_3$ receptor; CCE, capacitative calcium entry; SK&F, 1-(β-[3-(4-methoxy-phenyl)propoxy]-4-methoxyphenethyl)-1*H*-imidazole hydrochloride; 2-APB, 2-aminoethoxy-diphenylborate; LU52396, 1-[2-(4-fluorophenyl)cyclohexyl]-2-[4-(3-phenylalkyl)-piperazin-1-yl]-ethanol; L-651,582, 5-amino-[4-(4-chlorobenzoyl)-3,5-dichlorobenzyl]-1,2,3-triazole-4-carboxamide; NE, norepinephrine; CPA, cyclopiazonic acid; Ca_L, L-type voltage-gated Ca^{2+} channel; NO, nitric oxide; TRP, transient receptor potential channel(s); GPCR, G-protein coupled receptor(s); PKC, protein kinase C; Ach, acetylcholine; PKG, protein kinase G; CaM, Ca^{2+}-calmodulin kinase; BK, large conductance Ca^{2+}-activated K^+ channel; STOC, spontaneous transient outward current; PLC, phospholipase C; TMB-8, 8-(*N*,*N*-diethylamino)ocyl-3,4,5-trimethoxybenzonate; tBuBHQ, 2,5-di(*tert*-butyl)-1,4-benzohydroquinone; SAR, structure-activity relationship; TNP-ATP, 3′-*O*-(trinitrophenyl)adenosine-5′-triphosphate; PKG, cGMP-dependent protein kinase; Cch, carbachol; cADPR, cyclic ADP ribose; NAD, nicotinamide adenine dinucleotide; cADPcR, cADP-carbocyclic-ribose; cArisDPR, cyclic aristeromycin diphosphate ribose; ADPRC, ADP-ribosyl cyclase; cADPRH, cADPR hydrolase; MBED, 9-methyl-7-bromoeudistomin D; PDE, phosphodiesterase; LC_{20}, 20-kDa myosin light chain; MLCP, myosin light chain phosphatase; Cch, carbachol; SOCC, store-operated Ca^{2+} channel.

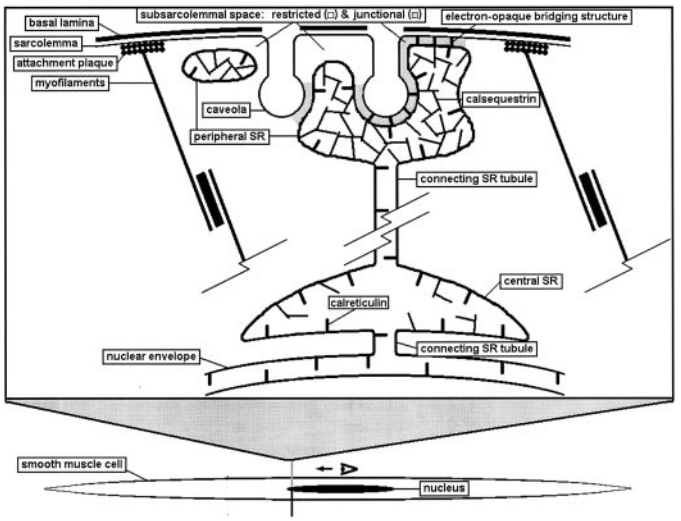

FIG. 1. Schematic transversal section of a smooth muscle cell illustrating the main topological relationships between SR and key ultrastructural elements. Sarcolemma = plasma membrane, subsarcolemmal = subplasmalemmal.

The SR has many structural features of the endoplasmic reticulum (ER), sharing many intracellular chaperone proteins and other histological features. The existence of a SERCA and of Ca^{2+} release channels reveals that the SR is, in fact, a region of the ER that specializes in Ca^{2+} homeostasis, predominantly Ca^{2+} release and uptake. Thus, the SR is in reality an intracellular networking system whereby different cytoplasmic domains are connected in an intercommunicating and interdependent manner. In reality, the SR and ER are constantly multitasking—some portions of the structures are involved in protein trafficking, while other portions are being earmarked for Ca^{2+} signaling (Berridge, 2002). These portions of the SR/ER are constantly remodeling, with this process being driven by stability of the proteins and the Ca^{2+} load (Berridge, 2002). The SR is also contiguous with the nuclear envelope and thus may play a role in Ca^{2+}-dependent gene regulation via Ca^{2+}-dependent transcription factors such as cAMP responsive element-binding proteins (CREB) and nuclear factor for activated T cells (NFAT) (Cartin et al., 2000; Gomez et al., 2003; Hill-Eubanks et al., 2003). $InsP_3R$ are also found in the SR membrane and may regulate the opening of the nuclear pores (Stehno-Bittel et al., 1995).

The release and accumulation of intracellular Ca^{2+} regulates many aspects of cellular functions, including hormone and neurotransmitter release, endothelial secretion, muscle contractile activity, cell division, growth and migration, and apoptosis. It is, in fact, difficult to imagine an aspect of mammalian cell function that is not in some way regulated by the availability of Ca^{2+}. With this in mind, it becomes apparent why there has been a burgeoning global interest in understanding how cells regulate all aspects of Ca^{2+} availability. Our interest in cellular Ca^{2+} handling owes much to the seminal observations of Ringer in 1883, who first demonstrated the absolute need for Ca^{2+} in muscle excitation-contractile activity coupling. The impetus for the search for drugs that modify the cellular responses to Ca^{2+} comes largely from the need to treat a variety of diseases thought to involve abnormal handling of Ca^{2+}. Thus, an extensive array of pharmacological tools altering Ca^{2+} entry, release, sensitization, and extrusion has been created. In this review, we summarize the pharmacology of drugs frequently used to modulate intracellular Ca^{2+} sequestration and release in smooth muscle.

Smooth muscle cells are spindle-shaped, with the widest part being ~2 to 5 μm, and the length ranging up to 500 μm in visceral muscle and to ~150 μm in vascular tissues. The plasma membrane and SR come into close contact with the SR membrane running parallel with the plasma membrane for distances of 1 μm or more (Devine et al., 1972; Gabella, 1983). The geometrical shape of smooth muscle cells ensures a disproportionate ratio of membrane (PM, sarcoplasmic membrane) surface/cytoplasm (cytosol, sarcoplasm) ratio. For example, visceral smooth muscle cells have a volume of 2500 to 3000 μm^3 and a cell surface area of 5000 μm^3 (not allowing for caveolae), producing an approximated cell surface/volume ratio of 1.5 μm^{-1}, which is equivalent to that of erythrocytes. For a comprehensive review of the ultrastructural features of smooth muscle, see the overview by Gabella (1983).

In vascular smooth muscle cells, there are 2.7 μm^2 of cell surface for every cubic micrometer of cell volume. This large cell surface/cell volume ratio in smooth muscle favors exquisite regulation of cell surface processes by instantaneous changes in intracellular composition, such as the regulation by (presumably) spontaneously released Ca^{2+} from the SR, known as "Ca^{2+} sparks", of Ca^{2+}-activated K^+ (K_{Ca}) (see reviews by Nelson et al., 1995; Jaggar et al., 2000; Wellman and Nelson, 2003) and chloride (Cl_{Ca}) channels (Kotlikoff and Wang, 1998). Earlier studies by Benham and Bolton (1986) and by Stehno-Bittel and Sturek (1992) lead to the suggestion that the frequently observed spontaneous K^+ currents recorded in smooth muscle (Benham and Bolton, 1986; Ohya et al., 1987; Desilets et al., 1989; Hume and Leblanc, 1989) occur in regions of the cell where the SR and the PM are closely apposed. This Ca^{2+} release from the SR, presumed to occur spontaneously, occurs in close proximity to K_{Ca} channels and reaches a $[Ca^{2+}]_{cyt}$ of 10 to 100 μM and an average size of 13 μm^2, which covers ~1% of the 1300 μm^2 of the smooth muscle membrane (Perez et al., 1999). This release of Ca^{2+} occurs via Ca^{2+}-gated channel/ryanodine receptor (RyR) channels, likely the RyR2 subtype with an ancillary role for RyR3 (Lohn et al., 2001). However, the global change in cytoplasmic Ca^{2+} due to the spontaneous release of Ca^{2+} sparks from the SR is less than 2 nM (Jaggar et al., 2000). Ca^{2+} sparks originating from the SR occur with a relatively low frequency of 1 Hz (allowing for a tonic

hyperpolarization throughout the electrically coupled smooth muscle), and the spreading distance in smooth muscle is ~1.0 to 2.5 μm (Jaggar et al., 2000). Thus, there is the appearance of a specialized subsarcolemmal signaling space where high local concentrations of Ca^{2+} (~10 μM) exist in microdomains without significant impact on global cytosolic Ca^{2+}.

B. Sarcoplasmic Reticulum

Unlike other membrane systems, such as the mitochondrial inner membrane, there is no potential difference across the SR membrane. The concentration of Ca^{2+} in the extracellular space is between 1 and 10 mM, whereas the $[Ca^{2+}]_{cyt}$ in the cytoplasm is in the order of 0.1 μM, thus creating a large inwardly directed electrochemical gradient forcing Ca^{2+} entry across the plasma membrane. The cell has several mechanisms for maintaining a low $[Ca^{2+}]_{cyt}$, which at the same time also ensures that the appropriate transient peak levels of Ca^{2+} are reached during activation. Notable among these are active processes such as Ca^{2+} extrusion across the plasma membrane into the extracellular reservoir by the plasma membrane Ca^{2+}-ATPase pump (PMCA) and also accumulation of the ion into the SR by the SERCA. Although these two pumps essentially accomplish the same effect of rapidly reducing $[Ca^{2+}]_{cyt}$ levels, they have different physicochemical properties and regulatory mechanisms (Grover and Khan, 1992; Raeymaekers and Wuytack, 1993). Using indirect methods in a large vein, Nazer and van Breemen (1998) concluded that nearly half the cytoplasmic free Ca^{2+} load is extruded via the PMCA, with an equal role for the SERCA and the plasma membrane Na^+-Ca^{2+} exchanger in removal of the remainder. Much is known about the molecular identity of the Na^+-Ca^{2+} exchanger in smooth muscle (Nakasaki et al., 1993; Juhaszova et al., 1996), although details of its isoform distribution and functionality awaits further characterization.

Some investigators have suggested that the plasma membrane pathways (PMCA and Na^+-Ca^{2+} exchanger) account for only 20 to 40% of Ca^{2+} removal (Cooney et al., 1991), whereas others have concluded that the PMCA removes only ~10 to 20% of Ca^{2+} from the cell (Kargacin and Fay, 1991). However, in a resistance artery from the brain, Kamishima and McCarron (1998) proposed roles only for the Ca-ATPase pumps (SERCA and PMCA), and not the Na^+-Ca^{2+} exchanger, in removal of free Ca^{2+} from the cytoplasm. In keeping with this, Kargacin and Kargacin (1995) proposed that the SERCA pumps are likely to make the largest single contribution to Ca^{2+} removal and can reduce Ca^{2+} at a rate of ~60 to 80% the rate of Ca^{2+} removal seen in cells during a Ca^{2+} transient. Thus, there exists some uncertainty about the precise roles and relative importance of the extrusion mechanisms for cytoplasmic Ca^{2+}. In part, this is related to the lack of specific inhibitors of the various processes that govern Ca^{2+} homeostasis. It is likely that many of the quantitative estimates described in the literature regarding Ca^{2+} pool sizes, diffusion rates, and other physicochemical parameters exhibit variations in estimates due largely to differences in methods, species, and tissues.

An important initial step in elucidating the contribution and role of the various modalities of Ca^{2+} extrusion mechanisms is the description of caloxin, a peptide that inhibits Ca^{2+} extrusion by the PMCA (Chaudhary et al., 2001; Holmes et al., 2003). The search for a selective and specific inhibitor for the PMCA is considered by many to be enigmatic; the limitation of caloxin [IC_{50} value ~0.4–1 mM in red cell leaky ghosts, which mainly express PMCA4 (Holmes et al., 2003)] is that it is a peptide and thus not amenable to routine use. However, it produces an endothelium-dependent relaxation in intact rings of rat aorta (0.34 mM) (Chaudhary et al., 2001). Caloxin does not inhibit Mg^{2+}-ATPase or Na^+/K^+-ATPase (Holmes et al., 2003) and has been shown to also inhibit PMCA activity in human mesenchymal stem cells (Kawano et al., 2003) and human embryonic kidney (HEK) cells (De Luisi and Hofer, 2003). A third and relatively novel family of Ca^{2+} pumps is the Ca^{2+}/Mn^{2+} ATPases, which occur predominantly in the Golgi compartment of eukaryotic cells (reviewed by Wuytack et al., 2002, 2003).

The rise of intracellular Ca^{2+} is vital to cell function, but Ca^{2+} availability must occur rapidly and in sufficient concentration at required intracellular targets. This is accomplished by Ca^{2+} release from the SR either as a regenerative release of Ca^{2+} via CICR occurring through activation of RyR, or as $InsP_3$-induced Ca^{2+} release (IICR, occurring through activation of $InsP_3R$/Ca^{2+} release channel) (see *Section I.G.2.*). The RyR was originally shown to bind [^{3}H]ryanodine (see *Section II.B.3.a.*), an agent that was then known to alter SR Ca^{2+} release events in skeletal muscle. Within the SR, a fraction of Ca^{2+} is bound to various Ca^{2+} storage proteins such as calsequestrin. (see *Section I.E.*). Once released, the diffusion rate of Ca^{2+} in the cytoplasm is limited by the presence of various high-affinity binding proteins, so that the rate of Ca^{2+} diffusion in the cytoplasm (10–100 μm^2/s) is ~3 to 30% the rate in free solution, which occurs at 320 μm^2/s (Tsien and Tsien, 1990).

The description of an intracellular network of membrane systems that was later to be named SR was first described in skeletal muscle more than 100 years ago (Veratti, 1902). It was appreciated that muscle had an intrinsic "relaxing activity", which was later ascribed to the ability of SR membranes to accumulate Ca^{2+} at the expense of ATP hydrolysis (Ebashi and Lipmann, 1962). The SR is a system of anastomosing intracellular membranes organized into tubules that occupy between 1.5 to 7.5% of the cell volume, with greater volumes being present for instance in smooth muscle cells from large, conduit type arteries (Devine et al., 1972). This distri-

bution of SR and its implications in arteries of varying sizes has not been revisited since the initial description by Devine et al.; it is likely that these estimates may be revised with the use of more modern techniques and the patterns of SR distribution better defined with regard to cell structure and colocalization with cellular elements. This represents a daunting task since we now know that the complex architecture of the SR is made functionally complicated by the presence of regions that specialize in Ca^{2+} uptake and release, with other adjoining parts involved in the assembly or degradation of proteins. The variable volume of SR in smooth muscle cells may also be a reflection of cell synthetic activity, so that large arteries, which synthesize more extracellular proteins than smaller diameter arteries, have a correspondingly larger SR volume (Somlyo, 1980), although this supposition has not been rigorously examined. Also, the SR volume of smooth muscle cells, at least in the uterus, is increased by estrogen and during pregnancy (Shoenberg, 1958; Ross and Klebanoff, 1971). Thus, proliferative, developing smooth muscle cells tend to have more SR (Campbell et al., 1971), as is the case for some injured and hypertensive vascular smooth muscle cells (Raeymaekers and Wuytack, 1993).

The SR contains several ionic species and of note is the following: 1) the Na^+ and Cl^- concentrations are similar to those present in the cytoplasm, indicating that the SR is not effectively in contact with the extracellular space, 2) the Ca^{2+} concentration in the SR measured by electron probe analysis is ~30 to 50 mmol/kg dry weight, and 3) the Ca^{2+} concentration near the plasma membrane is not uniformly distributed, with areas of low (~1 mmol/kg dry weight) and high ("hot spots") concentrations. There is a concordance of junctional elements of the SR (those portions close to the plasma membrane) and areas of Ca^{2+} hot spots. It is estimated that the average number of SR elements indicated by hot spots that lie within 50 nm from the plasma membrane is between 3 and 5 per cell (Bond et al., 1984b). One consequence of this is that sufficiently high local concentrations (in mM) of Ca^{2+} are reached near the plasma membrane, allowing for local, intracellular regulation of K^+ (Nelson and Quayle, 1995) and Ca^{2+} channels (Huang et al., 1989) in smooth muscle.

That the SR acts as a sink for Ca^{2+}, i.e., can actively accumulate Ca^{2+}, was initially demonstrated by Somlyo and Somlyo (1971). These investigators took advantage of the fact that the SR can accumulate Sr^{2+} and Ca^{2+} by the same transport mechanisms so that the SR became loaded to a greater extent with Sr^{2+} after incubation in a depolarizing solution. Based on the use of electron probe analysis, Somlyo and Somlyo (1971) estimated that the Ca^{2+} content of the central SR increases 3- to 4-fold following depolarization of smooth muscle. When Casteels and Droogmans (1981) used $^{45}Ca^{2+}$ to determine the content of the SR (junctional, central), they estimated it to be 60 μM/kg wet weight. Using the same technique, they also showed that 1) the maximal rate of filling of Ca^{2+} under normal conditions of external ionic composition (1.5 mM Ca^{2+}) is nearly 70 μmol/kg, and 2) the permeability of Ca^{2+} across the plasma membrane is regulated by the extent of filling of the agonist-sensitive pool of SR Ca^{2+} (Casteels and Droogmans, 1981). This was the forerunner of what would later be described as "capacitative Ca^{2+} entry", as described by Putney (1986).

C. Capacitative Ca^{2+} Entry

In addition to functioning as a store and a sink for Ca^{2+}, the SR is also at the origin of two cell signaling processes: 1) the SR generates Ca^{2+} sparks that, in smooth muscle cells, regulate the plasma membrane electrical potential through modulation of K_{Ca} channels (Nelson et al., 1995; Jaggar et al., 2000), and 2) the content of the SR determines entry of extracellular Ca^{2+} through "store-operated calcium entry" (Casteels and Droogmans, 1981) or "capacitative calcium entry (CCE)" (Putney, 1986; Putney et al., 2001). Thus, both Ca^{2+} sparks and CCE act to regulate Ca^{2+} entry, albeit through separate but related mechanisms.

The designation of CCE is by analogy with an electrical capacitor; a charged or full intracellular store prevents Ca^{2+} entry through this pathway, whereas a discharged or empty store facilitates Ca^{2+} entry and refilling of the store. The CCE model thus proposes that when the SR store is stimulated to discharge Ca^{2+}, either by $InsP_3$-generating signal such as stimulation of G-protein coupled (G_q/G_{11}-) receptors or by receptor/$InsP_3$-independent means, such as through SERCA inhibition, there is a fall in the Ca^{2+} content of the SR, which then signals a novel Ca^{2+} pathway on the plasma membrane so that refilling of the store can occur. The refilling is rapid and allows for a constant internal store of Ca^{2+} to be available for smooth muscle oscillations and maintained tone. The pharmacology of CCE is in its infancy, with agents of generally low specificity being used (Putney et al., 2001). Notable among these are [with attendant K_i values (μM)]: Gd^{3+}, <1; econozole, 2–10; miconazole, 1.0; flufenamic acid, 33; eicosatetraynoic acid, 4.0; SK&F 96365, 3–50; 2-aminoethoxydiphenylborate (2-APB), 30; LU52396, 2.0; and L-651,582, 1.2 (see Putney et al., 2001 for complete list). The lack of a specific inhibitor stems from a paucity of information regarding two key aspects of the model for CCE: 1) the molecular nature of the signaling between a depleted SR and the plasma membrane, and 2) the specific details of the membrane events (ion channels, receptor mechanisms) activated during the process. Notwithstanding these limitations, there has been progress made in unraveling details regarding CCE, and a clearer picture is starting to emerge, at least in some cell types.

In isolated portal vein smooth muscle cells, norepinephrine (NE) causes a transient increase in Ca^{2+} due to SR activation; this is rapidly followed by a more

sustained increase in Ca^{2+} due to entry from extracellular sources (Pacaud et al., 1993). In rat aorta, inhibition of SERCA with low concentrations (1 μM) of cyclopiazonic acid (CPA) increases $[Ca^{2+}]_{cyt}$ without causing contractile activity, suggesting that increases in $[Ca^{2+}]_{cyt}$ in noncontractile compartments are being affected by CPA (Tosun et al., 1998). Low concentrations of CPA induce increases in $[Ca^{2+}]_{cyt}$ that are similar to those produced by KCl, but unlike the latter, fail to induce contraction. On the other hand, higher concentrations of CPA (10–20 μM) appear to increase $[Ca^{2+}]_{cyt}$ beyond the noncontractile compartment. Of interest is that the increase in $[Ca^{2+}]_{cyt}$ produced by low concentrations of CPA is insensitive to L-type voltage-gated Ca^{2+} channel (Ca_L) blockers, such as verapamil, but was inhibited by Ni^{2+} (Tosun et al., 1998). Vasodilation in rabbit and mouse aorta by nitric oxide (NO) has been linked to inhibition of CCE, possibly by the effect of NO in rapidly filling the SR store via stimulation of SERCA (Cohen et al., 1999).

A unique but poorly characterized current, Ca^{2+} release-activated Ca^{2+} current (I_{CRAC}), characterizes the depletion-activated entry of Ca^{2+}. Hoth and Penner (1993) first identified a Ca^{2+} current activated by store depletion (in mast cells) and several aspects of this current were noted: It had a very low conductance (~0.02 pS), high Ca^{2+} selectivity, inward rectification, inhibition by intracellular Ca^{2+}, blockade by Ni^{+} and Cd^{2+}, and lack of voltage-dependent gating (Hoth and Penner, 1993). A current with similar characteristics has also been reported in the mouse anococcygeus muscle, where it is termed I_{DOC} and has a unitary conductance of ~10 pS (Wayman et al., 1998). CCE has been described in a number of smooth muscles (Ito et al., 2000; Weirich et al., 2001; Young et al., 2001); and these findings have been reviewed recently (Gibson et al., 1998; Albert and Large, 2002; McFadzean and Gibson, 2002). There is some evidence to support the notion that store depletion activates tyrosine kinases to signal Ca^{2+} entry in a number of cell types including smooth muscle (Pacaud and Bolton, 1991a; Wijetunge et al., 1992; Doi et al., 2000) and endothelial cells (Jacob, 1990; Sharma and Davis, 1996). In rat aortic smooth muscle cells, depletion of the SR with thapsigargin or bradykinin stimulates phospholipase D to generate phosphatidic acid, which enhances sustained Ca^{2+} entry (Walter et al., 2000). Pharmacological evidence in support of CCE in maintaining the basal tone in resistance arteries has been documented in the rat cremaster arterioles (Potocnik and Hill, 2001). Whereas the CCE was not altered by disruption of the cytoskeleton in cremaster arterioles (Potocnik and Hill, 2001), there is marked inhibition of CCE when actin filaments are disrupted in endothelial cells (Bishara et al., 2002).

Although the molecular identity of the channel responsible for CCE remains elusive, there is persuasive evidence that it has considerable homology with *Drosophila* transient receptor potential channel (TRP) proteins, which are involved in phototransduction in the fruit fly where they mediate CCE. TRP channels are a large family (at least 20 genes) of plasma membrane, nonselective cationic channels. This latter feature of being nonselective makes them depolarizing agents, and their Ca^{2+} permeability suggests a role in intracellular Ca^{2+} signaling. The TRP channels have six transmembrane segments and are activated by products of G-protein coupled receptor (GPCR) stimulation. The properties of TRP have recently been reviewed (Zhu and Birnbaumer, 1998; Nilius, 2003). TRP shares sequence homology with voltage- and second messenger-gated Ca^{2+} channels, and this homology has a long evolutionary history, being also present in *Caenorhabditis elegans*. However, a concern is that TRP channels are not highly selective for Ca^{2+}, and the available evidence indicates that none of the TRP proteins induce a conductance with the known properties of CCE (Vennekens et al., 2002). The TRP(C3) channel may be directly linked to $InsP_3R$ activation, whereby $InsP_3R$ activation leads to entry of extracellular Ca^{2+} (Boulay et al., 1999). It is likely then that CCE is not mediated by a single TRP protein but is possibly occurring through a channel formed by a multimeric structure containing various combinations of TRP and TRP-like proteins (Montell, 1997). The vagaries of the CCE have found detractors who present evidence that key elements of store-operated Ca^{2+} entry are incompatible with generating oscillatory $[Ca^{2+}]_{cyt}$ signals (Shuttleworth, 1999) or that depletion of the internal stores for Ca^{2+} does not always lead to CCE (Haller et al., 1996).

D. Sarcoplasmic Reticulum Fractions and Interaction with Mitochondria

Popescu and Diculescu (1975) segregated smooth muscle SR into three regions: peripheral, deep, and central. In general, the peripheral SR is located close to the plasma membrane and sometimes in apposition with the caveolae (equivalent to junctional SR described above). This SR element is in contact with the deep SR positioned near the myofilaments and is in continuity with the central SR deeper within the cell and associated with the nuclear membrane (Forbes et al., 1977, 1979). Notable details of the analogy of smooth muscle SR to that of striated muscle have been painstakingly pointed out by Forbes et al. (1979) who described as "peripheral SR" the collection of saccules, tubules, and cisternae lying in close apposition (gap of 10–20 nm) to the inner plasmalemmal surface. One functional implication of the peripheral SR is that it dampens the impact of the basal Ca^{2+} entry by acting as a "superficial buffer barrier" (SBB), which then reinforces this buffering capacity by causing a vectorial extrusion of Ca^{2+} to the extracellular space (van Breemen et al., 1995) (Fig. 2). Another implication of the close apposition of the SR and plasma membrane is that sufficiently high concentra-

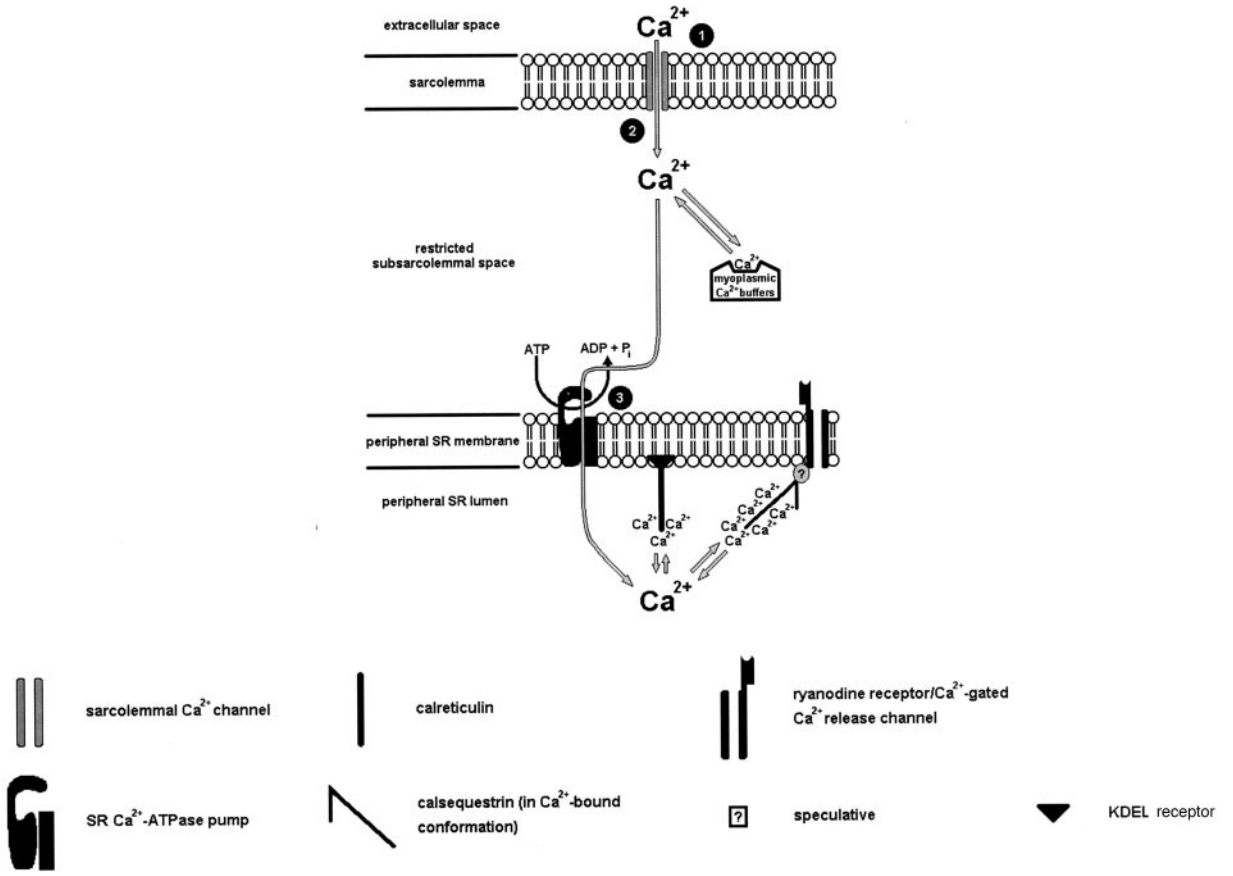

FIG. 2. Preferential sequestration by the peripheral SR of the extracellular Ca^{2+} entering the cell in the restricted subsarcolemmal space as proposed in the superficial buffer barrier model. 1, extracellular Ca^{2+} enters the vascular smooth muscle cells through voltage-dependent or -independent Ca^{2+} channels. 2, it accumulates in the restricted subsarcolemmal space. 3, it is taken up by the peripheral SR through its SERCA. Sarcolemma = plasma membrane, subsarcolemmal = subplasmalemmal, myoplasmic = cytoplasmic.

tions of local are reached to activate the Na^+-Ca^{2+} exchanger and also to activate spontaneous outward K^+ currents. This was recorded by Tomita and Bulbring (1969) and later visualized and described in detail by Nelson et al. (1995).

The concept of the SBB as proposed by van Breemen (see van Breemen et al., 1995) is being challenged. Using more direct approaches, McCarron's data suggests a different model of SR-plasma membrane arrangement that essentially argues against the SBB model. In elegant experiments, Bradley et al. (2002) made two important findings: first, that Ca^{2+} accumulation by the SR proceeds even when Ca^{2+} influx ceases, implying that for this to be possible, the SR and plasma membrane need not necessarily be closely apposed; and second, close apposition of the SR and plasma membrane is instead essential for Ca^{2+} removal by the Na^+-Ca^{2+} exchanger. Using an array of biophysical constants related to Ca^{2+} diffusion characteristics and microdomain constraints, Kargacin's group present intriguing data suggesting that the rate of Ca^{2+} uptake by the SR is insufficient to significantly alter the dynamics of a Ca^{2+} transient, either in its magnitude or spread (Bazzazi et al., 2003). Immunofluorescence imaging reveals no obvious differences in the density of Ca^{2+} pumps or phospholamban between the peripheral (superficial) SR and deep (central) SR.

In addition to the distinct distribution patterns of SR within the cell, there is also some evidence that SR fractions represent heterogeneous compartments of releasable Ca^{2+}. In this regard, Golovina and Blaustein (1997) reported that, in mesenteric arteries, there are two or possibly three functionally distinct compartments: a region (~55%) that empties and refills in a $InsP_3$- and RyR-independent manner (e.g., not affected by CPA and thapsigargin) and a second region (~22%) that empties and fills only in response to caffeine (RyR pool), with other regions (~16%) being responsive to CPA and caffeine. Consistent with this, there is a portion of the SR that appears to be more richly endowed with $InsP_3R$ than RyR (Wibo and Godfraind, 1994). Other studies propose two stores of Ca^{2+} that are distinguished by their Ca^{2+} refilling sources: the store that expresses only RyR is filled by cytoplasmic Ca^{2+}, whereas the store that expresses both RyR and $InsP_3R$ is filled by extracellular Ca^{2+} (Flynn et al., 2001). In contrast to these studies, Itoh et al. (1983) provided compelling evidence that the Ca^{2+} stores associated with IICR (NE-induced) and CICR (caffeine-induced) are identical; additional support for this also comes from

the findings of Leijten and van Breemen (1984) and more recently from Bradley et al. (2002), who depleted caffeine-sensitive Ca^{2+} stores through release with flash photolysis of caged $InsP_3$.

It has been known for some time that mitochondria frequently envelop the central and peripheral portions of the SR (Forbes et al., 1979). Furthermore, mitochondria isolated from smooth muscle cells actively sequester Ca^{2+}, as demonstrated by Somlyo and Somlyo (1971). The mitochondria are also, in many instances, located near the caveolae (Somlyo, 1975; Forbes et al., 1979), and this raises the possibility of transfer of ions between these three structures. Some direct evidence for an important regulatory role of mitochondria on intracellular Ca^{2+} homeostasis were provided by Loew et al. (1994), Drummond and Tuft (1999), and McCarron and Muir (1999). Keeping with this role for mitochondrial interaction with the SR and plasma membrane with regard to Ca^{2+} cycling are the recent findings of Kamishima and Quayle (2002) and Szado et al. (2003). Evidence in freshly dissociated vascular (Drummond and Tuft, 1999; Gurney et al., 2000) and visceral (McCarron and Muir, 1999) smooth muscle cells also suggest a functional integration between SR Ca^{2+} release and mitochondrial Ca^{2+} uptake under physiological conditions. For instance, membrane potential, and thus Ca^{2+} entry, can be regulated by mitochondrial Ca^{2+} accumulation, since mitochondrial Ca^{2+} uptake has recently been shown to modulate Ca^{2+} spark activity in isolated rat cerebral artery smooth muscle cells (Cheranov and Jaggar, 2004). Furthermore, new evidence from rat ventricular cardiac muscle cells (permeabilized cells, microsomes, and RyR2 reconstituted into planar lipid bilayers) demonstrated that physiological concentrations of NADH inhibit CICR and that NADH oxidation, likely right at the SR membranes level, is tightly linked to and essential for this effect. This suggests that it is an important physiological negative feedback mechanism, coupling SR Ca^{2+} fluxes and mitochondrial energy production (Cherednichenko et al., 2004). In contrast, there appears to be no role for mitochondria in Ca^{2+} decay following agonist activation, as shown in rat myometrial smooth muscle cells (Shmigol et al., 1999). The dependence of Ca^{2+} entry from the extracellular space on the status of ER Ca^{2+} content and the influence of the mitochondria on this interaction (Parekh, 2003), as well as the transmission of $InsP_3$-generated Ca^{2+} signals to the mitochondria, have recently been reviewed (Hajnoczky et al., 2000a,b, 2002; Pacher et al., 2000; Szalai et al., 2000; Csordas and Hajnoczky, 2001, 2003).

E. Ca^{2+} Storage by the Sarcoplasmic Reticulum

Once the SR accumulates Ca^{2+}, it is loosely bound and available for release; however, the divalent cation does not exist in an ionized form, since this would lead to inhibition of the SERCA, as mentioned above. Hence, there exist within the SR storage proteins capable of binding large quantities of Ca^{2+} in a complex that is readily available for dissociation when Ca^{2+} release is triggered. The total concentration of intracellular Ca^{2+} buffers in smooth muscle cells is estimated to be ~200 to 300 μM (Bond et al., 1984a; Carafoli, 1987; Allbritton et al., 1992) or 500 μM (Daub and Ganitkevich, 2000). The storage proteins that are expressed at the highest levels in the SR are calsequestrin and calreticulin. These proteins have high capacity (25–50 mol/mol) and low affinity (1–4 mM) for Ca^{2+}. Calsequestrin is the product of two different genes that have a 65% homology; smooth muscle is thought to express both isoforms but in much reduced quantities compared with other muscle types (Pozzan et al., 1994). On the other hand, calreticulin exists in multiple isoforms. There may be some structural similarity between these two Ca^{2+}-binding proteins (calsequestrin and calreticulin), since there is antibody cross-reactivity. It is of note that once the SR accumulates Ca^{2+}, there is preferential binding to proteins, such as calsequestrin, that are strategically located close to the Ca^{2+} release channels. In particular, calsequestrin is retained within the SR lumen by the presence of discrete string-like molecular anchors (Pozzan et al., 1994). In a detailed study of the vas deferens, Villa et al. (1993) provided intriguing evidence that the Ca^{2+} proteins are not uniformly distributed in the SR. They reported that the peripheral portion of SR is rich in calsequestrin (which, incidentally, is also enriched with $InsP_3R$), whereas calreticulin was more evenly distributed in the cell. This selective distribution of binding proteins is in agreement with the hot spots for Ca^{2+} stores reported earlier by Bond et al. (1984a). However, by combining immunogold labeling and immunohistochemical studies, Nixon et al. (1994) concluded that calsequestrin is absent in tonic muscles (aorta), although it was located in the superficial regions of cells from tonic smooth muscle (vas deferens), but the $InsP_3R$ distribution was largely in the peripheral SR in both tissue types. There is some evidence that protein kinase C (PKC) can directly reduce the Ca^{2+} storage by thapsigargin-sensitive [i.e., involving SERCA (see *Section II.A.1.b.*)] mechanisms in cells from the rat aorta. This unloading of the SR content by PKC is suggested to be defective in hypertension (Neusser et al., 1993).

F. Estimates of Ca^{2+} Content in the Sarcoplasmic Reticulum

There is a large variation in the estimate of Ca^{2+} concentration within mammalian intracellular stores, ranging from 1 μM to 5 mM, with these values being subject to the limitations of the method used [e.g., aequorin measures free Ca^{2+} in the SR, whereas electron probe X-ray microanalysis measures total Ca^{2+}] and the cell type studied (Meldolesi and Pozzan, 1998). With the advent of more precise technology, other more direct measurements of the Ca^{2+} content of the SR have been made. For example, Ganitkevich and Hirche (1996) de-

termined that the quantity of Ca^{2+} released by acetylcholine (Ach) is 680 attomoles in smooth muscle; this translates to ~230 μmoles of total Ca^{2+} per liter of cytoplasmic volume. Assuming that this released Ca^{2+} is derived only from the SR, then the SR content would be 7.5 mM per liter SR. In permeabilized smooth muscle cells where uptake of the SR was monitored with fura-2 acid, it is estimated that the SERCA pumps can remove Ca^{2+} at a rate that is 45 to 75% the rate at which Ca^{2+} is removed from the cytoplasm of intact cells during transient Ca^{2+} signals (Kargacin and Kargacin, 1995). Kargacin and Kargacin (1995) calculated that the SR of a single smooth muscle cell could store more than 10 times the amount of Ca^{2+} required to generate a single transient contractile response.

The use of fluorescent indicators has revolutionized the study and understanding of intracellular Ca^{2+} regulation and has also allowed a more accurate quantification of intraluminal free Ca^{2+} in smooth muscle SR. However, an important limitation of this technique is that frequently these dyes, particularly the acetomethoxy ester derivative-type dyes, are prone to compartmentalization in various other intracellular organelles as well (Takahashi et al., 1999). Thus, Hofer and Schulz (1996) have determined that, at least in fibroblasts, only 88% of the loaded low-affinity Ca^{2+} indicator mag-fura-2 (furaptra) (Martinez-Zaguilan et al., 1998) is restricted to the thapsigargin-sensitive ER. In fact, potential contribution of a confounding signal stemming from its accumulation in mitochondria must be kept in mind (Gurney et al., 2000) (see *Section I.D.* for discussion of functional significance). Despite this limitation, the indicator has been used to monitor SR free Ca^{2+} changes in several intact smooth muscle preparations (Hirose and Iino, 1994; Sugiyama and Goldman, 1995; Steenbergen and Fay, 1996; Golovina and Blaustein, 1997; Gomez-Viquez et al., 2003), as has been mag-indo-1, another low-affinity Ca^{2+} indicator (Pesco et al., 2001). Indeed, although it is possible to use high- affinity Ca^{2+} indicators such as fluo-3 or fura-2, the use of these lower affinity Ca^{2+} indicators may be more suitable to monitor dynamic changes in Ca^{2+} stores. The use of aequorin targeted to the ER, as initially described Kendall et al. (1992), has been a significant but technically limiting advance (Alvarez and Montero, 2002) and has been use only in limited number of smooth muscle preparations (Szado et al., 2003).

G. Ca^{2+} Uptake and Release by the Sarcoplasmic Reticulum

It has been known for some time that there is a basal leak of Ca^{2+} from the cell: it is likely that under resting physiological conditions, all cells are exposed to some endogenous low-level stimulation by Ca^{2+}-releasing agents, of which there are many. This will undoubtedly cause a basal leak of Ca^{2+} from the SR, which has been confirmed in a number of tissues by tracking increases in cytoplasmic Ca^{2+} or decreases in SR Ca^{2+} content after maximal inhibition of SERCA with pharmacological tools. This basal leak in various cell types is in the range of 20 to 200 μM/min (Camello et al., 2002; Lomax et al., 2002), and it was shown to be 22% per min in cultured smooth muscle cells (Missiaen et al., 1996). It is thus clear that, in the majority of cell types, this leak is of sufficient magnitude to deplete the SR in a few minutes and forms the largest source of Ca^{2+} efflux from the SR (Missiaen et al., 1996). To offset it, SERCA act to increase SR luminal Ca^{2+} by removing Ca^{2+} from the cytoplasm. Interestingly, pumping activity does not lead to the buildup of a membrane potential across the SR membrane during Ca^{2+} uptake (neither does it occur during Ca^{2+} release) because of the coupling of an efflux of H^+ to this uptake (Inesi and Hill, 1983). There is also evidence for an inward movement Cl^- (Pollock et al., 1998) helping to maintain SR electrical neutrality during Ca^{2+} uptake.

Thus, the SR performs several functions that are directly aided by the presence of SERCA: 1) it acts as a reservoir of releasable Ca^{2+} (the concentration of Ca^{2+} in the SR lumen is nearly three times greater than in the cytoplasm), 2) it buffers the Ca^{2+} leak into the cell that is driven by the steep electrochemical gradient according to the superficial buffer barrier hypothesis proposed by van Breemen and colleagues (1995), 3) it sequesters Ca^{2+} to facilitate smooth muscle relaxation, 4) it provides a pool of Ca^{2+} that is ideally located to activate hyperpolarizing currents via stimulation of K_{Ca} channels, although the spontaneous release of discreet amounts of Ca^{2+} termed Ca^{2+} sparks (Nelson et al., 1995), and 5) it provides Ca^{2+} from $InsP_3$-sensitive stores to activate Cl_{Ca} currents and therefore sustain regenerative changes in membrane potential in gastric muscle (Hirst, 1999; Hirst and Edwards, 2001; Hirst et al., 2002).

1. Ca^{2+} Pump (Sarco/Endoplasmic Reticulum Ca^{2+}-ATPase). The pumping of Ca^{2+} by the SERCA, which belongs to the P-type ion pumps family, is a cycle of chemical reactions leading to a series of conformational states divided into two main groups, termed E_1 and E_2, which are based on a general model describing P-type ATPases activity (the E_1/E_2 model) (Martonosi, 1996; Moller et al., 1996; Adebanjo et al., 1999; Lee, 2000). The E_1 conformations have a high affinity for Ca^{2+} (K_D = 10^{-7} M) and can be phosphorylated by MgATP to form a high-energy phosphorylated intermediate, E_1P. Furthermore, their Ca^{2+}-binding sites are only accessible from the cytoplasm and not from the SR lumen. By contrast, the E_2 conformations have a lower affinity for Ca^{2+} (K_D = 10^{-3} M) and can be phosphorylated by inorganic phosphate (P_i), in the absence of Ca^{2+}, to form a low energy phosphorylated intermediate (E_2P), and their Ca^{2+} binding sites are only accessible from the SR lumen and not from the cytoplasm.

The pumping cycle (Fig. 3) is thus initiated by the binding of two Ca^{2+} ions to high-affinity binding sites on the cytoplasmic surface of the SERCA that is in an E_1 conformation with high-affinity Ca^{2+} binding sites ($E_1{\cdot}[Ca_2]$), which is followed by the binding of a molecule of ATP ($MgATP{\cdot}E_1{\cdot}[Ca_2]$). This leads to autophosphorylation of the enzyme and release of MgADP resulting in an $E_1P{\cdot}[Ca_2]$ intermediate. The energy released from the high-energy phosphate bond leads to major conformational changes, through hinge-type or sliding motions, affecting the Ca^{2+} binding sites: the conversion from the high-energy E_1P to the low-energy E_2P ($E_2P{\cdot}[Ca_2]$). The Ca^{2+} ions are then released to the SR lumen from the now low-affinity Ca^{2+} binding sites (E_2P). The cycle is then terminated by hydrolysis of the bound phosphate (E_2), countertransport of H^+ ions to maintain electroneutrality of the SR membrane (although this countertransport of H^+ does not completely balance the charge carried by Ca^{2+}, making the Ca^{2+}-ATPase electrogenic), and the conversion of E_2 into E_1 to reset the Ca^{2+} pumping cycle. Variants of this model have been proposed (Martonosi, 1996; Moller et al., 1996; Adebanjo et al., 1999; Lee, 2000) as well as an alternative model not based on the E_1/E_2 dichotomy (Jencks, 1992). As Ca^{2+} accumulates within the lumen, the rate of SERCA activity would be expected to slow down due to a negative feedback. To overcome this limitation, the SR is endowed with Ca^{2+} buffering proteins (see above). The stoichiometry of 1ATP:2Ca has been proven only for SERCA1; in tissues such as smooth muscle, there is only indirect evidence from Hill coefficients (Mg ATPase being 1 and 2 for Ca^{2+}) for SERCA pump activation (Grover and Samson, 1986).

The SERCA are 110-kDa proteins and are encoded by three genes: SERCA1 is largely expressed in fast-twitch skeletal muscle, with 1a in adult and 1b in neonatal muscle, SERCA2a is mainly in cardiac and slow-twitch muscle, and SERCA2b is mainly in smooth muscle and most nonmuscle cells, whereas SERCA3 is present on a more widespread basis (East, 2000; Sorrentino and Rizzuto, 2001). Smooth muscle mainly expresses the SERCA2b isoform (>70%), with the SERCA2a and SERCA3 isoforms forming the remainder of the SERCA population (Lytton et al., 1989; Wuytack et al., 1989; Eggermont et al., 1990; Amrani et al., 1995; Trepakova et al., 2000; Wu et al., 2001). Both isoforms are splice variants transcribed from the SERCA2 gene (Wu and Lytton, 1993). The SERCA2b has a higher affinity for Ca^{2+} than SERCA2a (Verboomen et al., 1992) and a lower turnover rate for both Ca^{2+} transport and ATP hydrolysis (Lytton et al., 1992). The maximal rate of Ca^{2+} uptake by smooth muscle SR (loaded with oxalate to create linear kinetics) is ~100 nmol/kg/min, which is lower (by two times) than in striated muscle (Raeymaekers, 1982; Raeymaekers and Jones, 1986). This reduced rate of Ca^{2+} uptake is most likely due to the reduced density of SERCA in smooth muscle (Wuytack et al., 1989).

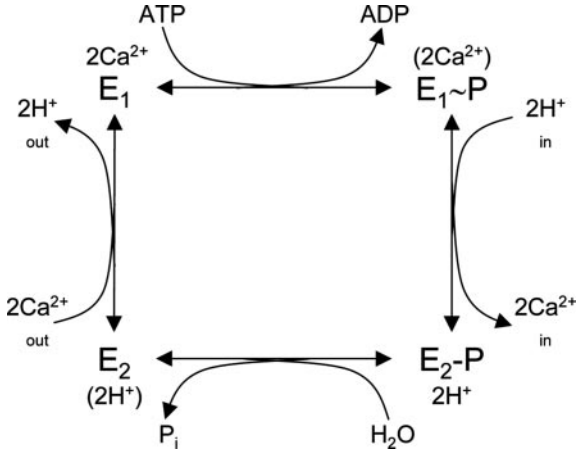

FIG. 3. SERCA pumping cycle. ( ): occlusion. See text for details.

The activity of SERCA is largely regulated by phospholamban, a small protein of 52 amino acids that forms a homopentamer and is present in the smooth muscle SR membranes. Although it was shown to be expressed in the porcine gastric smooth muscle (Raeymaekers and Jones, 1986) and rabbit aorta (Cornwell et al., 1991), there is species and tissue variability in the amount of phospholamban expressed (Raeymaekers and Jones, 1986). There is also variability in the sensitivity of SERCA isoforms to this regulatory protein; although SERCA2b is regulated by both phospholamban and calmodulin kinase, SERCA3 is not regulated by either of these proteins. In addition, SERCA3 is more resistant to reactive oxygen species than SERCA2b (Grover and Samson, 1997).

Unphosphorylated phospholamban 1) lowers the apparent turnover rate (global V_{max}) of SERCA2 through interactions with its cytoplasmic domain (likely by decreasing the Ca^{2+} transport portion of the cycle $E_1P{\cdot}[Ca_2] \rightarrow \ldots \rightarrow E_2P$ (Hughes et al., 1994, 1996) and 2) lowers its apparent affinity for Ca^{2+}, without affecting the true chemical affinity, through interactions with its transmembrane domain (James et al., 1989; Sasaki et al., 1992a; Cantilina et al., 1993). Its phosphorylation causes its dissociation from SERCA (Tada, 1992) and increases SERCA apparent affinity for Ca^{2+} by reducing the activation energy for a slow transition triggered by Ca^{2+} binding in the Ca^{2+} pumping cycle (Fig. 3), making the pump more "reactive" to cytoplasmic Ca^{2+} (Cantilina et al., 1993).

When phospholamban is phosphorylated, e.g., by cAMP or Ca^{2+}/calmodulin kinase, SERCA activity is increased resulting in an enhanced uptake of Ca^{2+} by the SR, although it should be noted that the extent of cAMP-stimulated phospholamban activity is considerably lower than in cardiac tissue (Watras, 1988). Phospholamban is also an excellent substrate for PKG (Raeymaekers et al., 1988). cGMP is more effective in reducing cytoplasmic Ca^{2+} and is thus a potent mediator of

smooth muscle relaxation (Felbel et al., 1988). Indeed, it is likely involved in NO-induced SERCA activation; NO activation of guanylate cyclase would increase cGMP concentration, which would activate SR membrane-located PKG, which would then phosphorylate phospholamban (Felbel et al., 1988; Raeymaekers et al., 1988; Twort and van Breemen, 1989; Cornwell et al., 1991; Karczewski et al., 1992; Andriantsitohaina et al., 1995). Several groups have also described a novel means of activation of SERCA by direct phosphorylation by a Ca^{2+}-calmodulin kinase (CaM kinase)—for example in heart (Xu et al., 1993), HEK cells (Toyofuku et al., 1994), skeletal muscle (Hawkins et al., 1994), and coronary arteries (Grover et al., 1996).

2. Ca^{2+} Release Channels. As mentioned earlier, release of Ca^{2+} from the SR can occur via a basal leak that is removed from the cytoplasm via a concerted action of mitochondrial uptake, SERCA activity, and plasma membrane extrusion through the Na^+-Ca^{2+} exchanger and PMCA. The most physiologically relevant SR Ca^{2+} release, however, occurs though activation of $InsP_3R$ and RyR. Interestingly, in many smooth muscle preparations, the SR Ca^{2+} pools released through these channels overlap (Missiaen et al., 1992b). Furthermore, there could be functional interactions between SERCA and the SR Ca^{2+} release channels (Gomez-Viquez et al., 2003).

There are three genes that encode $InsP_3R$ and also three genes that encode RyR, each generating a specific isoform. The sequences encoded by $InsP_3R$ and RyR genes house a basic similarity in structure, sharing fragmental amino acid residue homology concentrated in the ligand-binding and Ca^{2+} channel domains, implying fundamental roles of these domains in the activity of the SR Ca^{2+} channels (Yoshida and Imai, 1997) and suggesting a common ancestral history (Sorrentino and Rizzuto, 2001). Each of these release channels is indeed configured in as a tetrameric formation, with the RyR being homotetrameric, the $InsP_3R$ being heterotetrameric, and the molecular weights of purified $InsP_3R$ (500 kDa) and RyR (300 kDa) indicating large protein structures (Furuichi et al., 1989, 1994). However, despite the above molecular similarities, the three-dimensional structure at 24-Å resolution of these two classes of channels is quite different (Jiang et al., 2002) (see the two following sections).

Local accessory proteins tailor the functional properties of these channels within particular cells and subcellular domains (Mackrill et al., 1996). Some of these proteins modulate activity of all SR Ca^{2+} release channels, whereas others have class- or even isoform-specific effects. Some proteins exert both direct and indirect regulation, sometimes with opposing effects, whereas others are themselves modulated by $[Ca^{2+}]_{cyt}$ changes, thus being part of feedback loops.

a. Ca^{2+}-Gated Channel/Ryanodine Receptor. The RyR channel is activated when surrounding $[Ca^{2+}]_{cyt}$ increases sufficiently to trigger CICR (Fig. 4) (see below). The RyR is a homotetrameric protein approximately 2 MDa in molecular weight. In mammalian tissues (including smooth muscle), it forms a family of three isoforms, RyR1, RyR2, and RyR3, each encoded by a distinct gene, either *ryr1* (initially cloned and sequenced from skeletal muscle), *ryr2* (initially cloned and sequenced from cardiac muscle), and *ryr3* (initially cloned and sequenced from the brain) (Sutko et al., 1997). Two alternatively splice variants of RyR1 and one variant of RyR2 have also been identified. RyR knockout mice have also been developed; in mice lacking RyR3, caffeine and NE maintain their contractile effects (Yamazawa et al., 1996), whereas Ca^{2+} activity is significantly increased (Lohn et al., 2001). RyR2 knockout is lethal due to cardiac malformation (Takeshima et al., 1998). An interesting approach was used by Drega et al. (2001) to minimize the function of RyR: Using organ culture techniques (4 days, 10–100 μM ryanodine), RyR protein was recovered but RyR were nonfunctional. An interesting finding of this study is that although intracellular stores recover following chronic ryanodine treatment, RyR activity is essential for Ca^{2+}-spark activity but not for Ca^{2+} waves/oscillations (Dreja et al., 2001).

Expression patterns of RyR subtypes show variable distribution, with RyR1 and RyR2 being present in skeletal muscle and cardiac muscle, respectively; RyR2 is the predominant isoform in neural tissue. RyR3 is expressed mainly in embryonic tissue, and levels decrease during development (Rossi and Sorrentino, 2002). In smooth muscle cells, RyR2 and RyR3 are the primary isoforms (Sanders, 2001). Interestingly, although all three RyR isoforms are present in vascular smooth muscle of neonatal mice, where the SR content appears normal, these RyR do not become fully functional until further maturity of the animals (Gollasch et al., 1998). There is also a regional variability in the expression combination of the three RyR isoforms in smooth muscle from different organs. RyR2 is required for generation of Ca^{2+} sparks, with either a minimal (Mironneau et al., 2001) or inhibitory (Lohn et al., 2001) contribution for RyR3.

The channel is an assembly of four RyR subunits (protomers) of the same isoform (thus an homotetramer) forming a central Ca^{2+}-conducting pore, which has a diameter of 2 to 3 nm. RyR1 and RyR3 have been shown to differ significantly in vitro in terms of gating and activation. Topologically, various studies suggest that the RyR spans the membrane 4, 10, or 12 times (Michikawa et al., 1996), with highly conserved ion-channel-forming membrane-spanning regions that appear to be localized to the carboxyl terminal (20% of the protein), while the remaining amino-terminal region of the protein forms a large cytoplasmic foot domain that assumes a quatrefoil shape (Sutko et al., 1997; Welch et al., 1997; Wagenknecht and Samso, 2002). The RyR is anchored to the SR by interaction with the Ca^{2+} binding storage protein calsequestrin (see *Section I.E.*).

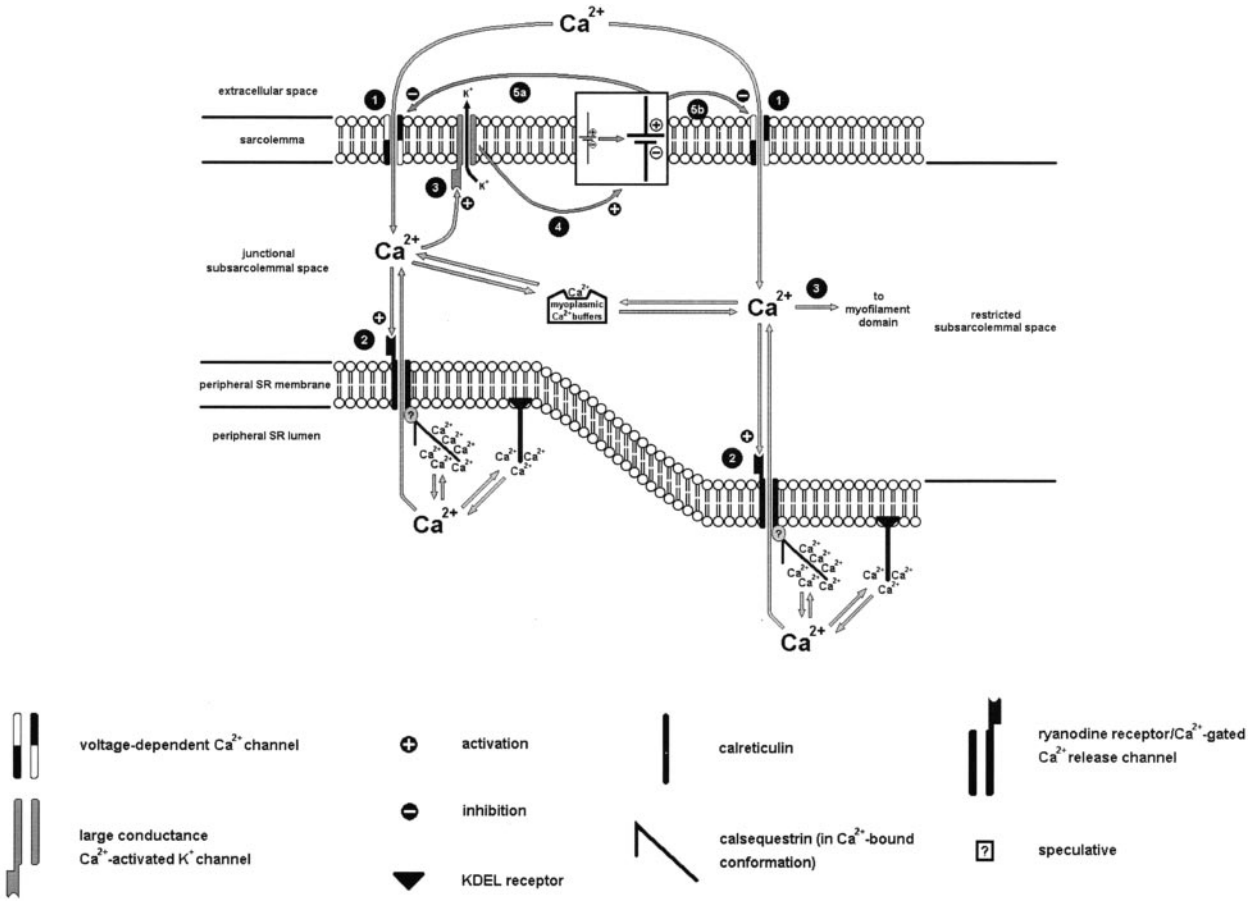

FIG. 4. CICR and Ca^{2+} sparks. 1, influx of extracellular Ca^{2+} occurs through opening of voltage-gated Ca^{2+} channels into both the junctional and the restricted subsarcolemmal spaces. 2, Ca^{2+} accumulation in these spaces activates Ca^{2+}-gated Ca^{2+}-release channel/RyR leading to the opening of the channel, a phenomenon termed CICR. 3, the resulting CICR into the junctional subsarcolemmal space (termed Ca^{2+} spark) raises the local Ca^{2+} concentration enough to activate large conductance Ca^{2+}-activated K^+ channel (BK) on the plasma membrane. 4, the resulting BK opening leads to K^+ efflux, which in turn induces membrane hyperpolarization. 5, this hyperpolarization promotes voltage-gated Ca^{2+} channel closure reducing Ca^{2+} influx both in the junctional subsarcolemmal space (5a) and in the restricted subsarcolemmal space (5b). Sarcolemma = plasma membrane, subsarcolemmal = subplasmalemmal, myoplasmic = cytoplasmic.

The distribution pattern of RyR follows that of the SR such that in where there is a patch distribution of SR in the cytoplasm, as in the guinea pig aorta, there is a sparse labeling with ryanodine markers, whereas tissues with a more prominent peripheral SR have a rich marking of RyR in the periphery—in other words, RyR distribution parallels that of the SR (Lesh et al., 1998). The physiological roles of RyR in smooth muscle cells are still being elucidated (Guerrero-Hernandez et al., 2002). Although its endogenous gating ligand is Ca^{2+} leading to CICR, as mentioned above, it appears that its basal Ca^{2+} sensitivity is in the micromolar range, a $[Ca^{2+}]_{cyt}$ not globally reached in the bulk of the cytoplasm (Sanders, 2001). Hence, RyR appears to be activated in proximity to the plasma membrane (e.g., on the SR face of the plasma membrane-SR junctional space) by extracellular Ca^{2+} influx through Ca_L to produce CICR of Ca^{2+} sparks, which in turn modulates plasma membrane excitability (e.g., hyperpolarization) through activation of small conductance K_{Ca} channels (SK), large conductance K_{Ca} (BK), and depolarization through Cl_{Ca} (Jaggar et al., 2000; Sanders, 2001). In cerebral artery smooth muscle cells, for instance, Ca^{2+} sparks-activated BK openings promote relaxation (Nelson et al., 1995). There may be a role, however, for regional vascular differences with regard to the role of Ca^{2+} sparks. For example, spontaneous transient outward currents (STOC), and hence Ca^{2+} sparks, are very active in fetal pulmonary arteries, and this activity diminishes with maturation (Pratusevich and Balke, 1996; Jaggar et al., 2000). This contrasts completely with the nearly 100-fold increase in Ca^{2+} spark activity and STOC frequency during maturation of systemic arterial cells (Gollasch et al., 1998). Thus, in pulmonary artery cells, endothelin, the potent endogenous vasoconstrictor, activates Ca^{2+} sparks by causing the cross-signaling of RyR and $InsP_3R$—in this case, increased smooth muscle Ca^{2+} activity is associated with constriction (Ge et al., 2003; Zhang et al., 2003). Another example of the physiological relevance of Ca^{2+} sparks is the finding that stretching of urinary bladder smooth muscle cells generates Ca^{2+} sparks from RyR sites on the SR (Ji et al., 2002).

The finer details of the organization of microdomains that underlie Ca^{2+} sparks are being unraveled with

insightful experimental analysis. It is now apparent that K_{Ca} channels that underpin STOC are exposed to a mean Ca^{2+} concentration on the order of 10 μM during a Ca^{2+} spark (ZhuGe et al., 2002). The membrane area over which a concentration of 10 μM or more (range 12–21 μM) is achieved has an estimated radius of 15 to 30 nm, corresponding to an area that is a fraction of one square micron (0.07–0.28 μm^2). It is also apparent that K_{Ca} channels are not uniformly distributed over the membrane but exist as clusters at sites of frequent discharge of Ca^{2+} sparks, where the K_{Ca} channels and RyR mediating Ca^{2+} sparks is in the order of 25 nM (ZhuGe et al., 2000, 2002). Indirect support for an intimate relationship between K_{Ca} channels and RyR comes from findings in smooth muscle-excised patches of portal vein (Xiong et al., 1992) and vas deferens (Ohi et al., 2001b), where there is evidence for clustering of K_{Ca} channels and an apparent attachment of SR membrane.

An emerging role for RyR is the development of hypertension, where Ca^{2+} spark regulation of BK channels is altered. Although the pore-forming α subunit is conserved and ubiquitously expressed, there are four distinct β regulatory subunits (Nelson and Quayle, 1995). The β_1 subunit is selectively expressed in smooth muscle. In a recent study of angiotensin I-induced hypertension, expression of the β_1 subunit (and not the α subunit) was shown to be reduced, thus uncoupling K_{Ca} channels from Ca^{2+} sparks from the RyR (Amberg et al., 2003). The reduced efficacy of vascular K_{Ca} channels is associated with greater depolarization and increased vascular tone (Amberg et al., 2003).

In contrast, CICR from RyR at SR locations further away from the plasma membrane could propagate Ca^{2+} waves that induce contractile activity (Collier et al., 2000). For instance, CICR could be triggered by IICR (Fig. 5) (see below), such as in the IICR-triggered and CICR-propagated Ca^{2+} waves induced by NE in portal vein (Boittin et al., 1999) and inferior vena cava (Lee et al., 2002b) smooth muscle cells. CICR could also be triggered by the spatially restricted $[Ca^{2+}]_{cyt}$ bursts induced by the newly identified Ca^{2+} releaser nicotinic acid adenine dinucleotide phosphate, a pyridine nucleotide derived from β-$NADP^+$, such as in the nicotinic acid adenine dinucleotide phosphate-triggered and CICR-propagated global Ca^{2+} wave and contractile activity in pulmonary artery smooth muscle cells (Boittin et al., 2002).

Smooth muscle CICR is a function of the net flux of Ca^{2+} ions into the cytoplasm rather than the single channel amplitude of Ca_L. Unlike CICR in cardiac muscle, RyR channel opening in smooth muscle is not tightly linked to the gating of Ca_L, and unlike CICR in striated muscle, Ca^{2+} release is completely eliminated by cytoplasmic Ca^{2+} buffering. Thus, Ca_L is loosely coupled to RyR through an increase in global $[Ca^{2+}]_{cyt}$ due to an increase in the effective distance between Ca_L and RyR compared with striated muscle.

The RyR sensitivity (hence CICR sensitivity) to Ca^{2+} could be increased by the endogenous cyclic ADP ribose (the only endogenous RyR agonist identified so far) (see *Section II.B.1.*), although its sensitivity could also be altered by many other endogenous factors (Ca^{2+}, Mg^{2+}, H^+, adenine nucleotide, calmodulin, and protein kinases A and C (PKC) (Rossi and Sorrentino, 2002). As CICR itself, this alteration of RyR sensitivity could promote either relaxation or contractile activity depending on the circumstances. For instance, it could relax through Ca^{2+} sparks generation, such as in β-adrenoceptor-activated (Boittin et al., 2003) or resting (Cheung, 2003) arterial smooth muscle. In contrast, this phenomenon could induce (i.e., without requiring extracellular Ca^{2+} influx) or amplify (i.e., by augmenting an initial $[Ca^{2+}]_{cyt}$ rise mediated by Ca^{2+} influx) contractile activity through global $[Ca^{2+}]_{cyt}$ increases. Examples of this are the Ca^{2+} influx-independent M_1 muscarinic receptor-induced coronary artery smooth muscle contractile activity (Ge et al., 2003) and the Ca^{2+} influx-triggered cholecystokinin-A receptor-induced longitudinal intestinal smooth muscle contractile activity (Kuemmerle and Makhlouf, 1995).

b. Inositol 1,4,5-Trisphosphate-Gated Channel/Inositol 1,4,5-Trisphosphate Receptor. The $InsP_3R$ family is formed in mammalian tissues of at least three isoforms, type 1 ($InsP_3R1$), type 2 ($InsP_3R2$), and type 3 ($InsP_3R3$), each encoded by a distinct gene and sharing 60 to 70% amino acid residue homology (Wilcox et al., 1993; Nakade et al., 1994; Michikawa et al., 1996; Yoshida and Imai, 1997; Taylor, 1998; Patel et al., 1999; Yule, 2001; Jiang et al., 2002). These isoforms, each ~300 kDa, share the same structural and functional organization (Yoshida and Imai, 1997; Wilcox et al., 1998): a bulbous ligand-binding domain in the N-terminal portion (~24% of the whole receptor molecule), a large coupling (a.k.a. regulatory, modulatory) domain in the middle portion (~60% of the molecule) that transduces the signal of ligand binding and contains sites for Ca^{2+} binding, ATP binding, and phosphorylation by protein kinases, and a short Ca^{2+} channel domain in the C-terminal portion. Only $InsP_3R1$ is known to undergo alternative splicing with two segments (Yoshida and Imai, 1997): the 15-residue-long S1 segment located in the ligand-binding domain predominantly expressed in peripheral tissues and the 40-residue long S2 segment located in the coupling domain and predominantly expressed in the nervous system. As is the case for the majority of cell types examined so far (Wilcox et al., 1993, 1998), smooth muscle cells express multiple $InsP_3R$ isoforms, although some could express none, such as the longitudinal intestinal smooth muscle cells (Kuemmerle et al., 1994).

The proportion of amino acid residue identity among isoforms is 68% in the ligand-binding domain, 53% in the coupling domain, and 59% in the Ca^{2+} channel domain (Yoshida and Imai, 1997). Poor conservation in the coupling domain suggests the possible operation of differential

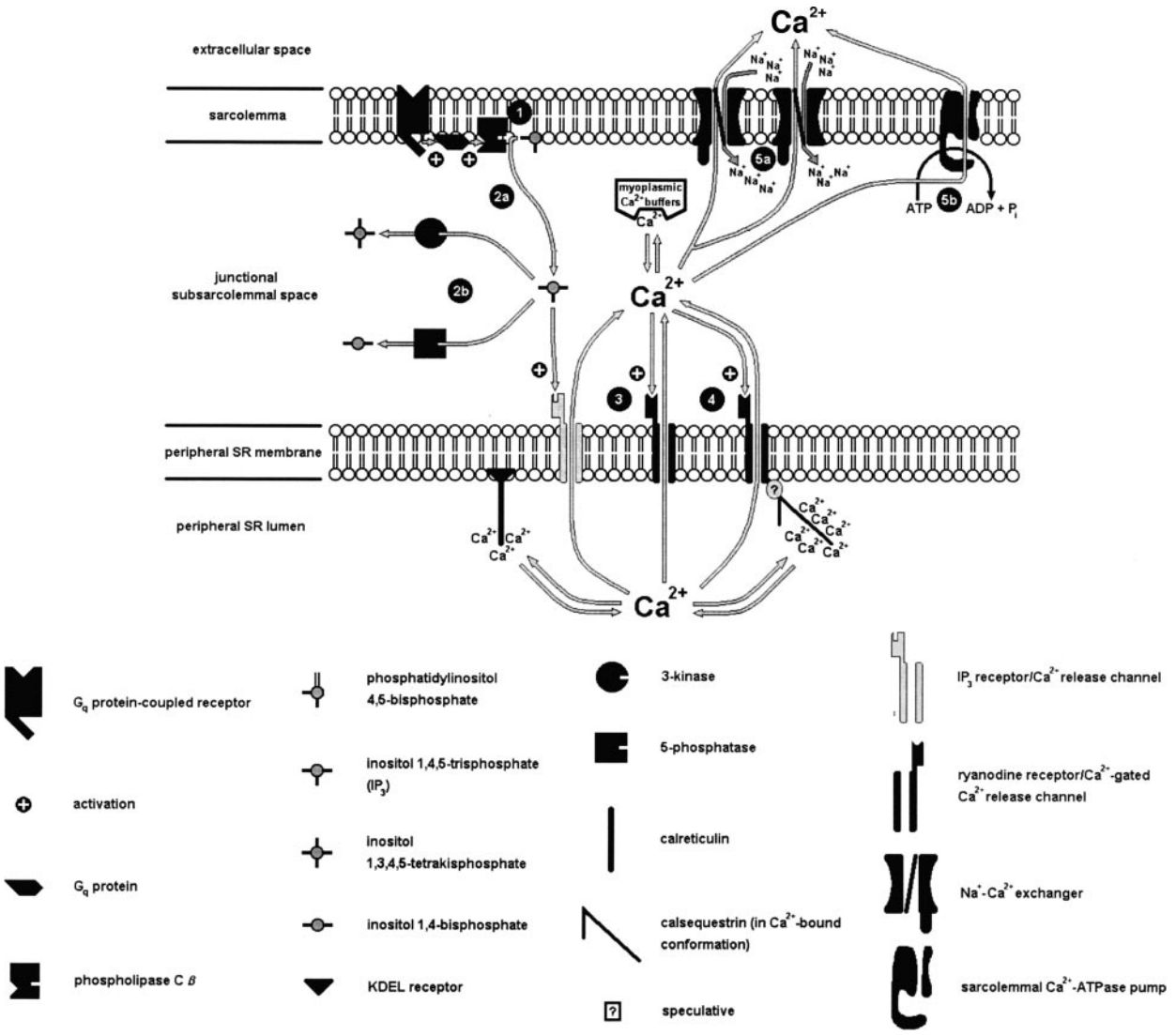

FIG. 5. Vectorial Ca^{2+} extrusion scheme from the peripheral SR toward the sarcolemma in the junctional subsarcolemmal space as proposed in the superficial buffer barrier model 1, the activity of G_q protein-coupled receptor-regulated phospholipase C β generates $InsP_3$ from phosphatidylinositol 4,5-bisphosphate. 2a, $InsP_3$ accumulates in the junctional subsarcolemmal space where it activates its receptor on the peripheral SR membrane leading to the opening of the associated Ca^{2+} release channel. 2b, $InsP_3$ is metabolized either by a 3-kinase into inositol 1,3,4,5-tetrakisphosphate or by a 5-phosphatase into inositol 1,4-bisphosphate before it could leave the junctional subsarcolemmal space. 3, the Ca^{2+} released by $InsP_3$ accumulates in the junctional subsarcolemmal space until it reaches a concentration triggering a CICR through activation of the Ca^{2+}-gated Ca^{2+} release channel/RyR. 4: the CICR process becomes regenerative. 5a, the Ca^{2+} released from the peripheral SR into the junctional subsarcolemmal space is eventually extruded from the cell mostly through the action of the Na^+-Ca^{2+} exchanger. 5b, some of this Ca^{2+} is also extruded by the plasma membrane Ca^{2+}-ATPase pump (PMCA). Sarcolemma = plasma membrane, subsarcolemmal = subplasmalemmal, myoplasmic = cytoplasmic.

regulation in that region among the three isoforms, as illustrated by their sensitivity to protein kinase A-mediated phosphorylation ($InsP_3R1 \gg InsP_3R3 > InsP_3R2$) (Wojcikiewicz and Luo, 1998b; Murthy and Zhou, 2003). Isoforms were also shown to differ in their sensitivities to breakdown by cellular proteases ($InsP_3R2$ relatively resistant versus $InsP_3R1$ and $InsP_3R3$) (Wojcikiewicz, 1995) and in their spatial distribution (Sugiyama et al., 2000; Tasker et al., 2000) (see *Section II.C.1.*).

The three-dimensional structure of $InsP_3R1$ has recently been determined by electron cryomicroscopy and single-particle reconstitution using immunopurified and functional bovine cerebellar $InsP_3R1$ (Serysheva et al., 2003). As expected, the channel forms a 4-fold symmetric structure divided into a peripheral large pinwheel (~80% total tetramer volume), created by four centrally interconnected radial curved spokes and a central smaller square (remaining tetramer volume). The $InsP_3R$-binding core domain (likely corresponding to the "coupling domain" mentioned above) was localized within each spoke of the pinwheel region through three-dimensional reconstruction. Putative assignment of the $InsP_3R1$ protomer amino acid sequence to domains within the three-dimensional map was also done, concurring with the topological model deduced from biochemical, electrophysiological, and molecular biology experiments (Joseph et al., 1997; Galvan et al., 1999; Ramos-Franco et al., 1999; Galvan and Mignery, 2002).

The pinwheel region is likely exposed to the cytoplasm, whereas the square region likely includes the transmembrane domain and faces the ER lumen, putting about 89% of the tetramer in the cytoplasm, with the remaining portion constituting the transmembrane channel domain. A model was also proposed where binding of $InsP_3$ on the pinwheel region far from the transmembrane channel domain induces long range conformational changes in the cytoplasmic region of $InsP_3R1$ to trigger channel opening.

The $InsP_3R$ isoform protomers, each traversing the SR membrane six times, much like voltage-gated and ligand-activated ion channels of the plasma membrane (Jan and Jan, 1992), associate via their C termini into homotetrameric, or in contrast with the RyR isoform protomers, heterotetrameric channels; at present, it is unclear to what extent differences in isoform composition influence ligand binding or Ca^{2+} release properties of the channels (Shears, 1998, 1989; Wilcox et al., 1998) (see *Section II.C.1*). The $InsP_3R$ is localized to the caveolae in vascular smooth muscle and endothelial cells (Fujimoto et al., 1992), and this distribution may be actin-linked (Fujimoto et al., 1995).

The density of $InsP_3R$ is over 100 times greater in brain than smooth muscle, but the ligand affinity (2.1 versus 2.4 nM) is similar in binding studies (Marks et al., 1990; Zhang et al., 1995). In permeabilized A7r5 (embryonic aortic smooth muscle cell line), the threshold for $InsP_3$-induced release of $^{45}Ca^{2+}$ is 32 nM under control conditions and was reduced to 4.5 nM when the affinity of $InsP_3R$ was increased by treatment with thimerosal (Missiaen et al., 1996).

Iino reported that IICR in smooth muscle is enhanced by submicromolar concentrations of cytoplasmic Ca^{2+} (Iino, 1987, 1989). The activity of the $InsP_3R$ was subsequently shown to depend on cytoplasmic concentrations of Ca^{2+} in a biphasic manner, with a peak near 300 nM (Iino, 1990). Ca^{2+} has immediate effects on the rate of release of (caged) Ca^{2+} induced by (caged) $InsP_3$ (Iino and Endo, 1992). Later studies by Iino's group demonstrated that $InsP_3$, even at very high concentrations, is not by itself sufficient to activate the $InsP_3R$ and that both $InsP_3$ and Ca^{2+} are required simultaneously for activation of the receptor (Hirose et al., 1998). Thus, it is evident that the $InsP_3R$ detect simultaneous increases in $InsP_3$ and Ca^{2+} such that Ca^{2+} potentiates IICR without changing the affinity of the $InsP_3R$ for $InsP_3$; increasing the cytoplasmic concentration of Ca^{2+} from 100 to 300 nM causes a nearly 7-fold increase in Ca^{2+} released by $InsP_3$ (Hirose et al., 1998). However, micromolar concentrations of Ca^{2+} decrease the affinity of the $InsP_3R$; 50% inhibition is caused by 0.3 μM Ca^{2+} (Benevolensky et al., 1994). It has recently been suggested for $InsP_3R1$ that such high Ca^{2+} concentrations regulate the rearrangement of the peripheral region of the molecule (Hamada et al., 2002). Taken together, these findings are of particular importance in the generation and propagation of Ca^{2+} waves (Hirose et al., 1998).

In most smooth muscle cell types, many excitatory agonists (e.g., neurotransmitters) can bind to a specific class of plasma membrane GPCR, those coupled to G_q or G_{11}, to activate phospholipase C (PLC) leading to the generation of $InsP_3$ from the breakdown of surrounding plasma membrane phosphoinositides (Sanders, 2001) (see *Section II.C.1.b.*). This water-soluble $InsP_3$ then diffuses into the cytoplasm away from the plasma membrane to bind to $InsP_3R$ in the SR membrane, where it induces the opening of the Ca^{2+} channel that they are forming leading to Ca^{2+} release (IICR). The diffusion coefficient for $InsP_3$ is 283 $\mu m^2/s$ without metabolism by specific phosphatases and kinases; the time scale of $InsP_3$ action is limited by its degradation to ~1 s, making the effective domain of second messenger action an area of ~24 μm (Michikawa et al., 1996). The $InsP_3R$ has a single high-affinity binding site (K_D value of 80 nM), and it is estimated that half-maximal release of Ca^{2+} from the SR requires 40 nM of $InsP_3$. The $InsP_3$ sensitivities of the isoforms vary to a limited extent and are ranking $InsP_3R1 > InsP_3R2 > InsP_3R3$ (K_D values of 1.5, 2.5, and 22.4 nM, respectively), consistent with the sensitivities for IICR of cell lines expressing predominantly homotetrameric forms of either of these isoforms (Wojcikiewicz and Luo, 1998a). This sensitivity is controlled by the SR luminal Ca^{2+} content such that a reduced content also reduces IICR sensitivity (Missiaen et al., 1992c). Likewise, moderate increases in $[Ca^{2+}]_{cyt}$ sensitize IICR, whereas higher $[Ca^{2+}]_{cyt}$ has an inhibitory effect (Iino, 1990; Iino and Endo, 1992). Pharmacological modulation of $InsP_3R$ sensitivity occurs with thimerosal, which increases the affinity of the receptor for $InsP_3$ (Bootman et al., 1992b; Michelangeli et al., 1995). Of notable interest is that IICR is quantal in nature (Bootman et al., 1992a; Ferris et al., 1992), whereby maximal $InsP_3$ concentrations release 40% of SR Ca^{2+} content in freshly isolated canine smooth muscle cells (Hashimoto et al., 1985) and 84% of SR Ca^{2+} store in cultured human smooth muscle cells (Twort and van Breemen, 1989).

This IICR can sum with agonist-activated Ca^{2+} entry mechanisms and contribute to global $[Ca^{2+}]_{cyt}$ transients and ensuing contractile activity. IICR can also result in very spatially localized increases in $[Ca^{2+}]_{cyt}$ (Ca^{2+} puffs) analogous to Ca^{2+} sparks (Bayguinov et al., 2000; Boittin et al., 2000; Burdyga and Wray, 2002). The response to these Ca^{2+} puffs could be either initiation of Ca^{2+} waves, which can then be propagated by RyR-induced CICR leading to contractile activity (see above), or alteration of plasma membrane Ca^{2+}-activated conductances (SK and BK channels) promoting relaxation (or contractile activity with Cl_{Ca}) as with Ca^{2+} sparks. As for CICR, the type of response to Ca^{2+} puffs depends on the spatial location of $InsP_3R$, which may vary between smooth muscle cell types (see *Section II.C.1.c.*).

An interesting development is the proposal by McCarron et al. (2002) that IP_3 evokes contractile activity of smooth muscle by suppressing STOC, which would promote Ca^{2+} entry via membrane depolarization and activation of voltage-gated Ca^{2+} channels.

II. Physiological and Pharmacological Agents

Physiological and pharmacological agents targeting SERCA, RyR, or $InsP_3R$ have been characterized mostly using isolated ER/SR membrane-enriched cell membrane fractions (lipidic spheres called microsomes) or the molecular target of interest partially purified from these microsomes and reconstituted into lipid membrane bilayers. Although the microsome approach allows the measurement of Ca^{2+} fluxes either using $^{45}Ca^{2+}$ loaded into the microsomes or high-affinity Ca^{2+} indicators outside the microsomes, the lipid bilayer reconstitution approach allows the measurement of specific membrane currents. However, both approaches may suffer from the loss of important cofactors or accessory proteins associated with the harshness of the preparatory methods and the unavoidable loss of cytoplasm and non-ER/SR subcellular structures. This could generate results conflicting with data obtained with the same agents in isolated smooth muscle cells or tissues. It could also lead to the oversight of important nonselective effects requiring the presence of other molecular targets in the cytoplasm or on non-ER/SR subcellular structures. It should also be considered that there might be variations in the nature and quantitative aspects of the response to an agent related to the nature of the cell type/tissue considered as well as the animal species. Finally, more than one cell type in an isolated tissue may respond the same way to a given agent, but the effect on one type of cell may inhibit or accentuate the effect of the agent on a neighboring cell of another type (e.g., endothelial cells versus vascular smooth muscle cells). Thus, each agent must be carefully evaluated with all these caveats in mind. One must also remain aware that selectivity versus all major relevant molecular targets involved in the Ca^{2+} handling process has not always been thoroughly assessed for every agent, and caution must be exerted accordingly in experimental design using these agents.

It should be noted that 8-(*N*,*N*-diethylamino)octyl-3,4,5-trimethoxybenzoate (TMB-8), chlorpromazine, and tetracaine, although affecting some of the molecular targets of interest here, are not discussed in this review because of their high degree of nonselectivity (Prozialeck et al., 1987; Ishihara and Karaki, 1991). Similarly, AlF_4^- and vanadate, although SERCA inhibitors, are not considered here because of their nonselectivity for P-type ATPases in general (e.g., PMCA, Na^+/K^+-ATPase) (Missiaen et al., 1988), with AlF_4^- also activating heterotrimeric G-proteins (Bigay et al., 1987) and vanadate-inhibiting protein-phosphotyrosine phosphatases (Gordon, 1991). Likewise, dantrolene is not discussed because of its important inhibition of Ca^{2+} influx, reducing its usefulness as a RyR inhibitor (Sanz et al., 1990; Satoh et al., 1994; Nasu et al., 1996). Although they have been reported as RyR agonists, 4-chloro-methyl-phenol and 4-chloro-3-ethylphenol are not considered because of their too-low potency (Larini et al., 1995; Yusufi et al., 2002). The $InsP_3R$ inhibitors flunarizine (difluorinated derivative of cinnarizine) and decavanadate are not reviewed either, the former because of its dominant calmodulin inhibitory effect and the latter because of its rapid decomposition in solution into vanadate species (Fohr et al., 1989; Strupish et al., 1991). Finally, the use of neutralizing rabbit polyclonal anti-RyR (Boittin et al., 1999, 2000) and anti-RyR3 (Mironneau et al., 2002) antibodies has been reported but is not reviewed here since all published studies so far originate from only one laboratory.

A. Ca^{2+} Pump (Sarco/Endoplasmic Reticulum Ca^{2+}-ATPase)

1. Thapsigargin.

a. Source and Chemical Structure. Thapsigargin is a sesquiterpene lactone isolated from the root and fruit of the Mediterranean umbelliferous (*Apiaceae*) plants *Thapsia garganica* (Linnaeus) and *Thapsia gymnesica* (Rosselo and Pujadas) (Fig. 6) (Rasmussen et al., 1981; Christensen et al., 1997). It is part of a group of naturally occurring hexaoxygenated 6,12-guaianolides found in several plant species of the genus *Thapsia* and often designated "thapsigargins" as a group (Christensen et al., 1997; Treiman et al., 1998). It is highly lipophilic and thus cell-permeant (Treiman et al., 1998).

b. Mechanism of Action. Following the seminal observation by Thastrup et al. (1990) that thapsigargin selectively inhibits SERCA in a variety of cells, it was subsequently shown that it does so by locking SERCA in its Ca^{2+}-free E_2 conformations (see *Section I.G.1.*) by forming a dead-end complex with them (Fig. 7) (Inesi and Sagara, 1992; Sagara et al., 1992). Indeed, although this reaction is in principle reversible, its negligible dissociation constant [K_D = 2.2 pM or less (Davidson and Varhol, 1995)] makes it irreversible in practice, hence the name "dead-end complex". Accordingly, high concentrations of free Ca^{2+} attenuate SERCA inhibition by thapsigargin (Kijima et al., 1991). Interestingly, in this respect, the fluorescent analog 8-*O*-(4-aminocinnamoyl)-8-*O*-debutanoylthapsigargin is almost as potent as thapsigargin in inhibiting $^{45}Ca^{2+}$ uptake by rabbit SERCA1-expressing skeletal muscle microsomes (IC_{50} = 168 versus 123 nM, respectively), and its fluorescence is sensitive to the E_1-E_2 conformational equilibrium, thus making it a conformational probe (Procida et al., 1998). This mechanism of action is also consistent with the localization of the thapsigargin-specific binding site on the SERCA within the S3 stalk segment, as shown in chimerical studies (Ma et al., 1999). The CPA-specific

binding site was also shown to significantly overlap it, making CPA a competitor of thapsigargin at the molecular level. It is proposed that the perturbation induced by binding of these inhibitors interferes with the long-range functional linkage between ATP utilization in the SERCA cytoplasmic region and Ca^{2+} binding in the membrane-bound region (uncoupling) (Ma et al., 1999).

SERCA1a, SERCA2a, SERCA2b, and SERCA3 expressed in COS cells are equally sensitive to thapsigargin (but see *Section II.A.1.c.*) (Lytton et al., 1991). Also, studies of chimeras made from SERCA1 and Na^+/K^+-ATPase have revealed that thapsigargin binding involves the third transmembrane segment (S3-M3) (Norregaard et al., 1993, 1994; Andersen and Vilsen, 1995; Zhong and Inesi, 1998), whereas studies of interaction between SERCA1 and a fluorescent thapsigargin analog have shown that thapsigargin is at less than 19 Å from tryptophan residue 272 (Hua et al., 1995). Consistent with these findings, the S3-M3 region is highly conserved among SERCA isoforms (Norregaard et al., 1994).

Thapsigargin is 4 to 10,000 times more potent than the two other selective SERCA inhibitors, CPA and 2,5-di-(*tert*-butyl)-1,4-benzohydroquinone (tBuBHQ) (see *Sections II.A.2.* and *II.A.3.*) (Mason et al., 1991; Foskett and Wong, 1992; Luo et al., 1993; Inesi and Sagara, 1994), potentially explaining the relatively more widespread use of thapsigargin. However, its potency is quite variable across experimental systems (IC_{50} values ranging from subnanomolar to micromolar) (Treiman et al., 1998). Since the interaction between SERCA1 and thapsigargin is stoichiometric (Lytton et al., 1991; Sagara et al., 1992), it would follow that, if this relationship is also applied to the other SERCA isoforms, the apparent inhibitory potency of thapsigargin would be influenced by the number of SERCA molecules per cell or per microgram of microsomal preparation, as shown in various preparations (Papp et al., 1991; Caspersen and Treiman, 1995; Hussain et al., 1995). Likewise, as for other highly lipophilic drugs, thapsigargin interaction with SERCA should be highly dependent on the ratio (lipid + SERCA protein)/thapsigargin (Heirwegh et al., 1988). In keeping with this, indeed, inhibition of purified SERCA by thapsigargin occurs more effectively when the membrane concentration is reduced (Sagara and Inesi, 1991).

Although its metabolism has not been studied thoroughly, thapsigargin is known to be quickly degraded by carboxyesterases at C(2) and C(8) in hepatocytes (Nielsen et al., 1994) (see Fig. 6 for numeration).

In terms of structure-activity relationships (SAR), very small changes in structure have very profound effects on the analogs' potency in inhibiting purified SERCA ATPase activity, suggesting that that the thapsigargin binding site is very restrictive (Christensen et al., 1992, 1997; Andersen et al., 1994; Nielsen et al., 1995). In particular, epimerization of C(8) decreases potency by more than 3000 times, and epimerization at C(3) reduces it by 40 times. Likewise, the acyl residue at O(10) is critical, as hydrolysis of this ester decreases potency by 40 times. The carboxylic acid residue at O(3) (angelic acid in thapsigargin) appears to have some importance, since its replacement with the larger octanoic acid reduces potency by 11 times. In contrast, the hydroxyl groups at C(7) and C(11), as well as the lactone carbonyl at C(12) and the octanoic acid residue at O(2), have marginal roles in potency as their modifications are well tolerated.

c. Selectivity. Although it has been proposed that thapsigargin inhibitory potency may vary to a small extent among the currently identified SERCA isoforms (see *Section I.G.*) (Papp et al., 1993; Cavallini et al., 1995; Engelender et al., 1995; Waldron et al., 1995), it is not sufficient to allow for a truly discriminating concentration-dependent pattern (Treiman et al., 1998).

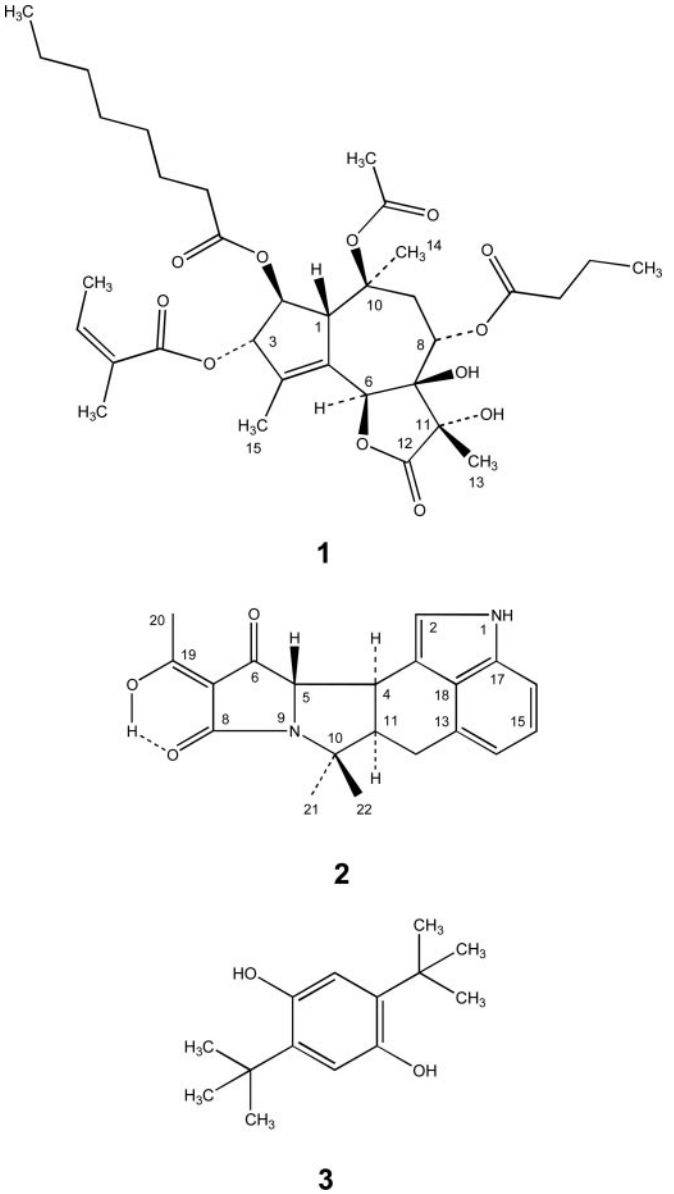

FIG. 6. Molecular structure of thapsigargin (1), CPA (2), and tBuBHQ (3).

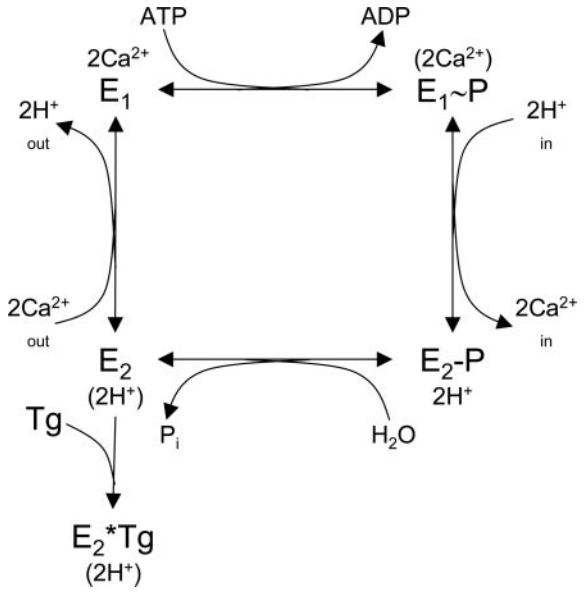

FIG. 7. Model of SERCA inhibition by thapsigargin. See text for details.

Interestingly, there is circumstantial evidence suggesting the existence of thapsigargin-insensitive Ca^{2+}-ATPase pumps in nonmitochondrial Ca^{2+} stores of various cultured cell lines (Bian et al., 1991; Tanaka and Tashjian, 1993). Furthermore, functional evidence indicates that long-term exposure of cell cultures to thapsigargin promotes the selection of cells with dominance of this thapsigargin-insensitive type of pump (Hussain et al., 1995; Waldron et al., 1995). In isolated vascular cells from the rat aorta, bradykinin releases Ca^{2+} from a thapsigargin-insensitive store (Neusser et al., 1999).

Recent evidence suggests that the thapsigargin-insensitive pump may be the mammalian homolog of Pmr1, a P-type Ca^{2+}-ATPase pump of the Golgi apparatus of *C. elegans* (Sorin et al., 1997). Transfection of Pmr1 in COS cells (which possess a functional ER) showed that 1) it localizes itself to the Golgi apparatus; 2) it transports Ca^{2+} and Mg^{2+} with high affinity; 3) its mediation of Ca^{2+} uptake is insensitive to thapsigargin, relatively insensitive to tBuBHQ (IC_{50} > 1 mM versus 1 μM for ER-mediated Ca^{2+} uptake), and about 400 times less sensitive to CPA than the ER (IC_{50} value ~300 μM; steeper concentration-response curve than for ER-mediated Ca^{2+} uptake); 4) its Ca^{2+} store is less leaky and less sensitive to $InsP_3$ and ATP than the ER; and 5) it allows generation of Ca^{2+} signals such as caffeine-sensitive regenerative oscillations and ilimaquinone-sensitive baseline spiking (Missiaen et al., 2001b; Wuytack et al., 2002). In A7r5 and 16HBE14o- cell lines, which possess an endogenous nonmitochondrial thapsigargin-sensitive Ca^{2+} store (~10% of total cell Ca^{2+} uptake) and express a mammalian homolog of Pmr1, Ca^{2+} accumulation in this store displays the same sensitivity pattern to the SERCA inhibitors as Pmr1-transfected COS cells (as well as a similar IC_{50} value), and although the store could be released by $InsP_3$ [or an $InsP_3$-generating receptor agonist such as arginine vasopressi] in A7r5 cells (EC_{50} ~5 μM versus ~1 μM for ER-mediated Ca^{2+} release), it is $InsP_3$-insensitive in 16HBE14o- cells (Wuytack et al., 2002).

Despite the fact that thapsigargin does not affect the various plasma membrane ATPases (PMCA, Na^+/K^+-ATPase) or mitochondrial membrane pumps (Thastrup et al., 1989, 1990; Lytton et al., 1991), it can inhibit capacitative Ca^{2+} entry (see *Section I.G.1.*) (Mason et al., 1991; Geiszt et al., 1995). Unlike CPA, but similarly to tBuBHQ (see *Section II.A.3.c.*), thapsigargin can inhibit Ca_L when used in the micromolar range (Rossier et al., 1993; Nelson et al., 1994; Buryi et al., 1995). However, in many preparations, maximal SERCA inhibition is obtained with lower concentrations of the compound, thus providing a selectivity window. In contrast, concentrations of CPA and tBuBHQ that inhibit SERCA also partially inhibit capacitative Ca^{2+} entry (see sections on these agents below and *Section I.C.*) (Mason et al., 1991).

Missiaen et al. (1992a) have shown that thapsigargin (2 μM), in contrast with CPA and tBuBHQ (50 μM) (see *Sections II.A.2.c.* and *II.A.3.c.*), does not alter the SR Ca^{2+} permeability in A7r5 cells (Missiaen et al., 1992a). Interestingly, Darby et al. (1996) observed that thapsigargin (3 μM) slightly decreases the slow phase of $^{45}Ca^{2+}$ efflux from smooth muscle membrane vesicles in an oxalate-dependent manner, as does CPA (30 μM). The authors proposed that this could be due to the specific obstruction of a putative transmembrane channel within the SERCA (de Meis and Inesi, 1992).

d. Use in Smooth Muscle Preparations. Thapsigargin has been successfully used to uncover the influence of SERCA activity in a variety of phasic and tonic vascular and nonvascular smooth muscle preparations. Thus, thapsigargin can be used effectively to deplete the SR stores of Ca^{2+}. The effective concentration range is between 0.1 to 10 μM, and the inhibition of SERCA isoforms occurs indiscriminately. Due to the highly lipophilic nature of the compound, the inhibition is long-lasting and difficult to overcome in intact preparations (Table 1). There is intriguing evidence of a thapsigargin-insensitive Ca^{2+} storage site, and it is therefore advisable to confirm findings with structurally unrelated SERCA inhibitors. Thapsigargin can inhibit capacitative Ca^{2+} entry, but at the concentrations used to inhibit SERCA, it does not affect other plasmalemmal and mitochondrial transporters. Thapsigargin can release relaxing factors from intact tissues with endothelium or epithelium by its interaction with SERCA in these cells. Rise in endothelial or epithelial Ca^{2+} has a faster time course (<1 min) than in smooth muscle (15–20 min). In some tissues, thapsigargin can release both endothelium-derived relaxing and contracting factors. Thapsigargin may have multiple sites of action in the endothelium of intact arteries. For example, in rat aorta, thapsigargin causes an endothelium-dependent NO-mediated vaso-

TABLE 1
Effective concentrations of thapsigargin in smooth muscle

Tissue	Animal Species	Experimental Details (Preparation; Measurement Method; Measured Response)	Effective Concentrations of Thapsigargin	Reference
Airways	Cattle	Isolated smooth muscle cells; fura-2 cellular loading, fluorometry; $[Ca^{2+}]_{cyt}$	0.3 μM	Ethier and Madison, 2002
Airways	Human	Isolated smooth muscle cells; indo-1 cellular loading, epifluorescence microscopy; $[Ca^{2+}]_{cyt}$ imaging	1 μM	Berger et al., 2001
Airways	Human	Isolated smooth muscle cells; fura-2 cellular loading, fluorometry; $[Ca^{2+}]_{cyt}$	0.3 μM	Ethier and Madison, 2002
Airways	Mouse	Lung slices; Oregon Green cellular loading, confocal fluorescence microscopy; $[Ca^{2+}]_{cyt}$ imaging	10 μM	Bergner and Sanderson, 2002
Aorta	Human	Isolated smooth muscle cells; whole-cell patch-clamping, fura-2 cellular loading, fluorometry; I_K, $[Ca^{2+}]_{cyt}$	2 μM	Karkanis et al., 2001
Aorta	Pig	Microsomes, F3 microsomal membranes fraction; inorganic phosphate-release assay; Ca^{2+}-ATPase activity	3 μM	Luo et al., 2000
Aorta	Rabbit	Microsomes; $^{45}Ca^{2+}$ loading; Ca^{2+} fluxes	10 μM	Adachi et al., 2001
Aorta	Rabbit	Isolated rings; isometric dynamometry; contractile activity	3 μM	Luo et al., 2000
Aorta	Rat	Saponin-permeabilized cultured A7r5 cell line; $^{45}Ca^{2+}$ cellular loading; Ca^{2+} fluxes	2 μM	Missiaen et al., 2001a
Aorta	Rat	Isolated cultured smooth muscle cells permeabilized by electroporation; fura-2 cellular loading, fluorometry; $[Ca^{2+}]_{cyt}$	500 nM	Walter et al., 2000
Aorta	Rat	Isolated smooth muscle cells; fura-2 cellular loading, epifluoresence microscopy; $[Ca^{2+}]_{cyt}$ imaging	500 nM	Vallot et al., 2001
Aorta	Rat	Isolated smooth muscle cells; fura-2 cellular loading, fluorometry; $[Ca^{2+}]_{cyt}$	1 μM	Neusser et al., 1999
Aorta	Rat	Isolated smooth muscle cells; fura-2 cellular loading, fluorometry; $[Ca^{2+}]_{cyt}$	2 μM	Neylon et al., 1992
Aorta	Rat	Isolated endothelium-denuded rings; isometric dynamometry; contractile activity	30 μM	Shen et al., 2001
Aorta	Rat	Isolated endothelium-denuded rings; isometric dynamometry; contractile activity	1 μM	Fusi et al., 1998
Aorta	Rat	Isolated endothelium-denuded rings; isometric dynamometry; contractile activity	1 μM	Low et al., 1993
Aorta	Rat	Isolated rings; isometric dynamometry; contractile activity	1-100 nM	Huang et al., 2000
Basilar artery	Rabbit	Isolated smooth muscle cells and endothelium-denuded strips; fura-2 cellular loading, fluorometry, isometric dynamometry; $[Ca^{2+}]_{cyt}$, contractile activity	1-2 μM	Szado et al., 2001
Carotid artery	Rat	Isolated endothelium-denuded strips; isometric dynamometry; contractile activity	100 nM	Nomura and Asano, 2000
Cerebellar artery	Rat	Isolated smooth muscle cells; whole-cell patch-clamping; $I_{K(Ca)}$	100 nM	Cheranov and Jaggar, 2004
Cerebellar resistance arteries	Rat	Isolated, cannulated and pressurized segments; fluo-3 cellular loading, confocal fluorescence microscopy, diameter monitoring by video microscopy; $[Ca^{2+}]_{cyt}$ imaging, contractile activity	100 nM	Jaggar, 2001
Cerebral arterioles	Rabbit	Isolated smooth muscle cells; fura-PE3 cellular loading, fluorometry; $[Ca^{2+}]_{cyt}$	1 μM	Guibert et al., 2002
Cerebral arterioles	Rat	Isolated smooth muscle cells; indo-1 cellular loading, confocal fluorescence microscopy; $[Ca^{2+}]_{cyt}$ imaging	1 μM (no effect)	Saino et al., 2002
Cerebral artery	Rat	Isolated smooth muscle cells; whole-cell patch-clamping; $I_{K(Ca)}$	100 nM	Cheranov and Jaggar, 2004
Cerebral artery	Rat	Isolated, cannulated and pressurized segments; fluo-3 cellular loading, confocal fluorescence microscopy, diameter monitoring by video microscopy; $[Ca^{2+}]_{cyt}$ imaging, contractile activity	100 nM	Jaggar, 2001
Colon	Guinea pig	Isolated smooth muscle cells; whole-cell patch-clamping, fluo-3 or fura-2 cellular loading, fluorometry; I_{Ca}, $[Ca^{2+}]_{cyt}$	500 nM	Bradley et al., 2002
Colon	Guinea pig	Isolated smooth muscle cells; whole-cell patch-clamping, fluo-3 cellular loading, epifluorescence microscopy; membrane currents, $[Ca^{2+}]_{cyt}$	500 nM	Flynn et al., 2001
Colon	Guinea pig	Isolated smooth muscle cells; whole-cell patch-clamping, fura-2 cellular loading, fluorometry; membrane currents, $[Ca^{2+}]_{cyt}$	100 nM	McCarron and Muir, 1999
Colon	Guinea pig	Isolated smooth muscle cells; whole-cell patch-clamping, fluo-3 cellular loading, fluorometry or wide-field fluorescence digital imaging; I_{Ca}, $[Ca^{2+}]_{cyt}$, $[Ca^{2+}]_{cyt}$ imaging	500 nM	Bradley et al., 2003
Coronary artery	Pig	F3 microsomal membranes fraction, isolated cultured smooth muscle cells and endothelium-denuded rings; fluo-3 loading (cells), $^{45}Ca^{2+}$ loading (microsomal membranes), epifluorescence microscopy (cells), isometric dynamometry (rings); $[Ca^{2+}]_{cyt,}$ (cells), Ca^{2+} fluxes (microsomal membranes), contractile activity (rings)	1 μM	Walia et al., 2003
Cremaster muscle arterioles	Hamster	Isolated, cannulated and pressurized segments isolated from 1st- and 2nd-order branches; fura-2 cellular loading, fluorometry, diameter monitoring by video microscopy; $[Ca^{2+}]_{cyt}$, conducted vasomotor responses	100 nM	Yashiro and Duling, 2003

TABLE 1
Continued

Tissue	Animal Species	Experimental Details (Preparation; Measurement Method; Measured Response)	Effective Concentrations of Thapsigargin	Reference
Cremaster muscle arterioles	Rat	Isolated, cannulated and pressurized endothelium-denuded segments; fura-2 cellular loading, fluorometry, diameter monitoring by video microscopy; $[Ca^{2+}]_{cyt}$, contractile activity	1 μM	Potocnik and Hill, 2001
Esophagus (lower sphincter, circular layer)	Cat	Isolated saponin-permeabilized smooth muscle cells; cell length monitoring by phase-contrast microscopy; contractile activity	3 μM	Sohn et al., 1993
Femoral artery	Rat	Isolated endothelium-denuded strips; isometric dynamometry; contractile activity	300 nM	Asano and Nomura, 2001
		Isolated endothelium-denuded strips; isometric dynamometry; contractile activity	100 nM	Nomura and Asano, 2000
Gall bladder	Guinea pig	Isolated tissue and smooth muscle cells; whole-cell patch-clamping, fluo-4 cellular loading, confocal fluorescence microscopy, isometric dynamometry; $[Ca^{2+}]_{cyt}$ imaging, contractile activity	1 μM	Pozo et al., 2002
Lung	Rat	Physiological salt solution-perfused lungs; perfusion pressure; vascular bed resistance	10 nM	Morio and McMurtry, 2002
Mesenteric artery	Dog	Microsomes; $^{45}Ca^{2+}$ loading; Ca^{2+} fluxes	3 μM	Darby et al., 1996
Mesenteric resistance arteries	Rat	Isolated endothelium-denuded strips; fura-2 cellular loading, fluorometry, isometric dynamometry; $[Ca^{2+}]_{cyt}$, contractile activity	1 μM	Lagaud et al., 1999
Pulmonary artery	Cattle	Microsomes; extramicrosomal fluo-3 and fluorometry or $^{45}Ca^{2+}$ loading; Ca^{2+} fluxes	10 nM	Stout et al., 2002
Pulmonary artery	Dog	Isolated smooth muscle cells; fura-2 cellular loading, fluorometry; $[Ca^{2+}]_{cyt}$	1 μM	Doi et al., 2000
Pulmonary artery	Rat	Isolated intact or β-escin-permeabilized strips; isometric dynamometry; contractile activity	1 μM	Gonzalez De La Fuente et al., 1995
Pulmonary artery	Rat	Isolated endothelium-denuded strips; isometric dynamometry; contractile activity	100 nM	Nomura and Asano, 2000
Renal artery	Pig	Isolated smooth muscle strips; fura-2 cellular loading, fluorometry, isometric dynamometry; $[Ca^{2+}]_{cyt}$, contractile activity	1 μM	Ihara et al., 1999
Small intestine	Mouse	Isolated segments; microelectrode; slow wave frequency	1 μM	Malysz et al., 2001
Stomach (antrum)	Cattle	Microsomes; extramicrosomal fluo-3 and fluorometry or $^{45}Ca^{2+}$ loading; Ca^{2+} fluxes	10 nM	Stout et al., 2002
Stomach (antrum)	Guinea pig	Isolated smooth muscle cells; whole-cell patch-clamping; I_{BK}	1 μM	Duridanova et al., 1997
Tail artery	Rat	Isolated cultured endothelium- denuded rings; fura-2 cellular loading, fluorometry, isometric dynamometry; $[Ca^{2+}]_{cyt}$, contractile activity	10 μM	Dreja et al., 2001
Testicular arterioles	Rat	Isolated smooth muscle cells; indo-1 cellular loading, confocal fluorescence microscopy; $[Ca^{2+}]_{cyt}$ imaging	1 μM (no effect)	Saino et al., 2002
Trachea	Guinea pig	Isolated smooth muscle cells and strips; fura-2 cellular loading, fluorometry, isometric dynamometry; $[Ca^{2+}]_{cyt}$, contractile activity	10 μM	Ito et al., 2002
Trachea	Guinea pig	Isolated smooth muscle strips; fura-2 cellular loading, fluorometry, isometric dynamometry; $[Ca^{2+}]_{cyt}$, contractile activity	1 μM	Ito et al., 2000
Trachea	Guinea pig	Isolated one-cartilage epithelium-denuded rings; isometric dynamometry; contractile activity	1 μM	Takahashi et al., 2000
Trachea	Guinea pig	Isolated smooth muscle strips; isometric dynamometry; contractile activity	1 μM	Yoshida et al., 2002
Urinary bladder	Guinea pig	Isolated smooth muscle cells; whole-cell patch-clamping, fura-2 (for $[Ca^{2+}]_{cyt}$) or mag-fura-2 (for $[Ca^{2+}]_{SR}$) cellular loading, fluorometry; STOCs, $[Ca^{2+}]_{cyt}$, $[Ca^{2+}]_{SR}$	100 nM-10 μM	Gomez-Viquez et al., 2003
Urinary bladder	Guinea pig	Isolated smooth muscle cells; whole-cell amphotericin B-perforated-patch-clamping, fluo-3 cellular loading, confocal fluorescence microscopy; I_{BK}, $[Ca^{2+}]_{cyt}$ imaging	100 nM	Herrera et al., 2001
Urinary bladder	Guinea pig	Isolated smooth muscle cells; fura-2 cellular loading, fluorometry; $[Ca^{2+}]_{cyt}$	100 nM	Rueda et al., 2002b
Uterus	Rat	Isolated smooth muscle cells; fura-2 (for $[Ca^{2+}]_{cyt}$) and mag-fluo-4 (for $[Ca^{2+}]_{SR}$) cellular loading, fluorometry; $[Ca^{2+}]_{cyt}$, $[Ca^{2+}]_{SR}$	0.2 μM	Shmigol et al., 2001
Vas deferens	Rat	Microsomes; $^{45}Ca^{2+}$ loading; Ca^{2+} fluxes	3 μM	Darby et al., 1996

dilation (1–100 nM), whereas at low concentrations (3 nM), it diminishes endothelium-dependent vasodilation to A23187 and Ach (Huang et al., 2000).

2. Cyclopiazonic Acid.

a. Source and Chemical Structure. CPA is a mycotoxin produced by some strains of the molds *Penicillium cyclopium* and *Aspergillus flavus* (Holzapfel, 1968). It is an indole tetramic acid metabolite derived from the amino acid tryptophan (Fig. 6) (Holzapfel, 1968). CPA is a natural contaminant of some cereal products and mold-fermented cheese or meat and is considered a toxic hazard to humans and animals. The usual clinical signs of its toxicity are related to skeletal muscle dysfunction, consistent with its accumulation in this tissue (Norred et al., 1985).

b. Mechanism of Action. CPA was originally shown to be a potent inhibitor of both SERCA activity and ATP-dependent Ca^{2+} sequestration in SR vesicles isolated from mammalian fast skeletal muscle (Goeger et al., 1988). This finding is consistent with its inhibition of oxalate-stimulated $^{45}Ca^{2+}$ uptake in mammalian visceral and vascular smooth muscle microsomal vesicles (Darby et al., 1996)—oxalate-stimulated uptake is an exclusive property of the SR-derived components of smooth muscle membrane fractions (Grover, 1985; Kwan, 1985). Maximal inhibition is achieved with 10 to 30 μM CPA (Darby et al., 1996), which corresponds with the concentrations required to prevent SR Ca^{2+} release and the accompanying contractile activity in different intact and permeabilized smooth muscle preparations. Furthermore, CPA inhibition of vesicular $^{45}Ca^{2+}$ uptake has a rapid onset and is rapidly and completely reversible both in intact and permeabilized smooth muscle preparations (Darby et al., 1996).

CPA mechanism of action was recently elucidated using mammalian fast skeletal muscle SR vesicles (Plenge-Tellechea et al., 1997). It decreases the SERCA affinity (K_D) for ATP under nonturnover conditions by approximately one order of magnitude. The net effect results in inhibition of enzymatic hydrolytic activity and hence, its Ca^{2+} pumping ability. Although the number of CPA binding sites on the ATPase is equivalent to that of the high-affinity ATP binding sites, they are distinct. Earlier studies (Seidler et al., 1989; Karon et al., 1994) proposed that CPA could compete for ATP-binding sites, but later findings reported that the decrease in the K_D for ATP is independent of CPA (Plenge-Tellechea et al., 1997). Furthermore, CPA does not modify the 2′(or 3′)-*O*-(trinitrophenyl)adenosine-5′-triphosphate (TNP-ATP) fluorescence signal, further supporting the absence of direct competition (Plenge-Tellechea et al., 1997). TNP-ATP fluorescence increases upon its binding to the SERCA in the absence of Ca^{2+} and competition by ATP for the binding site occupied by TNP-ATP decreases the fluorescence signal because of TNP-ATP displacement.

Early confusion was caused by the observations that CPA blockade of the SERCA turnover could be overcome if the ATP concentration is sufficiently increased. However, recent evidence suggests that CPA does not bind at the catalytic site, a conclusion supported by the observation that autophosphorylation of the Ca^{2+}-bound enzyme by ATP is not inhibited by CPA (Plenge-Tellechea et al., 1997). Nonetheless, CPA effect on the enzyme is likely not restricted to the ATP-binding process since it causes additional inhibition of the ATPase at concentrations above the stoichiometric levels (Plenge-Tellechea et al., 1997). With an ATP concentration of 1 mM, SERCA is completely inhibited at a CPA/SERCA molar ratio of approximately 10 (Soler et al., 1998). Furthermore, enzyme activity is observed to recover at a CPA/SERCA molar ratio of 1 when the Ca^{2+} concentration is raised, which is consistent with the competitive character of CPA and Ca^{2+} (Soler et al., 1998). These results suggest that ATP and Ca^{2+} can protect against CPA inhibition. Whether this mechanism of action documented in the SERCA1a isoform also applies to the other SERCA isoforms has not been shown.

In terms of the Ca^{2+} pumping cycle, CPA appears to stabilize the E_2 SERCA conformation (Seidler et al., 1989; Karon et al., 1994; Plenge-Tellechea et al., 1997; Soler et al., 1998). The onset of inhibition during SERCA enzymatic turnover is slow, implying that numerous cycles are required (Plenge-Tellechea et al., 1997). Under turnover conditions, the K_D for CPA is 7 nM (Soler et al., 1998). This suggests the existence of a slow isomerization step between binding of CPA to the SERCA E_2 conformations and the formation of E_2 conformations with lower ATP-binding affinity. This is consistent with the localization of the CPA-specific binding site on the SERCA within the S3 stalk segment, as shown in chimeric studies (Ma et al., 1999). The thapsigargin-specific binding site was also shown to significantly overlap it, thus making thapsigargin a competitor of CPA at the molecular level. It is proposed that perturbation induced by binding of these inhibitors interferes with the long-range functional linkage between ATP utilization in the SERCA cytoplasmic region and Ca^{2+} binding in the membrane-bound region (uncoupling) (Ma et al., 1999).

A model for the inhibition of the SERCA by CPA in the substoichiometric/stoichiometric range has been developed (Fig. 8) (Plenge-Tellechea et al., 1997). In the presence of a stoichiometric CPA concentration, all enzyme molecules would eventually bind CPA, such that hydrolytic activity could only be maintained by a high ATP concentration. However, the enzyme turnover displays a lower ATP affinity (K'_{ATP}) and a lower maximal velocity (V'_{max}). Consequently, at substoichiometric CPA and high ATP concentrations, the observed kinetic parameters correspond to the contribution of two different reaction cycles sustained by the CPA-free form of the enzyme (K_{ATP} and V_{max}) and its CPA-bound form (K'_{ATP} and V'_{max}).

As discussed earlier (see *Section I.G.1.*), the SERCA-inhibiting accessory protein phospholamban, which needs to be phosphorylation to be inactivated, is an excellent substrate for PKG (Raeymaekers et al., 1988), and as such, is likely involved in NO-induced SERCA activation. NO activation of guanylate cyclase would increase cGMP concentration, which would activate SR membrane-located cGMP-dependent PKG, which would then phosphorylate phospholamban (Raeymaekers et al., 1988; Twort and van Breemen, 1989; Cornwell et al., 1991; Karczewski et al., 1992; Andriantsitohaina et al., 1995). Indeed, the role of SERCA in this scheme is supported by the fact that NO donors suppress 1) CPA-induced extracellular Ca^{2+}-dependent contractile activity of the feline gastric fundus smooth muscle (Petkov and Boev, 1996) and 2) CPA-induced Cl_{Ca} activation in the mouse anococcygeus (Westerduin et al., 1992). In

addition, CPA inhibits the relaxation of phenylephrine-induced contractile activity triggered by NO donors in the endothelium-denuded rabbit aorta (Luo et al., 1993). Finally, CPA inhibits the relaxation of carbachol (Cch)-induced contractile activity triggered by an NO donor and by 8-bromo-cGMP in the canine tracheal smooth muscle (McGrogan et al., 1995).

It was proposed that phospholamban would act as an indirect competitor of CPA (Westerduin et al., 1992; Petkov and Boev, 1996), as shown in cardiac muscle for both CPA and thapsigargin (Mahaney et al., 1999). This is consistent with data in bladder from mice in which the phospholamban gene was ablated (phospholamban-knockout mice) showing that CPA amplifies the increase in $[Ca^{2+}]_{cyt}$ and the associated contractile activity induced by Cch, as it does to a more limited extent in the bladder from wild-type mice, and that this effect is virtually abolished in bladder from mice where phospholamban had been overexpressed in a smooth muscle-specific manner (Nobe et al., 2001).

c. Selectivity. There is no direct evidence indicating that SERCA1a and SERCA2a/b isoforms have different sensitivities to CPA; likewise, the three mammalian-homolog avian SERCA isoforms (SERCA1, SERCA2a, and SERCA2b), which are encoded by three distinct cDNAs, have identical sensitivities to CPA (Campbell et al., 1991). However, it should be kept in mind that CPA-insensitive/MgATP-independent SR Ca^{2+} uptake may exist in parallel with a CPA-sensitive/MgATP-dependent mechanism in some vascular (Stout, 1991; Low et al., 1992) and airway (Bourreau et al., 1993) smooth muscles. A direct but regulated communication between the extracellular space and the SR lumen has been postulated but seems unlikely based on existing structural and biophysical data.

CPA has no effect on cation ATPases other than the SERCA. It does not interact with brain and kidney Na^+/K^+-ATPase pumps, the gastric H^+/K^+-ATPase pump, the mitochondrial F_1 ATPase, or the erythrocyte and skeletal muscle PMCA (Seidler et al., 1989). However, CPA can inhibit Ca^{2+} uptake by the thapsigargin-insensitive Ca^{2+} store (IC_{50} value ~300 μM in A7r5 cells; steeper concentration-response curve than for ER-mediated Ca^{2+} uptake with threshold at ~100 μM), likely mediated by a Pmr1-like P-type Ca^{2+}-ATPase pump located in the Golgi apparatus (see *Section II.A.1.c.*) (Wuytack et al., 2003).

In smooth muscle, CPA has no effect on Ca_L- (in contrast with the inhibitory effect of thapsigargin and tBuBHQ) (see *Sections II.A.1.c.* and *II.A.3.c.*) and delayed rectifier K^+ channel-mediated currents in visceral smooth muscle (Suzuki et al., 1992). However, a supramaximal concentration of CPA for inhibition of the SERCA (300 μM) appears to inhibit Ca^{2+} influx through Ca_L in the myometrium (Imai et al., 1984). Whether this is due to a direct action on the channel is not known. CPA has no direct effect on the single-channel conductance or the open probability (P_o) of BK from visceral smooth muscle (Suzuki et al., 1992). In addition, CPA has no effect on plasmalemmal ATP-dependent Ca^{2+} extrusion; indeed, it does not alter saponin-sensitive microsomal Ca^{2+} uptake, believed to reflect the plasmalemmal-derived component of smooth muscle membrane fractions (Grover, 1985). Finally, CPA has no effect on the sensitivity of the contractile apparatus to Ca^{2+} in β-escin permeabilized visceral (Uyama et al., 1992) and vascular (Gonzalez De La Fuente et al., 1995) smooth muscle preparations. In the latter permeabilized preparations, CPA inhibits NE- and/or caffeine-induced contractile activity in absence of Ca^{2+} only if it is

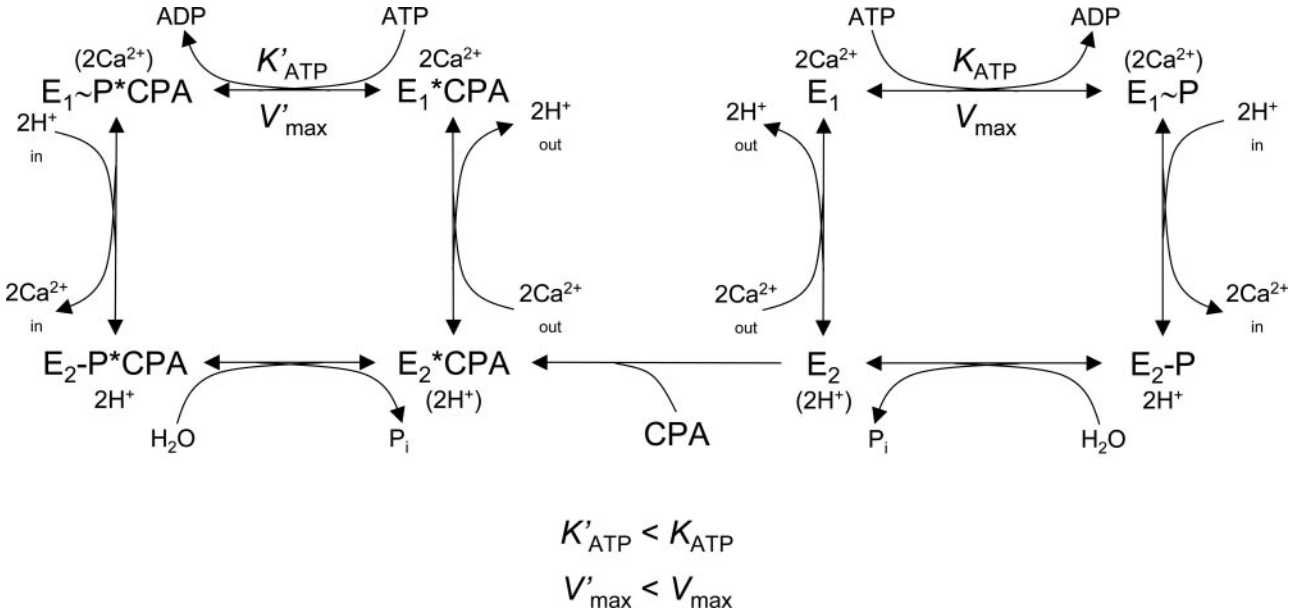

FIG. 8. Model of SERCA inhibition by CPA. See text for details.

TABLE 2
Effective concentrations of CPA in smooth muscle

Tissue	Animal Species	Experimental Details (Preparation; Measurement Method; Measured Response)	Effective Concentrations of CPA	Reference
			μM	
Airways	Cattle	Isolated smooth muscle cells; fura-2 cellular loading, fluorometry; $[Ca^{2+}]_{cyt}$	5	Bazan-Perkins et al., 2001
Anococcygeus	Mouse	Isolated smooth muscle cells; whole-cell patch-clamping; $I_{Cl(Ca)}$, I_{DOC}, I_{CRAC}	10	Wayman et al., 1998
Anococcygeus	Mouse	Isolated smooth muscle cells; whole-cell patch-clamping; $I_{Cl(Ca)}$, I_{DOC}	10	Wayman et al., 1997
Aorta	Pig	Microsomes, F3 microsomal membranes fraction; inorganic phosphate-release assay; Ca^{2+}-ATPase activity	30	Luo et al., 2000
Aorta	Rabbit	Isolated smooth muscle cells and endothelium-denuded rings; cells: $^{45}Ca^{2+}$ cellular loading, rings: fura-2 cellular loading, fluorometry, isometric dynamometry; cells: Ca^{2+} fluxes, rings: $[Ca^{2+}]_{cyt}$, contractile activity	20	Adachi et al., 2001
Aorta	Rabbit	Isolated rings; isometric dynamometry; contractile activity	30	Luo et al., 2000
Aorta	Rat	Isolated endothelium-denuded rings; isometric dynamometry; contractile activity	30	Shen et al., 2001
Aorta	Rat	Isolated endothelium-denuded rings; isometric dynamometry; contractile activity	10	Fusi et al., 1998
Aorta	Rat	Isolated endothelium-denuded rings; isometric dynamometry; contractile activity	30	Low et al., 1993
Carotid artery	Rat	Isolated endothelium-denuded strips; isometric dynamometry; contractile activity	10	Nomura and Asano, 2000
Cerebral arterioles	Rabbit	Isolated smooth muscle cells; fura-PE3 cellular loading, fluorometry; $[Ca^{2+}]_{cyt}$	10	Guibert et al., 2002
Cerebral artery	Dog	Isolated smooth muscle strips; isometric dynamometry; contractile activity	10	Asano et al., 1998
Colon	Mouse	Isolated smooth muscle cells; whole-cell amphotericin B-perforated patch-clamping, fluo-3 cellular loading, confocal fluorescence microscopy; STOCs, $[Ca^{2+}]_{cyt}$ imaging	10	Bayguinov et al., 2000
	Guinea pig	Isolated smooth muscle cells; whole-cell patch-clamping, fluo-3 or fura-2 cellular loading, fluorometry; I_{Ca}, $[Ca^{2+}]_{cyt}$	10	Bradley et al., 2002
	Guinea pig	Isolated smooth muscle cells; fluo-3 cellular loading, epifluorescence microscopy; $[Ca^{2+}]_{cyt}$	10	Flynn et al., 2001
Coronary artery	Pig	F3 microsomal membranes fraction, isolated cultured smooth muscle cells and endothelium-denuded rings; fluo-3 loading (cells), $^{45}Ca^{2+}$ loading (microsomal membranes), epifluorescence microscopy (cells), isometric dynamometry (rings); $[Ca^{2+}]_{cyt,}$ (cells), Ca^{2+} fluxes (microsomal membranes), contractile activity (rings)	10	Walia et al., 2003
Coronary artery	Rabbit	Isolated smooth muscle cells; fura-2 cellular loading, fluorometry; $[Ca^{2+}]_{cyt}$	10	Heaps et al., 2001
Coronary artery	Rabbit	Isolated smooth muscle cells; fura-2 cellular loading, fluorometry; $[Ca^{2+}]_{cyt}$	10	Heaps et al., 2000
Coronary artery	Rabbit	Isolated smooth muscle cells; fura-2 cellular loading, fluorometry; $[Ca^{2+}]_{cyt}$	10	Kang et al., 2002
Esophagus	Human	Isolated smooth muscle cells and strips; fura-2 cellular loading, fluorometry, isometric dynamometry; $[Ca^{2+}]_{cyt}$, contractile activity	10	Sims et al., 1997
Femoral artery	Rabbit	Isolated endothelium-denuded rings; isometric dynamometry; contractile activity	10	Jezior et al., 2001
Femoral artery	Rat	Isolated endothelium-denuded strips; fura-PE3 cellular loading, fluorometry, isometric dynamometry; $[Ca^{2+}]_{cyt}$, contractile activity	10	Asano and Nomura, 2001
Femoral artery	Rat	Isolated endothelium-denuded strips; isometric dynamometry; contractile activity	10	Nomura and Asano, 2000
Femoral artery	Rat	Isolated endothelium-denuded strips; fura-PE3 cellular loading, fluorometry, isometric dynamometry; $[Ca^{2+}]_{cyt}$, contractile activity	10	Nomura et al., 1997
Ileum	Guinea pig	Isolated β-escin-permeabilized smooth muscle strips; microelectrode, fura-2 cellular loading, fluorometry, isometric dynamometry; membrane potential, $[Ca^{2+}]_{cyt}$, contractile activity	10	Uyama et al., 1993
Lung	Rat	Physiological salt solution-perfused lungs; perfusion pressure; vascular bed resistance	5	Morio and McMurtry, 2002
Mesenteric arterioles	Rat	Isolated, cannulated and pressurized segments; fura-2 cellular loading, fluorometry, diameter monitoring by video microscopy; $[Ca^{2+}]_{cyt}$, contractile activity	10	Watanabe et al., 1993
Mesenteric artery	Dog	Microsomes; $^{45}Ca^{2+}$ loading; Ca^{2+} fluxes	30	Darby et al., 1996
Mesenteric artery	Dog	Isolated endothelium-denuded rings; isometric dynamometry; contractile activity	30	Low et al., 1992
Mesenteric artery	Rat	Isolated cultured smooth muscle cells; furaptra cellular loading, fluorometry; $[Ca^{2+}]_{SR}$	10	Golovina and Blaustein, 1997

TABLE 2
Continued

Tissue	Animal Species	Experimental Details (Preparation; Measurement Method; Measured Response)	Effective Concentrations of CPA	Reference
			μM	
Mesenteric artery	Rat	Isolated endothelium-denuded strips; isometric dynamometry; contractile activity	10	Nomura and Asano, 2000
Mesenteric artery	Rat	Isolated endothelium-intact or -denuded strips; isometric dynamometry; contractile activity	3	Huang and Cheung, 1997
Portal vein	Rabbit	Isolated smooth muscle cells; whole-cell and outside-out patch-clamping; I_{SOC}	10	Albert and Large, 2003
Pulmonary artery	Dog	Isolated smooth muscle cells; fura-2 cellular loading, fluorometry; $[Ca^{2+}]_{cyt}$	10	Doi et al., 2000
Pulmonary artery	Rabbit	Isolated smooth muscle cells; fura-2 cellular loading, fluorometry; $[Ca^{2+}]_{cyt}$	10	Kang et al., 2002
Pulmonary artery	Rat	Isolated intact or β-escin-permeabilized strips; isometric dynamometry; contractile activity	10	Gonzalez De La Fuente et al., 1995
Pulmonary resistance arteries	Dog	Smooth muscle cells isolated from 3rd- and 4th-order branches; fura-2 cellular loading, fluorometry; $[Ca^{2+}]_{cyt}$	10	Janiak et al., 2001
Pulmonary resistance arteries	Rat	Isolated endothelium-denuded rings; isometric dynamometry; contractile activity	10	Dipp and Evans, 2001
Renal pelvis	Guinea pig	Isolated urothelium-denuded strips; microelectrode, isometric dynamometry; membrane potential, contractile activity	10	Lang et al., 2002
Renal resistance arteries	Dog	Smooth muscle cells isolated from 3rd- and 4th-order branches; fura-2 cellular loading, fluorometry; $[Ca^{2+}]_{cyt}$	10	Janiak et al., 2001
Skeletal muscle arterioles	Rat	Isolated, cannulated and pressurized segments; fura-2 cellular loading, fluorometry, diameter monitoring by microscopy; $[Ca^{2+}]_{cyt}$, contractile activity	10	Watanabe et al., 1993
Small intestine	Mouse	Isolated segments; microelectrode; slow wave frequency	2	Malysz et al., 2001
Stomach	Rat	Isolated smooth muscle cells; microelectrode, fura-2 cellular loading, fluorometry; I_{Ca}, $[Ca^{2+}]_{cyt}$	5	White and McGeown, 2000
Stomach (antrum)	Guinea pig	Isolated smooth muscle cells; whole-cell patch-clamping; I_{BK}	1	Duridanova et al., 1997
Stomach (antrum)	Rat	Isolated smooth muscle cells; Oregon Green BAPTA 5N cellular loading, fluorometry; $[Ca^{2+}]_{SR}$	5	White and McGeown, 2002
Stomach (antrum, circular layer)	Guinea pig	Isolated smooth muscle bundles; microelectrode, fura-2 cellular loading, fluorometry; membrane potential, $[Ca^{2+}]_{cyt}$	10	Fukuta et al., 2002
Stomach (pylorus)	Guinea pig	Isolated smooth muscle strips; microelectrode; slow wave frequency	16	Van Helden et al., 2000
Tail artery	Rat	Isolated freshly or cultured endothelium-denuded rings; isometric dynamometry; contractile activity	10	Dreja et al., 2001
Tail artery	Rat	Isolated smooth muscle cells; whole-cell patch-clamping; $I_{Ca(L)}$	10	Fusi et al., 2001
Trachea	Cattle	Isolated smooth muscle cells; fura-2 cellular loading, fluorometry; $[Ca^{2+}]_{cyt}$	5	Ethier et al., 200
Trachea	Trachea	Isolated smooth muscle cells and strips; fura-2 cellular loading, fluorometry, isometric dynamometry; $[Ca^{2+}]_{cyt}$ contractile activity	30	Tao et al., 2000
Trachea	Dog	Isolated smooth muscle cells; fura-2 cellular loading, fluorometry; $[Ca^{2+}]_{cyt}$	60	Janssen et al., 2001
Ureter	Rat and guinea pig	Isolated α-toxin- or β-escin-permeabilized strips; isometric dynamometry; contractile activity	20	Burdyga et al., 1998
Urinary bladder	Guinea pig	Isolated smooth muscle cells; fluo-2 cellular loading, fluorometry; $[Ca^{2+}]_{cyt}$	20	Wu et al., 2002
Urinary bladder	Guinea pig	Isolated smooth muscle cells; fura-2 cellular loading, fluorometry; $[Ca^{2+}]_{cyt}$	1	Rueda et al., 2002a
Urinary bladder	Guinea pig	Isolated smooth muscle cells; whole-cell patch-clamping, fluo-3 cellular loading, confocal fluorescence microscopy; I_{BK}, $[Ca^{2+}]_{cyt}$ imaging	3	Ohi et al., 2001b
Urinary bladder	Guinea pig	Isolated smooth muscle cells; indo-1 FF cellular loading, fluorometry;$[Ca^{2+}]_{cyt}$	10	Ganitkevich, 1999
Urinary bladder	Mouse	Isolated rings, phospholamban-knockout mice; fura-PE3 cellular loading, fluorometry, isometric dynamometry; $[Ca^{2+}]_{cyt}$, contractile activity	10	Nobe et al., 2001
Urinary bladder	Rabbit	Isolated urothelium-denuded strips; isometric dynamometry; contractile activity	10	Jezior et al., 2001
Uterus	Human	Isolated myometrial strips; indo-1 cellular loading, fluorometry, isometric dynamometry; $[Ca^{2+}]_{cyt}$, contractile activity	20	Kupittayanant et al., 2002
Uterus	Rat	Isolated smooth muscle cells; microelectrode, indo-1 cellular loading, fluorometry; transmembrane currents, $[Ca^{2+}]_{cyt}$	10	Shmigol et al., 1999
Vas deferens	Guinea pig	Isolated smooth muscle cells; whole-cell patch-clamping, fluo-3 cellular loading, confocal fluorescence microscopy; I_{BK}, $[Ca^{2+}]_{cyt}$ imaging	3	Ohi et al., 2001b
Vas deferens	Rat	Microsomes; $^{45}Ca^{2+}$ loading; Ca^{2+} fluxes	30	Darby et al., 1996

present during the loading of the intracellular Ca^{2+} stores. This indicates that the inhibition of contractile activity occurs via the effects of CPA on SR loading.

Missiaen et al. (1992a) proposed that CPA, at 50 μM, like tBuBHQ (see *Section II.A.3.c.*), nonselectively decreases Ca^{2+} permeability of isolated smooth muscle cells. This is based on the fact that CPA inhibits passive Ca^{2+} efflux from permeabilized A7r5 cells. The nonspecificity of this effect was suggested by the fact that it persists even after prior exposure to 2 μM of the SERCA inhibitor thapsigargin, which has no effect on passive Ca^{2+} efflux at this concentration. However, these findings have to be reconciled with the absence of effect of CPA on D-[^{14}C(U)]sorbitol efflux in skeletal muscle SR vesicles (Goeger and Riley, 1989). Indeed, this latter finding indicates that CPA does not affect SR permeability nonselectively. Interestingly, Darby et al. (1996) observed that both CPA (30 μM) and thapsigargin (3 μM) slightly decrease the slow phase of $^{45}Ca^{2+}$ efflux from smooth muscle membrane vesicles in an oxalate-dependent manner. The authors proposed that this could be due to the specific obstruction of a putative transmembrane channel within the SERCA (de Meis and Inesi, 1992).

Finally, CPA (10 μM) inhibits ecto-ATPase activity in the guinea pig urinary bladder and vas deferens to some extent (<25%) (Ziganshin et al., 1994). It also substantially potentiates neuronal ATP release induced by transmural electrical field stimulation of the vas deferens (15-fold). However, these effects did not significantly influence the ATP-induced P_{2x}-purinoceptor-mediated contractile activity of these smooth muscle preparations (Ziganshin et al., 1994).

d. Use in Smooth Muscle Preparations. CPA is a water-soluble inhibitor of all SERCA isoforms that is effective in concentrations of 10 to 30 μM (Table 2). The inhibition of Ca^{2+} uptake by the SR is rapid in onset and fully reversible. CPA inhibits the ATP hydrolytic activity of SERCA, thus reducing its pumping ability. CPA does not affect the other pumps, such as the Na^+/K^+-ATPases and PMCA, the Ca^{2+} and K^+ channels, or contractile protein activity. In intact mesenteric arteries, CPA causes an initial endothelium-dependent dilation and a subsequent endothelium-dependent maintained rhythmic vasomotion that may be the result of released hyperpolarizing factors that activate K^+ channels on the smooth muscle cells (Huang and Cheung, 1997).

3. 2,5-Di-(tert-butyl)-1,4-benzohydroquinone.

a. Source and Chemical Structure. 2,5-Di-(*tert*-butyl)-1,4-benzohydroquinone (tBuBHQ) is a synthetic phenolic compound, originally studied for its antioxidant properties (Wilson and Poley, 1960; Ershoff, 1963, 1969), characterized by a repeated bifunctionality consisting of a hydrophilic group associated with a lipophilic area (the latter making it cell-permeant) (Fig. 6). In aqueous solution at physiological pH, as a hydroquinone, it very easily undergoes superoxide dismutase-inhibitable spontaneous oxidation (auto-oxidation) to form semiquinone radicals and donate an electron to molecular oxygen, thus generating the membrane-impermeant superoxide anion (Marklund and Marklund, 1974; Fusi et al., 1999).

A caged form of tBuBHQ, *O*[*o*-nitromandelyloxycarbonyl]-tBuBHQ, has been designed (Rossi and Kao, 1997), although it is not available commercially. Its carboxylate group can be used to attach an acetoxymethyl-ester moiety to make the caged compound cell-permeant (Rossi and Kao, 1997). Irradiation of *O*[*o*-nitromandelyloxycarbonyl]-tBuBHQ with UV light (<400 nm wavelength) results in the formation of tBuBHQ-bicarbonate, which would rapidly decompose under physiological conditions to tBuBHQ and carbon dioxide (Rossi and Kao, 1997).

b. Mechanism of Action. tBuBHQ was originally shown to impair ER/SR-mediated Ca^{2+} sequestration in hepatocytes (expressing SERCA2b and 3) by relatively potent inhibition of SERCA activity (Moore et al., 1987). In rabbit skeletal muscle microsomes, containing SERCA1a, and canine cardiac muscle microsomes, containing SERCA2a, tBuBHQ inhibits ATP hydrolysis by up to 80 and 90%, respectively, at less than 10 μM with an IC_{50} value ~1.5 μM for both preparations (Nakamura et al., 1992b). More specifically, at 5 to 10 μM, tBuBHQ inhibits by 35 to 40% the decomposition rate of the phosphorylated SERCA intermediate (EP), probably due to a decreased rate of conversion of high Ca^{2+} affinity (E_1P) to the low Ca^{2+} affinity (E_2P) form. It also inhibits, by almost 90%, the formation of EP by decreasing the rate of Ca^{2+} binding to the Ca^{2+}-free, nonphosphorylated SERCA (mostly E_1) (Nakamura et al., 1992b) (see Fig. 3 and *Section I.G.1.*). This suggests that tBuBHQ has at least two sites of action in the SERCA Ca^{2+} pumping cycle (Fig. 9).

Another comparative study looking at the inhibitory activity of tBuBHQ in microsomes from platelets [human; SERCA2b and 3 (Bobe et al., 1994; Kovacs et al., 1997)], smooth muscle (pig and rat aorta; mostly SERCA2b), cardiac muscle, and skeletal muscle showed that tBuBHQ inhibits EP formation in the 0.1- to 1-μM range with maximal inhibition at 5 μM, whereas hydroquinone (lacking the two tertiary butyl groups of tBuBHQ; see *Section II.A.2.a.*) is inactive, supporting the selectivity of effect of tBuBHQ (Papp et al., 1992). However, there is a clear insensitivity of the smooth muscle microsomes to this effect (SERCA2b; ~5% at 10 μM), while the amplitude of this effect in the other preparations is ranking as platelet (SERCA3; ~70%) > skeletal muscle (SERCA1a; ~60%) > cardiac muscle (SERCA2a; ~45%).

c. Selectivity. As is the case for thapsigargin and CPA, tBuBHQ can inhibit all three families of SERCA isoforms, although SERCA2b may be resistant (Moore et al., 1987; Nakamura et al., 1992b; Papp et al., 1992). tBuBHQ is also without effect on mitochondrial Ca^{2+} fluxes and PMCA activity (Moore et al., 1987) and on the Ca^{2+} sensitivity of contractile proteins (Westerblad and Allen, 1994). How-

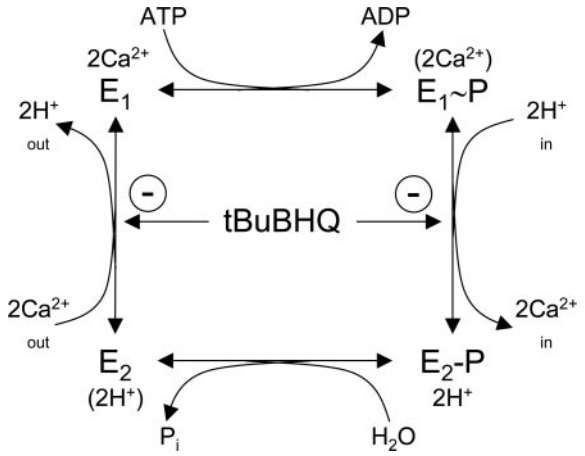

FIG. 9. Model of SERCA inhibition by tBuBHQ. See text for details.

ever, at high concentrations (50 μM), within the minimal range required for maximal SERCA inhibition, it can partially inhibit capacitative Ca^{2+} entry presumably through a direct effect on the plasma membrane permeability for divalent cations (Mason et al., 1991; Foskett and Wong, 1992). Furthermore, also at high concentrations (IC_{50} value ~67 μM), in contrast with CPA but similar to thapsigargin, tBuBHQ inhibits the Ca_L currents in freshly isolated rat tail artery smooth muscle cells (Fusi et al., 2001). It does so in a partially reversible and voltage-dependent manner; its auto-oxidation into superoxide anion impairs channel function from the extracellular side of the plasma membrane (possibly by stabilizing it in its inactivated state) (Fusi et al., 2001). This effect is consistent with the Ca_L blockade observed in GH3 pituitary cells (Nelson et al., 1994)—tBuBHQ was also shown, in contrast with thapsigargin and CPA, to block N-, P-, and Q- but not T-, L-, or R-type Ca^{2+} current in central and peripheral neurons (Scamps et al., 2000). tBuBHQ (50 μM), like CPA (see *Section II.A.3.c.*), nonselectively decreases SR Ca^{2+} permeability as it inhibits passive Ca^{2+} efflux from permeabilized A7r5 cells (Missiaen et al., 1992a). Evidence for a nonspecific effect was suggested by the observation that the inhibition persists after cells are exposed to thapsigargin (2 μM) at a concentration that does not affect passive Ca^{2+} efflux.

d. Use in Smooth Muscle Preparations. tBuBHQ is a SERCA inhibitor, the use of which is limited by its rapid conversion to superoxide radicals in solution. This compound can inhibit capacitative Ca^{2+} entry while not affecting mitochondrial Ca^{2+} fluxes, PMCA activity, or contractile protein sensitivity. By formation of free radicals, tBuBHQ can readily inhibit various Ca^{2+} channels. SERCA inhibition in various smooth muscle preparations is fast and readily reversible and requires 50 to 100 μM (Table 3).

B. Ca^{2+}-Gated Ca^{2+} Release Channel/Ryanodine Receptor

1. Cyclic ADP-Ribose and Analogs.

a. Source and Chemical Structure. Cyclic ADP-ribose (cADPR) is a pyridine nucleotide metabolite derived from nicotinamide adenine dinucleotide (NAD^+, β-NAD^+) (Lee et al., 1989). Cyclization is at the N1-position of the adenine ring linked to the anomeric carbon C1′ of the terminal ribose with the linkage in β-configuration (Lee et al., 1994) (Fig. 10, Fig. 11). The NAD nicotinamide group is released during the cyclization reaction.

Several cADPR analogs with either agonistic or antagonistic activity have been synthesized by enzymatic and chemoenzymatic methods owing to the broad substrate specificity of ADP-ribosylcyclase from *Aplysia californica*, the mollusk where cADPR was first discovered (Lee et al., 1989). However, new enzyme-independent methods (Fukuoka et al., 2001; Shuto et al., 2001) should allow for more analogs with structural diversity.

To date, five significantly potent agonist analogs have been designed (in decreasing order of potency): 3-deaza-cADPR, cADP-carbocyclic-ribose (cADPcR), $2'_A$-deoxy-

TABLE 3
Effective concentrations of tBuBHQ in smooth muscle

Tissue	Animal Species	Experimental Details (Preparation; Measurement Method; Measured Response)	Effective Concentrations of tBuBHQ	Reference
			μM	
Aorta	Pig	Microsomes, F3 microsomal membranes fraction; inorganic phosphate-release assay; Ca^{2+}-ATPase activity	30-50	Luo et al., 2000
Aorta	Rabbit	Isolated rings; isometric dynamometry; contractile activity	30-50	Luo et al., 2000
Aorta	Rat	Saponin-permeabilized cultured A7r5 cell line; $^{45}Ca^{2+}$ cellular loading; Ca^{2+} fluxes	50	Missiaen et al., 1992a
Aorta	Rat	Isolated smooth muscle cells; fura-2 cellular loading, fluorometry; $[Ca^{2+}]_{cyt}$	20	Neylon et al., 1992
Aorta	Rat	Isolated endothelium-denuded rings; isometric dynamometry; contractile activity	50	Fusi et al., 1998
Aorta	Rat	Isolated endothelium-denuded rings; isometric dynamometry; contractile activity	10-100	Shimamoto et al., 1992
Coronary artery	Pig	Isolated smooth muscle cells; fura-2 cellular loading, fluorometry; $[Ca^{2+}]_{cyt}$	1	Weirich et al., 2001
Tail artery	Rat	Isolated smooth muscle cells; whole-cell patch-clamping; $I_{Ca(L)}$	10-100	Fusi et al., 2001

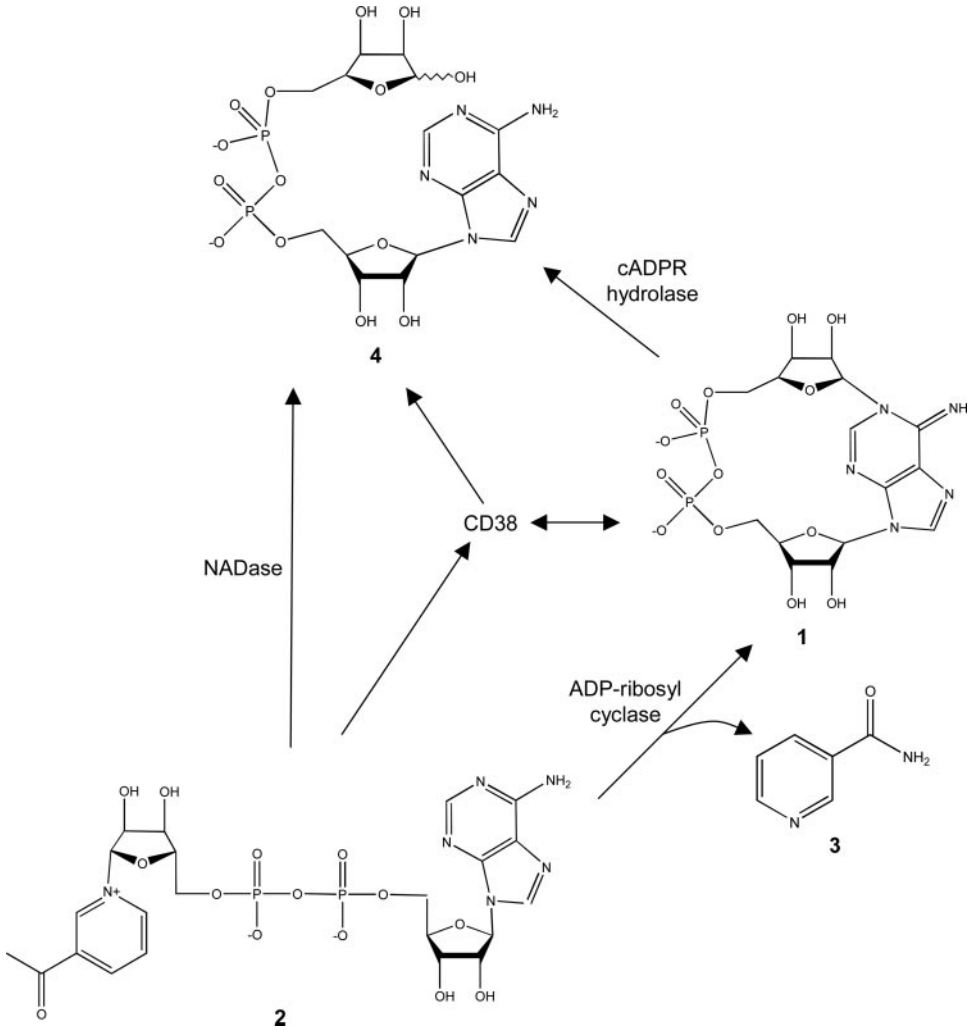

FIG. 10. Formation and metabolism of cADPR (1). cADPR is synthesized from nicotinamide adenine dinucleotide (NAD^+) (2) by ADP-ribosyl cyclase, with release of nicotinamide (3) and hydrolyzed to its inactive metabolite ADPR (4). CD38 is a bifunctional enzyme that catalyzes both their synthesis and degradation of cADPR. Adapted with permission from Ashamu et al. (1997).

cADPR, cyclic aristeromycin diphosphate ribose (cArisDPR), and $3'_A$-deoxy-cADPR (Fig. 11). 3-Deaza-cADPR differs from cADPR by the substitution of carbon for nitrogen at the purine ring 3-position (Wong et al., 1999). In cADPcR, the oxygen atom in the cADPR *N*-1-ribose ring is substituted by a methylene group (Fukuoka et al., 1999; Shuto et al., 2001). $2'_A$-Deoxy-cADPR has a deletion of the cADPR 2′-position hydroxyl group of the ribose moiety linked to the adenine, i.e., the adenosine ribose (Ashamu et al., 1997). cArisDPR was the first carbocyclic cADPR analog synthesized, wherein the adenosine ribosyl moiety is replaced with a carbocyclic 5-membered ring (Bailey et al., 1996). Finally, $3'_A$-deoxy-cADPR has deletion of cADPR 3′-position hydroxyl group of the adenosine ribose (Ashamu et al., 1997).

Five antagonists of reasonable potencies have been designed to date (in decreasing order of potency): 8-NH_2-cADPR, 7-deaza-8-Br-cADPR, 8-N_3-cADPR, 8-Br-cADPR, and 3′-OMe-cADPR (Fig. 11). 8-NH_2-cADPR has an amine moiety substituting for cADPR hydrogen atom on adenine ring 8-position, whereas 8-N_3-cADPR has an azide moiety, and 8-Br-cADPR has a bromine atom (Walseth and Lee, 1993). 7-Deaza-8-Br-cADPR has, in addition to the latter analog, the nitrogen atom in 7-position of the adenine ring of cADPR substituted by a carbon atom (Sethi et al., 1997). Finally, 3′-OMe-cADPR has a methoxyl moiety substituting for cADPR 3′-position hydroxyl group of the adenosine ribose (Ashamu et al., 1997).

A caged form of cADPR has also been designed (Aarhus et al., 1995a; Walseth et al., 1997) and contains one photolabile (2-nitrophenyl)ethyl group on either of the two phosphates of cADPR (Fig. 12). The two resulting isomers have similar photolysis efficiency [quantum yield of 0.11 (Walseth et al., 1997)] and are both biologically inactive until photolysis with UV light (<400-nm wavelength), and therefore, do not need to be separated for biological applications (Aarhus et al., 1995a).

b. Mechanism of Action.

i. Synthesis and Degradation. The cell-impermeant cADPR is generated from NAD^+ by an ADP-ribosyl cyclase (ADPRC) and is degraded to ADP-ribose by a

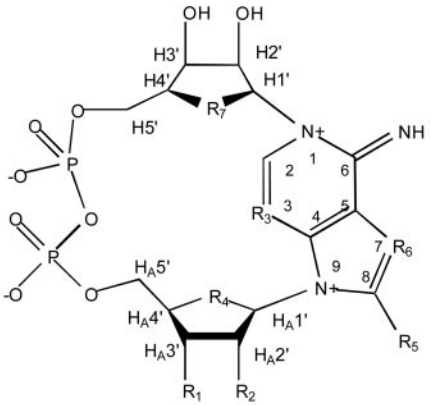

Analog	R_1	R_2	R_3	R_4	R_5	R_6	R_7	Activity	Cell Permeability	Enzymatic Stability
3-deaza-cADPR	OH	OH	CH	O	H	N^+	O	Full Agonist	No	Yes
cADP-carbocyclic-ribose	OH	OH	N^+	O	H	N^+	CH_2	Superagonist	No	Yes
cADPR	OH	OH	N^+	O	H	N^+	O	Full Agonist	No	No
$2'_A$-deoxy-cADPR	OH	H	N^+	O	H	N^+	O	Full Agonist	No	No
cArisDPR	OH	OH	N^+	CH_2	H	N^+	O	Full Agonist	No	Yes
$3'_A$-deoxy-cADPR	H	OH	N^+	O	H	N^+	O	Full Agonist	No	No
8-NH_2-cADPR	OH	OH	N^+	O	NH_2	N^+	O	Competitive Antagonist	No	No
8-N_3-cADPR	OH	OH	N^+	O	N_3	N^+	O	Competitive Antagonist	No	No
7-deaza-8-Br-cADPR	OH	OH	N^+	O	Br	CH	O	Antagonist	Yes	Yes
8-Br-cADPR	OH	OH	N^+	O	Br	N^+	O	Antagonist	Yes	No
3'-OMe-cADPR	OCH_3	OH	N^+	O	H	N^+	O	Antagonist	No	No

FIG. 11. Molecular structure of cADPR and analogs in decreasing order of potency in each class of activity as measured in the sea urchin homogenate Ca^{2-}-releasing assay. Core structure adapted with permission from Ashamu et al. (1997).

cADPR hydrolase (cADPRH) (Guse, 2002) (Fig. 10). Presently, there are no details on the physiological mechanisms that lead to activation of ADPRC. In mammals, ADPRC and cADPRH activities are expressed as ectoenzymes by the type II transmembrane glycoprotein CD38 (Lee, 2000, 2001; Higashida et al., 2001). For instance, ADPRC and cADPRH activities were both demonstrated in plasma membrane-enriched tracheal smooth muscle crude membranes but not in the SR-enriched fractions (White et al., 2000). It is possible, however, that in smooth muscle cells, CD38 or closely related enzymes are expressed in nuclear membranes or at other intracellular sites (Adebanjo et al., 1999; Khoo et al., 2000). Both activities of ADPRC and cADPRH also comigrate at a molecular weight of ~40 kDa on SDS-PAGE, which was confirmed by sucrose gradient density fractionation and gel filtration chromatography. Kinetic analysis has yielded K_m values of 30.4 and 695.3 μM and V_{max} values of 330.4 and 102.8 nmol/mg/h for ADPRC and cADPRH activities, respectively (White et al., 2000). This is consistent with the observation that both ADPRC and cADPRH activities are associated with a single-membrane protein fraction in rat myometrial smooth muscle (Dogan et al., 2002). Interestingly, in membranes from rat aortic smooth muscle cells, an ADPRC is detected on Western blot with an anti-CD38 antibody, but

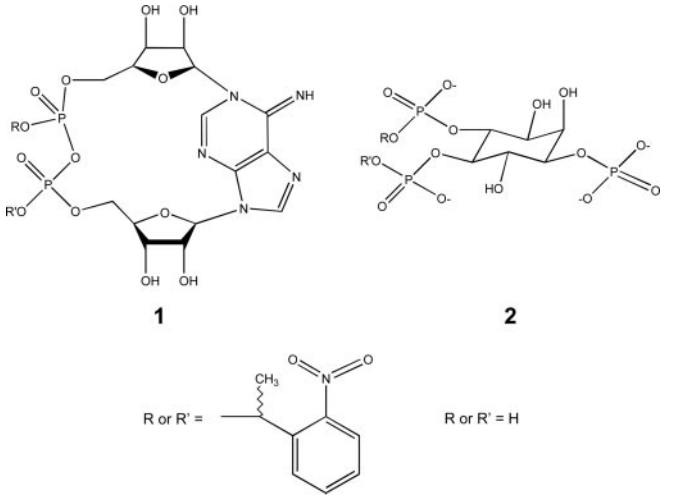

FIG. 12. Molecular structure of caged cADPR (1) and caged $InsP_3$ (2). Each caged compound is formed of two constitutional isomers, each with the caging group, (2-nitrophenyl)ethyl, on either of the two phosphates. The methyl group orientation could vary, as denoted by the wavy line.

it was shown to be pharmacologically distinct from the classical CD38 (de Toledo et al., 2000).

The bifunctional activity of CD38 is regulated in smooth muscle cells, thus influencing cADPR levels. For instance, in porcine tracheal smooth muscle cell membranes, NO donors produce a concentration-dependent decrease in ADPRC but not cADPRH activity through a cGMP-independent pathway involving *S*-nitrosylation of thiols, resulting in reduced cADPR synthesis and in part mediating NO-induced inhibition of intracellular Ca^{2+} mobilization (White et al., 2002). NO inhibits the Ca^{2+} mobilization induced by endogenous cADPR in bovine coronary arterial smooth muscle cells (Yu et al., 2000). In rat myometrial smooth muscle, estradiol-17β increases CD38 mRNA and protein expression and significantly enhances ADPRC, but not cADPRH, activity. This differential regulation could result in increased cADPR synthesis and influence myometrial Ca^{2+} regulation and contractility (Dogan et al., 2002). cADPRH activity was also shown to be differentially regulated in rabbit pulmonary arterial smooth muscle where, in homogenates, cADPR levels are increased by reduction of the β-NAD^+/β-NADH ratio, at least in part due to the inhibition of cADPRH by β-NADH (Wilson et al., 2001). This mechanism, reflecting the cellular redox state, may mediate the SR Ca^{2+} release-induced hypoxic pulmonary vasoconstriction and associated hypertension (Wilson et al., 2001).

An important contrast with other second messenger molecules, such as adenylate cyclase or PLC, that act on plasma membrane or intracellular substrates is that CD38 is an ecto-NADase, as alluded above; thus, it acts on extracellular substrates (Lee, 2000, 2001). Such an extracellular active site makes its role still a matter of debate given the intracellular function of cADPR. However, an evolving model proposes that CD38 ADPRC activity is sensitive to extracellular stimuli through receptor-mediated phosphorylation and/or G-protein- or ATP-mediated modulation (Guse, 2002). In this model, NAD^+ needs to be exported from the cytoplasm, probably by connexin 43 hemichannels (Bruzzone et al., 2001). The cell-impermeant cADPR subsequently formed must then be transported back into the cell, probably by dimeric or oligomeric CD38 itself or by an unknown transport system (Zocchi et al., 1999).

Consistent with such a model is that tracheal mucosa strips release NAD^+ and increase $[Ca^{2+}]_{cyt}$ in a cADPR-dependent manner, suggesting the existence of a paracrine mechanism whereby mucosa-released extracellular NAD^+ plays a hormone-like function and where cADPR behaves as second messenger (Franco et al., 2001). Additional support for the model is that extracellularly applied cADPR (100 μM) potentiates Ach-induced $[Ca^{2+}]_{cyt}$ increases and contractile activity in tracheal smooth muscle cells (Franco et al., 2001). Furthermore, this latter effect is mimicked by extracellular application of the more potent and metabolically stable cell-impermeant analog 3-deaza-cADPR (Wong et al., 1999) (see below). This suggests that, by formation of NAD^+, cADPR could play an autocrine/paracrine role in addition to its second messenger role.

ii. Interaction with Ca^{2+}-Gated Ca^{2+} Release Channel/Ryanodine Receptor. cADPR is the only known endogenous RyR agonist apart from Ca^{2+}. Its ability to activate smooth muscle RyR was directly shown using RyR from bovine coronary arterial smooth muscle cells SR reconstituted into planar lipid bilayers; cADPR (0.01–1 μM) increases RyR P_o up to 8 times in a ryanodine-sensitive manner and sensitizes RyR activation by Ca^{2+} (Li et al., 2001). cADPR (10 μM) reduces [^{3}H]ryanodine binding to microsomes from freshly cultured rat aortic smooth muscle cells that express RyR1–3 (Yusufi et al., 2002). However, a direct interaction of cADPR with the RyR has not been demonstrated in any type of cellular preparation thus far.

In cultured bovine coronary arterial smooth muscle cells, cADPR activation of RyR requires the tacrolimus (FK-506)-binding protein 12.6 (FKBP12.6) (Tang et al., 2002), a RyR accessory protein. This protein was shown to bind in a stoichiometry of four RyR protomers: four FKBP12.6 molecules using either RyR1 from skeletal muscle, RyR2 from cardiac muscle, or RyR3 cloned from lung epithelial cells (Timerman et al., 1996; Bultynck et al., 2001; Jeyakumar et al., 2001). FK-506, an immunosuppressant drug, increases the P_o of reconstituted RyR channels from the SR of these cells by interacting with FKBP12.6 (Tang et al., 2002). FK-506 dissociates FKBP12.6 from RyR, and this is believed to activate or delay the inactivation/closing of the Ca^{2+} channel; it is assumed that cADPR acts similarly (Higashida et al., 2001). The lower sensitivity of RyR to cADPR in microsomal and permeabilized smooth muscle preparations (micromolar) compared with that observed in sea urchin egg homogenates (nanomolar—the standard assay for cADPR) may be due to the fact that small accessory proteins, such as FKBP12.6 or calmodulin, which would be lost in membrane or permeabilized preparations, are necessary for expression of cADPR full potency [either directly (Lee et al., 1994; Tanaka and Tashjian, Jr., 1995) or indirectly (Takasawa et al., 1995)].

It was recently demonstrated in preparations from striated muscles (rabbit skeletal and canine cardiac) that 1) RyR is insensitive to cADPR (up to 10 μM) when reconstituted into planar lipid bilayers (channel P_o) or in purified or crude microsomes (energized Ca^{2+} uptake or passive Ca^{2+} leak), 2) [^{32}P]cADPR does not bind significantly (<1/10,000 equivalent of binding) to purified or crude microsomes, and 3) cADPR does not affect FKBPs 12 or 12.6 association to crude microsomes (Copello et al., 2001). Care was taken to use cADPR from several sources to optimize the experimental conditions for cADPR activity (Iino et al., 1997; Thomas et al., 2001), verify retention of FKBP in crude microsomes, and demonstrate the classical effects of known RyR modulators

(Ca^{2+}, caffeine, ruthenium red). Thus, this study calls attention to the need to appreciate the molecular details of cADPR action in other mammalian tissues, including smooth muscles, and to take caution in extrapolating results.

Caged cADPR has been successfully used in non-smooth muscle mammalian cell types (Varadi and Rutter, 2002), including cardiac muscle cells (Guo et al., 1996; Cui et al., 1999). However, only one report has been published so far on its use in a smooth muscle preparation. In this study, caged cADPR was used to examine the effect of cADPR on Ca^{2+} signaling in voltage-clamped isolated guinea pig colon smooth muscle cells that express RyR but lack FKBP12.6 (Bradley et al., 2003). Photoreleased cADPR (50–500 μM) does not alter global or subsarcolemmal $[Ca^{2+}]_{cyt}$ through CICR, nor does it enhance caffeine-induced CICR, despite the fact that it is releasing Ca^{2+} in sea urchin eggs. Furthermore, this lack of cADPR activity on Ca^{2+} release is unchanged by introduction of recombinant FKBP12.6 into the smooth muscle cells. However, photoreleased cADPR increases the rate of Ca^{2+} removal from the cytoplasm, an effect that is slowed by the cADPR antagonist 8-bromo-cADPR (see *Section II.B.1.b.3.*). These results suggest that cADPR modulates $[Ca^{2+}]_{cyt}$ by promoting Ca^{2+} extrusion but not via RyR.

iii. Structure-Activity Relationships. In terms of SAR, the design of five noticeably potent, but cell-impermeant, cADPR full agonists has been possible. The most potent of these is 3-deaza-cADPR (Fig. 11), which can induce Ca^{2+} release at a threshold concentration of 0.3 nM and with an EC_{50} value of 1 nM (in sea urchin egg homogenates), making it ~70 times more potent that cADPR (Wong et al., 1999). This action is potentiated by caffeine (1 mM) and concentration-dependently (60–300 nM) inhibited by the cADPR antagonist 8-NH_2-cADPR (see below) suggesting that it acts through the same mechanism as cADPR (Wong et al., 1999). The increased potency is likely due to the fact that, in contrast with cADPR, 3-deaza-cADPR is resistant to both heat- and enzymatically-induced hydrolysis—most probably because of an increase in electronegativity at the N1-position making it a poorer leaving group in a hydrolytic reaction (Wong et al., 1999). An increased lag time for Ca^{2+} release by 3-deaza-cADPR compared with cADPR suggests that binding of cADPR may involve formation of a hydrogen bond or electrostatic interaction between N3 of adenine and its receptor (Foskett and Wong, 1992; Wong et al., 1999).

The second most potent cADPR agonist is cADPcR (Fig. 11). In intact sea urchin eggs, injection of cADPcR (30–500 nM) increases $[Ca^{2+}]_{cyt}$ by more than the levels produced with equivalent concentrations of injected cADPR, making cADPcR a superagonist (Shuto et al., 2001). This is very likely related to its almost complete enzymatic stability compared with cADPR when assayed in rat brain extract in the presence of recombinant CD38 (Shuto et al., 2001).

The third most potent cADPR agonist is $2'_A$-deoxy-cADPR (Fig. 11), which acts as a full agonist (in a sea urchin egg homogenate Ca^{2+} releasing assay) with an EC_{50} value of 58 nM compared with 32 nM for cADPR (Ashamu et al., 1997). Furthermore, $2'_A$-deoxy-cADPR (200 nM) desensitizes Ca^{2+} release induced by cADPR (100 nM), suggesting a similar mechanism of action for the two ligands (Ashamu et al., 1997). Enzymatically, its stability is similar to cADPR (Ashamu et al., 1997). The SAR suggests the importance of potential hydrogen bonding with cADPR binding sites by proton donation from the 2′-position hydroxyl moiety as a means of gaining potency.

Interestingly, substitution of the hydroxyl moiety in position 2′ by a phosphate group results in an analog inactive in sea urchin egg homogenates (Aarhus et al., 1995b; Ashamu et al., 1997) but which is at least as effective as cADPR in releasing Ca^{2+} from rat brain microsomes (Vu et al., 1996) and permeabilized T-lymphocytes (Guse et al., 1997). This may reflect subtle differences between cADPR-sensitive Ca^{2+}-releasing mechanisms for the RyR of sea urchin eggs and mammalian cells (Ashamu et al., 1997; Lee, 1997), and it is unclear whether inactivity in the sea urchin eggs is the result of charge addition and/or increase in steric volume (Ashamu et al., 1997). In this regard, it is worth mentioning the discovery of a new Ca^{2+} current activated by cADPR in sea urchin egg microsomes reconstituted into planar lipid bilayers; this current has different unitary conductance than RyR, despite the fact that it is similarly modulated by caffeine, ruthenium red, and calmodulin (Perez et al., 1998).

The fourth agonist of significant potency is cArisDPR (Fig. 11). In the sea urchin egg homogenate Ca^2-releasing assay, cArisDPR is a full agonist with an EC_{50} value of 80 nM compared with 30 nM for cADPR, thus having about one-third the potency of cADPR (Bailey et al., 1996). However, it is degraded significantly more slowly in the homogenates, with a $t_{1/2}$ of 170 min versus 15 min for cADPR (Bailey et al., 1996).

The last agonist of noticeable potency is $3'_A$-deoxy-cADPR (Fig. 11), with an EC_{50} value of ~5 μM, which is a potency of ~100-fold lower than that of $2'_A$-deoxy-cADPR (EC_{50} value of 58 nM) and ~150-fold lower than that of cADPR (EC_{50} value of 32 nM) (Ashamu et al., 1997). Consistent with these findings, like $2'_A$-deoxy-cADPR, $3'_A$-deoxy-cADPR also desensitizes Ca^{2+} release induced by cADPR (100 nM) but at a concentration 100 times larger (20 μM) (Ashamu et al., 1997). This difference in potency does not appear to be due to a difference in enzymatic stability, suggesting that the 3′-position hydroxyl group of the adenosine ribose is more critical to cADPR that the 2′-position one for agonist activity (Ashamu et al., 1997).

The design of significantly potent antagonists has been quite successful using position-8 substitutions, with potency roughly decreasing with increasing size of the substituting groups, thus highlighting the crucial importance of the cADPR hydrogen atom on adenine ring 8-position in its agonistic effect. For instance, it has led to 8-NH_2-cADPR (Fig. 11), the most potent antagonist known, which competitively and fully antagonizes at a nearly maximally effective concentration of cADPR (135 nM) with an IC_{50} value ~10 nM in the sea urchin egg homogenate Ca^{2+}-releasing assay (Walseth and Lee, 1993). Furthermore, this effect is immediate, as 8-NH_2-cADPR is effective even when added after cADPR-induced Ca^{2+} release had been initiated (Walseth and Lee, 1993). In contrast, this analog is ineffective in blocking either ryanodine- or caffeine-induced Ca^{2+} release, demonstrating the selective nature of its antagonist activity and suggesting that the cADPR binding site is distinct from those of ryanodine and caffeine (Walseth and Lee, 1993).

The second most potent antagonist designed so far is 8-N_3-cADPR with an IC_{50} value ~0.45 μM against cADPR (135 nM) in the sea urchin egg microsomal Ca^{2+}-releasing assay (Walseth and Lee, 1993). 8-N_3-cADPR and cADPR reciprocally displace each other in binding to the microsomes. However, its most remarkable property is that it is a photoaffinity probe for cADPR binding sites; photolysis of microsomes preincubated with [^{32}P]8-N_3-cADPR resulted in specific labeling of proteins of 140 and 100 kDa, which could be specifically prevented by 8-N_3-cADPR or by nanomolar concentrations of cADPR (Walseth and Lee, 1993). Interestingly, caffeine preferentially inhibits the labeling of the 100-kDa protein as compared with the 140-kDa protein. In keeping with the cADPR requirement for the protein FKBP12.6 in cultured coronary arterial smooth muscle cells (discussed above), these results also suggest that cADPR may not directly interact with the RyR to alter its activity but could do so by acting through accessory proteins (Walseth and Lee, 1993).

The third most potent antagonist is 7-deaza-8-Br-cADPR (Fig. 11), which has an IC_{50} value ~0.7 μM against cADPR (100 nM) (Sethi et al., 1997). However, its most remarkable properties, in contrast to the other 8-substituted antagonists, are its resistance to hydrolysis (heat- and enzymatically-mediated), owing to its substitution of the 7-position nitrogen atom by a carbon atom (Bailey et al., 1997), and its cell permeability, owing to the lipophilic character of its 8-bromo and 7-CH moieties (Sethi et al., 1997).

The fourth most potent antagonist is 8-Br-cADPR (Fig. 11), with an IC_{50} value of ~1 μM against cADPR (100 nM) (Sethi et al., 1997). Like 7-deaza-8-Br-cADPR, this analog is also cell-permeant due to the lipophilicity of it 8-bromo moiety; however, it lacks the enzymatic stability of 7-deaza-8-Br-cADPR (Sethi et al., 1997).

3′-OMe-cADPR (Fig. 11) is the last antagonist of significant potency with an IC_{50} value of ~5 μM against cADPR (100 nM) (Ashamu et al., 1997). In contrast with the OH moiety in the 3′-position of the adenosine ribose in cADPR, the methoxyl group is larger and cannot donate a proton for potential hydrogen bonding with cADPR binding site, although it can still act as an acceptor (Ashamu et al., 1997). Thus, it appears that proton donation may indeed be critical for agonist activity, whereas an oxygen atom is sufficient for recognition of the cADPR binding site (Ashamu et al., 1997).

c. Selectivity. It is unknown whether cADPR can affect the activity of all three known mammalian RyR isoforms. For instance, cADPR (1 μM) augments Ca^{2+}-induced (100 μM) Ca^{2+} release and reduces its inhibition by ryanodine (50 μM) in brain and cardiac microsomes (which express RyR2). In addition, cADPR (1 μM) increases [^{3}H]ryanodine binding to cardiac microsomes in the presence of Ca^{2+} (100 μM) (Meszaros et al., 1993), which concurs with the observation that cADPR (10 μM) augments the P_o of sheep cardiac SR Ca^{2+} channels (presumably RyR2) reconstituted into planar lipid bilayers (Sitsapesan et al., 1994). Interestingly, the latter effect is inhibited by physiologic concentrations of ATP (100 μM-1 mM), suggesting that a direct interaction of cADPR with RyR2 is unlikely to occur in the intact cardiac muscle cell (Sitsapesan et al., 1994). However, both studies are at odds with the lack of effect of cADPR (0.1–5 μM) on the activity of SR Ca^{2+} channel reconstituted into planar lipid bilayers or on [^{3}H]ryanodine binding to microsomes from procine cardiac muscle (Fruen et al., 1994).

In sheep skeletal muscle SR Ca^{2+} channel (RyR1) reconstituted into planar lipid bilayers, cADPR (1–10 μM) increases P_o with a $[Ca^{2+}]_{cyt}$ of 10 μM (Sitsapesan and Williams, 1995). However, this effect is proportional to luminal $[Ca^{2+}]$ (1–50 mM), and channel conductance is still susceptible to partial inhibition by ryanodine (1 μM), suggesting that the cADPR effect is on the RyR and not on another type of SR channel (Sitsapesan and Williams, 1995). This may explain why other groups have been unable to show an effect of cADPR on CICR in skeletal muscle microsomes (Meszaros et al., 1993; Morrissette et al., 1993) since their luminal $[Ca^{2+}]$ may have been too low (e.g., 1–4 μM) (Sitsapesan and Williams, 1995).

Although the lack of effect of cADPR (0.1–5 μM) on the activity of SR Ca^{2+} channel reconstituted into planar lipid bilayers or on [^{3}H]ryanodine binding to microsomes from procine cardiac muscle (Fruen et al., 1994) still remains to be reconciled, more recent studies support a stimulatory role of cADPR on RyR1. Indeed, cADPR enhances a ruthenium red (1 μM)- and ryanodine (100 μM)-sensitive CICR in rabbit skeletal muscle (Yamaguchi and Kasai, 1997); however, cADPR increases $[Ca^{2+}]_{cyt}$ in a ruthenium red-resistant manner when microinjected in intact porcine skeletal muscle fibers

without changes in plasma membrane potential (Lopez et al., 2000). Also, in RyR1-expressing microsomes from RyR3 knockout mouse diaphragm muscle (which normally only expresses RyR1 and RyR3), cADPR (0.1–2 μM) amplifies caffeine-induced (10 mM) Ca^{2+} release (Fulceri et al., 2001), although at 1 μM, it does not affect the P_o of the SR Ca^{2+} channel when reconstituted into planar lipid bilayers (Sonnleitner et al., 1998). In contrast, cADPR (1 μM) increases the P_o of reconstituted SR Ca^{2+} channels from wild-type mouse diaphragm muscle (10-fold leftward shift of the Ca^{2+}-P_o curve) (Sonnleitner et al., 1998), suggesting that it also affects RyR3 activity.

cADPR appears selective for CICR versus IICR in smooth muscle. For instance, in microsomes from freshly cultured rat aortic smooth muscle cells that express RyR1–3, cADPR (1–10 μM) induces Ca^{2+} release that is fully inhibited by 8-Br-cADPR (40 μM) and ruthenium red (10 μM), whereas $InsP_3$ stimulates (1–8 μM) Ca^{2+} release that is fully inhibited by heparin (1 mg/ml) (Yusufi et al., 2002). Although both agents induce maximal Ca^{2+} release of similar magnitude, the cADPR effect is insensitive to heparin (Yusufi et al., 2002). Likewise, in saponin-permeabilized freshly cultured seminiferous peritubular smooth muscle cells from rat testis that express $InsP_3$R1–3 but only RyR2 among RyR isoforms, cADPR-induced (10 μM) Ca^{2+} release from a SR Ca^{2+} store was shown to be independent from that released by $InsP_3$ (10 μM) but fully inhibited by 8-Br-cADPR (50 μM) or ryanodine (5 μM) (Barone et al., 2002). In contrast, CADPR (10 μM)-induced Ca^{2+} release was shown to be resistant to heparin (10 μg/ml), which is nevertheless able to fully inhibit the $InsP_3$ effect (Barone et al., 2002). It was observed in inside-out plasma membrane patches that cADPR (1–10 μM) concentration-dependently reduces K_{Ca} P_o by up to 75% (Li et al., 1997).

d. Use in Smooth Muscle Preparations. The role of cADPR in the regulation of smooth muscle function is unclear; there are no studies indicating that the inhibition of the synthesis or activity of this endogenous ligand for the RyR causes alteration in either mechanical or electrical activity under basal conditions. In an exhaustive study of smooth muscle from three animal species (human, guinea pig, and rabbit), Iizuka et al. (1998) were unable to detect any Ca^{2+} release even with supramaximal concentrations of cADPR, either under resting or stimulated conditions. The synthesis of membrane-permeant analogs has assisted in the use of cADPR agonists and antagonists. Some success in smooth muscle has been reported with the use of 10 μM cADPR or 100 μM 8Br-cADPR (Table 4). However, the constriction with exogenously administered cADPR requires high concentrations and is delayed in onset, with a plateau response occurring some 25 min after administration.

The evidence that cADPR has a functional role in smooth muscle is relatively weak. For example, Nixon et al. (1994) were unable to elicit responses with cADPR in permeabilized rat aorta and vas deferens. Important persuasive evidence that cADPR is ineffective as an RyR modulator in smooth muscle comes from the detailed study by McCarron's group (Bradley et al., 2003), discussed above (see *Section II.B.1.b.*), where caged cADPR failed to cause Ca^{2+} release, with no detectable changes in either subsarcolemmal or global $[Ca^{2+}]_{cyt}$. As discussed by Bradley et al. (2003), cADPR is also ineffective in other nonvascular (bronchial, intestinal, and vas deferens) and vascular (aorta, coronary, and cerebral arteries) smooth muscle preparations. Rather than mediating constriction, cADPR is proposed to increase the rate of Ca^{2+} removal from the cytoplasm, likely through an action on the PMCA (Bradley et al., 2003).

2. Caffeine and 9-Methyl-7-bromoeudistomin D.

a. Source and Chemical Structure. Caffeine is an alkaloid occurring in plants that are geographically widely distributed (e.g., *Thea sinensis* L). It is a methylated xanthine derivative (1,3,7-trimethylxanthine; Fig. 13). Xanthine is a dioxypurine structurally related to uric acid. 9-Methyl-7-bromoeudistomin D (MBED; Fig. 13) is a synthesized compound (Nakamura et al., 1986; Kobayashi et al., 1989a; Seino et al., 1991; Takahashi et al., 1995) derived from a natural product, eudistomin D (Fig. 13), from the Caribbean tunicate *Eudistoma olivaceum* (Kobayashi et al., 1984). However, in terms of physicochemical properties, MBED is a larger molecule than caffeine and possesses a much higher affinity for phospholipid membranes, which may explain its distinct effect compared with caffeine (see *Section II.B.2.b.*).

b. Mechanism of Action. The primary site of action for caffeine is believed to be the RyR (Zucchi and Ronca-Testoni, 1997). Essentially, caffeine increases the RyR Ca^{2+} sensitivity by increasing its P_o without changing its conductance, as shown in single-channel experiments done with RyR purified from cardiac (Rousseau et al., 1987; Rousseau and Meissner, 1989; Sitsapesan and Williams, 1990) and skeletal (Rousseau et al., 1988) muscles and reconstituted into planar lipid bilayers. At low concentrations (0.5 to 2 mM), RyR activation requires submicromolar Ca^{2+} and P_o is increased by a reduction of the channel closed-state lifetime, whereas at higher concentrations (>5 to 10 mM), RyR activation requires picomolar Ca^{2+} and P_o is increased by a prolongation of the open-state lifetime. The specific binding site of caffeine on the RyR has not yet been established. However, it is unlikely to be that of adenine nucleotides, despite the structural resemblance of caffeine to these molecules (Zucchi and Ronca-Testoni, 1997). In terms of its pharmacological action on the RyR, caffeine is a class II activator as are Ca^{2+} and adenine nucleotides (Zucchi and Ronca-Testoni, 1997); they all increase RyR P_o without altering its conductance, and they increase its affinity for [^{3}H]ryanodine. It has been proposed that their binding sites are distinct but interacting synergistically (Pessah et al., 1987).

TABLE 4
Effective concentrations of cADPR and analogs in smooth muscle

Tissue	Animal Species	Experimental Details (Preparation; Measurement Method; Measured Response)	Effective Concentrations of cADPR and Analogs	Reference
Airways	Human	Isolated α-toxin-permeabilized strips; isometric dynamometry; contractile activity	No effect at up to 300 μM (cADPR)	Iizuka et al., 1998
Aorta	Guinea pig	Isolated α-toxin-permeabilized strips; isometric dynamometry; contractile activity	100 μM (no effect) (cADPR)	Nixon et al., 1994
Aorta	Rat	Microsomes; $^{45}Ca^{2+}$ loading; Ca^{2+} fluxes	10 and 40 μM (8-Br-cADPR)	Yusufi et al., 2002
Colon	Guinea pig	Isolated smooth muscle cells; whole-cell patch-clamping, fluo-3 cellular loading, fluorometry or wide-field fluorescence digital imaging; I_{Ca}, $[Ca^{2+}]_{cyt}$, $[Ca^{2+}]_{cyt}$ imaging	50-500 μM (caged cADPR) 20 μM (8-Br-cADPR)	Bradley et al., 2003
Coronary artery	Cattle	Microsomal membranes, stripped or not of FKBP-12.6, incorporated into planar lipid bilayers; bilayer clamp amplification; single Ca^{2+} channel currents	10 μM (cADPR)	Tang et al., 2002
Coronary artery	Cattle	Microsomal membranes, stripped or not of FKBP-12.6, incorporated into planar lipid bilayers; bilayer clamp amplification; single Ca^{2+} channel currents	0.01-1 μM (cADPR)	Li et al., 2001
Coronary artery	Cattle	Isolated α-toxin-permeabilized smooth muscle cells; fura-2 cellular loading, fluorometry; $[Ca^{2+}]_{cyt}$	5 μM (cADPR) 100 μM (8-Br-cADPR)	Yu et al., 2000
Coronary artery	Cattle	Isolated rings; isometric dynamometry; contractile activity	30 μM (8-Br-cADPR)	Geiger et al., 2000
Coronary artery	Pig	Isolated β-escin-permeabilized smooth muscle cells; fura-2 cellular loading; $[Ca^{2+}]_{cyt}$	2 μM (cADPR)	Kannan et al., 1996
Ileum	Guinea pig	Isolated α-toxin-permeabilized strips; isometric dynamometry; contractile activity	No effect at up to 300 μM (cADPR)	Iizuka et al., 1998
Mesenteric resistance arteries	Rabbit	Isolated 2nd- and 3rd-order branches endothelium-intact or -denuded rings and saponin-permeabilized smooth muscle cells; whole-cell patch-clamping (cells), isometric dynamometry (rings); membrane potential (cells), contractile activity (rings)	30 μM (cADPR) 300 μM (8-Br-cADPR)	Wilson et al., 2001
Pulmonary artery	Cattle	Microsomes; extramicrosomal fluo-3 and fluorometry or $^{45}Ca^{2+}$ loading; Ca^{2+} fluxes	10 nM-1 μM (cADPR)	Stout et al., 2002
Pulmonary resistance arteries	Rabbit	Isolated 2nd- and 3rd-order branches endothelium-intact or -denuded rings and saponin-permeabilized smooth muscle cells; whole-cell patch-clamping (cells), isometric dynamometry (rings); membrane potential (cells), contractile activity (rings)	30 and 300 μM (8-Br-cADPR)	Wilson et al., 2001
Pulmonary resistance arteries	Rat	Isolated endothelium-denuded rings; isometric dynamometry; contractile activity	300 μM (8-Br-cADPR)	Dipp and Evans, 2001
Renal resistance arteries	Rat	Isolated, cannulated and pressurized segments and β-escin-permeabilized cells; fura-2 cellular loading, fluorometry, diameter monitoring by video microscopy; $[Ca^{2+}]_{cyt}$, contractile activity	10 μM (cADPR)	Li et al., 2000
Stomach (antrum)	Pig	Microsomes; extramicrosomal fluo-3 and fluorometry or $^{45}Ca^{2+}$ loading; Ca^{2+} fluxes	10 nM-1 μM (cADPR)	Stout et al., 2002
Testicular peritubules	Rat	Isolated saponin-permeabilized smooth muscle cells; fura-2 cellular loading, fluorometry; $[Ca^{2+}]_{cyt}$	10 and 50 μM (cADPR) 50 μM (8-NH_2-cADPR)	Barone et al., 2002
Trachea	Cattle	Isolated smooth muscle cells; fura-2 cellular loading, fluorometry; $[Ca^{2+}]_{cyt}$	100 μM (cADPR)	Franco et al., 2001
Trachea	Pig	Isolated β-escin-permeabilized smooth muscle cells; fluo-3 cellular loading, confocal fluorescence microscopy; $[Ca^{2+}]_{cyt}$ imaging	1-10 μM (cADPR) 20 μM (8-NH_2-cADPR)	Prakash et al., 1998
Trachea	Rabbit	Isolated α-toxin-permeabilized strips; isometric dynamometry; contractile activity	No effect at up to 300 μM (cADPR)	Iizuka et al., 1998
Vas deferens	Guinea pig	Isolated α-toxin-permeabilized strips; isometric dynamometry; contractile activity	100 μM (no effect) (cADPR)	Nixon et al., 1994

Such detailed information is not yet available in smooth muscle. However, it has been shown that caffeine (2 mM) increases by a factor of 10 the P_o of partially purified RyR from porcine and canine aortic smooth muscle reconstituted into planar lipid bilayers (Herrmann-Frank et al., 1991). By comparison, 5 mM caffeine increases the sensitivity of CICR by ~30 times, as assessed by fura-2-reported $[Ca^{2+}]_{cyt}$, in saponin-permeabilized guinea pig taenia caeci (Iino, 1989). Caffeine also increases the rate of SR Ca^{2+} release in a concentration-dependent manner (1 to 25 mM). Furthermore, caffeine by itself (i.e., without Ca^{2+}) has no Ca^{2+}-releasing effect.

Interestingly, low temperature amplifies CICR induced by caffeine as monitored by the $[Ca^{2+}]_{cyt}$ transient reported by fura-2 in endothelium-free rat aorta strips

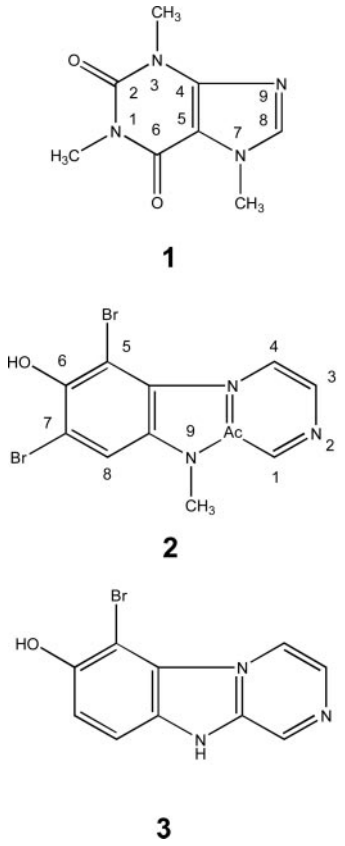

FIG. 13. Molecular structure of caffeine (1), MBED (2), and eudistomin D (3).

(Sato et al., 1988). This is likely due to the effect of temperature on the RyR itself, as shown in single-channel experiments in RyR purified from cardiac muscle and reconstituted into planar lipid bilayers (Sitsapesan et al., 1991). With Ca^{2+} as the sole activating ligand, cooling increases P_o through an increase in channel open lifetime with no significant alteration in the frequency of channel opening and without changing the activating Ca^{2+} dependence of P_o. Despite the fact that single-channel conductance is reduced when temperature is decreased, the net effect of temperature reduction is an increased Ca^{2+} current through the channel.

It is noteworthy that caffeine (up to 50 mM) does not induce contractile activity in saponin-permeabilized longitudinal myometrial smooth muscle from pregnant rats, despite the functional demonstration of RyR presence (Savineau et al., 1988; Savineau and Mironneau, 1990). Similarly, caffeine (10 to 50 mM) does not release $^{45}Ca^{2+}$ in freshly cultured smooth muscle cells from the human uterine artery (Lynn and Gillespie, 1995) and uterus (Lynn et al., 1993, 1995) where RyR presence has been demonstrated. Yet, permeabilized cells from the uterine artery have a CICR process sensitive to ryanodine and ruthenium red (Lynn et al., 1993, 1995; Lynn and Gillespie, 1995). In fresh pregnant and nonpregnant myometrium, as well as in freshly cultured myometrial cells (Lynn et al., 1995), RyR1 and RyR3 are expressed. In contrast, RyR2 is present only in pregnant human myometrium and in TGF-β-exposed cultured human myometrial cells (Awad et al., 1997). TGF-β exposure creates a caffeine-induced $^{45}Ca^{2+}$ efflux from these cultured cells that are normally unresponsive to caffeine, constitutively expressing only RyR3. This is consistent with the fact that the RyR3 isoform expressed in mink lung epithelial cells is caffeine insensitive (Giannini et al., 1992; Morgan and Gillespie, 1995). Curiously, caffeine (10 mM) amplifies the ryanodine-induced $^{45}Ca^{2+}$ efflux in permeabilized human myometrial cells, which may indicate the action of caffeine on the RyR1 isoform to promote the actions of ryanodine on P_o (Lynn et al., 1995).

In β-escin-permeabilized guinea pig mesenteric artery and longitudinal ileum smooth muscles, caffeine causes a contractile activity and Ca^{2+} transient that is accompanied by STOC through BK channels (Imaizumi et al., 1993, 1996). Interestingly, MBED, a compound structurally related to caffeine (see *Section II.B.2.a.*) and originally shown to be a potent releaser of Ca^{2+} from skeletal muscle microsomes (Seino et al., 1991) and to bind to RyR like caffeine (Fang et al., 1993; Adachi et al., 1994), fails to activate Ca^{2+} transients or contractile activity, even at high concentrations (up to 300 μM), despite the fact that it activates BK channels (at 30 μM) like caffeine (5–10 mM) (Imaizumi et al., 1993, 1996). The basis for these contrasting profiles was recently elucidated using confocal Ca^{2+} imaging and whole-cell voltage-clamp methods in guinea pig urinary bladder isolated smooth muscle cells (Ohi et al., 2001a). It was shown that MBED increases $[Ca^{2+}]_{cyt}$, mainly in the subplasmalemmal space synchronously with BK channels activation. This suggests that MBED selectively induces superficial SR Ca^{2+} release that activates BK channels but does not stimulate the contractile apparatus. Since MBED does not directly activate BK channels (Imaizumi et al., 1996), it is likely that this selective action is due to its high lipophilicity compared with caffeine that may concentrate it in the junctional SR areas (see *Section I.B.*) (Ohi et al., 2001a)—this is consistent with the longer exposure of isolated smooth muscle cells (2 min versus few seconds) required to decrease the amount of Ca^{2+} releasable by a subsequent exposure to caffeine (Ohi et al., 2001a).

c. Selectivity. Caffeine has several nonselective effects in smooth muscle. First, the SR Ca^{2+} release induced by $InsP_3$ could be inhibited by caffeine, as shown in permeabilized A7r5 cells (Missiaen et al., 1994). However, in these cells, caffeine does not affect the binding of $InsP_3$ to its purified receptor, isocaffeine (differing from caffeine by the position of one methyl group) is ineffective in inhibiting $InsP_3$-induced SR Ca^{2+} release, and ATP prevents the inhibitory effect of caffeine. This suggests that caffeine has to bind to a specific site on the $InsP_3R$ different from that of $InsP_3$ but very likely that of ATP, given the structural resemblance of the two

molecules. Caffeine binding at this latter site probably induces a conformational change in the $InsP_3R$ modifying its gating properties and inhibiting its opening upon $InsP_3$ binding, hence inhibiting IICR. Consistent with these findings, caffeine decreases the P_o of purified $InsP_3R$ reconstituted into planar lipid bilayers without reducing specific [^{3}H]$InsP_3$ binding to its receptor (Bezprozvanny et al., 1994).

Second, caffeine can inhibit plasmalemmal Ca_L in cultured myometrial cells from pregnant rats (Martin et al., 1989). In these cells, caffeine inhibits the depolarization-induced Ca^{2+} current with an IC_{50} value of 35 mM. This effect shows no use-dependence, and caffeine does not alter the steady-state inactivation of the Ca^{2+} current. Furthermore, caffeine inhibits the specific binding of [^{3}H]isradipine, a specific Ca_L blocker, to myometrial membranes with a similar IC_{50} value without altering the dissociation constant. Caffeine also causes a rapid and reversible concentration-dependent (1 to 30 mM) blockade of the Ba^{2+} current (occurring through Ca_L) in freshly isolated smooth muscle cells from the rabbit ear artery (Hughes et al., 1990). This effect has no voltage- or use-dependence, and caffeine does not alter the steady-state inactivation of the Ba^{2+} current. Also, inhibition of the Ba^{2+} current is unaffected by ryanodine and intracellular Ca^{2+} buffering with EGTA or 1,2-bis(*o*-aminophenoxy)ethane-*N*,*N*,*N*′*N*′-tetraacetic acid. The effect on the Ba^{2+} current is not due to caffeine-induced cAMP phosphodiesterase (PDE) inhibition (Poch and Umfahrer, 1976), as nonmethylxanthine cAMP PDE inhibitors do not inhibit the Ba^{2+} current. These findings are consistent with data obtained in freshly isolated smooth muscle cells from the guinea pig ileum (Zholos et al., 1991), where caffeine (10 mM) substantially inhibits depolarization pulse-induced Ca^{2+} currents. This latter effect occurs in a biphasic manner: a transient component, associated with Ca^{2+}-dependent inactivation of $Ca^{2+}{}_L$ resulting from SR Ca^{2+} release, and a tonic component. This latter tonic component is not due to activation of additional ionic currents of opposite direction or to inhibition of PDE activity, and it is unaffected by $Ca^{2+}{}_{cyt}$ buffering by EGTA, RyR blockers procaine and ruthenium red, or by ryanodine. In summary, results obtained in three different types of smooth muscles suggest that caffeine can block Ca_L by specifically occupying a binding site on the channel independently of its SR Ca^{2+} releasing ability or of its potential cAMP PDE inhibition.

Third, caffeine can activate a plasmalemmal Ca^{2+}-permeant nonselective cation channel as shown in the freshly isolated toad gastric smooth muscle cells (Guerrero et al., 1994). Current through such a channel (~20% of this current was estimated to be carried by Ca^{2+}) is elicited by caffeine (20 mM) in 85% of the cells studied; ryanodine only partially prevents the increase in $[Ca^{2+}]_i$ accompanying exposure to caffeine. Almost complete blockade of the current and the associated $[Ca^{2+}]_{cyt}$ increase occurs with Gd^{3+}, a nonselective cation channel and Ca_L blocker, or by decreasing the Ca^{2+} influx electrochemical driving force. Intracellular Ca^{2+} buffering with 1,2-bis(*o*-aminophenoxy)ethane-*N*,*N*,*N*′*N*′-tetraacetic acid does not prevent the activation of the current by caffeine, although this maneuver eliminates the associated $[Ca^{2+}]_{cyt}$ increase. Finally, the cAMP PDE-resistant cAMP analog 8-bromo-cAMP is not able to induce the current, nor is it able to inhibit the current activation by caffeine. These results suggest that caffeine can activate a plasmalemmal nonselective cation channel independent of its SR Ca^{2+}-releasing ability or of its potential cAMP PDE inhibition. It has been proposed (Guerrero et al., 1994) that this proceeds either through a direct interaction between caffeine and the channel or through a linkage between RyR on the peripheral SR and the channel. Caffeine then acts on the latter indirectly through its direct interaction with the RyR. Whether this channel or its analog exists in mammalian smooth muscle is unknown. Related to this observation, caffeine can increase a voltage-sensitive Ca^{2+} influx in freshly isolated guinea pig jejunal smooth muscle cells (Pacaud and Bolton, 1991b). However, the identity of the plasmalemmal structure involved in this effect of caffeine is unknown.

Fourth, caffeine directly inhibits the contractile apparatus in Triton X-100-permeabilized chicken gizzard smooth muscle (Ozaki et al., 1990). In this tissue, caffeine (1 to 40 mM) inhibits the contractile activity induced by 3 μM of free Ca^{2+}. These concentrations of caffeine also inhibit the phosphorylation of the regulatory 20-kDa myosin light chain (LC_{20}) in native actomyosin preparations. LC_{20} steady-state phosphorylation is the result of the activity ratio of myosin light chain kinase and myosin light chain phosphatase (MLCP), and Ca^{2+}-induced LC_{20} phosphorylation is triggered by activation of MLCK through binding of Ca^{2+}-activated calmodulin (Walsh, 1994). However, calmodulin activity is not affected by 20 mM of caffeine. Likewise, time-dependent dephosphorylation of LC_{20} upon removal of Ca^{2+}, an indicator of MLCP activity, is not affected by caffeine. These results suggest that caffeine inhibits MLCK directly. Caffeine also inhibits the Ca^{2+}-independent contractile activity in thiophosphorylated tissue, where contractile activity is due to the irreversible thiophosphorylation of LC_{20} (MLCP cannot hydrolyze thiophosphate bonds). Thus, caffeine also inhibits the basic actin-myosin interactions leading to force production.

In contrast, data obtained in saponin-permeabilized guinea pig mesenteric artery shows that caffeine (25 mM) does not alter either the minimum free $[Ca^{2+}]$ required to induce contractile activity, the maximal Ca^{2+}-induced contractile activity, or the slope of the free $[Ca^{2+}]$-force relationship (Itoh et al., 1981). Likewise, caffeine (5 mM) does not alter the free $[Ca^{2+}]$-force relationship in saponin-permeabilized porcine coronary artery (Itoh et al., 1982a). However, caffeine (10 mM)

slightly suppresses contractile activity of saponin-permeabilized rabbit mesenteric artery (Itoh et al., 1983), and high concentrations of caffeine (50 mM) inhibit the maximal Ca^{2+}-induced contractile activity in saponin-permeabilized longitudinal myometrial smooth muscle from pregnant rats (Savineau et al., 1988). It is possible that the inhibitory effects of caffeine reported in chicken gizzard smooth muscle are avian-specific and/or variable among mammalian smooth muscles.

It is unlikely that inhibition of contractile activity with caffeine is due to inhibition of cAMP PDE, although cAMP concentration was increased by caffeine (≤5 mM) during relaxation of intact gizzard smooth muscle (Ozaki et al., 1990). cAMP-induced relaxation of phenylephrine- or histamine-induced contractile activity in the porcine carotid artery is not associated with an alteration of the Ca^{2+} dependence of LC_{20} phosphorylation or the LC_{20} phosphorylation dependence of force production (McDaniel et al., 1991).

It should be mentioned that caffeine could affect other molecular targets such as 5′-nucleotidase (inhibition), adenosine receptors (nonselective antagonism), and GABA/benzodiazepine receptors (antagonism) (Sawynok and Yaksh, 1993), although the significance of these effects in smooth muscle preparations is not likely to be significant.

Caffeine also has secondary effects in smooth muscle either directly associated with Ca^{2+} released from the SR or associated with the subsequent Ca^{2+} depletion of the SR. First, caffeine increases $[Ca^{2+}]_{cyt}$ in the subplasmalemmal space. For instance, the $[Ca^{2+}]_{cyt}$ increase induced by caffeine (20 mM) through SR Ca^{2+} release in the freshly isolated toad gastric smooth muscle cell rises ~15 times faster as reported by the membrane-associating low-affinity fluorescent Ca^{2+} probe FFP-18 (>65% being located near or at the plasmalemma) than as reported by fura-2 (uniformly distributed throughout the cytoplasm) (Etter et al., 1996). Also, $[Ca^{2+}]_{cyt}$ reported by FFP-18 reaches levels about 3 times higher than that reported by fura-2. In freshly isolated bovine, porcine, and guinea pig coronary artery smooth muscle cells (Stehno-Bittel and Sturek, 1992; Ganitkevich, 1996), the K_{Ca}-mediated current was used to report subplasmalemmal $[Ca^{2+}]_{cyt}$. It was monitored simultaneously with fura-2 "global" $[Ca^{2+}]_{cyt}$ signals. It was shown that caffeine-induced (5 or 10 mM) SR Ca^{2+} release raises K_{Ca}-mediated current faster than the fura-2 signal. The current also peaks and decays faster. This could be interpreted as a faster caffeine-induced Ca^{2+} release from the peripheral SR, because caffeine reaches peripheral SR before it can stimulate central SR (Ganitkevich, 1996). The transient increase in K_{Ca}-mediated current could explain the transient plasmalemmal hyperpolarization associated with exposure to caffeine (10 mM) (Itoh et al., 1992). It also reflects the potential ability of caffeine to activate plasmalemmal Ca^{2+}-dependent processes through Ca^{2+} release from the peripheral SR. Currents mediated by Cl_{Ca} (for review, see Carl et al., 1996) and Ca^{2+}-activated nonspecific cation channels (Loirand et al., 1991; Janssen and Sims, 1992; Sims, 1992; Wang and Kotlikoff, 1997) are transiently induced by caffeine in vascular and visceral smooth muscle cells. Caffeine also transiently inhibits $Ca^{2+}{}_L$-mediated currents in freshly isolated smooth muscle cells from the guinea pig ileum (Zholos et al., 1991), an effect that is inhibited by the RyR blockers procaine and ruthenium red, suggesting that this transient inhibition of $Ca^{2+}{}_L$-mediated current is due to Ca^{2+}-dependent inactivation of $Ca^{2+}{}_L$ caused by the caffeine-induced SR Ca^{2+} release.

Second, a long exposure time to caffeine (more than several minutes) prevents access of Ca^{2+} influx to the myofilaments in the porcine carotid artery (Rembold et al., 1995). In this tissue, caffeine (20 mM) first induces synchronized transient increases in aequorin-reported $[Ca^{2+}]_{cyt}$, fura-2-reported $[Ca^{2+}]_{cyt}$, LC_{20} phosphorylation, and force peaking within 1.5 min. Both the aequorin and the fura-2 signals decline to steady-state levels within 10 min of exposure to higher than resting values, whereas LC_{20} phosphorylation and force go back to resting values. The transient in aequorin signal is larger than that in fura-2 signal. After 10 min of exposure to caffeine, the tissue was depolarized in the presence of caffeine for 10 more minutes. In the presence of caffeine (20 mM), high $[K^+]$-induced (109 mM) depolarization lead to Ca^{2+} influx through $Ca^{2+}{}_L$ associated with a maintained increase in the aequorin signal but in only a transient increase in the fura-2 signal. This is not accompanied by LC_{20} phosphorylation of force production. However, withdrawal of caffeine leads to an increase in fura-2 signal within 5 min to a steady-state level comparable to that reached by the transient peak initially induced, whereas the aequorin signal is not significantly altered. Also, within 10 min, LC_{20} phosphorylation and force increase to steady-state levels. Based on these observations, the authors proposed that a ratio of the aequorin and fura-2 light signals could reflect the relative spatial heterogeneity of $[Ca^{2+}]_{cyt}$ distribution within the smooth muscle cells; the aequorin signal would report local changes in $[Ca^{2+}]_{cyt}$, whereas fura-2 would report average changes in $[Ca^{2+}]$i, assuming that both Ca^{2+} probes are distributed in the same tissue volume and that the cellular responses across the tissue are synchronized and identical (Rembold et al., 1995). The following scheme is suggested by the results: 1) the initial transient increase in $[Ca^{2+}]_{cyt}$ induced by caffeine promotes LC_{20} phosphorylation and subsequent force production; 2) the sustained increase in $[Ca^{2+}]_{cyt}$ persisting after the fading of both LC_{20} phosphorylation and force could be due to persistent leakage of Ca^{2+} taken up by the SR caused by caffeine-promoted opening of RyR (and also potentially to stimulated Ca^{2+} influx indirectly induced by caffeine, see above); 3) the increase in the aequorin/fura-2 ratio accompanying these events

TABLE 5

Effective concentrations of caffeine and 9-methyl-7-bromoeudistomin D (MBED) in smooth muscle

Tissue	Animal Species	Experimental Details (Preparation; Measurement Method; Measured Response)	Effective Concentrations of Caffeine and MBED	Reference
Airways	Cattle	Isolated smooth muscle cells; fura-2 cellular loading, fluorometry; $[Ca^{2+}]_{cyt}$	10 mM	Ethier and Madison, 2002
Airways	Cattle	Isolated smooth muscle cells; fura-2 cellular loading, fluorometry; $[Ca^{2+}]_{cyt}$	10 mM	Bazan-Perkins et al., 2001
Airways	Human	Isolated smooth muscle cells; fura-2 cellular loading, fluorometry; $[Ca^{2+}]_{cyt}$	10 mM	Ethier and Madison, 2002
Airways	Human	Isolated α-toxin-permeabilized strips; isometric dynamometry; contractile activity	30 mM	Iizuka et al., 1998
Anococcygeus	Mouse	Isolated smooth muscle cells; whole-cell patch-clamping; $I_{Cl(Ca)}$, I_{DOC}	10 mM	Wayman et al., 1998
Anococcygeus	Mouse	Isolated smooth muscle cells; whole-cell patch-clamping; $I_{Cl(Ca)}$, I_{DOC}	10 mM	Wayman et al., 1997
Aorta	Guinea pig	Isolated α-toxin-permeabilized strips; isometric dynamometry; contractile activity	20 mM	Nixon et al., 1994
Aorta	Pig	Microsomes, F3 microsomal membranes fraction; inorganic phosphate-release assay; Ca^{2+}-ATPase activity	20 mM	Luo et al., 2000
Aorta	Rabbit	Isolated intact or saponin-permeabilized smooth muscle cells; mag-fura-2 cellular loading, fluorometry; $[Ca^{2+}]_{SR}$, $[Ca^{2+}]_{mito}$	10–20 mM	Gurney et al., 2000
Aorta	Rabbit	Isolated endothelium-denuded strips; fura-2-cellular loading, fluorometry, isometric dynamometry; $[Ca^{2+}]_{cyt}$, contractile activity	10 mM	Ahn and Karaki, 1988
Aorta	Rabbit	Isolated rings; isometric dynamometry; contractile activity	20 mM	Luo et al., 2000
Aorta	Rat	Microsomes; $^{45}Ca^{2+}$ loading; Ca^{2+} fluxes	20 mM	Yusufi et al., 2002
Aorta	Rat	Isolated cultured saponin-permeabilized smooth muscle cells; $^{45}Ca^{2+}$ cellular loading; Ca^{2+} fluxes	30 mM	Yamamoto et al., 1991
Aorta	Rat	Isolated smooth muscle cells; fura-2 cellular loading, epifluorescence microscopy; $[Ca^{2+}]_{cyt}$ imaging	5–40 mM	Vallot et al., 2001
Aorta	Rat	Isolated endothelium-denuded strips; fura-2 cellular loading, fluorometry, isometric dynamometry; $[Ca^{2+}]_{cyt}$, contractile activity	20 mM	Sato et al., 1988
Basilar artery	Rabbit	Isolated endothelium-denuded strips; isometric dynamometry; contractile activity	10 mM	Szado et al., 2001
Carotid artery	Rat	Isolated endothelium-denuded strips; isometric dynamometry; contractile activity	20 mM	Nomura and Asano, 2000
Cerebral artery	Mouse	Isolated smooth muscle cells and segments, phospholamban-knockout mice; whole-cell amphotericin B-perforated patch-clamping, fura-2 or fluo-3 cellular loading, confocal fluorescence microscopy; I_{BK}, $[Ca^{2+}]_{cyt}$	10 mM	Wellman et al., 2001
Colon	Guinea pig	Isolated smooth muscle cells; whole-cell patch-clamping, fluo-3 cellular loading, fluorometry or wide-field fluorescence digital imaging; I_{Ca}, $[Ca^{2+}]_{cyt}$, $[Ca^{2+}]_{cyt}$ imaging	10 mM	Bradley et al., 2003
Colon	Guinea pig	Isolated smooth muscle cells; whole-cell patch-clamping, fluo-3 or fura-2 cellular loading, fluorometry; I_{Ca}, $[Ca^{2+}]_{cyt}$	10 mM	Bradley et al., 2002
Colon	Guinea pig	Isolated smooth muscle cells; whole-cell patch-clamping, fluo-3 cellular loading, epifluorescence microscopy; membrane currents, $[Ca^{2+}]_{cyt}$	10 mM	Flynn et al., 2001
Colon	Mouse	Isolated smooth muscle cells; fluo-3 cellular loading, confocal fluorescence microscopy; $[Ca^{2+}]_{cyt}$ imaging	1 mM	Bayguinov et al., 2001
Colon	Mouse	Isolated smooth muscle cells; fluo-3 cellular loading, confocal fluorescence microscopy; $[Ca^{2+}]_{cyt}$ imaging	1 mM	Bayguinov et al., 2000
Colon	Guinea pig	Isolated smooth muscle cells; fluo-3 cellular loading, wide-field fluorescence digital imaging; $[Ca^{2+}]_{cyt}$ imaging	10 mM	McCarron et al., 2004
Coronary artery	Cattle	Microsomal membranes stripped or not of FKBP-12.6, reconstituted into planar lipid bilayers; bilayer clamp amplification; single Ca^{2+} channel currents	1–5 mM	Li et al., 2001
Coronary artery	Dog	Isolated fibers; isometric dynamometry; contractile activity	25 mM	Imai et al., 1984
Coronary artery	Pig	Isolated intact or saponin-permeabilized smooth muscle cells; quin-2 cellular loading, $^{45}Ca^{2+}$ cellular loading (intact or permeabilized); cellular Ca^{2+} fluxes, Ca^{2+} fluxes from intracellular stores, $[Ca^{2+}]_{cyt}$	20 mM	Ueno et al., 1987
Coronary artery	Pig	Isolated smooth muscle cells; fura-2 cellular loading, fluorometry; $[Ca^{2+}]_{cyt}$	5 mM	Heaps et al., 2001
Cremaster muscle arterioles	Rat	Isolated, cannulated and pressurized endothelium-denuded segments; fura-2 cellular loading, fluorometry, diameter monitoring by video microscopy; $[Ca^{2+}]_{cyt}$, contractile activity	20 mM	Potocnik and Hill, 2001
Esophagus	Human	Isolated smooth muscle cells; fura-2 cellular loading, fluorometry; $[Ca^{2+}]_{cyt}$	5 mM	Sims et al., 1997
Femoral artery	Rabbit	Isolated endothelium-denuded rings; isometric dynamometry; contractile activity	20 mM	Jezior et al., 2001
Femoral artery	Rat	Isolated endothelium-denuded strips; isometric dynamometry; contractile activity	20 mM	Asano and Nomura, 2001
Femoral artery	Rat	Isolated endothelium-denuded strips; isometric dynamometry; contractile activity	20 mM	Nomura and Asano, 2000
Gall bladder	Guinea pig	Isolated smooth muscle cells; whole-cell amphotericin B-perforated patch-clamping; I_{BK}	250 μM and 1 mM	Pozo et al., 2002
Ileum	Guinea pig	Isolated intact smooth muscle cells and β-escin-permeabilized strips; whole-cell and outside-out patch-clamping, indo-1 cellular loading, fluorometry, isometric dynamometry; I_{BK}, STOCs, $[Ca^{2+}]_{cyt}$, contractile activity	3–30 mM 30 and 300 μM (MBED)	Imaizumi et al., 1996
Ileum	Guinea pig	Isolated α-toxin-permeabilized strips; isometric dynamometry; contractile activity	30 mM	Iizuka et al., 1998
Ileum (circular layer)	Guinea pig	Isolated β-escin-permeabilized strips; isometric dynamometry; contractile activity	20 mM	Fukami et al., 1993
Mesenteric artery	Guinea pig	Isolated smooth muscle cells; microelectrode, alumina adsorption; membrane potential, excitatory junction potential	10 μM–5 mM	Fujii et al., 1985
Mesenteric artery	Rabbit	Isolated saponin-permeabilized strips; isometric dynamometry; contractile activity	3 and 25 mM	Kanmura et al., 1989
Mesenteric artery	Rat	Isolated cultured smooth muscle cells; furaptra cellular loading, fluorometry; $[Ca^{2+}]_{SR}$	10 mM	Golovina and Blaustein, 1997
Mesenteric artery	Rat	Isolated endothelium-denuded strips; fura-2 cellular loading, fluorometry, isometric dynamometry; $[Ca^{2+}]_{cyt}$, contractile activity	2 and 20 mM	Akata et al., 2001
Mesenteric artery	Rat	Isolated endothelium-denuded strips; isometric dynamometry; contractile activity	20 mM	Nomura and Asano, 2000
Mesenteric resistance arteries	Rat	Isolated smooth muscle cells; fluo-4 cellular loading, confocal fluorescence microscopy; $[Ca^{2+}]_{cyt}$ imaging	10 mM	Zang et al., 2001
Mesenteric resistance arteries	Rat	Isolated endothelium-denuded strips; fura-2 cellular loading, fluorometry, isometric dynamometry; $[Ca^{2+}]_{cyt}$, contractile activity	10 mM	Lagaud et al., 1999
Mesenteric resistance arteries	Rat	Isolated 3rd-order branches; isometric dynamometry; contractile activity	10 mM	Rubio et al., 2002
Mesenteric resistance arteries	Rat	Isolated, cannulated and pressurized endothelium-intact or -denuded segments isolated from 3rd- and 4th-order branches; fluo-4 cellular loading, confocal fluorescence microscopy, diameter monitoring by video microscopy; $[Ca^{2+}]_{cyt}$ imaging, contractile activity	20 μM	Lamont and Wier, 2004 [in press]
Mesenteric resistance arteries	Rat	Isolated, cannulated and pressurized vessels isolated from 5th-order branches; diameter monitoring by video microscopy; contractile activity	10 μM	Giulumian et al., 2000
Portal vein	Guinea pig	Isolated β-escin-permeabilized strips; isometric dynamometry; contractile activity	3–30 mM 30 and 300 μM (MBED)	Imaizumi et al., 1996

TABLE 5
Continued

Tissue	Animal Species	Experimental Details (Preparation; Measurement Method; Measured Response)	Effective Concentrations of Caffeine and MBED	Reference
Portal vein	Guinea pig	Isolated strips; isometric dynamometry; contractile activity	1–100 mM	Yagi et al., 1985
Portal vein	Guinea pig	Saponin-permeabilized smooth muscle cells and strips; microelectrode, isometric dynamometry; membrane potential, contractile activity	1–10 mM	Nanjo, 1984
Portal vein	Rabbit	Isolated smooth muscle cells; fluo-4 cellular loading, confocal fluorescence microscopy; $[Ca^{2+}]_{cyt}$ imaging	10 mM	Povstyan et al., 2003
Pulmonary artery	Cattle	Microsomes; extramicrosomal fluo-3 and fluorometry or $^{45}Ca^{2+}$ loading; Ca^{2+} fluxes	20 mM	Stout et al., 2002
Pulmonary artery	Rabbit	Isolated smooth muscle cells and endothelium-denuded strips; fura-2 cellular loading, fluorometry; $[Ca^{2+}]_{cyt}$, contractile activity	10 mM	Dipp et al., 2001
Pulmonary artery	Rabbit	Isolated smooth muscle cells and strips; double sucrose gap, microelectrode, isometric dynamometry; membrane potential, ionic current, contractile activity	0.1–10 mM	Ito et al., 1977
Pulmonary resistance arteries	Dog	Smooth muscle cells isolated from 3rd- and 4th-order branches; fura-2 and fluo-3 or fluo-4 cellular loading, fluorometry, confocal fluorescence microscopy; $[Ca^{2+}]_{cyt}$ imaging	10 mM	Janiak et al., 2001
Pulmonary resistance arteries	Rabbit	Isolated saponin-permeabilized smooth muscle cells; whole-cell patch-clamping; membrane potential	10 mM	Wilson et al., 2001
Pulmonary resistance arteries	Rabbit	Smooth muscle cells isolated from 3rd- and 4th-order branches; whole-cell patch-clamping, fura-2 cellular loading, fluorometry; membrane current, $[Ca^{2+}]_{cyt}$	5 mM	Smani et al., 2001
Pulmonary resistance arteries	Rat	Isolated endothelium-denuded rings; isometric dynamometry; contractile activity	10 mM	Dipp and Evans, 2001
Renal pelvis	Guinea pig	Isolated urothelium-denuded strips; microelectrode, isometric dynamometry; membrane potential, contractile activity	1 mM	Lang et al., 2002
Renal resistance arteries	Dog	Smooth muscle cells isolated from 3rd- and 4th-order branches; fura-2 and fluo-3 or fluo-4 cellular loading, fluorometry, confocal fluorescence microscopy; $[Ca^{2+}]_{cyt}$ imaging	10 mM	Janiak et al., 2001
Small intestine	Mouse	Isolated segments; microelectrode; slow wave frequency	5 mM	Malysz et al., 2001
Stomach	Mouse	Isolated smooth muscle cells and strips; whole-cell patch-clamping, fura-2 cellular loading, fluorometry, isometric dynamometry; I_{Cch}, STOCs, $[Ca^{2+}]_{cyt}$, contractile activity	5–10 mM	Tokutomi et al., 2001
Stomach (antrum)	Cattle	Microsomes; extramicrosomal fluo-3 and fluorometry or $^{45}Ca^{2+}$ loading; Ca^{2+} fluxes	20 mM	Stout et al., 2002
Stomach (antrum)	Rat	Isolated smooth muscle cells; Oregon Green BAPTA 5 cellular loading, fluorometry; $[Ca^{2+}]_{SR}$	10 mM	White and McGeown, 2002
Stomach (antrum, circular layer)	Guinea pig	Isolated smooth muscle bundles; microelectrode, fura-2 cellular loading, fluorometry; membrane potential, $[Ca^{2+}]_{cyt}$	1 mM	Fukuta et al., 2002
Stomach (antrum, circular layer)	Guinea pig	Isolated smooth muscle strips; isometric dynamometry; contractile activity	1–10 mM	Itoh et al., 1982b
Stomach (pylorus)	Guinea pig	Isolated smooth muscle strips; microelectrode; slow wave frequency	0.3–1 mM	Van Helden et al., 2000
Taenia caeci	Guinea pig	Isolated strips; isometric dynamometry; contractile activity	1–100 mM	Yagi et al., 1985
Taenia coli	Guinea pig	Isolated smooth muscle cells; whole-cell amphotericin B-perforated patch-clamping; STOCs	1 mM	Kong et al., 2000
Tail artery	Rat	Isolated freshly or cultured cells and endothelium-denuded rings; fura-2 cellular loading, fluorometry, isometric dynamometry; $[Ca^{2+}]_{cyt}$, contractile activity	5 mM	Dreja et al., 2001
Trachea	Cat	Isolated smooth muscle cells; whole-cell nystatin perforated patch-clamping; I_{Cch}	10 mM	Waniishi et al., 1998
Trachea	Cat	Isolated mucosa- and adventitia-denuded strips; double sucrose-gap, isometric dynamometry; membrane potential, contractile activity	10 mM	Ito and Itoh, 1984
Trachea	Cattle	Isolated smooth muscle cells and strips; fura-2 cellular loading, fluorometry, isometric dynamometry; $[Ca^{2+}]_{cyt}$, contractile activity	10 mM	Tao et al., 2000
Trachea	Dog	Isolated cultured smooth muscle cells; fura-2 cellular loading, fluorometry; $[Ca^{2+}]_{cyt}$	5 mM	Mitchell et al., 2000
Trachea	Rabbit	Isolated α-toxin-permeabilized strips; isometric dynamometry; contractile activity	30 mM	Iizuka et al., 1998
Ureter	Rat	Isolated smooth muscle cells; fluo-4 cellular loading, confocal fluorescence microscopy; $[Ca^{2+}]_{cyt}$ imaging	10–20 mM	Burdyga et al., 2003
Urinary bladder	Guinea pig	Isolated smooth muscle cells; whole-cell patch-clamping, fura-2 (for $[Ca^{2+}]_{cyt}$) or mag-fura-2 (for $[Ca^{2+}]_{SR}$) cellular loading, fluorometry; STOCs, $[Ca^{2+}]_{cyt}$, $[Ca^{2+}]_{SR}$	20 mM	Gomez-Viquez et al., 2003
Urinary bladder	Guinea pig	Isolated smooth muscle cells; whole-cell patch-clamping, fura-2 cellular loading, fluorometry; membrane potential, ionic current, $[Ca^{2+}]_{cyt}$	20 mM	Wu et al., 2002
Urinary bladder	Guinea pig	Isolated smooth muscle cells; fura-2 cellular loading, fluorometry; $[Ca^{2+}]_{cyt}$	20 mM	Rueda et al., 2002a
Urinary bladder	Guinea pig	Isolated smooth muscle cells; whole-cell patch-clamping, indo-1 cellular loading, confocal fluorescence microscopy; STOCs, $[Ca^{2+}]_{cyt}$ imaging	1–10 mM	Ohi et al., 2001a
Urinary bladder	Guinea pig	Isolated smooth muscle cells; whole-cell patch-clamping, indo-1 cellular loading, fluorometry; I_K, $[Ca^{2+}]_{cyt}$	20 mM	Weidelt and Isenberg, 2000
Urinary bladder	Guinea pig	Isolated smooth muscle cells; whole-cell and outside-out patch-clamping, indo-1 cellular loading, fluorometry; I_{BK}, STOCs, $[Ca^{2+}]_{cyt}$	3–30 mM 30 and 300 μM (MBED)	Imaizumi et al., 1996
Urinary bladder	Guinea pig	Isolated smooth muscle cells; indo-1 cellular loading, fluorometry; $[Ca^{2+}]_{cyt}$	10 mM	Ganitkevich and Isenberg, 1992
Urinary bladder	Rabbit	Isolated urothelium-denuded strips; isometric dynamometry; contractile activity	20 mM	Jezior et al., 2001
Uterus	Human	Isolated myometrial strips; indo-1 cellular loading, fluorometry, isometric dynamometry; $[Ca^{2+}]_{cyt}$, contractile activity	10 mM	Kupittayanant et al., 2002
Vas deferens	Guinea pig	Isolated smooth muscle cells; fura-2 cellular loading, fluorometry; $[Ca^{2+}]_{cyt}$	10 mM	White and McGeown, 2003
Vas deferens	Guinea pig	Isolated smooth muscle cells; inside-out patch-clamping; I_{BK}	5 mM	Ohi et al., 2001b
Vas deferens	Guinea pig	Isolated β-escin-permeabilized strips; isometric dynamometry; contractile activity	20 mM	Nixon et al., 1994
Vena cava (inferior)	Rabbit	Isolated smooth muscle cells and endothelium-denuded rings; fura-2 and fluo-3 cellular loading, fluorometry (fura-2), confocal fluorescence microscopy (fluo-3), isometric dynamometry; $[Ca^{2+}]_{cyt}$ imaging, contractile activity	0.5–50 mM	Ruehlmann et al., 2000
Ventricles	Rabbit	Isolated smooth muscle cells; fluo-3 cellular loading, confocal fluorescence microscopy; $[Ca^{2+}]_{cyt}$ imaging	10 mM	Haddock et al., 1999

suggests that caffeine induces a nonuniform increase in $[Ca^{2+}]_{cyt}$ in the smooth muscle cells; 4) the increase in $[Ca^{2+}]_{cyt}$ induced by high $[K^+]$ in the presence of caffeine occurs away from the myofilaments since it does not increase LC_{20} phosphorylation; 5) the sustained increase in the aequorin/fura-2 ratio upon exposure to high $[K^+]$ suggests further spatial heterogeneity in $[Ca^{2+}]_{cyt}$ distribution; and 6) upon removal of caffeine, the ratio value collapses because of an even redistribution of $[Ca^{2+}]_{cyt}$, which is associated with an increase of

$[Ca^{2+}]_{cyt}$ in the vicinity of the myofilaments as revealed by the increase in LC_{20} phosphorylation. Thus, these results suggest that caffeine can prevent access of Ca^{2+} to the myofilaments by localizing the increase in $[Ca^{2+}]_{cyt}$ at remote sites. This could explain the often observed dissociation between Ca^{2+} influx or $[Ca^{2+}]_{cyt}$ increase from LC_{20} phosphorylation and force production in the presence of caffeine (for review, see Karaki et al., 1997).

Third, caffeine could affect smooth muscle by depleting SR Ca^{2+}. For instance, spontaneous Ca^{2+}-activated currents mediated by K_{Ca} and Cl_{Ca}, termed STOCs and STICs (for spontaneous transient inward currents), respectively, are inhibited following caffeine-induced SR Ca^{2+} depletion in vascular and visceral smooth muscle cells (for review, see Carl et al., 1996). Inhibition of such spontaneous currents by caffeine leads to plasmalemmal depolarization and increased smooth muscle excitability (Itoh et al., 1981, 1982b; Savineau, 1988; Savineau and Mironneau, 1990). Caffeine-induced SR Ca^{2+} depletion can also lead to capacitative Ca^{2+} entry, a Ca^{2+} store depletion-activated Ca^{2+} influx (Janssen and Sims, 1993; Ohta et al., 1995).

Little information is available on MBED selectivity for RyR. However, it has been shown that its parent compound, bromo-eudistomin D (up to 30 μM), has no effect on the activity of skeletal muscle SERCA or Na^+/K^+-ATPase (Nakamura et al., 1986). On the other hand, it was shown that, in bovine aortic smooth muscle homogenates, [^{3}H]MBED has non-negligible soluble binding sites, suggesting that it may interact with non-RyR caffeine molecular targets such as phosphodiesterases (Adachi et al., 1994).

d. Use in Smooth Muscle Preparations. Caffeine has long been used to deplete SR Ca^{2+} stores in smooth muscle; this is frequently done in a Ca^{2+}-free medium containing Ca^{2+} chelators such as EGTA. The transient contractile response obtained under such conditions is a qualitative estimate of the average size of the Ca^{2+} stores in the SR, assuming a linear relationship between Ca^{2+} released from the SR and the size of the contractile activity. Effective concentrations for caffeine range from 5 to 25 mM (Table 5). The use of caffeine in smooth muscle comes with several concerns: 1) it inhibits PDE and therefore raises cAMP, 2) it inhibits voltage-gated Ca^{2+} entry and activates a nonspecific inward current, 3) it has the potential to augment capacitative Ca^{2+} entry by depletion of the SR, and 4) it can also redistribute Ca^{2+} within cells such that it predominately remains at superficial sites.

3. Ryanodine.

a. Source and Chemical Structure. Ryanodine is a complex polycyclic, polyhydroxylic diterpene (+)-ryanodol esterified at C3 with pyrrole-2-carboxylic acid (Fig. 14). Although this molecule is electrically neutral, it has a hydrophilic face with five hydroxyl groups at C2, C4, C6, C12, and C10 and a lipophilic surface defined by the isopropyl group and the hydrogens attached to C14, C20, C7, C8, and C21 (Sutko et al., 1997). Ryanodine is an alkaloid found in members of the genus *Ryania*, shrubs or slender trees growing in several tropical locations in Central and South America, including Trinidad and the Amazon basin (Sutko et al., 1997). In acidic medium, ryanodine dehydrates easily to give anhydroryanodine with loss of activity (Fig. 14).

b. Mechanism of Action. The pharmacology of ryanodine receptors has been elegantly reviewed by Guerrero-Hernandez et al. (2002). Ryanodine has complex effects on the conductance and gating of single RyR channels that are concentration-dependent (Sutko et al., 1997). At submicromolar concentrations, it has one of two effects. In the first instance, ryanodine increases channel activity to a full conductance state (Pessah and Zimanyi, 1991). Alternately, and more typically, ryanodine makes the channel partially conducting (Rousseau et al., 1987), and although multiple subconductance states have been observed (Ding and Kasai, 1996), the most common state is one near 50% full conductance (Sutko et al., 1997). Finally, at micromolar or greater concentrations, ryanodine induces the channel to adopt a closed state (Meissner, 1994). Micro- to millimolar concentrations of ryanodine induce a permanently closed state in RyR partially purified from canine and porcine aortic microsomal protein fractions and reconstituted into planar lipid bilayers (Herrmann-Frank et al., 1991), whereas a subconductance state is observed with lower concentrations of ryanodine (0.1–10 μM) in similar preparation from the bovine coronary arteries (Li et al., 2001). Higher concentrations of ryanodine (20 and 50 μM) close the channel. It is still unclear whether ryanodine modifies conductance by stabilizing the RyR channel in a specific conformation via allosteric effects or whether it physically interferes with the flux of ions through the pore of the channel (Sutko et al., 1997), although recent structure-activity data from experiments on the RyR2 channel favor an allosteric mechanism (Welch et al., 1997) as discussed below.

There is consensus that [^{3}H]ryanodine binds to high- (K_D ~ 1–10 nM) and low-affinity sites (K_D ~ 1–10 μM) on the RyR channel, likely localized to the C-terminal 76-kDa fragment of the receptor (Sutko et al., 1997). There is also agreement that high-affinity binding results in channel activation or subconductivity, whereas low-affinity binding leads to channel inhibition (Sutko et al., 1997). The density of [^{3}H]ryanodine binding is ~100 fmol/mg protein, although in the rat portal vein it is reported to reach nearly 6 pmol/mg protein (Boittin et al., 1999). In general, the RyR density in smooth muscle is about 10 times lower than that in striated muscle (Guerrero-Hernandez et al., 2002), this presumably being a reflection of a lower SR volume in smooth muscle. The binding of [^{3}H]ryanodine to smooth muscle microsomes is increased by agents that also modulate RyR activity, such as Ca^{2+}, caffeine, ATP, and pH, whereas it is decreased by

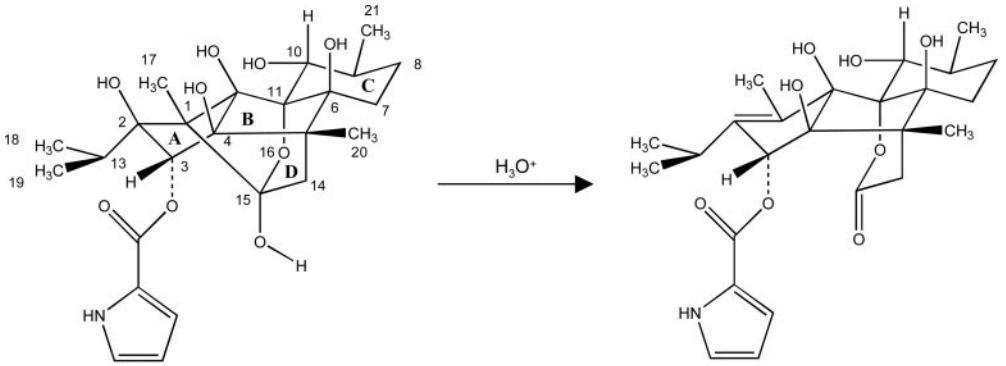

1 2

FIG. 14. Molecular structure of ryanodine (1) and anhydroryanodine (2). Adapted with permission from Sutko et al. (1997).

ruthenium red and Mg^{2+} (for review, see Guerrero-Hernandez et al., 2002).

Ryanodine-induced activation also exhibits use-dependence; high-affinity binding occurs in the RyR channel open state. Furthermore, there is suggestive evidence that the tetrameric form of the channel is required for high-affinity binding (Lai et al., 1989), consistent with a stoichiometry of 1 mol of [^{3}H]ryanodine/1 mol of RyR tetramer (Pessah and Zimanyi, 1991). In contrast, stoichiometries of either 3:1 (Lai et al., 1989) or 1:1 (Wang et al., 1993) have been reported for the low-affinity binding site.

These variable stoichiometries allows for at least two models of ryanodine binding to its receptor: the distinct site model and the interconvertible site model (Sutko et al., 1997). The distinct site model states that the two binding sites are physically distinct on the RyR tetramer in a 1:1 stoichiometry, with binding of ryanodine to the high-affinity site stabilizing the channel in a subconductance state, and subsequent binding of ryanodine to the low-affinity site leading to channel closure (Wang et al., 1993). Although both sites are distinct, it is proposed that ryanodine binding to the low-affinity site reduces the dissociation rate of ryanodine from the high-affinity site (Wang et al., 1993), although the nature of this interaction, be it steric or allosteric, has not been determined (Sutko et al., 1997). In contrast, the interconvertible site model envisions four initially identical (i.e., high-affinity) interacting binding sites per RyR tetramer that can be either high- or low-affinity sites; binding of ryanodine to one site exerts a negatively cooperative effect on the remaining sites, lowering their affinity. It has been shown that this decrease in affinity is equivalent among the three remaining sites, with channel closure requiring binding of ryanodine to all three (Carroll et al., 1991). Alternately, the decrease was proposed to be sequential, with binding of ryanodine to each site successively lowering the affinity of the remaining unbound sites, thus leading to four classes of sites with different K_D values, with binding to each site successively lowering channel conductance to reach closure once the four sites are occupied by ryanodine (Pessah and Zimanyi, 1991). It remains to be resolved how switching between conductance states occurs, as it may be an important regulator of the average quantity of Ca^{2+} released per unit of time by a RyR channel (Sutko et al., 1997).

In terms of SAR, naturally occurring ryanoids (i.e., ryanodine congeners) have been found to differ in their biological activity (Sutko et al., 1997), with the most interesting case being that of ester A, which has a methoxyl moiety instead of a hydroxyl in the 10-position (Fig. 14). Ryanodine ester A only activates the RyR channel at concentrations up to 3 mM (Sutko et al., 1990) and binds to the high-affinity site with a K_D of 110 nM (Welch et al., 1994), although its binding to the low-affinity site is unknown. Quantitative SAR analysis of various ryanoids has revealed that both physical bulk (van der Waals contacts in the pyrrole region) and electrostatic interactions (localized in the hydroxyl regions) correlate with high-affinity binding to the RyR channel (Welch et al., 1994). These correlations have led to a binding model for ryanodine with the pyrrole locus buried within the high-affinity binding site and 9- and 10-positions extending outside beyond the pyrrole carbonyl group (Welch et al., 1994) and possibly involving hydrogen bonding (Sutko et al., 1997). One end of ryanodine (3-position) appears to primarily determine binding affinity, whereas the opposite end (9- and 10-positions) seems to primarily control channel behavior (e.g., conductivity) (Sutko et al., 1997).

c. Selectivity. Although there are no RyR-isoform-specific ryanodine analogs, affinity of ryanoids for RyR2 is generally 2- to 3-fold higher than for RyR1 (ryanodine being close to 3-fold selective), with the most discriminating ryanoid reaching a 10-fold selectivity (Sutko et al., 1997).

d. Use in Smooth Muscle Preparations. Ryanodine is frequently used to deplete the SR by causing the Ca^{2+} release channels to remain in a semiconducting state. This leak of Ca^{2+} from the SR has several consequences, such as preventing the SR from storing any Ca^{2+} it may

TABLE 6
Effective concentrations of ryanodine in smooth muscle

Tissue	Animal Species	Experimental Details (Preparation; Measurement Method; Measured Response)	Effective Concentrations of Ryanodine	Reference
Airways	Mouse	Lung slices; Oregon Green cellular loading, confocal fluorescence microscopy; $[Ca^{2+}]_{cyt}$ imaging	200 μM	Bergner and Sanderson, 2002
Airways	Pig	Isolated intact or β-escin-permeabilized cells; fluo-3 cellular loading, confocal fluorescence microscopy; $[Ca^{2+}]_{cyt}$	20 μM	Pabelick et al., 2001a
Anococcygeus	Mouse	Isolated smooth muscle cells; whole-cell patch-clamping; I_{DOC}, $I_{Cl(Ca)}$	3 and 30 μM	Wayman et al., 1997
Anococcygeus	Mouse	Isolated smooth muscle cells and whole tissue; whole-cell patch-clamping, isometric dynamometry; I_{DOC}, $I_{Cl(Ca)}$, contractile activity	3–30 μM	Wayman et al., 1998
Aorta	Rabbit	Isolated intact or saponin-permeabilized smooth muscle cells; mag-fura-2 cellular loading, fluorometry; $[Ca^{2+}]_{SR}$, $[Ca^{2+}]_{mito}$	20 μM	Gurney et al., 2000
Aorta	Rat	Microsomes; $^{45}Ca^{2+}$ loading; Ca^{2+} fluxes	30 nM ($[^3H]$-ryanodine)	Yusufi et al., 2002
Aorta	Rat	Isolated endothelium-denuded rings; isometric dynamometry; contractile activity	30 μM	Low et al., 1993
Basilar artery	Mouse	Isolated smooth muscle cells; whole-cell nystatin perforated patch-clamping; I_{BK}	10 μM	Lohn et al., 2001
Basilar artery	Rabbit	Isolated smooth muscle cells and endothelium-denuded strips; fura-2 cellular loading, fluorometry, isometric dynamometry; $[Ca^{2+}]_{cyt}$, contractile activity	10 μM	Szado et al., 2001
Cerebellar artery	Rabbit	Isolated endothelium-intact or -denuded strips; isometric dynamometry; contractile activity	10 μM	Jewell et al., 2004
Cerebral artery	Human	Isolated smooth muscle cells; fluo-3 cellular loading, confocal fluorescence microscopy, isometric dynamometry; $[Ca^{2+}]_{cyt}$ imaging, contractile activity	10 μM	Wellman et al., 2002
Cerebral artery	Mouse	Isolated segments, phospholamban-knockout mice; fluo-3 cellular loading, confocal fluorescence microscopy; $[Ca^{2+}]_{cyt}$ imaging	10 μM	Wellman et al., 2001
Cerebral artery	Rabbit	Isolated endothelium-intact or -denuded strips; isometric dynamometry; contractile activity	10 μM	Jewell et al., 2004
Cerebral artery	Rat	Isolated, cannulated and pressurized segments; fluo-3 cellular loading, confocal fluorescence microscopy, diameter monitoring by video microscopy; $[Ca^{2+}]_{cyt}$ imaging, contractile activity	10 μM	Jaggar, 2001
Colon	Guinea pig	Isolated smooth muscle cells; whole-cell patch-clamping, fluo-3 cellular loading, epifluorescence microscopy; membrane currents, $[Ca^{2+}]_{cyt}$	50 μM	Flynn et al., 2001
Colon	Guinea pig	Isolated smooth muscle cells; whole-cell patch-clamping, fluo-3 or fura-2 cellular loading, fluorometry; I_{Ca}, $[Ca^{2+}]_{cyt}$	50 μM	Bradley et al., 2002
Colon	Mouse	Isolated smooth muscle cells; whole-cell amphotericin B-perforated patch-clamping, fluo-3 cellular loading, confocal fluorescence microscopy; STOCs, $[Ca^{2+}]_{cyt}$ imaging	10 μM	Bayguinov et al., 2000
Colon (circular layer)	Dog	Isolated non-inflamed and inflamed saponin-permeabilized smooth muscle cells; fura-2 cellular loading or $^{45}Ca^{2+}$ cellular loading, cell length monitoring by phase-contrast microscope; Ca^{2+} fluxes, $[Ca^{2+}]_{cyt}$, contractile activity	10 μM	Shi and Sarna, 2000
Coronary artery	Cattle	Microsomal membranes, stripped or not of FKBP-12.6, reconstituted into planar lipid bilayer; patch-clamping, bilayer clamp amplification; open channel probability (path clamping), single Ca^{2+} release channel currents (bilayer clamp amplification)	0.1–50 μM	Li et al., 2001
Coronary artery	Cattle	Isolated α-toxin-permeabilized smooth muscle cells; fura-2 cellular loading, fluorometry; $[Ca^{2+}]_{cyt}$	10 μM	Yu et al., 2000
Coronary artery	Cattle	Isolated cultured smooth muscle cells and microsomes, FKBP12.6-stripped; patch-clamping, bilayer clamp amplification; open channel probability (path clamping), single Ca^{2+} release channel currents (bilayer clamp amplification)	0.1 μM	Tang et al., 2002
Coronary artery	Cow	Isolated smooth muscle cells, and cannulated and pressurized endothelium-denuded rings; fura-2 cellular loading, fluorometry, diameter monitoring by video microscopy; $[Ca^{2+}]_{cyt}$, contractile activity	30 μM	Ge et al., 2003
Coronary artery	Human	Isolated smooth muscle cells; whole-cell nystatin perforated patch-clamping, fluo-3 cellular loading, confocal fluorescence microscopy; $I_{K(Ca)}$, $[Ca^{2+}]_{cyt}$ imaging	50 μM	Furstenau et al., 2000
Coronary artery	Rabbit	Isolated smooth muscle cells; fura-2 cellular loading, fluorometry; $[Ca^{2+}]_{cyt}$	5 μM	Kang et al., 2002
Esophagus	Human	Isolated smooth muscle cells and strips; fura-2 cellular loading, fluorometry, cell length monitoring by phase-contrast microscopy; $[Ca^{2+}]_{cyt}$, contractile activity	1 μM	Sims et al., 1997
Femoral artery	Rat	Isolated endothelium-denuded strips; fura-PE3 cellular loading, isometric dynamometry; $[Ca^{2+}]_{cyt}$, contractile activity	0.1–10 μM	Asano and Nomura, 2001
Gall bladder	Guinea pig	Isolated smooth muscle cells; whole-cell amphotericin B-perforated patch-clamping; I_{BK}	10 μM	Pozo et al., 2002
Ileum	Guinea pig	Isolated smooth muscle cells; whole-cell and outside-out patch-clamping; I_{BK}	10 μM	Imaizumi et al., 1996
Irideal arterioles	Rat	Isolated, cannulated and pressurized segments; diameter monitoring by video microscopy; contractile activity	10 μM	Haddock et al., 2002
Mesenteric arterioles	Rat	Isolated, cannulated and pressurized segments; fura-2 cellular loading, fluorometry, diameter monitoring by video microscopy; $[Ca^{2+}]_{cyt}$, contractile activity	10 μM	Watanabe et al., 1993
Mesenteric artery	Dog	Isolated endothelium-denuded rings; isometric dynamometry; contractile activity	30–100 μM	Low et al., 1992
Mesenteric resistance arteries	Rat	Isolated 3rd-order branches; isometric dynamometry; contractile activity	20 μM	Rubio et al., 2002
Mesenteric resistance arteries	Rat	Isolated smooth muscle cells; fluo-4 cellular loading, confocal fluorescence microscopy; $[Ca^{2+}]_{cyt}$ imaging	10 μM	Zang et al., 2001
Mesenteric resistance arteries	Rat	Isolated endothelium-denuded strips; isometric dynamometry; contractile activity	10 μM	Lagaud et al., 1999
Mesenteric resistance arteries	Rat	Isolated, cannulated and pressurized endothelium-intact or -denuded segments isolated from 3rd- and 4th-order branches; fluo-4 cellular loading, confocal fluorescence microscopy, isotonic dynamometry; $[Ca^{2+}]_{cyt}$ imaging, contractile activity	40 μM	Lamont and Wier, 2004 [in press]
Mesenteric resistance arteries	Rat	Isolated, cannulated and pressurized vessels isolated from 5th-order branches; diameter monitoring by video microscopy; contractile activity	10 μM	Giulumian et al., 2000
Portal vein	Rabbit	Isolated smooth muscle cells; fluo-4 cellular loading, confocal fluorescence microscopy; $[Ca^{2+}]_{cyt}$ imaging	1 μM	Gordienko et al., 2001
Pulmonary artery	Cattle	Microsomes; extramicrosomal fluo-3 and fluorometry or $^{45}Ca^{2+}$ loading; Ca^{2+} fluxes	10 nM–750 μM	Stout et al., 2002
Pulmonary artery	Rabbit	Isolated smooth muscle cells and endothelium-denuded strips; fura-2 cellular loading, fluorometry, isometric dynamometry; $[Ca^{2+}]_{cyt}$, contractile activity	10 μM	Dipp et al., 2001
Pulmonary artery	Rat	Physiological salt solution-perfused lungs; perfusion pressure; vascular bed resistance	10–300 μM	Morio and McMurtry, 2002
Pulmonary resistance arteries	Dog	Smooth muscle cells isolated from 3rd- and 4th-order branches; fura-2 and fluo-3 or fluo-4 cellular loading, fluorometry (fura-2), confocal fluorescence microscopy (fluo-3 and fluo-4); $[Ca^{2+}]_{cyt}$ imaging	10–300 μM	Janiak et al., 2001
Pulmonary resistance arteries	Rabbit	Isolated saponin-permeabilized smooth muscle cells; whole-cell patch-clamping; membrane potential	10 μM	Wilson et al., 2001

TABLE 6
Continued

Tissue	Animal Species	Experimental Details (Preparation; Measurement Method; Measured Response)	Effective Concentrations of Ryanodine	Reference
Pulmonary resistance arteries	Rat	Isolated endothelium-denuded rings; isometric dynamometry; contractile activity	10 μM	Dipp and Evans, 2001
Renal pelvis	Guinea pig	Isolated urothelium-denuded strips; microelectrode, isometric dynamometry; membrane potential, contractile activity	30 μM	Lang et al., 2002
Renal resistance arteries	Dog	Smooth muscle cells isolated from 3rd- and 4th-order branches; fura-2 and fluo-3 or fluo-4 cellular loading, fluorometry, confocal fluorescence microscopy; $[Ca^{2+}]_{cyt}$ imaging	10–300 μM	Janiak et al., 2001
Skeletal muscle arterioles	Rat	Isolated, cannulated and pressurized segments; fura-2 cellular loading, fluorometry, diameter monitoring by video microscopy; $[Ca^{2+}]_{cyt}$, contractile activity	10 μM	Watanabe et al., 1993
Small intestine	Mouse	Isolated segments; microelectrode; slow wave frequency	50 μM	Malysz et al., 2001
Stomach	Guinea pig	Isolated smooth muscle cells; whole-cell patch-clamping; $I_{K(Ca)}$	10 μM	Duridanova et al., 1996
Stomach	Mouse	Isolated smooth muscle cells; whole-cell patch-clamping, fura-2 cellular loading, fluorometry; I_{Cch}, STOCS, $[Ca^{2+}]_{cyt}$	1 μM	Tokutomi et al., 2001
Stomach	Rat	Isolated smooth muscle cells; microelectrode, fura-2 cellular loading, fluorometry; I_{Ca}, $[Ca^{2+}]_{cyt}$	10 μM	White and McGeown, 2000
Stomach (antrum)	Cattle	Microsomes; extramicrosomal fluo-3 and fluorometry or $^{45}Ca^{2+}$ loading; Ca^{2+} fluxes	10 nM–750 μM	Stout et al., 2002
Stomach (antrum, circular layer)	Guinea pig	Isolated smooth muscle bundles; microelectrode, fura-2 cellular loading, fluorometry; membrane potential, $[Ca^{2+}]_{cyt}$	10 μM	Fukuta et al., 2002
Taenia coli	Guinea pig	Isolated smooth muscle cells; whole-cell amphotericin B-perforated patch-clamping; STOCs	10 μM	Kong et al., 2000
Tail artery	Rat	Isolated freshly or cultured endothelium-denuded rings; fura-2 cellular loading, fluorometry, isometric dynamometry; $[Ca^{2+}]_{cyt}$, contractile activity	10 μM	Dreja et al., 2001
Testicular peritubules	Rat	Isolated saponin-permeabilized smooth muscle cells; fura-2 cellular loading, fluorometry; $[Ca^{2+}]_{cyt}$	5 μM	Barone et al., 2002
Trachea	Cat	Isolated smooth muscle cells; whole-cell nystatin perforated patch-clamping; I_{Cch}	4 μM	Waniishi et al., 1998
Trachea	Cattle	Isolated smooth muscle cells and strips; fura-2 cellular loading, fluorometry, isometric dynamometry; $[Ca^{2+}]_{cyt}$, contractile activity	30 μM	Tao et al., 2000
Trachea	Dog	Isolated cultured smooth muscle cells; fura-2 cellular loading, fluorometry; $[Ca^{2+}]_{cyt}$	50 μM	Mitchell et al., 2000
Trachea	Rabbit	Isolated α-toxin-permeabilized strips; isometric dynamometry; contractile activity	30 μM	Iizuka et al., 1998
Ureter	Guinea pig	Isolated α-toxin- or β-escin-permeabilized strips; isometric dynamometry; contractile activity	10 μM	Burdyga et al., 1998
Ureter	Rat	Isolated smooth muscle cells; fluo-4 cellular loading, confocal fluorescence microscopy; $[Ca^{2+}]_{cyt}$ imaging	50 μM	Burdyga et al., 2003
Ureter	Rat	Isolated smooth muscle cells; fluo-3 cellular loading, confocal fluorescence microscopy; $[Ca^{2+}]_{cyt}$ imaging	10 μM	Boittin et al., 2000
Ureter	Rat	Isolated α-toxin- or β-escin-permeabilized strips; isometric dynamometry; contractile activity	10 μM	Burdyga et al., 1998
Urinary bladder	Guinea pig	Isolated smooth muscle cells; whole-cell amphotericin B-perforated patch-clamping; I_{BK}, I_{SK}, I_{Ca}	10 μM	Herrera and Nelson, 2002
Urinary bladder	Guinea pig	Isolated smooth muscle cells; fura-2 cellular loading, fluorometry; $[Ca^{2+}]_{cyt}$	10 μM	Rueda et al., 2002b
Urinary bladder	Guinea pig	Isolated smooth muscle cells; whole-cell and outside-out patch-clamping; I_{BK}	10 μM	Imaizumi et al., 1996
Urinary bladder	Guinea pig	Isolated smooth muscle cells; whole-cell amphotericin B-perforated patch-clamping, fluo-3 cellular loading, confocal fluorescence microscopy; I_{BK}, $[Ca^{2+}]_{cyt}$ imaging	10 μM	Herrera et al., 2001
Urinary bladder	Mouse	Isolated smooth muscle cells; fluo-4 cellular loading, confocal fluorescence microscopy; $[Ca^{2+}]_{cyt}$ imaging	10 μM	Ji et al., 2002
Uterus	Human	Isolated myometrial strips; indo-1 cellular loading, fluorometry, isometric dynamometry; $[Ca^{2+}]_{cyt}$, contractile activity	50 μM	Kupittayanant et al., 2002
Vas deferens	Guinea pig	Isolated smooth muscle cells; fluo-4 cellular loading, confocal fluorescence microscopy; local $[Ca^{2+}]_{cyt}$ imaging	100 μM	White and McGeown, 2003
Vena cava (inferior)	Rabbit	Isolated smooth muscle cells, fluo-3 cellular loading, confocal fluorescence microscopy; local $[Ca^{2+}]_{cyt}$ imaging	100 μM	Ruehlmann et al., 2000

accumulate (loss of buffering activity), loss of K_{Ca} regulation by Ca^{2+} sparks, and loss of regulation of Cl_{Ca} activity. Ryanodine effectively depletes caffeine-sensitive Ca^{2+} stores in both isolated smooth muscle cells and intact smooth muscle. Ryanodine actions are complicated by having distinct actions on the RyR that are concentration-dependent, such that at low-intermediate concentrations (submicromolar/micromolar range) the channel is locked in a semiconducting state, whereas at higher concentrations the channel remains in a closed state (Table 6). A comprehensive review of ryanodine receptor properties and functions has recently been published (Guerrero-Hernandez et al., 2002).

4. Procaine.

a. Source and Chemical Structure. Procaine is a synthetic amphiphilic (pK_a = 8.9) local anesthetic tertiary amine, which exists predominantly in its cationic (versus neutral) form at physiological pH (Burdyga and Magura, 1986) (Fig. 15). It was originally derived from cocaine (Fig. 15), which was used medicinally for its local anesthetic and vasoconstrictive effects in an attempt to isolate the anesthesiophoric part of the latter molecule to eliminate its undesirable hallucinogenic and euphoric effects (Virji et al., 1969). It was initially found that the cocaine complex ring system was not essential to its local anesthetic activity (Virji et al., 1969). By comparing results obtained from alkyl para-aminobenzoates with the degradation residues of cocaine, the anesthesiophoric group was identified as the aromatic acid esterified with a tertiary amino alcohol. This led to the synthesis of procaine.

b. Mechanism of Action. Procaine was one of the first agents to be identified as an inhibitor of caffeine and CICR from the skeletal muscle SR (Feinstein, 1963). Its mechanism of action has been characterized on partially purified RyR from dog cardiac muscle microsomes reconstituted into planar lipid bilayers (Zahradnikova and Palade, 1993). In contrast with other RyR inhibitors, it does not reduce single-channel conductance, nor does it significantly shorten the channel P_o, but rather it in-

creases the longest closed time. This suggests that procaine interacts selectively with a closed state of the channel rather than with an open state, consistent with computer simulation of RyR gating (Zahradnikova and Palade, 1993). This mechanism of action is also consistent with the long-known inhibitory effect of procaine on caffeine-induced contractile activity in vascular and visceral smooth muscles. For instance, in the porcine coronary artery, procaine (5 mM) inhibits caffeine (20 mM)-induced contractile activity of isolated strips in the absence of extracellular Ca^{2+} (Itoh et al., 1982a) and inhibits (1–10 mM) the associated reduction in cellular Ca^{2+} content in saponin-permeabilized smooth muscle cells (Ueno et al., 1987). Likewise, in guinea pig taenia caeci, procaine (1 mM) inhibits caffeine-induced (1–25 mM) contractile activity in the absence of extracellular Ca^{2+} (Yagi et al., 1985), consistent with the inhibition of CICR rate by procaine (millimolar concentrations) in fura-2-loaded saponin-permeabilized smooth muscle fiber bundles (Iino, 1989).

c. Selectivity. Procaine has no effect on the pCa-force relationship in permeabilized arterial smooth muscle cells (Itoh et al., 1981, 1982b), and at up to 10 mM, it does not affect basal permeability of intracellular Ca^{2+} stores as shown in dispersed and saponin-permeabilized porcine coronary artery smooth muscle cells (Ueno et al., 1987). Likewise, procaine (at up to 1 mM) does not affect PMCA activity in membranes from pig coronary artery and human myometrium, in contrast with its concentration-dependent (at 0.1–1 mM) inhibition of human erythrocyte PMCA (Popescu et al., 1987).

However, in reserpinized rat vas deferens, procaine (10 mM) prevents NE-induced increase in Ca^{2+} efflux (NE = 100 μM), increases tissue Ca^{2+} content (NE = 10 μM), and completely inhibits NE-induced (10 μM) contractile activity in the absence of extracellular Ca^{2+} (Khoyi et al., 1993). Similarly, in the absence of extracellular Ca^{2+}, procaine (1 mM) inhibits Cch-induced (1–1000 μM) guinea pig taenia caeci contractile activity (Yagi et al., 1985). The same concentration of procaine also inhibits Ach-induced (10 μM) contractile activity of the porcine coronary artery in absence of extracellular Ca^{2+}. Furthermore, in dispersed and saponin-permeabilized smooth muscle cells from this blood vessel, the reduction in cellular Ca^{2+} content induced by Ach (3 μM) is prevented by 1 mM of procaine (Ueno et al., 1987). This is consistent with the complete inhibition by procaine (5 mM) of the intracellular Ca^{2+} transients elicited by Ach (10 μM) in intact cells (Ueno et al., 1987).

Although all of the above effects of procaine on agonist-induced responses might be related to the fact that, as shown in permeabilized coronary artery cells, it concentration-dependently (1–10 mM) inhibits $InsP_3$-induced (3 μM) release of cellular Ca^{2+} content (although with only partial effectiveness (Ueno et al., 1987)), they are more likely due to inhibition of agonist-induced $InsP_3$ production. Indeed, in intact strips of porcine coronary artery, procaine (1–10 mM) concentration-dependently inhibits and eventually completely suppresses Ach-induced (10 μM) production of phosphatidyl inositol 4,5-bisphosphate, a surrogate marker of $InsP_3$ (Ueno et al., 1987). Likewise, in reserpinized rat vas deferens, procaine (10 mM) prevents NE-induced (10 μM) tissue increase in total inositol phosphates and in $InsP_3$ in particular (Khoyi et al., 1993). Whether this effect is mediated by a direct inhibition of phospholipase C and/or of an upstream event (e.g., by affecting plasma membrane fluidity, see below) is still undetermined.

Procaine (1–20 mM) also inhibits Ca^{2+} influx (through Ca_L) associated with K^+-induced depolarization both in spontaneously active [e.g., guinea pig taenia caeci (Spedding and Berg, 1985; Ahn and Karaki, 1988), urinary bladder (Kurihara and Sakai, 1976a), rat duodenum (Ozturk et al., 1990)] and quiescent smooth muscle [e.g., rabbit aorta (Ahn and Karaki, 1988), and sheep carotid artery (Jacobs and Kretinge, 1974)]. Similarly, procaine (10 mM) increases Ca^{2+} influx induced by NE (10 μM) in reserpinized rat vas deferens (Khoyi et al., 1993) and by Cch in guinea pig taenia caeci (Ahn and Karaki, 1988), occurring in both cases through Ca_L. This Ca^{2+}-channel inhibition may be a consequence of procaine membrane stabilizing effect on depolarized plasma membrane that it shares with other local anesthetics, an effect that can be overcome by extracellular Ca^{2+} (Ahn and Karaki, 1988) but not by activators of Ca_L (Ahn and Karaki, 1988). Salicylic acid, which incorporates itself in the plasma membrane to increase negative surface charge and therefore favors the incorporation of cationic drugs (McLaughlin, 1973), potentiates the membrane effects of procaine (Spedding and Berg, 1985).

Procaine (≥1 mM) depolarizes tissues mainly by inhibiting K^+ conductance, thus enhancing spike frequency and amplitude in spontaneously active smooth muscles [e.g., guinea pig urinary bladder (Kurihara, 1975; Kurihara and Sakai, 1976a,b; Fujii et al., 1990), ureter (Burdyga and Magura, 1986), and portal vein (Hara et al., 1980)] and enabling outward current pulses to evoke action potentials in electrically quiescent smooth muscles [e.g., rabbit (Casteels et al., 1977; Ito et al., 1977) and guinea pig (Hara et al., 1980) pulmonary artery, dog trachea (Imaizumi and Watanabe, 1982), and sheep carotid artery (Jacobs and Kretinge, 1974)].

In contrast, procaine (up to 0.1 mM) was shown to be unable to displace radiolabeled batrachotoxin, a Na^+ channel selective blocker, or to inhibit specific guanidine uptake, a surrogate marker of Na^+ fluxes, in rat brain crude synaptosomal preparations (Pauwels et al., 1986), suggesting that procaine does not affect Na^+ conductance.

d. Use in Smooth Muscle Preparations. Procaine interacts with RyR by prolonging their closed state, and thus it is able to deplete caffeine-sensitive Ca^{2+} stores. Procaine also inhibits IICR and has little effect Ca^{2+} extrusion by the PMCA. Although it does not affect basal

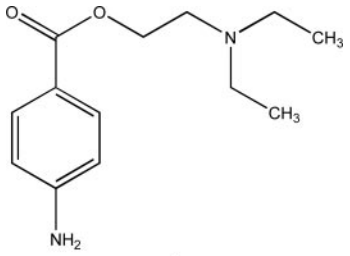

1

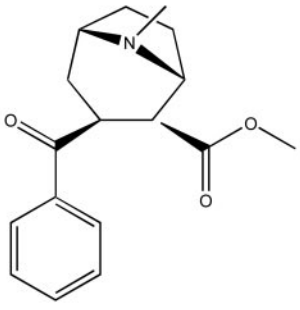

2

FIG. 15. Molecular structure of procaine (1) and cocaine (2).

Ca^{2+} permeability, it inhibits voltage-gated Ca^{2+} channel activity. In intact rat aorta, procaine causes a vasodilation that may reflect a multitude of effects, including release of NO, direct inhibition of extracellular Ca^{2+} entry, and reduction in the release of intracellular Ca^{2+} (Huang et al., 1999). The concentrations of procaine used in smooth muscle are shown in Table 7.

5. Ruthenium Red.

a. Source and Chemical Structure. Ruthenium red is a water-soluble and intensely colored inorganic synthetic dye that is obtained from the reaction of $RuCl_3$ and NH_3 in solution (Joly, 1892), is defined as ammoniated ruthenium oxychloride, and is a hexavalent cation in an aqueous environment (Carrondo et al., 1980) (Fig. 16). It is a complex compound of relatively high molecular weight that was originally used as a histochemical stain for its ability to bind to acidic glycosaminoglycans and other negatively charged polyanions (Charuk et al., 1990). Ruthenium red has an electron-dense character (Dierichs, 1979). This dye is relatively cell-impermeant.

b. Mechanism of Action. Ruthenium red (30 μM) fully inhibits RyR channels partially purified from canine and porcine aortic microsomal protein fractions and reconstituted into planar lipid bilayers (see Guerrero-Hernandez et al., 2002). Binding of [^{3}H]ryanodine to microsomes obtained from cultured rat aortic smooth muscle cells is inhibited by ruthenium red (10 μM) (Yusufi et al., 2002). This is consistent with its inhibition, at 20 μM, of caffeine (3–10 mM)-induced contractile activity of saponin-permeabilized rabbit mesenteric artery smooth muscle (Kanmura et al., 1989) and with its inhibition (at 10 μM) of cADPR (10 μM)- and caffeine (20 mM)-induced Ca^{2+} release from rat aortic microsomes (Yusufi et al., 2002).

c. Selectivity. Relatively low concentrations (1–20 μM) of ruthenium red inhibit RyR1, RyR2, and RyR3 isoforms equally well (Sonnleitner et al., 1998; Marx et al., 2001). Neither basal Mg^{2+}-ATPase, nor the Na^+/K^+-ATPase, are affected by ruthenium red in erythrocyte membranes (Watson et al., 1971). However, in various tissues and cell types, ruthenium red has several nonselective effects: 1) it inhibits voltage-gated Ca^{2+} channels (most likely by its binding in a 1:1 stoichiometry at a site in the extracellular entrance of the pore (Cibulsky and Sather, 1999)—e.g., millimolar concentrations block depolorization-induced Ca^{2+} uptake (Greenberg et al., 1973), inhibition of I_{ca} in isolated smooth muscle cells from guinea pig urinary bladder by externally applied ruthenium red (IC_{50} = 5.6 μM) (Sasaki et al., 1992; Hamilton and Lundy, 1995; Hirano et al., 1998); 2) it inhibits PMCA—e.g., K_D = 25 μM in purified PMCA from pig gastric antral smooth muscle—it reduces V_{max} for Ca^{2+} without affecting affinity for Ca^{2+} by inhibiting the stimulant effect of negatively charged (i.e. acidic) phospholipids on the cytoplasmic face of the pump (Missiaen et al., 1990); 3) it inhibits BK—e.g., at 10 μM in guinea pig urinary bladder dissociated smooth muscle cells, likely by interacting with BK cytoplasmic Ca^{2+}-binding site (Hirano et al., 1998); 4) it inhibits SERCA—e.g., at 10 to 100 μM, ruthenium red inhibits oxalate-dependent Ca^{2+} uptake in pig gastric antral smooth muscle microsomes (Kanmura et al., 1989), possibly through adsorption to negatively charged phospholipids in the SR membrane (Voelker and Smejtek, 1996a,b) resulting in altered phosphorylation kinetics (Meszaros and Ikemoto, 1985); 5) it inhibits IICR—e.g., ruthenium red (20 μM) inhibits $InsP_3$ (20 μM)-induced contractile activity in saponin-permeabilized rabbit mesenteric artery smooth muscle (Kanmura et al., 1989), but it is inactive at 10 μM on the $InsP_3$ (8 μM)-induced Ca^{2+} release from microsomes from freshly cultured rat aortic smooth muscle cells (Yusufi et al., 2002); 6) it inhibits the mitochondrial Ca^{2+} uniporter responsible for energy-dependent Ca^{2+} uptake (noncompetitive inhibition in rat liver mitochondria, K_i = 30 nM) (Moore, 1971; Ash and Bygrave, 1977; Matlib et al., 1998); and 7) it inhibits various Ca^{2+}-binding proteins, including actin-activated myosin Mg^{2+}-ATPase (it specifically interacts with F-actin binding site competitively (K_i = 4.4 μM with purified enzyme from chicken gizzard smooth muscle), thus preventing ATPase activation) (Nakamura et al., 1992), calmodulin (K_D = 18 μM) (Sasaki et al., 1992), and calsequestrin (K_i = 72 μM versus Ca^{2+} with purified enzyme from rabbit skeletal muscle) (Charuk et al., 1990).

Ruthenium red also increases the Ca^{2+} sensitivity of contractility in β-escin-permeabilized porcine smooth muscle from urinary bladder (EC_{50} = 60 μM at pCa 6.0), ileal longitudinal layer, and mesenteric artery without affecting E_{max} (at pCa 4.5). These effects are associated with increased LC_{20} phosphorylation (Yamada et al.,

TABLE 7
Effective concentrations of procaine in smooth muscle

Tissue	Animal Species	Experimental Details (Preparation; Measurement Method; Measured Response)	Effective Concentrations of Procaine	Reference
Anococcygeus	Rat	Isolated smooth muscle fibers; isotonic dynamometry; contractile activity	10 μM-1 mM	Babul'ova et al., 1981
Aorta	Rabbit	Isolated endothelium-denuded strips; fura-2 cellular loading, fluorometry, isometric dynamometry; $[Ca^{2+}]_{cyt}$, contractile activity	10 mM	Ahn and Karaki, 1988
Aorta	Rat	Isolated endothelium-intact or -denuded rings; isometric dynamometry; contractile activity	10 mM	Huang et al., 1999
Carotid artery	Sheep	Isolated smooth muscle strips; sucrose-gap; electrical activity, contractile activity	up to 50 mM	Jacobs and Kretinge, 1974
Coronary artery	Dog	Isolated fibers; isometric dynamometry; contractile activity	10 mM	Imai et al., 1984
Coronary artery	Pig	Isolated intact or saponin-permeabilized smooth muscle cells; quin-2 cellular loading, $^{45}Ca^{2+}$ cellular loading (intact or permeabilized); cellular Ca^{2+} fluxes, Ca^{2+} fluxes from intracellular stores, $[Ca^{2+}]_{cyt}$	10 mM	Ueno et al., 1987
Femoral artery	Rabbit	Isolated strips; isometric dynamometry; contractile activity	10 mM	Yagi et al., 1985
Mesenteric artery	Guinea pig	Isolated smooth muscle cells; microelectrode, alumina adsorption; membrane potential, excitatory junction potentials	5 mM	Fujii et al., 1985
Nasal mucosa	Dog	Isolated septal mucosa; dynamometry; contractile activity	100 μM	Wang and Jackson, 1988
Portal vein	Guinea pig	Isolated saponin- or β-escin-permeabilized strips; fluo-3 cellular loading, epifluorescence microscopy; $[Ca^{2+}]_{cyt}$ imaging	5 mM	Somlyo et al., 1992
Portal vein	Guinea pig	Isolated saponin-permeabilized cells and strips; microelectrode, isometric dynamometry; membrane potential, contractile activity	1 mM	Nanjo, 1984
Portal vein	Guinea pig	Isolated smooth muscle cells and strips; microelectrode, isometric dynamometry; membrane potential, contractile activity	1 mM	Hara et al., 1980
Portal vein	Guinea pig	Isolated strips; isometric dynamometry; contractile activity	10 mM	Yagi et al., 1985
Pulmonary artery	Guinea pig	Isolated smooth muscle cells and strips; microelectrode, isometric dynamometry; membrane potential, contractile activity	1 mM	Hara et al., 1980
Pulmonary artery	Rabbit	Isolated smooth muscle cells; microelectrode, $^{42}K^{+}$-cellular loading; membrane potential, K^{+} efflux	5 mM	Casteels et al., 1977
Pulmonary artery	Rabbit	Isolated smooth muscle cells and strips; double sucrose-gap, microelectrode, isometric dynamometry; membrane potential, ionic current, contractile activity	5 and 10 mM	Ito et al., 1977
Stomach (antrum, circular layer)	Guinea pig	Isolated circular muscle strips; isometric dynamometry; contractile activity	10 mM	Itoh et al., 1982b
Taenia caeci	Guinea pig	Isolated endothelium-denuded strips; fura-2 cellular loading, fluorometry, isometric dynamometry; $[Ca^{2+}]_{cyt}$, contractile activity	10 mM	Ahn and Karaki, 1988
Taenia caeci	Guinea pig	Isolated strips without myenteric plexus; single sucrose gap, isotonic dynamometry; electrical activity, contractile activity	30 μM-10 mM	Ishii and Shimo, 1984
Taenia caeci	Guinea pig	Isolated strips; isometric dynamometry; contractile activity	10 mM	Yagi et al., 1985
Trachea	Cat	Isolated mucosa- and adventitia-denuded strips; isometric dynamometry; contractile activity	10 mM	Ito and Itoh, 1984
Trachea	Cattle	Isolated tissue; isometric dynamometry; contractile activity	6 μM	Nakahara et al., 2000
Trachea	Dog	Isolated mucosa- and adventitia-denuded strips; microelectrode, $^{86}Rb^{+}$-cellular loading, isometric dynamometry; membrane potential, Rb^{+} efflux, contractile activity	1-10 mM	Imaizumi and Watanabe, 1982
Trachea	Guinea pig	Isolated smooth muscle fibers; isotonic dynamometry; contractile activity	10 μM-1 mM	Babul'ova et al., 1981
Trachea	Guinea pig	Isolated rings; isometric dynamometry; contractile activity	7 μM-6 mM	Okumura and Denborough, 1980
Trachea	Rabbit	Isolated α-toxin-permeabilized strips; isometric dynamometry; contractile activity	20 mM	Iizuka et al., 1998
Ureter	Guinea pig	Isolated strips; double sucrose-gap; membrane potential, contractile activity	10 mM	Burdyga and Magura, 1986
Urinary bladder	Guinea pig	Isolated strips; microelectrode, isometric dynamometry; membrane potential, contractile activity	10 mM	Fujii et al., 1990
Urinary bladder	Guinea pig	Isolated tissue; single sucrose-gap, microelectrode; membrane potential, contractile activity	1, 7, and 15 mM	Kurihara and Sakai, 1976b
Urinary bladder	Guinea pig	Isolated tissue; single sucrose-gap; membrane potential, contractile activity	15 mM	Kurihara, 1975
Vas deferens	Rat	Isolated tissue; $^{45}Ca^{2+}$ cellular loading, [^{3}H]-myo-inositol incubated, isometric dynamometry; Ca^{2+} fluxes, accumulation of inositol phosphates, contractile activity	10 mM	Khoyi et al., 1993
Vas deferens	Rat	Isolated segments; isometric dynamometry; contractile activity	10 mM	Huang, 1995

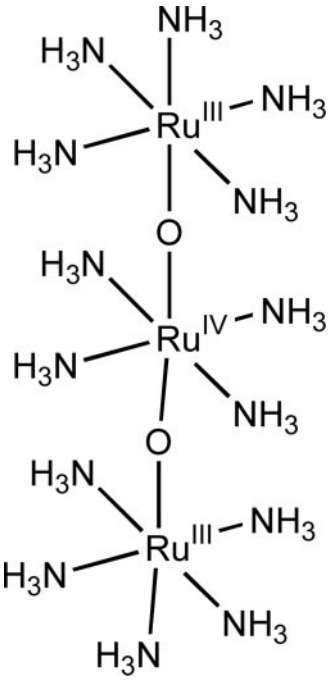

FIG. 16. Molecular structure of ruthenium red. Adapted with permission from Amann and Maggi (1991).

1999). Conversely, the relaxation of ileal longitudinal smooth muscle induced by decreasing [Ca^{2+}] is reduced by ruthenium red (100 μM) (Yamada et al., 1999). These effects are mediated by a direct concentration-dependent inhibition of MLCP, as shown with MLCP purified from guinea pig ileum longitudinal smooth muscle (IC_{50} = 23 μM) (Yamada et al., 2000).

Apart from the above effects on Ca^{2+} homeostasis, ruthenium red inhibits Ca^{2+}/calmodulin-dependent PDE (Ca^{2+}/CaM-PDE) isolated from rat brain (IC_{50} = 15 μM) (Masuoka et al., 1990). This effect could be completely reversed by calmodulin, and in contrast with Ca^{2+}/CaM-PDE inhibition by a typical calmodulin antagonist such as fluphenazine, this effect could also be overcome by increasing Ca^{2+} concentration (Masuoka et al., 1990). This suggests that the inhibitory effect of ruthenium red could be due to its effects on both Ca^{2+} and PDE binding to calmodulin at sites distinct from those of typical calmodulin antagonists.

Ruthenium red also inhibits Ca^{2+}-dependent neurotransmitter release (e.g., Ach) by blocking mainly N-type voltage-gated Ca^{2+} channels both in central synapses and peripheral junctions (e.g., K_D = 3.7 μM in brain synaptosomal membranes) (Tapia et al., 1985; Hamilton and Lundy, 1995; Tapia and Velasco, 1996), probably by binding to negatively charged sialic residues of gangliosides and glycoproteins on the external surface of the neuronal membranes. Ruthenium red (0.1–20 μM) can also inhibit Ca^{2+}-dependent release of neuropeptides from primary afferent sensory nerve fibers that is induced by capsaicin activation of Ca^{2+} influx through the VR1 receptor, a nonselective cation channel (Amann and Maggi, 1991). This is consistent with the selective noncompetitive inhibition of capsaicin-induced (10–10,000 nM) contractile activity of isolated rat vas deferens (with 3 μM) and urinary bladder (with 10–30 μM) (Maggi et al., 1993).

d. Use in Smooth Muscle Preparations. Ruthenium red is a water-soluble inhibitor of RyR that is relatively impermeant in intact cells. It inhibits all isoforms of RyR and effectively competes for binding with [^{3}H]ryanodine in isolated membranes. Although ruthenium red depletes caffeine-sensitive Ca^{2+} stores, its use is made unattractive due to its myriad of nonspecific effects that can occur at concentrations normally used to inhibit RyR. Included in the list of nonspecific effects are ruthenium red-induced inhibition of voltage-gated Ca^{2+} channel activity, PMCA, K_{Ca}, IICR, mitochondrial Ca^{2+} uniporter, and calmodulin activity. There are also important direct effects on MLCK and MLCP. Table 8 summarizes the use of ruthenium red in various smooth muscle preparations.

C. Inositol 1,4,5-Triphospate-Gated Ca^{2+} Release Channel/Inositol 1,4,5-Triphospate Receptor

1. Inositol 1,4,5-Triphosphate.

a. Source and Chemical Structure. D-*myo*-Inositol 1,4,5-trisphosphate [Ins(1,4,5)P_3, $InsP_3$, IP_3] is a phosphorylated species of the *myo*-stereoisomeric form of inositol 1,2,3,4,5,6-hexahydroxycyclohexane, a monosaccharide that is a member of the vitamin B complex (Fig. 17). This *myo* isomer is the most abundant of nine naturally occurring stereoisomers found in plant and animal tissues.

A caged form of $InsP_3$ has also been designed (Walker et al., 1987); it contains one photolabile (2-nitrophenyl) ethyl group esterified with either 4- or 5-position phosphate of $InsP_3$ (Fig. 12). The two resulting isomers have a quantum yield of 0.6 and are both biologically inactive (and resistant to phosphatase activity) until photolysis with UV light (<400 nm wavelength). Since the publication of Somlyo's group seminal paper (Walker et al., 1987), the compound has been used extensively in many cell types, including smooth muscle cells (Iino and Endo, 1992; Somlyo et al., 1992; McCarron and Muir, 1999; Boittin et al., 2000; Bradley et al., 2002; Zhang et al., 2003).

A new form of caged $InsP_3$ analog, 2,3-methoxymethylene $InsP_3$, has been designed with the advantage of being cell-permeant, although not available commercially (Li et al., 1998). It bears propionyloxymethyl groups on 4– and 5–positions phosphates of $InsP_3$ that confer cell permeability and are hydrolyzed once the compound is inside the cells, and a photolabile group on the 6–position hydroxyl, 4,5-dimethoxy-2-nitrobenzyl. The caged compound was shown to accumulate in the cytoplasm in 1321N1 astrocytoma cells at concentrations of hundreds of micromolar without $InsP_3R$ activation (Li et al., 1998). UV illumination uncages the $InsP_3$ analog that is nearly as potent as $InsP_3$. Because of the large accumulation of compound, repetitive flashes

TABLE 8
Effective concentrations of ruthenium red in smooth muscle

Tissue	Animal Species	Experimental Details (Preparation; Measurement Method; Measured Response)	Effective Concentrations of Ruthenium Red	Reference
			μM	
Airways	Human	Isolated α-toxin-permeabilized strips; isometric dynamometry; contractile activity	100-300	Iizuka et al., 1998
Airways	Human	Isolated rings; isometric dynamometry; contractile activity	10	Molimard et al., 1994
Aorta	Dog	Microsomal membranes incorporated into planar lipid bilayers, microsomes; bilayer clamp amplification (for membranes), extra-microsomal anti-pyridylazo-III (for microsomes); single Ca^{2+} channel currents (for membranes), Ca^{2+} fluxes (for microsomes)	up to 20 (no effect)	Ehrlich and Watras, 1988
Aorta	Rat	Microsomes; $^{45}Ca^{2+}$ loading; Ca^{2+} fluxes	10	Yusufi et al., 2002
Colon (circular layer)	Dog	Isolated non-inflamed and inflamed saponin-permeabilized smooth muscle cells; fura-2 cellular loading or $^{45}Ca^{2+}$ cellular loading, cell length monitoring by phase-contrast microscope; Ca^{2+} fluxes, $[Ca^{2+}]_{cyt}$, contractile activity	10	Shi and Sarna, 2000
Coronary artery	Cattle	Microsomal membranes, stripped or not of FKBP-12.6, incorporated into planar lipid bilayers; bilayer clamp amplification; single Ca^{2+} channel currents	80	Li et al., 2001
Ileum	Guinea pig	Isolated intact or β-escin-permeabilized strips; immunoblotting, isometric dynamometry; myosin light chain phosphorylation, contractile activity	300	Yamada et al., 2000
Ileum	Guinea pig	Isolated α-toxin-permeabilized strips; isometric dynamometry; contractile activity	100	Iizuka et al., 1998
Mesenteric artery	Rabbit	Isolated saponin-permeabilized strips; isometric dynamometry; contractile activity	20	Kanmura et al., 1989
Mesenteric resistance arteries	Guinea pig	Isolated intact or β-escin-permeabilized strips isolated from 4th-order branches; immunoblotting, isometric dynamometry; myosin light chain phosphorylation, contractile activity	60-600	Yamada et al., 1999
Pulmonary artery	Cattle	Microsomes; extramicrosomal fluo-3 and fluorometry or $^{45}Ca^{2+}$ loading; Ca^{2+} fluxes	20	Stout et al., 2002
Stomach (antrum)	Pig	Microsomes; extramicrosomal fluo-3 and fluorometry or $^{45}Ca^{2+}$ loading; Ca^{2+} fluxes	20	Stout et al., 2002
Stomach (antrum)	Pig	Microsomes; $^{45}Ca^{2+}$ loading; Ca^{2+} fluxes	1-100	Kanmura et al., 1989
Trachea	Cattle	Microsomal membranes incorporated into planar lipid bilayers; bilayer clamp amplification; single Ca^{2+} channel currents	50	Gaburjakova et al., 1999
Trachea	Pig	Isolated β-escin-permeabilized smooth muscle cells; fura-3 cellular loading, confocal fluorescence microscopy; $[Ca^{2+}]_{cyt}$ imaging	10	Kannan et al., 1997
Trachea	Rabbit	Isolated β-escin-permeabilized strips; isometric dynamometry; contractile activity	100	Iizuka et al., 1998
Urinary bladder	Guinea pig	Isolated smooth muscle cells; whole-cell patch-clamping; I_{BK}, I_{caf}, STOCs	10	Hirano et al., 1998
Urinary bladder	Guinea pig	Isolated smooth muscle cells; indo-1 FF cellular loading; $[Ca^{2+}]_{cyt}$ decay	20	Ganitkevich, 1999
Urinary bladder	Guinea pig	Isolated intact or β-escin-permeabilized strips; immunoblotting, isometric dynamometry; myosin light chain phosphorylation, contractile activity	100	Yamada et al., 1999
Urinary bladder	Rat	Isolated strips; isometric dynamometry; contractile activity	3-30	Maggi et al., 1993
Uterus	Rat	Isolated digitonin-permeabilized smooth muscle cells; $^{45}Ca^{2+}$ mitochondrial loading; mitochondrial Ca^{2+} fluxes	10	Shinlova et al., 1996
Uterus	Rat	Isolated myometrial strips; isometric dynamometry; contractile activity	30	Phillippe and Basa, 1996
Vas deferens	Rat	Isolated strips; isometric dynamometry; contractile activity	3-30	Maggi et al., 1993

could be used to generate oscillations in $[Ca^{2+}]_{cyt}$ at approximately physiological rates (Li et al., 1998).

b. Mechanism of Action. The cell-impermeant $InsP_3$ is an important second messenger produced simultaneously with diacylglycerol from the phosphoinositide-specific PLC (also known as phosphoinositidase C or phosphoinositidase)-mediated hydrolysis of plasma membrane phosphatidylinositol 4,5-bisphosphate (phosphatidylinositol 4,5-bisphosphate, phosphatidylinositol 4,5-bisphosphate) (Berridge and Irvine, 1984). PLC, also found in the nucleus (Cocco et al., 2001), is a multidomain phosphodiesterase forming a family of more than 11 isoforms grouped into four subtypes (β, γ, δ, and ε) (Rebecchi and Pentyala, 2000; Rhee, 2001; Fukami, 2002). In the plasma membrane, depending on its subtype, PLC can be activated either through interactions with the heterotrimeric G proteins G_q or G_{11} following stimulation of numerous GPCR or through direct interactions with receptor and nonreceptor tyrosine kinases (Rhee, 2001). Plasma membrane-generated $InsP_3$ then

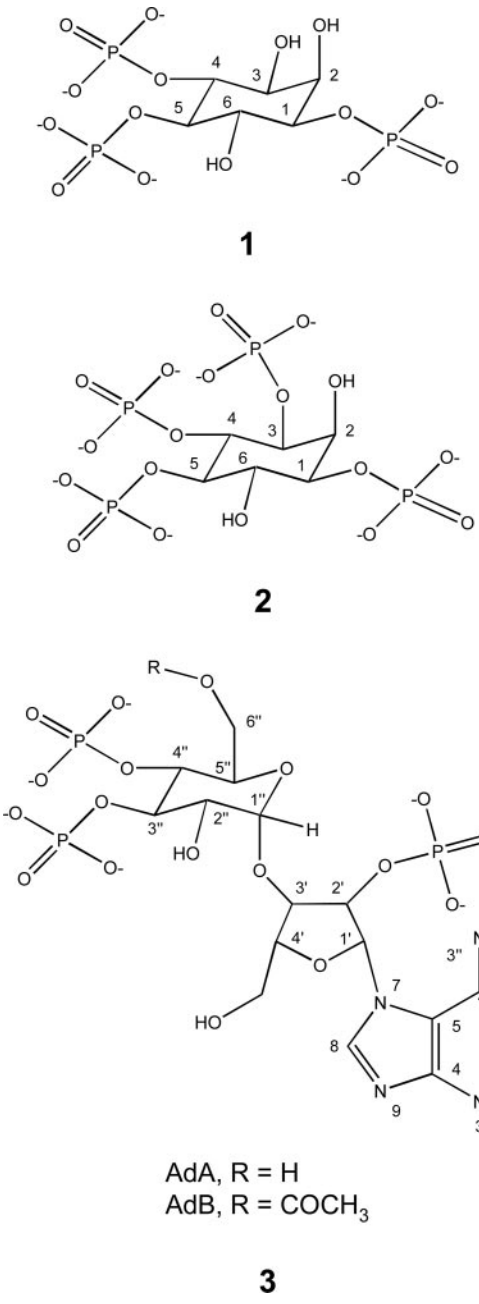

FIG. 17. Molecular structure of inositol 1,4,5-trisphosphate ($InsP_3$; 1), inositol 1,3,4,5-tetrakisphosphate [$Ins(1,3,4,5)P_4$; 2], and adenophostins A (AdA) and B (AdB). Adapted with permission from Wilcox et al. (1998).

diffuses in the cytoplasm to induce SR Ca^{2+} release by binding to $InsP_3R$ (see *Section II.C.*).

In mammalian cells, the $InsP_3$ signal is rapidly terminated by metabolism through two known routes (Connolly et al., 1987; Shears, 1989): dephosphorylation to D-*myo*-inositol 1,4-diphosphate [$Ins(1,4)P_2$] by an inositol polyphosphate 5-phosphatase located in both cytoplasmic and membrane cellular fractions (Downes et al., 1982; Verjans et al., 1994) or phosphorylation by a predominantly cytoplasmic ATP-dependent $InsP_3$ 3-kinase to D-*myo*-inositol 1,3,4,5-tetrakisphosphate [$Ins(1,3,4,5)P_4$, Fig. 17], which is further metabolized by the above 5-phosphatase and a 3-phosphatase (Irvine et al., 1986; Hoer et al., 1988). In its substrate interactions, the $InsP_3$3-kinase exhibits high stereo- and positional selectivity and constitutes a family of at least three isoforms (Communi et al., 1995), whereas the inositol polyphosphate 5-phosphatase seems relatively nonspecific (Nahorski and Potter, 1989) and forms a family of at least 10 mammalian members (Mitchell et al., 2002; Whisstock et al., 2002). However, little is known about the expression and regulation of these enzymes in smooth muscle. Interestingly, although $Ins(1,4)P_2$ is inactive in terms of Ca^{2+} movements, $Ins(1,3,4,5)P_4$ is a weak agonist at the $InsP_3R$ (Wilcox et al., 1994a) and has a controversial role in the regulation of extracellular Ca^{2+} influx (Hermosura et al., 2000).

In terms of SAR (Fig. 18), the interaction of $InsP_3$ with its receptor is highly stereospecific, with the D-isomer being over 1000 times more potent than the L-isomer (Nahorski and Potter, 1989). The most critical structural feature of $InsP_3$ is its vicinal D-4,5-bisphosphate motif, with the 5-phosphate being the dominant partner in receptor interaction (Wilcox et al., 1997). The 1-phosphate also contributes to the receptor interaction specificity (Nahorski and Potter, 1989), potency (Willcocks et al., 1989; Jenkinson et al., 1992), and efficacy (Wilcox et al., 1995, 1997). The hydroxyl group in 6-position appears to make a major contribution to the binding interactions with the receptor (Safrany et al., 1991), whereas

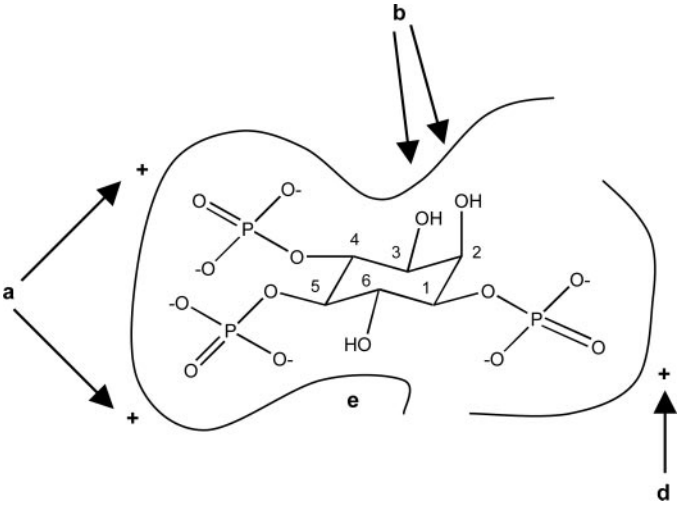

FIG. 18. The significant structure-activity features of the inositol 1,4,5-trisphosphate receptor-binding pocket. a, positively charged amino acids in the binding pocket, such as arginine and lysine, interact with each of the phosphate groups. b, 2- and 3-position hydroxyl groups are not essential per se for receptor binding. However, equatorial 3-position substituents larger than OH groups attenuate interaction with the receptor. c, the 2-position microdomain of the binding pocket does not significantly influence the efficiency of receptor binding. However, the axial position of the OH group might have crucial effects on adjacent groups. d, an auxiliary microdomain that significantly enhances binding stability via its relatively long-range interaction with the 1-position phosphate. Highly efficient interaction with this microdomain might contribute to enhancing the activity of the adenophostins. e, the anchoring receptor microdomain for the 4,5-bisphosphate and 6-hydroxyl motif. The vicinal 4- and 5-phosphate groups are the crucial structural features defining receptor interaction, with the 5-phosphate being the dominant partner. Adapted with permission from Wilcox et al. (1998).

TABLE 9
Effective concentrations of $InsP_3$ in smooth muscle

Tissue	Animal Species	Experimental Details (Preparation; Measurement Method; Measured Response)	Effective Concentrations of $InsP_3$	Reference
			μM	
Airways	Human	Isolated α-toxin-permeabilized strips; isometric dynamometry; contractile activity	300	Iizuka et al., 1998
Aorta	Dog	Microsomal membranes incorporated into planar lipid bilayers, microsomes; bilayer clamp amplification (for membranes), extra-microsomal anti-pyridylazo-III (for microsomes); single Ca^{2+} channel currents (for membranes), Ca^{2+} fluxes (for microsomes)	7 (vesicles) 1 (bilayer)	Ehrlich and Watras, 1988
Aorta	Guinea pig	Isolated α-toxin-permeabilized strips; isometric dynamometry; contractile activity	100	Nixon et al., 1994
Aorta	Pig	Microsomes; extramicrosomal fluo-3, fluorometry; Ca^{2+} fluxes	10 and 30	Tovey et al., 2000
Aorta	Rabbit	Isolated saponin-permeabilized smooth muscle cells; mag-fura-2 cellular loading; $[Ca^{2+}]_{SR}$, $[Ca^{2+}]_{mito}$	100	Gurney et al., 2000
Aorta	Cattle	Purified $InsP_3R$ incorporated into planar bilayers; bilayer clamp amplification; single Ca^{2+} channel currents	0.5	Mayrleitner et al., 1991
Aorta	Rat	Microsomes; $^{45}Ca^{2+}$ loading; Ca^{2+} fluxes	8	Yusufi et al., 2002
Aorta	Rat	Isolated cultured saponin-permeabilized smooth muscle cells; $^{45}Ca^{2+}$ cellular loading; Ca^{2+} fluxes	10 and 100	Yamamoto et al., 1991
Aorta	Rat	Saponin-permeabilized cultured A7r5 cell line; $^{45}Ca^{2+}$ cellular loading; Ca^{2+} fluxes	0.3-100	Missiaen et al., 2001a
Cerebellum	Pig	Microsomes; extramicrosomal fluo-3, fluorometry; Ca^{2+} fluxes	10 and 30	Tovey et al., 2000
Colon	Guinea pig	Isolated smooth muscle cells; fluo-3 cellular loading, wide-field fluorescent digital imaging; $[Ca^{2+}]_{cyt}$ imaging	10	McCarron et al., 2004
Colon	Guinea pig	Isolated smooth muscle cells; whole-cell patch-clamping, fluo-3 cellular loading, fluorometry or wide-field fluorescence digital imaging;I_{Ca}, $[Ca^{2+}]_{cyt}$, $[Ca^{2+}]_{cyt}$ imaging	25 (caged $InsP_3$)	Bradley et al., 2003
Colon	Guinea pig	Isolated smooth muscle cells; fluo-3 cellular loading, wide-field fluorescent digital imaging; $[Ca^{2+}]_{cyt}$ imaging	20 (caged $InsP_3$)	McCarron and Muir, 1999
Colon (circular layer)	Dog	Isolated non-inflamed and inflamed saponin-permeabilized smooth muscle cells; fura-2 cellular loading or $^{45}Ca^{2+}$ cellular loading, cell length monitoring by phase-contrast microscope; Ca^{2+} fluxes, $[Ca^{2+}]_{cyt}$, contractile activity	1	Shi and Sarna, 2000
Coronary artery	Cattle	Microsomal membranes, stripped or not of FKBP-12.6, incorporated into planar lipid bilayers; bilayer clamp amplification; single Ca^{2+} channel currents	10	Li et al., 2001
Coronary artery	Cattle	Isolated α-toxin-permeabilized smooth muscle cells; fura-2 cellular loading, fluorometry; $[Ca^{2+}]_{cyt}$	70	Yu et al., 2000
Coronary artery	Pig	Isolated intact or saponin-permeabilized smooth muscle cells; quin-2 cellular loading, $^{45}Ca^{2+}$ cellular loading (intact or permeabilized); cellular Ca^{2+} fluxes, Ca^{2+} fluxes from intracellular stores, $[Ca^{2+}]_{cyt}$	3	Ueno et al., 1987
Gall bladder	Cat	Isolated saponin-permeabilized smooth muscle cells; cell length monitoring by phase-contrast microscopy; contractile activity	1	Yu et al., 1998
Heart	Pig	Microsomes; extramicrosomal fluo-3, fluorometry; Ca^{2+} fluxes	10 and 30	Tovey et al., 2000
Ileum	Guinea pig	Isolated α-toxin-permeabilized strips; isometric dynamometry; contractile activity	300	Iizuka et al., 1998
Ileum (circular layer)	Guinea pig	Isolated β-escin-permeabilized strips; isometric dynamometry; contractile activity	40	Fukami et al., 1993
Ileum (longitudinal layer)	Guinea pig	Isolated β-escin- or reversibly-permeabilized strips; fura-2 cellular loading, fluorometry, isometric dynamometry; $[Ca^{2+}]_{cyt}$, contractile activity	40	Kobayashi et al., 1989b
Internal anal sphincter	Rabbit	Isolated saponin-permeabilized smooth muscle cells; cell length monitoring by phase-contrast microscopy; contractile activity	1	Bitar et al., 1991
Mesenteric artery	Rabbit	Isolated saponin-permeabilized strips; isometric dynamometry; contractile activity	20	Kanmura et al., 1989
Mesenteric resistance arteries	Rabbit	Isolated β-escin-permeabilized smooth muscle cells; fura-2 cellular loading, fluorometry; $[Ca^{2+}]_{cyt}$	20	Itoh et al., 1992
Portal vein	Guinea pig	Isolated β-escin-permeabilized smooth muscle cells; furaptra cellular loading, fluorometry; $[Ca^{2+}]_{SR}$	10	Hirose et al., 1998
Portal vein	Guinea pig	Isolated saponin- or β-escin-permeabilized strips; fluo-3 cellular loading, epifluorescence microscopy, isometric dynamometry; $[Ca^{2+}]_{cyt}$ imaging, contractile activity	25	Somlyo et al., 1992

TABLE 9
Continued

Tissue	Animal Species	Experimental Details (Preparation; Measurement Method; Measured Response)	Effective Concentrations of $InsP_3$	Reference
			μM	
Pulmonary artery	Cattle	Microsomes; extramicrosomal fluo-3 and fluorometry or $^{45}Ca^{2+}$ loading; Ca^{2+} fluxes	50	Stout et al., 2002
Pulmonary artery	Rabbit	Isolated β-escin- or reversibly-permeabilized strips; fura-2 cellular loading, fluorometry, isometric dynamometry; $[Ca^{2+}]_{cyt}$, contractile activity	40	Kobayashi et al., 1989b
Pulmonary artery	Rabbit	Isolated saponin- or digitonin-permeabilized strips; Ca^{2+}-selective electrodes (extracellular), isometric dynamometry; Ca^{2+} efflux, contractile activity	0.5-30	Somlyo et al., 1985
Stomach	Rabbit	Isolated saponin-permeabilized smooth muscle cells; cell length monitoring by phase-contrast microscopy; contractile activity	1	Murthy, 2001
Stomach (antrum)	Cattle	Microsomes; extramicrosomal fluo-3 and fluorometry or $^{45}Ca^{2+}$ loading; Ca^{2+} fluxes	50	Stout et al., 2002
Stomach (antrum)	Rat	Isolated smooth muscle cells; Oregon Green BAPTA 5N cellular loading; $[Ca^{2+}]_{SR}$	10	White and McGeown, 2002
Testicular peritubules	Rat	Isolated saponin-permeabilized smooth muscle cells; fura-2 cellular loading, fluorometry; $[Ca^{2+}]_{cyt}$	10	Barone et al., 2002
Trachea	Cat	Isolated smooth muscle cells; whole-cell nystatin perforated patch-clamping, I_{Cch}	200 (caged)	Waniishi et al., 1998
Trachea	Cattle	Microsomal membranes incorporated into planar lipid bilayers; bilayer clamp amplification; single Ca^{2+} channel currents	6	Gaburjakova et al., 1999
Trachea	Pig	Isolated smooth muscle cells; whole-cell patch-clamping; $I_{Cl(Ca)}$	10	Liu and Farley, 1996
Trachea	Pig	Isolated β-escin-permeabilized smooth muscle cells; fluo-3 cellular loading, confocal fluorescence microscopy; $[Ca^{2+}]_{cyt}$ imaging	1	Kannan et al., 1997
Trachea	Rabbit	Isolated β-escin-permeabilized strips; isometric dynamometry; contractile activity	300	Iizuka et al., 1998
Uterus (pregnant)	Rat	Isolated myometrial smooth muscle cells; $^{45}Ca^{2+}$ cellular loading; Ca^{2+} efflux	10	Molnar and Hertelendy, 1995
Vas deferens	Guinea pig	Isolated β-escin-permeabilized strips; isometric dynamometry; contractile activity	100	Nixon et al., 1994

the axial 2-hydroxyl and the equatorial 3-hydroxyl groups do not seem as important for either binding or Ca^{2+} release (Hirata et al., 1989). In fact, the $InsP_3R$ has a remarkable tolerance for electronic and steric changes in either axial or equatorial substituents of the $InsP_3$ 2-position, which suggests that the 2-hydroxyl is not closely associated with the binding pocket (Hirata et al., 1989; Wilcox et al., 1994a). This is not the case for the 3-hydroxyl group; increasing steric bulk of the equatorial 3-position (Wilcox et al., 1994a) or even simple inversion of the hydroxyl moiety (Hirata et al., 1993) is detrimental to activity. Interestingly, it seems that bulkiness is tolerated for the axial 3-position (Wilcox et al., 1994b). Likewise, linking the 2- and 3-positions is also well tolerated (Li et al., 1998). These last two observations suggest that the interactions at these positions with the $InsP_3R$-binding pocket are complex (Wilcox et al., 1998). Indeed, data indicate that the axial orientation of the 2-hydroxyl group may play a critical role in modulating the interaction of the 3-hydroxyl group with the binding pocket (Murphy et al., 1997); this may contribute to the high potency of adenophostins (see *Section II.C.2.b.*).

Unfortunately, despite this relatively detailed SAR information, the rational design of potent agonist and antagonist $InsP_3$ analogs has not been successful, making the design of $InsP_3R$ isoform-specific analogs even less tenable. Progress in the development of pharmacological tools has relied mostly on the discovery of natural products, such as the adenophostins (agonists) and xestospongins (antagonists), and the design of neutralizing anti-$InsP_3R$ antibodies, as detailed in the following sections. However, a major limitation for most of the tools remains cell impermeability.

c. Selectivity. Affinity for $InsP_3$ varies to a limited extent among isoforms with $InsP_3R1 > InsP_3R2 > InsP_3R3$ (K_D values of 1.5, 2.5, and 22.4 nM, respectively), consistent with the sensitivities for IICR of cell lines expressing predominantly homotetrameric forms of either of these isoforms (Wojcikiewicz and Luo, 1998a) (see *Section II.C.*). Differences in modulation by Ca^{2+} of $InsP_3$ binding also occur with $InsP_3R1$ and $InsP_3R3$ (Newton et al., 1994; Mackrill et al., 1996).

Interestingly, $InsP_3R$ is intracellularly localized in structures other than the ER/SR. For instance, it has been found in the nuclear envelope in many cell types, including vascular (Tasker et al., 2000) and visceral (Villa et al., 1993) smooth muscles. However, although nuclear Ca^{2+} signaling is tightly coupled to transcriptional events and cell growth, the role of $InsP_3$ in these processes is still unclear. In A7r5 and 16HBE14o- cell lines possessing an endogenous nonmitochondrial thapsigargin-insensitive/CPA-sensitive Ca^{2+} store (~10% of

total cell Ca^{2+} uptake), likely corresponding to the Golgi apparatus (see *Section II.1.c.*) where $InsP_3R$ has also been localized (Surroca and Wolff, 2000), $InsP_3$ (or an $InsP_3$-generating receptor agonist such as arginine vasopressin) can release Ca^{2+} in A7r5 cells (EC_{50} values ~5 μM versus ~1 μM for ER-mediated Ca^{2+} release) but not in 16HBE14o- cells (Missiaen et al., 2002). It is unclear what role this type of IICR has and whether it is of significance in differentiated smooth muscle cells.

$InsP_3$ appears very selective for IICR versus CICR in smooth muscle. For instance, in microsomes from freshly cultured rat aortic smooth muscle cells that express RyR1–3, $InsP_3$ induces concentration-dependent (1–8 μM) Ca^{2+} release that is fully inhibited by heparin (1 mg/ml), whereas cADPR induces concentration-dependent (1–10 μM) Ca^{2+} release that is fully inhibited by 8-Br-cADPR (40 μM) and ruthenium red (10 μM). Although both agents induced maximal Ca^{2+} release of similar order of magnitude, $InsP_3$ effect is insensitive to ruthenium red (Yusufi et al., 2002). Likewise, $InsP_3$ (10 μM) is ineffective at changing the P_o of RyR partially purified from bovine coronary arteries microsomal protein fractions and reconstituted into planar lipid bilayers, which is fully sensitive to caffeine (0.5–5 mM), ryanodine (0.1–50 μM), ruthenium red (40 and 80 μM), and cADPR (0.01–1 μM) (Li et al., 2001).

In saponin-permeabilized freshly cultured seminiferous peritubular smooth muscle cells from rat testis expressing $InsP_3R1$–3 but only RyR2 among RyR isoforms, cADPR-induced (10 μM) Ca^{2+} release from a SR Ca^{2+} store is independent from Ca^{2+} released by $InsP_3$ (10 μM) but fully inhibited by 8-Br-cADPR (50 μM) or ryanodine (5 μM) (Barone et al., 2002).

d. Use in Smooth Muscle Preparations. $InsP_3$ does not cross cell membranes, complicating its routine use in either isolated smooth muscle cells or intact tissue. As shown in Table 9, the preferred methods of use of this endogenous SR Ca^{2+} releaser are via either direct injection through intracellular application (e.g., with a patch pipette) or photolytic release of caged $InsP_3$. When caged $InsP_3$ is released, there is a delay of ~5 to 10 ms before Ca^{2+} release occurs (Somlyo et al., 1992). This release raises $[Ca^{2+}]_{cyt}$ from 100 nM (basal) to 175 nM in guinea pig portal vein (Somlyo et al., 1992). Nonetheless, there is variable affinity of $InsP_3$ for its receptors: 2 nM for $InsP_3R1$ and $InsP_3R2$ and 22 nM for $InsP_3R3$. The D-isomer of $InsP_3$ is >1000 times more potent than the L-isomer. Smooth muscle (e.g., intestinal) has at least 10 times more $InsP_3R$ than RyR (Bolton et al., 1999). The EC_{50} value for $InsP_3$ is reportedly 1 μM, with maximal Ca^{2+} release requiring 4 μM (Somlyo et al., 1992). The general applicability of this differential density profile in smooth muscle (vascular and nonvascular) that differ in location (different vascular beds or various hollow organs), size (resistance versus conduit arteries), orientation (circular versus longitudinal), and function (phasic versus tonic) has not been examined so far.

2. Adenophostins.

a. Source and Chemical Structure. The gluconucleosides adenophostins A (3′-*O*-(α-D-glucopyranosyl)-adenosine-2′,3″,4″-trisphosphate) and B (the 6″-*O*-acetyl derivative) are metabolic products of the fungus *Penecillium brevicompactum* (Takahashi et al., 1993) (Fig. 17). Apart from a vicinal bisphosphate group and a third phosphate, adenophostins bear little resemblance to $InsP_3$, two of the major differences being the adenosine component and the hydroxymethyl substituent (acetylated in adenophostin B).

b. Mechanism of Action. The cell-impermeant adenophostins are the most potent $InsP_3R$ agonists known. They are full $InsP_3R$ agonists in rat cerebellar microsomes (which express $InsP_3R1$ almost exclusively) (Wojcikiewicz, 1995) with potencies about 100 times higher than $InsP_3$ potency (EC_{50} values: adenophostin A = 1.4 nM, adenophostin B = 1.5 nM, and $InsP_3$ = 170 nM). In binding data, adenophostin A has an affinity about seven times higher than $InsP_3$ in rat cerebellar microsomes (K_D values: 0.91 nM versus 6.75 nM) (Marchant et al., 1997a) and about five times higher in hepatic membranes (Beecroft et al., 1999). Consistent with this, the displacement of $[^3H]InsP_3$ by adenophostin has an IC_{50} value about 20 to 50 times lower than $InsP_3$ in rat cerebellar microsomes (Takahashi et al., 1994; Murphy et al., 1997) and about 10 times lower than in porcine cerebellar microsomes (Shuto et al., 1998). At the purified $InsP_3R1$, adenophostin B is about 10 times more potent than $InsP_3$ (EC_{50} values: 11 nM versus 100 nM) and exhibits a positive cooperativity in binding that is not observed with $InsP_3$ (Hirota et al., 1995). Adenophostin A is also about a 10-fold more potent Ca^{2+} releaser than $InsP_3$ in permeabilized hepatocytes (Marchant et al., 1997b; Beecroft et al., 1999) that have predominance of $InsP_3R2$ versus $InsP_3R1$ (>80% versus <20%) (Wojcikiewicz, 1995; De Smedt et al., 1997).

Adenophostins are resistant (Takahashi et al., 1993) to the metabolic enzymes inositol polyphosphate 5-phosphatase and $InsP_3$ 3-kinase (Nahorski and Potter, 1989) that are involved in the generation of the full but weaker SR $InsP_3R$ agonist $InsP_4$ (Wilcox et al., 1993) (see *Section II.C.1.b.*). As such, adenophostins are able to produce a sustained Ca^{2+} release in rat cerebral microsomes (Takahashi et al., 1994) and rabbit permeabilized platelets (Murphy et al., 1997) with potencies 10 to 100 times higher than $InsP_3$.

Adenophostins possess important structural features for agonism at the $InsP_3R$. The 4- and 3-positions of the glucose 3,4-bisphosphate moiety and the 2-position hydroxyl group were shown by molecular modeling to be similar to 4-, 5-, and 6-positions, respectively, of $InsP_3$ (Takahashi et al., 1994; Wilcox et al., 1995), and both structural features are as essential for Ca^{2+}-releasing activity in rabbit permeabilized platelets (Murphy et al., 1997). The third phosphate of adenophostins (2′-phos-

phate) is essential for high potency (Shuto et al., 1998); its removal causes a 1000-fold decrease in binding affinity in rat cerebellar microsomes (Takahashi et al., 1994) and a 2000-fold lower affinity to purified rat cerebellar $InsP_3R$ (Takahashi et al., 1993). The adenosine component at the 1″-position of the glucopyranose ring is also necessary for the high potency of adenophostins (Wilcox et al., 1995; Murphy et al., 1997; Shuto et al., 1998; de Kort et al., 2000).

c. Selectivity. Adenophostins, at a concentration of 10 μg/ml (~15 μM), do not bind to Ca_l or to a series of receptors of functional significance for smooth muscle function (α_1 and β adrenergic, angiotensin II, cholecystokinin A and B, dopamine D2, leukotriene B4 and D4, Ach muscarinic, neurokinin, NMDA, serotonin 5-HT1, 5-HT2 and 5-HT3, and thromboxane receptors) (Takahashi et al., 1993).

d. Use in Smooth Muscle Preparations. The adenophostins (A and B) are cell-impermeant and represent the most potent agonists for $InsP_3R$. They are 10 to 100 times more potent than $InsP_3$ in binding and Ca^{2+}-release studies. Unlike $InsP_3$, the adenophostins are metabolically stable and produce lasting effects. As can be seen from Table 10, the use of these compounds in smooth muscle has not been favorably received thus far.

3. Xestospongins.

a. Source and Chemical Structure. The macrocyclic *bis*-1-oxaquinolizidines xestospongins (xestospongins A, C, and D, araguspongine B, and demethylxestospongin B) are alkaloids from the Australian marine sponge *Xestospongia* sp. (Nakagawa et al., 1984; Vassas et al., 1996; Gafni et al., 1997) (Fig. 19).

b. Mechanism of Action. The xestospongins are potent blockers of IICR in rabbit cerebellar microsomes with IC_{50} values ranging from ~300 nM to ~6 μM, with the most potent form, xestospongin C, being cell-permeant (Gafni et al., 1997). The more potent xestospongins (xestospongin C, araguspongine B, and xestospongin D) produce a multiphasic inhibition of IICR in these microsomes, which may be explained by the existence of multiple $InsP_3R$ isoforms in preparations from whole cerebella. This would imply that these receptor isoforms have different affinities for these xestospongins (Gafni et al., 1997). There is indeed evidence that the cerebellum contains more than one of the three known $InsP_3R$ isoforms (Nakanishi et al., 1991; Ross et al., 1992). The blockade appears to be noncompetitive for $InsP_3$ as xestospongin C (7.5 μM) completely blocks Ca^{2+} release from rabbit cerebellar microsomes but cannot decrease [^{3}H]$InsP_3$-specific binding to the same microsomes (at 10 μM) (Gafni et al., 1997). Although not yet elucidated, the specific mechanism could be either blockade of the Ca^{2+} channel pore or an allosteric interaction uncoupling $InsP_3$ binding from Ca^{2+} release (Gafni et al., 1997). Consistent with the above findings, xestospongin C concentration-dependently (6–10 μM) inhibits ATP-induced transient increase in $[Ca^{2+}]_{cyt}$ in bovine aortic endothelial cells (Bishara et al., 2002).

In terms of SAR, the combination of a *cis*-fused and *trans*-fused oxaquinolizidines, such as in xestospongin C, is about 10 times more potent than a *trans/trans* system, such as in xestospongin A (Gafni et al., 1997). Because of purity issues, it is still not clear whether a *cis/trans* system would be superior in potency (about 2 times) to a *cis/cis* system, such as in araguspongine B (Gafni et al., 1997). The addition of a hydroxyl group to C9 of xestospongin C, such as in xestospongin D, reduces the potency about two times (Gafni et al., 1997). Substitution of the *cis*-fused oxaquinolizidine of xestospongin D for a *trans*-fused one, such as in demethylxestospongin B, further reduces the potency about 7 times (Gafni et al., 1997). Interestingly, xestospongins A, C, and D were recognized as vasodilators at the time of their discovery (Nakagawa et al., 1984), likely as a consequence of their $InsP_3R$ blocking activity.

c. Selectivity. Xestospongins display a high selectivity for the $InsP_3R$ over RyR1 (Gafni et al., 1997). In rabbit skeletal muscle, xestospongin C (10 μM) decreases [^{3}H]ryanodine binding to SR preparations by 22% and caffeine-induced Ca^{2+} release by 46%. The IC_{50} value for blocking caffeine-induced Ca^{2+} release in skeletal muscle is more than 30 times greater than that for blocking Ca^{2+} release in rabbit cerebellar microsomes. Likewise, in smooth muscle, xestospongin inhibits $InsP_3R$ and not RyR (Ozaki et al., 2002). In permeabilized smooth muscle, xestospongin C inhibits both K^+- and Cch-induced contractile activity (3–10 μM), whereas in isolated smooth muscle cells from this tissue, the inhibition of voltage-gated currents has an IC_{50} value of 0.63 μM (Ozaki et al., 2002). Thus, at least in the ileum, xestospongin is selective for $InsP_3R$ when applied to permeabilized tissue but not when applied to intact cells or tissue (Bishara et al., 2002; Ozaki et al., 2002).

Much like 2-APB (see *Section II.C.4.c.*), but with greater potency, xestospongin C (3–10 μM) inhibits agonist (ATP)- and receptor-independent (thapsigargin, ionomycin)-induced capacitative Ca^{2+} entry in bovine aortic endothelial cells (Bishara et al., 2002). Interestingly, in human platelets, xestospongin C, but not 2-APB, disrupts the thapsigargin-induced structural coupling (Rosado and Sage, 2000) between $InsP_3R2$ and

TABLE 10
Effective concentrations of adenophostins in smooth muscle

Tissue	Animal Species	Experimental Details (Preparation; Measurement Method; Measured Response)	Effective Concentrations of Adenophostins	Reference
Aorta	Pig	Microsomes; extramicrosomal fluo-3, fluorometry; $[Ca^{2+}]_{cyt}$	1 μM (adenophostin A)	Tovey et al., 2000

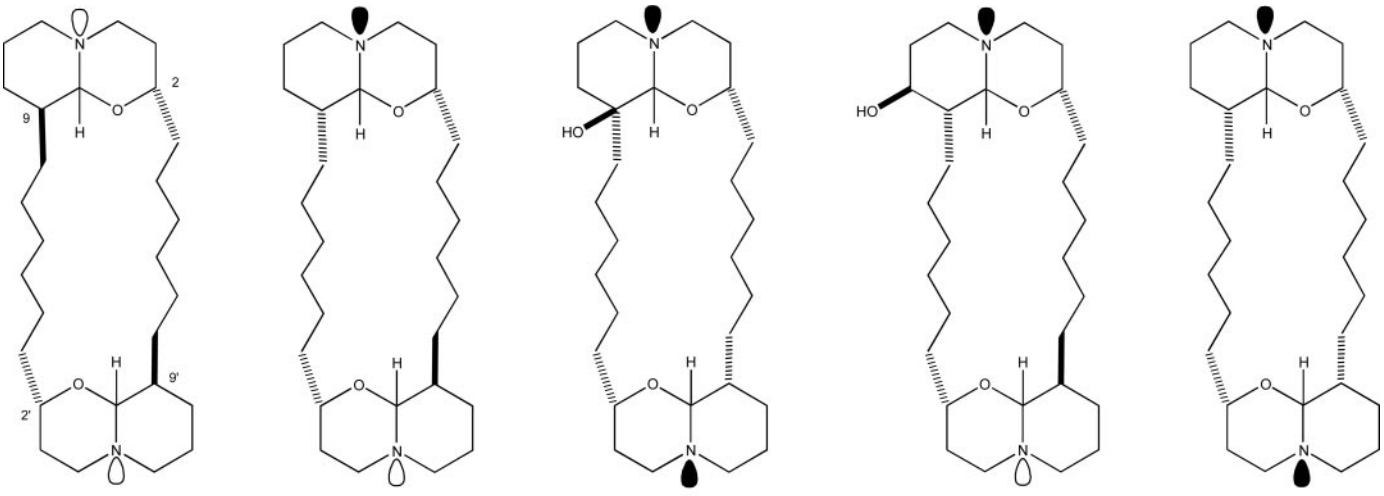

FIG. 19. Molecular structure of xestospongin A (1), xestospongin C (2), demethylxestospongin B (3), xestospongin D (4), araguspongine B (5). Adapted with permission from Gafni et al. (1997).

the putative capacitative Ca^{2+} protein Trp1 (see *Section I.C.*) (Rosado et al., 2002).

Also like 2-APB (see *Section II.C.4.c.*), xestospongin C was shown to inhibit SERCA in saponin-permeabilized A7r5 cells with a potency (IC_{50} value = 67 μM) similar to its potency to inhibit $InsP_3R$ in this smooth muscle preparation (IC_{50} value = 55 μM), resulting in depletion of SR Ca^{2+} stores (De Smet et al., 1999). Such a depletion of ER/SR Ca^{2+} stores in presence of xestospongin C has also been observed in nonpermeabilized A7r5 cells (Broad et al., 1999) and PC12 cells (Gafni et al., 1997).

d. Use in Smooth Muscle Preparations. The xestospongins are a composite of several structures including xestospongins A, C, and D. They are cell-permeant, potent inhibitors of $InsP_3R$ with little effect on RyR, with the most potent being xestospongin C. The various isoforms of $InsP_3R$ differ in their sensitivities to xestospongins. Xestospongins are vasodilators in intact tissues, but this may be due to a multitude of actions, including inhibition of voltage-gated Ca^{2+} channels, since the selectivity for inhibition of $InsP_3R$ appears to be unique for permeabilized cells and microsomal preparations (Table 11).

4. 2-Aminoethoxy-Diphenylborate.

a. Source and Chemical Structure. 2-APB is a synthetic monomer that can form a five-membered boroxazolidine heterocyclic ring (boroxazolidone) when an internal coordinate bond is formed between the nitrogen in the ethanolamine side chain and the tricoordinated boron (Strang et al., 1989) (Fig. 20). This heterocyclic ring species would be more hydrophobic than the primary amine open-chain species that could be protonated at physiological pH; it should thus permeate cells more rapidly (Dobrydneva and Blackmore, 2001). The heterocyclic ring species forms crystals in staggered arrays of molecules, with each molecule linking with two others through hydrogen bonds (Rettig and Trotter, 1976). This hydrogen bonding ability is likely the basis of 2-APB water solubility (Dobrydneva and Blackmore, 2001).

b. Mechanism of Action. The cell-permeant 2-APB was originally characterized as an inhibitor of IICR in rat cerebellar microsomes (Maruyama et al., 1997). Furthermore, high concentrations of 2-APB (up to 1 mM) do not affect $[^3H]InsP_3$ binding to its receptor, which is consistent with the inability of 2-APB (200 μM) to affect $[^3H]InsP_3$ binding to microsomes from the A7r5 cell line (Missiaen et al., 2001a), suggesting that 2-APB inhibits $InsP_3R$ channel opening allosterically (Maruyama et al., 1997). In human platelets and neutrophils, 2-APB (3–100 μM) inhibits thrombin- and 9,11-epithio-11,12-methano-thromboxane A_2 [synthetic thromboxane A_2 (STA_2)]-induced $[Ca^{2+}]_{cyt}$ increase but does not affect (at 100 μM) STA_2-induced $InsP_3$ production in human platelets (Maruyama et al., 1997; Diver et al., 2001; Dobrydneva and Blackmore, 2001). Likewise, 2-APB (100 μM) does not affect ATP-induced $InsP_3$ production in bovine aortic endothelial cells (Bishara et al., 2002). The inhibitory effect of 2-APB on IICR in A7r5 cells is independent of the concentration of $InsP_3$, ATP, or $[Ca^{2+}]_{cyt}$ (Missiaen et al., 2001a). In rabbit thoracic aorta, 2-APB (10 μM–1 mM) blocks angiotensin II-, NE-, and STA_2-induced contractile activity in a noncompetitive manner (Maruyama et al., 1997).

c. Selectivity. 2-APB (up to 100 μM) has no effect on caffeine-induced Ca^{2+} release from ryanodine-sensitive Ca^{2+} stores of rat cardiac and skeletal SR vesicles (Maruyama et al., 1997). It also has no effect, at concentrations up to 1 mM, on K^+-induced rabbit thoracic aorta contractile activity (Maruyama et al., 1997).

However, more recently, 2-APB was shown to affect the function of several molecular targets involved in Ca^{2+} handling besides the $InsP_3R$. First, it inhibits (1–100 μM) thapsigargin-activated store-operated (i.e., capacitative) Ca^{2+} entry in human platelets (Diver et al.,

TABLE 11
Effective concentrations of xestospongins in smooth muscle

Tissue	Animal Species	Experimental Details (Preparation; Measurement Method; Measured Response)	Effective Concentrations of Xestospongins	Reference
			μM	
Airways	Cattle	Isolated smooth muscle cells; fura-2 cellular loading, fluorometry; $[Ca^{2+}]_{cyt}$	20 (Xestospongin C)	Ethier and Madison, 2002
Airways	Human	Isolated smooth muscle cells; fura-2 cellular loading, fluorometry; $[Ca^{2+}]_{cyt}$	20 (Xestospongin C)	Ethier and Madison, 2002
Airways	Human	Isolated smooth muscle cells; indo-1 cellular loading, epifluorescence microscopy; $[Ca^{2+}]_{cyt}$ imaging	10 (Xestospongin C)	Berger et al., 2001
Airways	Mouse	Lung slices; Oregon Green cellular loading, confocal fluorescence microscopy; $[Ca^{2+}]_{cyt}$ imaging	10	Bergner and Sanderson, 2002
Airways	Pig	Isolated intact or β-escin-permeabilized smooth muscle cells; fluo-3 cellular loading, confocal fluorescence microscopy; $[Ca^{2+}]_{cyt}$ imaging	20 (Xestospongin D)	Pabelick et al., 2001a
Aorta	Rat	Saponin-permeabilized cultured A7r5 cell line; $^{45}Ca^{2+}$ cellular loading; Ca^{2+} fluxes	100 (Xestospongin C)	Bultynck et al., 2002
Colon	Mouse	Isolated smooth muscle cells; whole-cell amphotericin B-perforated patch-clamping, fluo-3 cellular loading, confocal fluorescence microscopy; STOCs, $[Ca^{2+}]_{cyt}$ imaging	5 (Xestospongin C)	Bayguinov et al., 2000
Colon	Mouse	Isolated smooth muscle cells; fluo-3 cellular loading, confocal fluorescence microscopy; $[Ca^{2+}]_{cyt}$ imaging	5 (Xestospongin C)	Bayguinov et al., 2001
Ileum	Guinea pig	Isolated smooth muscle cells and α-toxin-permeabilized strips; whole-cell patch-clamping, fura-2 cellular loading, fluorometry, isometric dynamometry; I_{Ba}, $[Ca^{2+}]_{cyt}$, contractile activity	3-10 (Xestospongin C)	Ozaki et al., 2002
Renal pelvis	Guinea pig	Isolated urothelium-denuded strips; isometric dynamometry; contractile activity	1 (Xestospongin C)	Lang et al., 2002
Small intestine	Mouse	Isolated segments; microelectrode; slow wave frequency	0.5 and 1 (Xestospongin C)	Malysz et al., 2001
Taenia coli	Guinea pig	Isolated smooth muscle cells; whole-cell amphotericin B-perforated patch-clamping; STOCs	1 (Xestospongin C)	Kong et al., 2000
Trachea	Dog	Isolated cultured smooth muscle cells; fura-2 cellular loading, fluorometry; $[Ca^{2+}]_{cyt}$	10 (Xestospongin C)	Mitchell et al., 2000

2001; Dobrydneva and Blackmore, 2001), consistent with its concentration-dependent (3–300 μM) inhibition of agonists (ATP, bradykinin)- and receptor-independent (thapsigargin, ionomycin)-induced capacitative Ca^{2+} entry in bovine aortic and rat cardiac endothelial cells (Bishara et al., 2002). 2-APB (1–100 μM) also readily blocks Sr^{2+}, Ba^{2+}, and Mn^{2+} entry in unstimulated human platelets following SR Ca^{2+} store depletion by thapsigargin, suggesting a direct action of 2-APB on store-operated Ca^{2+} channels (SOCC) (Diver et al., 2001; Dobrydneva and Blackmore, 2001), although it cannot be discounted that it also interacts with a non-$InsP_3R$ protein that regulates SOCC. However, complete inhibition by 2-APB of single-channel recordings of a putative SOCC in excised plasma membrane patches of rat basophilic leukemia cells (RBL-2H3 m1), an immortalized mucosal mast cell line, supports a direct action on the channel (Braun et al., 2001). However, the effects on capacitative Ca^{2+} entry may not be simple though. Indeed, in Jurkat human T cells, DT40 chicken B-lymphocytes, and RBL cells, 2-APB has a dichotomous action; at low concentrations (1–5 μM), it enhances the size of the I_{CRAC} and speeds up its fast Ca^{2+}-dependent inactivation, whereas at higher concentrations (≥10 μM), it inhibits I_{CRAC} and blocks its Ca^{2+}-dependent inactivation (Prakriya and Lewis, 2001). This latter inhibition is likely mediated through an extracellular site, as 2-APB is more potent when applied extracellularly and as this inhibition is unaffected by increased protonation of 2-APB (which reduces its cell permeability) (Prakriya and Lewis, 2001). The mechanism underlying these concentration-dependent effects is unknown, but different binding sites (i.e., high versus low affinity) could be involved by analogy with RyR (see *Section II.B.1.b.*) (Sutko et al., 1997), or different 2-APB species may exist at different concentrations (i.e., monomer at low concentrations versus dimer at high concentrations; see *Section II.C.4.a.*; Fig. 20) (Prakriya and Lewis, 2001). In terms of SAR, the inhibition of capacitative Ca^{2+} entry is dependent on diphenyl groups attached to a tetrahedral atom of a five-membered ring (e.g., 2-APB heterocyclic ring; see *Section II.C.4.a*) (Dobrydneva and Blackmore, 2001). Interestingly, in human platelets, thapsigargin induces structural coupling (Rosado and Sage, 2000) between $InsP_3R2$ and the putative SOCC Trp1 (Rosado et al., 2002) that is unchanged by 2-APB despite abolishment of capacitative Ca^{2+} entry (Diver et al., 2001). This is contrasting with the effects of xestospongin C (see above). In this respect, it is relevant to note that 2-APB blocks capacitative Ca^{2+} entry and I_{CRAC} in both wild-type DT40 chicken B-lymphocytes and a variant where all three types of $InsP_3R$ are knocked out (Broad et al., 2001; Prakriya and Lewis, 2001), suggesting that an interaction of 2-APB with an $InsP_3R$ is not required for its inhibition of capacitative Ca^{2+} entry.

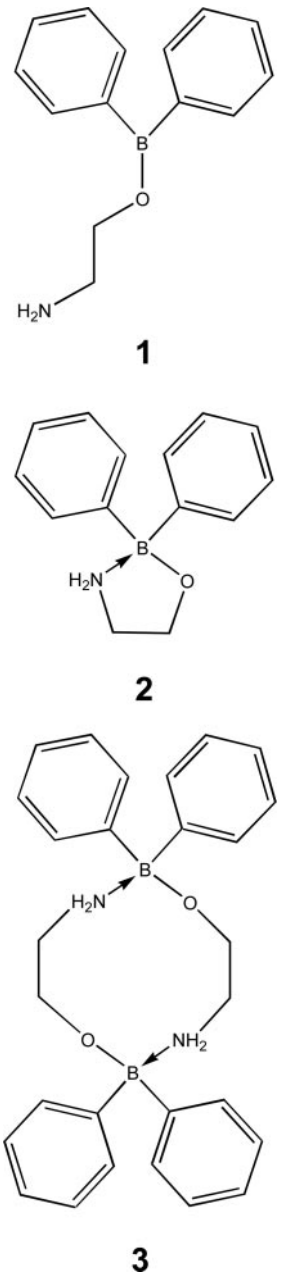

FIG. 20. Molecular structure of 2-APB monomer (1), monomer ring (2), and dimer (3). Adapted with permission from Dobrydneva and Blackmore (2001).

Second, 2-APB (5–50 μM) can inhibit Ca^{2+} efflux from mitochondria [believed to be mostly mediated by a Na^+-Ca^{2+} exchanger on the mitochondrial inner membrane (Gunter et al., 2000)] based on $[Ca^{2+}]_{cyt}$ measurements made in the absence of extracellular Ca^{2+} in Jurkat human T cells (Prakriya and Lewis, 2001). This effect needs to be confirmed more directly, as well as the finding that 2-APB may electrically uncouple smooth muscle cells in an intact blood vessel (Lamont and Wier, 2004).

Third, 2-APB can inhibit Ca^{2+} pumps (e.g., SERCA) and the nonspecific Ca^{2+} leak from nonmitochondrial Ca^{2+} stores in saponin-permeabilized A7r5 cells (Missiaen et al., 2001a). In this smooth muscle preparation, the IC_{50} values for these effects are 91 μM and >100 μM, respectively, compared with an IC_{50} value of 36 μM for inhibition of IICR.

Finally, it was shown recently that 2-APB completely and reversibly blocks gap junctional intercellular communication in monolayers of normal rat kidney cells (NRK/49F) with an IC_{50} value of 5.7 μM (maximal effect at 50 μM), the same concentration range required for inhibition of $PGF_{2\alpha}$-induced $[Ca^{2+}]_{cyt}$ increases (Harks et al., 2003). It displays a similar potency in human embryonic kidney epithelial cells (HEK293/tsA201) with an IC_{50} value of 10.3 μM (Harks et al., 2003).

d. Use in Smooth Muscle Preparations. There is increasing usage of 2-APB as a selective inhibitor of $InsP_3R$, as summarized in Table 12. 2-APB inhibits the $InsP_3R$ channel opening without affecting $InsP_3$ synthesis or binding. Although 2-APB does not interact with RyR or voltage-gated Ca^{2+} entry, it reduces capacitative Ca^{2+} entry, possibly by directly inhibiting store-operated Ca^{2+} channels. 2-APB also reduces Ca^{2+} efflux from mitochondria by inhibition of the Na^+-Ca^{2+} exchanger and may potentially block gap junctional intercellular communication.

5. mAb18A10 and Other Neutralizing Anti-Inositol 1,4,5-Triphosphate Receptor Antibodies.

a. Source and Chemical Structure. A monoclonal antibody, mAb18A10, has been raised in rats against the partially purified 2749-residue-long mouse cerebellar $InsP_3R$ produced by fusing spleen cells with mouse Sp2 myeloma cells (Maeda et al., 1988). Its epitope is located within residues 2736 and 2747 at the very end of the mouse $InsP_3R1$ C-terminal tail (Swiss-Prot Access Number P11881) (Furuichi et al., 1989; Nakade et al., 1991). A polyclonal antiserum, named $3'\beta_1$, has also been raised in rabbits against a 95-residue synthetic polypeptide corresponding to residue sequence 2604–2698 of $InsP_3R$, but its epitope has not been defined (Sullivan et al., 1995). Another neutralizing monoclonal antibody, named IPR.1, has been produced in mice using an 11-residue synthetic polypeptide corresponding to residue sequence 2546–2556 of the mouse $InsP_3R1$ (Bourguignon et al., 1993a), and a neutralizing rabbit polyclonal antibody has also been raised against the same polypeptide (Boittin et al., 2000).

b. Mechanism of Action. The cell-impermeant mAb18A10 has two effects in mouse cerebellar microsomes (Nakade et al., 1991): it suppresses IICR and increases the ability of the $InsP_3R$ to bind $InsP_3$. Suppression of Ca^{2+} release is only observed at submaximally effective $InsP_3$ concentrations (manifested by a rightward shift of $InsP_3$ threshold concentration to ~60 nM from a basal value of ~20 nM and a 5-fold increase in the EC_{50} values, which are 500 nM versus 110 nM) as the antibody does not affect maximal response. Binding of $InsP_3$ to the $InsP_3R$ is maximally increased by ~25%

TABLE 12
Effective concentrations of 2-APB in smooth muscle

Tissue	Animal Species	Experimental Details (Preparation; Measurement Method; Measured Response)	Effective Concentrations of 2-APB	Reference
			μM	
Aorta	Rat	Saponin-permeabilized cultured A7r5 cell line; $^{45}Ca^{2+}$ cellular loading; Ca^{2+} fluxes	200	Missiaen et al., 2001a
Aorta	Rat	Isolated endothelium-denuded rings; isometric dynamometry; contractile activity	50	Shen et al., 2001
Coronary artery	Cow	Isolated smooth muscle cells, and cannulated and pressurized endothelium-denuded rings; fura-2 cellular loading, fluorometry, diameter monitoring by video microscopy; $[Ca^{2+}]_{cyt}$, contractile activity	30	Ge et al., 2003
Cremaster muscle arterioles	Rat	Isolated, cannulated and pressurized endothelium-denuded segments; fura-2 cellular loading, fluorometry, diameter monitoring by video microscopy; $[Ca^{2+}]_{cyt}$, contractile activity	50	Potocnik and Hill, 2001
Femoral artery	Rabbit	Isolated endothelium-denuded rings; isometric dynamometry; contractile activity	10	Jezior et al., 2001
Gall bladder	Guinea pig	Isolated smooth muscle cells; whole-cell amphotericin B-perforated patch-clamping; I_{BK}	50	Pozo et al., 2002
Mesenteric resistance arteries	Rat	Isolated, cannulated and pressurized endothelium-intact or -denuded segments isolated from 3rd- and 4th-order branches; fluo-4 cellular loading, confocal fluorescence microscopy, isotonic dynamometry; $[Ca^{2+}]_{cyt}$ imaging, contractile activity	30	Lamont and Wier, 2004 [in press]
Stomach (antrum, circular layer)	Guinea pig	Isolated smooth muscle bundles; microelectrode, fura-2 cellular loading, fluorometry; membrane potentials, $[Ca^{2+}]_{cyt}$	10	Fukuta et al., 2002
Stomach (antrum, circular layer)	Guinea pig	Isolated, cannulated and pressurized segments; diameter monitoring by video microscopy; contractile activity	60	Haddock et al., 2002
Urinary bladder	Mouse	Isolated smooth muscle cells; fluo-4 cellular loading, confocal fluorescence microscopy; $[Ca^{2+}]_{cyt}$ imaging	100	Ji et al., 2002
Urinary bladder	Rabbit	Isolated urothelium-denuded strips; isometric dynamometry; contractile activity	10	Jezior et al., 2001
Vas deferens	Guinea pig	Isolated smooth muscle cells; whole-cell patch-clamping, fura-2 and fluo-4 cellular loading, fluorometry (fura-2), confocal fluorescence microscopy (fluo-4); STOCS, $[Ca^{2+}]_{cyt}$ imaging	100	White and McGeown, 2003

with a K_D value decreased to ~25 nM from a basal value of ~45 nM (Nakade et al., 1991).

Since the effective concentration range of the antibody (2–50 μg/ml) is the same for both suppressing IICR and decreasing the ability of the $InsP_3R$ to bind $InsP_3$, it is likely that these effects are related (Nakade et al., 1991). Because the $InsP_3R$ C-terminal tail is located close to the central membrane pore of the tetrameric Ca^{2+} release channel, it may be that inhibition of channel activity occurs either as an allosterically-mediated change in channel conformation suppressing activity, or as steric hindrance of the pore by the $InsP_3R$-bound antibody (Nakade et al., 1991). The increased $InsP_3$ binding to the $InsP_3R$ may be due to an allosterically induced conformational change (Nakade et al., 1991). However, an explanation as to why mAb18A10 can only inhibit Ca^{2+} release at submaximally effective concentrations of $InsP_3$, which would reconcile the Ca^{2+} release inhibition with $InsP_3$-binding promotion, may be that channel opening is delayed after $InsP_3$ binds to the receptor (Nakade et al., 1991). At low concentrations, $InsP_3$ may be degraded by inositol polyphosphate 5-phosphatase faster than the time required for channel opening under the influence of the antibody. This effect would be overcome if the initial $InsP_3$ concentration was sufficiently high and remained above threshold level long enough. Detailed kinetic studies are required to test this hypothesis. However, one might predict that, if this hypothesis was correct, mAb18A10 would be ineffective against Ca^{2+} release by nonhydrolysable $InsP_3$ agonists, such as the adenophostins, or by $InsP_3$ in presence of a 5-phosphatase inhibitor (Qazi and Trimmer, 1999).

Interestingly, the polyclonal antiserum 3′β_1 is able to inhibit IICR from a *Xenopus* oocyte membrane fraction, but in contrast with mAb18A10, does not alter receptor affinity (K_D) for $InsP_3$ (Sullivan et al., 1995). This suggests that 3′β_1 and mAb18A10 inhibit $InsP_3R$ channel activity by different mechanisms.

Although mAb18A10 has been extensively used in ascidian, hamster, and mouse oocytes (Miyazaki et al., 1992; Fujiwara et al., 1993; Miyazaki and Shirakawa, 1993; Xu et al., 1994; Shirakawa and Miyazaki, 1995; Mehlmann et al., 1996; Pesty et al., 1998; Yoshida et al., 1998), to our knowledge, neither mAb18A10 nor the polyclonal antibody 3′β_1 has been used in smooth muscle preparations.

c. Selectivity. Although selectivity against other relevant molecular targets, such as RyR, has not been experimentally demonstrated, the 12-residue-long sequence containing the epitope to which mAb18A10 binds

is shared only by the mouse, rat, and human $InsP_3R1$. This sequence is not present in $InsP_3R1$ and $InsP_3R2$.

Interestingly, although the polypeptide used to raise the neutralizing monoclonal antibody IPR.1 corresponds to a residue sequence also found in the mouse, rat, and human $InsP_3R1$ (Bourguignon et al., 1993a,b), homologs of this sequence also occur in the $InsP_3R2$ and $InsP_3R3$ from these species. IPR.1 thus recognizes all three known $InsP_3R$ isoforms. In enzymatically dissociated smooth muscle cells from porcine trachea, IPR.1 inhibits the Cl_{Ca} oscillations induced by Ach, as does heparin (5 mg/ml in pipette solution), another $InsP_3R$ channel blocker (Table 13; see *Section II.C.6.b.*) (Liu and Farley, 1996). In contrast, neither IPR.1 nor heparin affect the caffeine-induced transient Cl_{Ca} that is presumably caused by RyR-induced SR Ca^{2+} release (Liu and Farley, 1996) (Table 13; see *Section II.B.2.b.*), suggesting that IPR.1 is selective for $InsP_3R$ versus RyR. In agreement with this finding, a rabbit polyclonal antibody raised against the same polypeptide used to raise IPR.1 inhibits Ach- and caged $InsP_3$-induced Ca^{2+} waves in enzymatically dissociated rat ureteric smooth muscle cells, an effect shared by heparin (1 mg/ml in pipette solution) (Boittin et al., 2000).

d. Use in Smooth Muscle Preparations. mAb18A10, a targeted monoclonal antibody against $InsP_3R$ and the polyclonal antiserum $3'\beta_1$, have not been used extensively in smooth muscle; only results with IPR.1 and the associated polyclonal antibody have been published (see Table 13). mAb18A10 has two important effects: it reduces IICR (possibly by delaying $InsP_3R$ channel opening) and also increases $InsP_3$ binding to its receptor by ~25%.

6. Heparin.

a. Source and Chemical Structure. Heparin is a component of various tissues (especially liver and lung) and mast cells in man and several mammalian species; its principle and active constituent is a highly sulfated (thus highly anionic), polydisperse polysaccharide (glycosaminoglycan) of molecular weight 4 to 20 kDa consisting of alternating D-glucosamine and D-glucuronic acid residues, both sulfated, in a 1,4-linkage (Ueno and Shimada, 2001). Sulfation has been characterized as mainly 2-*N*,6-*O*-disulfated D-glucosamine, and 2-*O*-sulfated L-iduronic acid and D-glucuronic acid (Lindahl and Hook, 1978). A subset of heparin molecules in the lower end of its molecular weight range (4 to 6 kDa), termed low molecular weight heparin, is usually used in the experiments cited below, and it is presently unknown whether this is critical to its mechanism of action and selectivity as an $InsP_3R$ inhibitor. Although recent advances in carbohydrate analysis and biochemistry have shed light on heparin fine structure, its precise chemical structure remains undetermined.

b. Mechanism of Action. Heparin, which is cell-impermeant, potently and competitively inhibits $InsP_3$ binding to the $InsP_3R$, as initially shown in rat cerebellum membranes (Worley et al., 1987) [IC_{50} value ~2–5 μg/ml, similar values in human myometrium (Varney et al., 1990), rat vas deferens (Mourey et al., 1990), and bovine aortic smooth muscle (Chadwick et al., 1990)]. It has a similar potency in isolated membranes and for inhibition of $InsP_3$-induced contractile activity in β-escin-permeabilized rabbit main pulmonary artery (IC_{50} = 5 μg/ml) (Kobayashi et al., 1988). Heparin (20 μg/ml) prolongs the delay, slows the rate, and reduces the amplitude of SR Ca^{2+} release induced by photolysis of caged $InsP_3$ in β-escin-permeabilized guinea pig portal vein, as the kinetics of caged $InsP_3$ are similar to that of low concentrations of $InsP_3$ (Somlyo et al., 1992).

In terms of SAR, the effects of heparin appear to be specific as equivalent concentrations of chondroitin sulfate, a highly sulfated glycosaminoglycan of very similar chemical composition, and are ineffective in rat cerebellar membranes (Worley et al., 1987). Likewise, neither de-*N*-sulfated heparin, obtained by specific de-*N*-sulfation of native heparin, nor heparin sulfate (a structurally similar molecule to heparin but without 2-*N*,6-*O*-disulfated D-glucosamine and no 2-*O*-sulfated L-iduronic acid, are effective in blocking IICR in saponin-permeabilized aortic smooth muscle cells (Yamamoto et al., 1990). Consistent with these findings, de-*N*-sulfated heparin was also shown to be unable to inhibit IICR in the DDT_1MF-2 smooth muscle cell line (Ghosh et al., 1988). These results suggest that the sulfate groups at C-2-N and C-6 of D-glucosamine and at C-2 of L-iduronic acid of heparin are important for the inhibitory effect (Yamamoto et al., 1990, 1991).

An activity profile similar to heparin was described for low molecular weight dextran sulfate (average 5 kDa), the salt of sulfuric acid esters of the glucose polymer dextran having an average of two sulfate groups per glucose unit. This compound inhibits $InsP_3$-induced decrease in cellular Ca^{2+} content in saponin-permeabilized primary cultured rat aortic smooth muscle cells with an IC_{50} value of ~173 μg/ml [(versus IC_{50} ~7 μg/ml for heparin in this preparation (Yamamoto et al., 1990)]

TABLE 13
Effective concentrations of anti-$InsP_3R$ antibodies in smooth muscle

Tissue	Animal Species	Experimental Details (Preparation; Measurement Method; Measured Response)	Effective Concentrations of Anti-$InsP_3$-R Antibody	Reference
Trachea	Pig	Isolated smooth muscle cells; whole-cell patch-clamping, fluo-3 cellular loading, confocal fluorescence microscopy; $I_{Cl(Ca)}$, STOCs, STICs, $[Ca^{2+}]_{cyt}$ imaging	5 μg/ml (clone IPR.1)	Liu and Farley, 1996
Ureter	Rat	Isolated smooth muscle cells; fluo-3 cellular loading, confocal fluorescence microscopy; $[Ca^{2+}]_{cyt}$ imaging	10 μg/ml (polyclonal)	Boittin et al., 2000

without affecting the caffeine-induced decrease in cellular Ca^{2+}content (at up to 10 mg/ml) (Yamamoto et al., 1991). This suggests selectivity for IICR versus CICR, as it is the case for heparin (see *Selectivity* section). Consistent with this functional effect, dextran sulfate also concentration-dependently inhibits $InsP_3$ binding to these permeabilized cells, although here too it has lower potency than heparin (IC_{50} ~120 μg/ml versus 10 μg/ml for heparin) (Yamamoto et al., 1991). Unlike heparin, dextran sulfate has no sulfate group at C-6 of the D-glucose, because the D-glucose units are α-(1→6)-linked to each other. In contrast, the D-glucosamine of heparin is α-(1→4)-linked to L-iduronic acid. Thus, there may be differences between these two compounds regarding the relative orientation of the sulfate groups on two adjacent units. In any case, the inhibitory activity of both compounds suggests that at least two sulfate groups, one presumably at C-2 of a D-glucose unit and the other on the adjacent unit, are essential for interaction with the $InsP_3R$ (Yamamoto et al., 1991).

In bovine adrenal cortex membranes, heparin does not to change the affinity of binding sites for $InsP_3$ but decreases the number of sites available for $InsP_3$ binding (Guillemette et al., 1989). Heparin inhibits $InsP_3$-dependent gating of $InsP_3R$ Ca^{2+}-channel conductance in rat aortic smooth muscle microsomes incorporated into planar lipid bilayers (Ehrlich and Watras, 1988). Interestingly, the affinity of $InsP_3R$ for heparin does not always correlate with the affinity of $InsP_3R$ for $InsP_3$ and is not species-specific (Varney et al., 1990). However, heparin is a much larger molecule than $InsP_3$, which may give rise to access difficulties creating artifactual differences between tissues and preparations (Varney et al., 1990).

c. Selectivity. At a concentration maximally effective in inhibiting $InsP_3$ action (300 μg/ml (Kobayashi et al., 1988), heparin is ineffective at preventing caffeine-induced (20 mM) contractile activity in saponin-permeabilized rabbit main pulmonary artery (Kobayashi et al., 1988) or caffeine-induced (20 mM) Ca^{2+} release and contractile activity in permeabilized rabbit main pulmonary artery and ileum longitudinal smooth muscle layer (Kobayashi et al., 1988, 1989b). Furthermore, heparin (25 mg/ml) is ineffective at changing the P_o of RyR partially purified from bovine coronary arteries microsomal protein fractions and reconstituted into planar lipid bilayers, which is fully sensitive to caffeine (0.5–5 mM), ryanodine (0.1–50 μM), ruthenium red (40 and 80 μM), and cADPR (0.01–1 μM) (Li et al., 2001). These results suggest that heparin inhibition of SR Ca^{2+} release is selective for $InsP_3R$ versus RyR. However, heparin induces Ca^{2+} release from skeletal muscle microsomes (Ritov et al., 1985). In rabbit skeletal muscle microsomes incorporated into planar lipid bilayers, heparin (0.1–1 μg/ml on *cis* chamber, equivalent to the cytoplasmic side) increases the P_o of RyR in a ryanodine (5 μM)- and ruthenium red (2 μM)-sensitive manner (characteristic of RyR1) and does so in a Ca^{2+}-dependent manner (requires free $[Ca^{2+}] \geq 80$ nM in *cis* chamber, inactive if <20 nM) (Bezprozvanny et al., 1993). This effect is mimicked, but with reduced potency, by other polyanions such as pentosan polysulfate and polyvinyl sulfate, suggesting that these agents act by increasing the local concentration of Ca^{2+} near regulatory sites on the RyR-channel complex (Bezprozvanny et al., 1993). That this potentiating effect is relevant for smooth muscles, where RyR2 and/or RyR3 isoforms can be expressed instead of or in addition to RyR1, is evidenced by the fact that heparin (300 μg/ml), which inhibits histamine (100 μM)- and $InsP_3$ (40 μM)-induced contractile activity, tends to potentiate subsequent caffeine (20 mM)-induced contractile activity in β-escin-permeabilized guinea pig ileum longitudinal smooth muscle layer (Fukami et al., 1993), although this effect could also be explained by a functional overlap of $InsP_3$- and caffeine-sensitive SR Ca^{2+} stores.

Heparin (300 μg/ml) does not affect K^+ (143 mM)-induced contractile activity in reversibly permeabilized rabbit ileum longitudinal smooth muscle layer (Kobayashi et al., 1988), suggesting that it does not affect Ca^{2+} sensitivity of contractile proteins. Consistent with this finding, heparin, at a concentration that maximally inhibits $InsP_3$ action (300 μg/ml), is ineffective in blocking the potentiation of Ca^{2+}-induced contractile activity by Cch or GTPγ S in β-escin-permeabilized rabbit ileum longitudinal smooth muscle, suggesting that it does not affect G-protein-dependent sensitization of the contractile apparatus to Ca^{2+} (Kobayashi et al., 1989b). Likewise, heparin (300 μg/ml) does not affect calmodulin-induced potentiation of Ca^{2+}-induced contractile activity in β-escin-permeabilized rabbit tracheal smooth muscle (Iizuka et al., 1998).

However, although heparin has no effect on I_{CRAC} in mast cells (Hoth and Penner, 1992), its highest molecular weight fraction (14–17 kDa) inhibits capacitative Ca^{2+} entry in human neutrophils (100 μg/ml on cytoplasmic side) (Davies-Cox et al., 2001). Neither microinjected neutralizing monoclonal antibody IPR.1 (250 kDa) nor albumin-conjugated heparin (>200 kDa) inhibits capacitative Ca^{2+} entry, whereas all three agents reduce intracellular Ca^{2+} release induced by the peptide formylmethionyl-leucylphenylalanine (f-Met-Leu-Phe) (Davies-Cox et al., 2001). This suggests that the capacitative Ca^{2+} entry mechanism in these cells involves a heparin-sensitive step that is not accessible to higher molecular weight $InsP_3R$ inhibitors. Consistent with these findings, heparin inhibits an $InsP_3$-activated Ca^{2+} current in plasma membranes by inhibiting the P_o of 1) an $InsP_3R$-like Ca^{2+} channel in excised plasma-membrane patches from cultured bovine aortic epithelial cells (1 μg/ml) (Vaca and Kunze, 1995), 2) an $InsP_3R$ purified from rat liver plasma membrane (IC_{50} value ~20 μg/ml; effective concentration range = 10–40 μg/ml) (Mayrleitner et al., 1995), and 3) I_{CRAC}-like channels, termed miniature Ca^{2+} channels, in excised plasma-membrane patches from mouse macrophage (Kiselyov et

al., 1999; Semenova et al., 1999) and from A431 cells (human carcinoma cell line) (Kiselyov et al., 1997) (100–500 μg/ml on cytoplasmic side).

At high concentrations (≥1 mg/ml), heparin significantly chelates free Ca^{2+} (K_D = 0.64 mM = 3.2 mg/ml), which likely explains its inhibition of K^+ (143 mM)- and Cch (10 μM)-induced contractile activity (IC_{50} values ~20 mg/ml and >50 mg/ml, respectively) of intact rabbit ileum longitudinal smooth muscle (Kobayashi et al., 1989b).

Heparin also inhibits bovine adrenal cortex $InsP_3$ 3-kinase in a noncompetitive manner with an IC_{50} value of ~0.4 μg/ml (versus an IC_{50} value of ~10–20 μg/ml for blocking $InsP_3R$ in this tissue). In contrast, it is without effect on inositol polyphosphate 5-phosphatase (at up to 2 mg/ml) (Guillemette et al., 1989). Given that these enzymes are responsible for $InsP_3$ inactivation in the cytoplasm (see *Section II.C.1.b.*), these results raise the possibility that, at low concentrations, heparin might potentiate the effect of $InsP_3$ by inhibiting its inactivation, although the relevance of this mechanism in smooth muscle preparations is unknown.

d. Use in Smooth Muscle Preparations. Heparin is considered prototypical inhibitor of $InsP_3R$ (Table 14). Although it is cell-impermeant, it is frequently used as a competitive inhibitor of $InsP_3$ binding to microsomes and IICR in permeabilized smooth muscle. Heparin does not inhibit voltage-gated Ca^{2+} entry or G-protein-mediated intracellular Ca^{2+} sensitization, although it has other selectivity problems. The IC_{50} value for heparin in reducing IICR in permeabilized vascular smooth muscle is 5 μg/ml (Kobayashi et al., 1989b), a fairly low potency. At high concentrations however, heparin chelates Ca^{2+}. In intact tissue, low concentrations of heparin (up to 2 mg/ml) do not effect contractile responses to K^+ depolarization or agonist (Cch) stimulation, whereas higher concentrations (>20 mg/ml) are inhibitory (Kobayashi et al., 1989b).

III. Conclusions and Perspectives

We provide an overview of the pharmacology of research tools useful in understanding SR function in smooth muscle. Although we attempted to be comprehensive, there undoubtedly are oversights and omissions, which we hope will not detract from the usefulness of this overview. This review is aimed as a starting point for those who are new to the field and also as a summative document for more established investigators. Advances in our understanding of the physiology and pharmacology of the SR in smooth muscle has benefited greatly from the availability of an array of reagents that interact with various elements affecting SR function. Although such compounds have revealed the complex role of this organelle in regulating cell function, there is no doubt much more to be unearthed. Thus, there is a continuing need to develop improved ligands, coupled with a greater understanding of the strengths and limitations of currently available compounds. This, together with the application with more direct techniques, will greatly assist in the design of insightful experiments that will yield more detailed information.

Until relatively recently, contraction of smooth muscle was thought to depend almost exclusively on the entry of Ca^{2+} from extracellular sources, mainly through the activation of voltage-gated Ca^{2+} channels. However, the combined use of high-resolution imaging techniques and a variety of pharmacological modulators of SR function has revealed a complex system that has a far greater reliance on SR Ca^{2+} for the initiation, maintenance, and decay of smooth muscle tone. As recently summarized by Wier and Morgan (2003), smooth muscle SR serves a multitude of functions with regard to smooth muscle excitation-contraction coupling, including: 1) regulation of contraction (activation of contractile proteins) and relaxation (activation of K_{Ca} channels, SERCA-mediated Ca^{2+} uptake), 2) interception of a portion of Ca^{2+} that enters a cell (superficial buffer barrier), 3) generation of Ca^{2+} waves and oscillations, and 4) interaction with Ca^{2+}-store-operated channels (possibly through the interaction of $InsP_3R$ and Trp channels). Smooth muscle contains isoforms of RyR as well as isoforms of $InsP_3R$, and there is a clear interaction between release events occurring at these receptor sites (Iino, 2002). The Ca^{2+} stores in smooth muscle have variously been described as those containing only a single Ca^{2+}-release channel (RyR or IP_3R) or both. Thus, RyR and $InsP_3R$ can work cooperatively as Ca^{2+} is a ligand at both sites (Iino, 2002).

Elementary Ca^{2+} release events, termed Ca^{2+} sparks, frequently occur in discreet but preferred areas of the cell. These preferred areas are adjacent to the superficially located SR and lie within ~15 nm of the plasma membrane (Somlyo and Franzini-Armstrong, 1985; Gordienko et al., 2001). Both RyR1 and RyR2 are required for Ca^{2+} spark activity, with the role of RyR3 thought to be minimal (Boittin et al., 2000) or inhibitory (Lohn et al., 2001). It has been proposed that microsparks, which are smaller in duration, point spread, and amplitude, may form the basis of Ca^{2+} sparks (Pucovsky et al., 2002). Thus, smooth muscle tone is accompanied by a decrease in Ca^{2+} spark frequency (Bonev et al., 1997; Jaggar and Nelson, 2000; Mauban et al., 2001). Under certain conditions, which are not well defined, increased Ca^{2+} spark activity generates oscillations that are comprised of repetitive Ca^{2+} transients; these oscillations can then propagate as Ca^{2+} waves (see Bradley et al., 2003). The average Ca^{2+} concentration recorded, e.g., with intracellular recorder dyes, represents the summation of the asynchronous Ca^{2+} waves of the individual smooth muscle cells. Therefore, an important consequence of SR Ca^{2+}release/depletion during the generation of Ca^{2+} waves is the stimulation of Ca^{2+} influx.

In addition to the now familiar concept of Ca^{2+} sparks, there are other modalities of spontaneously oc-

TABLE 14
Effective concentrations of heparin in smooth muscle

Tissue	Animal Species	Experimental Details (Preparation; Measurement Method; Measured Response)	Effective Concentrations of Heparin	Reference
Anococcygeus	Mouse	Isolated smooth muscle cells; whole-cell patch-clamping; I_{DOC}, $I_{Cl(Ca)}$	5 mg/ml	Wayman et al., 1998
Aorta	Dog	Microsomal membranes incorporated into planar lipid bilayers, microsomes; bilayer clamp amplification (for membranes), extra-microsomal anti-pyridylazo-III (for microsomes); single Ca^{2+} channel currents (for membranes), Ca^{2+} fluxes (for microsomes)	1 mg/ml	Ehrlich and Watras, 1988
Aorta	Pig	Microsomes; extramicrosomal fluo-3, fluoroscopy; Ca^{2+} fluxes	50 μg/ml	Tovey et al., 2000
Aorta	Cattle	Purified $InsP_3R$ incorporated into planar bilayers; bilayer clamp amplification; single Ca^{2+} channel currents	25 μg/ml	Mayrleitner et al., 1991
Aorta	Rat	Microsomes; $^{45}Ca^{2+}$ loading; Ca^{2+} fluxes	1 mg/ml	Yusufi et al., 2002
Basilar artery	Rat	Isolated smooth muscle cells; whole-cell patch-clamping; $I_{K(Ca)}$	100 μg/ml	Kim et al., 1998
Colon (circular layer)	Dog	Isolated non-inflamed and inflamed saponin-permeabilized smooth muscle cells; $^{45}Ca^{2+}$-cellular loading, cell length monitoring by phase-contrast microscopy; Ca^{2+} fluxes, contractile activity	100 μg/ml	Shi and Sarna, 2000
Coronary artery	Cattle	Microsomal membranes, stripped or not of FKBP-12.6, incorporated into planar lipid bilayers; bilayer clamp amplification; single Ca^{2+} channel currents	25 mg/ml	Li et al., 2001
Esophagus	Cat	Isolated saponin-permeabilized smooth muscle cells; cell length monitoring by phase-contrast microscopy; contractile activity	20 μM	Shim et al., 2002
Esophagus (lower sphincter, circular layer)	Cat	Isolated saponin-permeabilized smooth muscle cells; cell length monitoring by phase-contrast microscopy; contractile activity	10 μg/ml	Sohn et al., 1993
Gall bladder	Cat	Isolated saponin-permeabilized smooth muscle cells; cell length monitoring by phase-contrast microscopy; contractile activity	10 μM	Yu et al., 1998
Ileum (circular layer)	Guinea pig	Isolated β-escin-permeabilized strips; isometric dynamometry; contractile activity	0.3 and 1 mg/ml	Fukami et al., 1993
Mesenteric resistance arteries	Rabbit	Isolated β-escin-permeabilized smooth muscle cells; fura-2 cellular loading, fluorometry; $[Ca^{2+}]_{cyt}$	500 μg/ml	Itoh et al., 1992
Portal vein	Guinea pig	Isolated saponin- or β-escin-permeabilized strips; fluo-3 cellular loading, epifluorescence microscopy, isometric dynamometry; $[Ca^{2+}]_{cyt}$ imaging, contractile activity	20 μg/ml	Somlyo et al., 1992
Stomach (antrum)	Guinea pig	Isolated smooth muscle cells; whole-cell patch-clamping; I_{BK}	Dialyzed with 0.1 μM	Duridanova et al., 1997
Testicular peritubules	Rat	Isolated saponin-permeabilized smooth muscle cells; fura-2 cellular loading, fluorometry; $[Ca^{2+}]_{cyt}$	10 μg/ml	Barone et al., 2002
Trachea	Cat	Isolated smooth muscle cells; whole-cell nystatin perforated patch-clamping; I_{Cch}	3 mg/ml	Waniishi et al., 1998
Trachea	Cattle	Microsomal membranes incorporated into planar lipid bilayers; bilayer clamp amplification; single Ca^{2+} channel currents	10 μM	Gaburjakova et al., 1999
Trachea	Pig	Isolated β-escin-permeabilized smooth muscle cells; fluo-3 cellular loading, confocal fluorescence microscopy; $[Ca^{2+}]_{cyt}$ imaging	0.5 mg/ml	Kannan et al., 1997
Trachea	Pig	Isolated smooth muscle cells; whole-cell patch-clamping; $I_{Cl(Ca)}$	5 mg/ml	Liu and Farley, 1996
Trachea	Rabbit	Isolated β-escin-permeabilized strips; isometric dynamometry; contractile activity	300 μg/ml	Iizuka et al., 1998
Ureter	Guinea pig	Isolated α-toxin- or β-escin-permeabilized strips; isometric dynamometry; contractile activity	50 and 100 μM	Burdyga et al., 1998
Ureter	Rat	Isolated α-toxin- or β-escin-permeabilized strips; isometric dynamometry; contractile activity	50 and 100 μM	Burdyga et al., 1998
Vas deferens	Guinea pig	Isolated smooth muscle cells; fluo-4 cellular loading, confocal fluorescence microscopy; local $[Ca^{2+}]_{cyt}$ imaging	5 mg/ml	White and McGeown, 2003

curring Ca^{2+} release events. Two such types are Ca^{2+} ripples and Ca^{2+} flashes, as observed in individual smooth muscle cells within intact segments of rat tail artery (Asada et al., 1999). Ca^{2+} ripples, which are modest in amplitude and frequency, are thought to be $InsP_3R$-generated. On the other hand, Ca^{2+}flashes are described as large Ca^{2+} discharges occurring in small areas (<20 μm) of the cell and that spread in a passive manner. Although ripples occur in about half the cell population studied, Ca^{2+} flashes are considerably more infrequent (Asada et al., 1999). These different patterns of Ca^{2+} delivery within the cell (sparks, waves, oscillations, etc.) encodes signaling information that determines the characteristics (e.g., amplitude, frequency,

and duration) of smooth muscle cell function at level as diverse as excitability/contractility, secretion, proliferation, migration, and cell cycling.

It is clear that Ca^{2+} released from the SR can activate either contraction or relaxation. As reviewed by Wier and Morgan (2003), Ca^{2+} released via $InsP_3R$ channels initiates contraction, whereas Ca^{2+} release through RyR channels mediates smooth muscle relaxation. The spread of the Ca^{2+} wave generated by IICR is sufficiently slow (~20 μm sec^{-1}) to allow for activation of the contractile machinery. Smooth muscle activation generates asynchronous Ca^{2+} waves, the frequency of which is increased with agonist concentration (Ruehlmann et al., 2000). When first observed by Hirose and Iino (1994), it was suggested that asynchronous Ca^{2+} waves were likely due to regenerative IICR. Support for this comes from more recent observations in arteries lacking functional RyR, where plasma membrane receptor activation was still able to produce apparently normal Ca^{2+} waves (Dreja et al., 2001). There is also evidence for a central role for RyR in the establishment of agonist-generated Ca^{2+} waves (Peng et al., 2001). In contrast to the asynchronous Ca^{2+} waves generated by agonists through discrete openings of $InsP_3R$, arteries can also undergo vasomotion or rhythmic contractions that are due to spatially uniform changes in Ca^{2+}, most likely generated by oscillatory changes in membrane potential (Mauban et al., 2001).

Regardless of the events leading to the generation of the Ca^{2+} signal, to be effective as a messenger, mechanisms must exist that allow for this ion to cause discrete and targeted cellular activation in a manner that has spatial and temporal characteristics consistent with physiological events. The assembly of various combinations of SR, ion transporters, exchangers, pumps, and channels makes feasible the creation of gradients of Ca^{2+} in various domains within the cell. A restricted space (15–30 nm) is created by the close opposition of a portion of the SR that extends toward the cell membrane (superficial SR) (see *Section I.D.*). This superficially located SR acts as a Ca^{2+} buffer by accumulating a component of Ca^{2+} that enters the cell; the SERCA pump thus diverts part of the Ca^{2+} that enters the cell away from the deeper elements of the cell for storage and subsequent extrusion (Poburko et al., 2004). Ca^{2+} removal mechanisms, primarily comprised of the Na^+-Ca^{2+} exchanger, and the PMCA maintain the buffering capacity of the SR.

There are currently no promising leads that implicate a therapeutic potential for reagents that disturb SR function in smooth muscle, be it vascular or nonvascular. One intriguing possibility may be in the manipulation of the basal leak of the relatively high basal leak of Ca^{2+} in unstimulated smooth muscle—this would require characterization of the Ca^{2+} leak pathway and selective inhibitors thereof. Presently, this would appear to be a somewhat distant possibility, since the Ca^{2+} leak may not necessarily require specific structural elements in cell membrane. A more likely therapeutic application lies in the manipulation of the "spontaneous Ca^{2+} release" from the SR—Ca^{2+} sparks—in vascular (e.g., small arteries) and nonvascular (e.g., bladder) smooth muscles. It is highly likely that the properties of Ca^{2+} sparks are altered in hyperactive smooth muscle. One approach to this would be to target the response elements associated with Ca^{2+} sparks, since the sites of release (RyR) may be a more problematic site of manipulation as these receptors required for a host of normal functions including those related to organ development.

The development of more selective reagents will enable us to ask more refined and better-focused questions related to cell function. Included among these is better definition of the precise role of the PMCA in health and disease states. In addition, it may be possible to gain a greater understanding of possible cross-talk by the various elements regulating SR function, for instance, between the RyR and $InsP_3R$. Uncovering the distribution patterns of these Ca^{2+} release sites and appreciating their interaction will generate fruitful insights in spontaneous contractile activity, such as pacemaker currents in the gut, spontaneous fluctuations of resistance artery tone, and the spread and function of intracellular Ca^{2+} waves. Likewise, availability of newer reagents with known specificities will help to establish the possibility of dynamic interactions of the peripheral SR with elements of the plasma membrane such as caveolae (and possibly gap junctions). Such compounds will be a valuable tool in ongoing research on the structure-function aspects regulating the activity of phasic versus tonic smooth muscle.

The urgent need to develop cell-permeant reagents cannot be understated since the goal is to integrate these findings in intact, functional systems. This is particularly evident in the study of the functional roles $InsP_3$ and, more so, cADPR. Those who have advanced technologies generate meaningful data with agents that regulate these endogenous Ca^{2+} releasing agents. One example is the need to understand the role of cADPR in smooth muscle—it produces no electrical or mechanical events when applied under acute conditions in smooth muscle, even though smooth muscle has the biochemical machinery for the synthesis and degradation of cADPR. With appropriate cell-permeant pharmacological tools, one can explore the possibility that cADPR has a more permissive or accessory role in excitation-contraction coupling, or even that it may have some trophic effects.

An emerging area is in the understanding of capacitative Ca^{2+} entry and the pharmacology of Ca^{2+} entry pathways that are activated by a depleted SR, e.g., trp channels. This is complicated immensely by several factors, one of which remains an overarching enigma—what is the sensing mechanism that couples SR content

with extracellular Ca^{2+} entry? How does the luminal content of the SR signal the plasma membrane? Resolution of these details will undoubtedly spur the development of pharmacological strategies aimed at augmenting or attenuating the actions of such processes. This then leads to another layer of complexity in multiple isoforms of trp channels and combination patterns, which again may vary regionally. These issues will increase in importance if there is evidence linking capacitative Ca^{2+} entry and trp channel function/density to disease states.

It is apparent that these pharmacological tools, which in many cases were in routine use for striated muscle research, have found homes in smooth muscle research. There are some notable exceptions in the literature; for example, the dearth of reports in the use of adenophostins in smooth muscle as is evident from this review of the available literature. Important strides are being made through innovative approaches with existing reagents, e.g., down-regulation of RyR using organ culture techniques.

As the possibilities made available by advances in techniques in molecular biology are better integrated with functional correlates, important insights in the (many) physiological roles of SR will emerge. Some efforts in this direction have produced some unexpected findings, such as the embryonic importance of RyR. Other opportunities may lie in manipulation of storage mechanisms for Ca^{2+} in the SR and understanding how this would impact on other functions such as SERCA and Ca^{2+} release mechanisms.

It is evident that the appropriate and judicious use of the pharmacological tools regulating SR function in smooth muscle has produced many interesting findings and greatly extended our appreciation of the complex nature of this intracellular organelle. Findings that the SR that is associated with the nuclear membrane may also regulate transcriptional events are just one promissory note for radical changes in our appreciation of the role of the SR in various aspects of smooth muscle function.

Acknowledgments. To our friends who gave so generously of their time, expertise, and insight: Christian Aalkjaer, Vladimir Ganitkevich, Ashok Grover, Mike Hill, Yu Huang, Gary and Meg Kargacin, Harry Knot, Holger Nilsson. We remain indebted for their lasting collegiality. We were particularly encouraged by the support provided by Yongzheng Liu, Julie Liu Laporte, and Ayesha Laher. This work was supported by grants from the Heart and Stroke Foundation of Canada.

References

Aarhus R, Gee K, and Lee HC (1995a) Caged cyclic ADP-ribose. Synthesis and use. *J Biol Chem* **270:**7745–7749.

Aarhus R, Graeff RM, Dickey DM, Walseth TF, and Lee HC (1995b) ADP-ribosyl cyclase and CD38 catalyze the synthesis of a calcium-mobilizing metabolite from NADP. *J Biol Chem* **270:**30327–30333.

Adachi M, Fang Y, Yamakuni T, Kobayashi J, and Ohizumi Y (1994) Properties of the binding sites of [3H]9-methyl-7-bromoeudistomin D in bovine aortic smooth muscle microsomes. *J Pharm Pharmacol* **46:**771–773.

Adachi T, Matsui R, Weisbrod RM, Najibi S, and Cohen RA (2001) Reduced sarco/endoplasmic reticulum Ca^{2+} uptake activity can account for the reduced response to NO, but not sodium nitroprusside, in hypercholesterolemic rabbit aorta. *Circulation* **104:**1040–1045.

Adebanjo OA, Anandatheerthavarada HK, Koval AP, Moonga BS, Biswas G, Sun L, Sodam BR, Bevis PJ, Huang CL, Epstein S, et al. (1999) A new function for CD38/ADP-ribosyl cyclase in Nuclear Ca^{2+} homeostasis. *Nat Cell Biol* **1:**409–414.

Ahn HY and Karaki H (1988) Inhibitory effects of procaine on contraction and calcium movement in vascular and intestinal smooth muscles. *Br J Pharmacol* **94:**789–796.

Akata T, Nakashima M, and Izumi K (2001) Comparison of volatile anesthetic actions on intracellular calcium stores of vascular smooth muscle: investigation in isolated systemic Resistance arteries. *Anesthesiology* **94:**840–850.

Albert AP and Large WA (2002) A Ca^{2+}-permeable non-selective cation channel activated by depletion of internal Ca^{2+} stores in single rabbit portal vein myocytes. *J Physiol (Lond)* **538:**717–728.

Albert AP and Large WA (2003) Store-operated Ca(2+)-permeable non-selective cation channels in smooth muscle cells. *Cell Calcium* **33:**345–356.

Allbritton NL, Meyer T, and Stryer L (1992) Range of messenger action of calcium ion and inositol 1,4,5-trisphosphate. *Science (Wash DC)* **258:**1812–1815.

Alvarez J and Montero M (2002) Measuring [Ca(2+)] in the endoplasmic reticulum with aequorin. *Cell Calcium* **32:**251–260.

Amann R and Maggi CA (1991) Ruthenium red as a capsaicin antagonist. *Life Sci* **49:**849–856.

Amberg GC, Bonev AD, Rossow CF, Nelson MT, and Santana LF (2003) Modulation of the molecular composition of large conductance, Ca(2+) activated K(+) channels in vascular smooth muscle during hypertension. *J Clin Investig* **112:**717–724.

Amrani Y, Magnier C, Enouf J, Wuytack F, and Bronner C (1995) Ca^{2+} increase and Ca(2+)-influx in human tracheal smooth muscle cells: role of Ca^{2+} pools controlled by sarco-endoplasmic reticulum Ca(2+)-ATPase 2 isoform. *Br J Pharmacol* **115:**1204–1210.

Andersen A, Cornett C, Lauridsen A, Olsen CE, and Broegger Christensen S (1994) Selective transformations of the Ca^{2+} pump inhibitor thapsigargin. *Acta Chem Scand* **48:**340–346.

Andersen JP and Vilsen B (1995) Structure-function relationships of cation translocation by Ca(2+)- and Na+, K(+)-ATPases studied by site-directed mutagenesis. *FEBS Lett* **359:**101–106.

Andriantsitohaina R, Lagaud GJ, Andre A, Muller B, and Stoclet JC (1995) Effects of cGMP on calcium handling in ATP-stimulated rat resistance arteries. *Am J Physiol* **268:**H1223–H1231.

Asada Y, Yamazawa T, Hirose K, Takasaka T, and Iino M (1999) Dynamic Ca^{2+} signalling in rat arterial smooth muscle cells under the control of local renin-angiotensin system. *J Physiol (Lond)* **521:**497–505.

Asano M, Kuwako M, Nomura Y, Suzuki Y, and Shibuya M (1998) Possible mechanism underlying the potent vasoconstrictor actions of cyclopiazonic acid on dog cerebral arteries. *Eur J Pharmacol* **352:**215–221.

Asano M and Nomura Y (2001) Calcium buffering of resting, voltage-dependent Ca^{2+} influx by sarcoplasmic reticulum in femoral arteries from spontaneously hypertensive rats at prehypertensive stage. *Hypertens Res* **24:**271–282.

Ash GR and Bygrave FL (1977) Ruthenium red as a probe in assessing the potential of mitochondria to control intracellular calcium in liver. *FEBS Lett* **78:**166–168.

Ashamu GA, Sethi JK, Galione A, and Potter BV (1997) Roles for adenosine ribose hydroxyl groups in cyclic adenosine 5′-diphosphate ribose-mediated Ca^{2+} release. *Biochemistry* **36:**9509–9517.

Awad SS, Lamb HK, Morgan JM, Dunlop W, and Gillespie JI (1997) Differential expression of ryanodine receptor RyR2 mRNA in the non-pregnant and pregnant human myometrium. *Biochem J* **322:**777–783.

Babul'ova A, Bauer V, Buran L, Benes L, Todorov S, Zamfirova R, and Petkov V (1981) The effect of new local anesthetics on tracheal and anococcygeal smooth muscle. *Acta Physiol Pharmacol Bulg* **7:**3–8.

Bailey VC, Fortt SM, Summerhill RJ, Galione A, and Potter BV (1996) Cyclic aristeromycin diphosphate ribose: a potent and poorly hydrolysable Ca(2+)-mobilising mimic of cyclic adenosine diphosphate ribose. *FEBS Lett* **379:**227–230.

Bailey VC, Sethi JK, Fortt SM, Galione A, and Potter BV (1997) 7-Deaza cyclic adenosine 5′-diphosphate ribose: first example of a Ca(2+)-mobilizing partial agonist related to cyclic adenosine 5′-diphosphate ribose. *Chem Biol* **4:**51–61.

Barone F, Genazzani AA, Conti A, Churchill GC, Palombi F, Ziparo E, Sorrentino V, Galione A, and Filippini A (2002) A pivotal role for cADPR-mediated Ca^{2+} signaling: regulation of endothelin-induced contraction in peritubular smooth muscle cells. *FASEB J* **16:**697–705.

Bayguinov O, Hagen B, Bonev AD, Nelson MT, and Sanders KM (2000) Intracellular calcium events activated by ATP in murine colonic myocytes. *Am J Physiol* **279:**C126–C135.

Bayguinov O, Hagen B, and Sanders KM (2001) Muscarinic stimulation increases basal Ca^{2+} and inhibits spontaneous Ca^{2+} transients in murine colonic myocytes. *Am J Physiol* **280:**C689–C700.

Bazan-Perkins B, Sanchez-Guerrero E, Carbajal V, Barajas-Lopez C, and Montano LM (2001) Sarcoplasmic reticulum Ca^{2+} depletion by caffeine and changes of [Ca2+]i during refilling in bovine airway smooth muscle cells. *Arch Med Res* **31:**558–563.

Bazzazi H, Kargacin ME, and Kargacin GJ (2003) Ca^{2+} regulation in the near-membrane microenvironment in smooth muscle cells. *Biophys J* **85:**1754–1765.

Beecroft MD, Marchant JS, Riley AM, Van Straten NCR, van der Marel GA, van Boom JH, Potter BVL, and Taylor CW (1999) Acyclophostin: a ribose-modified analog of adenophostin A with high affinity for inositol 1,4,5-trisphosphate receptors and pH-dependent efficacy. *Mol Pharmacol* **55:**109–117.

Benevolensky D, Moraru II, and Watras J (1994) Micromolar calcium decreases affinity of inositol trisphosphate receptor in vascular smooth muscle. *Biochem J* **299:**631–636.

Benham CD and Bolton TB (1986) Spontaneous transient outward currents in single visceral and vascular smooth muscle cells of the rabbit. *J Physiol (Lond)* **381:**385–406.

Berger P, Tunon-De-Lara JM, Savineau JP, and Marthan R (2001) Selected contri-

bution: tryptase-induced PAR-2-mediated Ca^{2+} signaling in human airway smooth muscle cells. *J Appl Physiol* **91:**995–1003.
Bergner A and Sanderson MJ (2002) Acetylcholine-induced calcium signaling and contraction of airway smooth muscle cells in lung slices. *J Gen Physiol* **119:**187–198.
Berridge MJ (2002) The endoplasmic reticulum: a multifunctional signaling organelle. *Cell Calcium* **32:**235–249.
Berridge MJ and Irvine RF (1984) Inositol trisphosphate, a novel second messenger in cellular signal transduction. *Nature (Lond)* **312:**315–321.
Bezprozvanny I, Bezprozvannaya S, and Ehrlich BE (1994) Caffeine-induced inhibition of inositol(1,4,5)-trisphosphate-gated calcium channels from cerebellum. *Mol Biol Cell* **5:**97–103.
Bezprozvanny IB, Ondrias K, Kaftan E, Stoyanovsky DA, and Ehrlich BE (1993) Activation of the calcium release channel (ryanodine receptor) by heparin and other polyanions is calcium dependent. *Mol Biol Cell* **4:**347–352.
Bian JH, Ghosh TK, Wang JC, and Gill DL (1991) Identification of intracellular calcium pools. Selective modification by thapsigargin. *J Biol Chem* **266:**8801–8806.
Bigay J, Deterre P, Pfister C, and Chabre M (1987) Fluoride complexes of aluminium or beryllium act on G-proteins as reversibly bound analogues of the gamma phosphate of GTP. *EMBO (Eur Mol Biol Organ) J* **6:**2907–2913.
Bishara NB, Murphy TV, and Hill MA (2002) Capacitative Ca^{2+} entry in vascular endothelial cells is mediated via pathways sensitive to 2 aminoethoxydiphenyl borate and xestospongin C. *Br J Pharmacol* **135:**119–128.
Bitar KN, Hillemeier C, Biancani P, and Balazovich KJ (1991) Regulation of smooth muscle contraction in rabbit internal anal sphincter by protein kinase C and Ins(1,4,5)P3. *Am J Physiol* **260:**G537–G542.
Bobe R, Bredoux R, Wuytack F, Quarck R, Kovacs T, Papp B, Corvazier E, Magnier C, and Enouf J (1994) The rat platelet 97-kDa Ca^{2+}ATPase isoform is the sarco-endoplasmic reticulum Ca^{2+}ATPase 3 protein. *J Biol Chem* **269:**1417–1424.
Boittin FX, Coussin F, Morel JL, Halet G, Macrez N, and Mironneau J (2000) Ca^{2+} signals mediated by Ins(1,4,5)P3-gated channels in rat ureteric myocytes. *Biochem J* **349:**323–332.
Boittin FX, Dipp M, Kinnear NP, Galione A, and Evans AM (2003) Vasodilation by the calcium-mobilizing messenger cyclic ADP-ribose. *J Biol Chem* **278:**9602–9608.
Boittin FX, Galione A, and Evans AM (2002) Nicotinic acid adenine dinucleotide phosphate mediates Ca^{2+} signals and contraction in arterial smooth muscle via a two-pool mechanism. *Circ Res* **91:**1168–1175.
Boittin FX, Macrez N, Halet G, and Mironneau J (1999) Norepinephrine-induced Ca(2+) waves depend on InsP(3) and ryanodine receptor activation in vascular myocytes. *Am J Physiol* **277:**C139–C151.
Bolton TB, Prestwich SA, Zholos AV, and Gordienko DV (1999) Excitation-contraction coupling in gastrointestinal and other smooth muscles. *Annu Rev Physiol* **61:**85–115.
Bond M, Kitazawa T, Somlyo AP, and Somlyo AV (1984a) Release and recycling of calcium by the sarcoplasmic reticulum in guinea-pig portal vein smooth muscle. *J Physio (Lond)* **355:**677–695.
Bond M, Shuman H, Somlyo AP, and Somlyo AV (1984b) Total cytoplasmic calcium in relaxed and maximally contracted rabbit portal vein smooth muscle. *J Physiol (Lond)* **357:**185–201.
Bonev AD, Jaggar JH, Rubart M, and Nelson MT (1997) Activators of protein kinase C decrease Ca^{2+} spark frequency in smooth muscle cells from cerebral arteries. *Am J Physiol* **273:**C2090–C2095.
Bootman MD, Berridge MJ, and Taylor CW (1992a) All-or-nothing Ca^{2+} mobilization from the intracellular stores of single histamine-stimulated HeLa cells. *J Physiol (Lond)* **450:**163–178.
Bootman MD, Petersen OH, and Verkhratsky A (2002) The endoplasmic reticulum is a focal point for co-ordination of cellular activity. *Cell Calcium* **32:**231–234.
Bootman MD, Taylor CW, and Berridge MJ (1992b) The thiol reagent, thimerosal, evokes Ca^{2+} spikes in HeLa cells by sensitizing the inositol 1,4,5-trisphosphate receptor. *J Biol Chem* **267:**25113–25119.
Boulay G, Brown DM, Qin N, Jiang M, Dietrich A, Zhu MX, Chen Z, Birnbaumer M, Mikoshiba K, and Birnbaumer L (1999) Modulation of Ca(2+) entry by polypeptides of the inositol 1,4, 5-trisphosphate receptor (IP3R) that bind transient receptor potential (TRP): evidence for roles of TRP and IP3R in store depletion-activated Ca(2+) Entry. *Proc Natl Acad Sci USA* **96:**14955–14960.
Bourguignon LY, Iida N, and Jin H (1993a) The involvement of the cytoskeleton in regulating IP3 receptor-mediated internal Ca^{2+} release in human blood platelets. *Cell Biol Int* **17:**751–758.
Bourguignon LY, Jin H, Iida N, Brandt NR, and Zhang SH (1993b) The involvement of ankyrin in the regulation of inositol 1,4,5-trisphosphate receptor-mediated internal Ca^{2+} release from Ca^{2+} storage vesicles in mouse T-lymphoma cells. *J Biol Chem* **268:**7290–7297.
Bourreau JP, Kwan CY, and Daniel EE (1993) Distinct pathways to refill ACh-sensitive internal Ca^{2+} stores in canine airway smooth muscle. *Am J Physiol* **265:**C28–C35.
Bradley KN, Currie S, MacMillan D, Muir TC, and McCarron JG (2003) Cyclic ADP-ribose increases Ca^{2+} removal in smooth muscle. *J Cell Sci* **116:**4291–4306.
Bradley KN, Flynn ERM, Muir TC, and McCarron JG (2002) Ca(2+) Regulation in guinea-pig colonic smooth muscle: the role of the Na(+)-Ca(2+) exchanger and the sarcoplasmic reticulum. *J Physiol (Lond)* **538:**465–482.
Braun FJ, Broad LM, Armstrong DL, and Putney JW Jr (2001) Stable activation of single Ca^{2+} release-activated Ca^{2+} channels in divalent cation-free solutions. *J Biol Chem* **276:**1063–1070.
Broad LM, Braun FJ, Lievremont JP, Bird GS, Kurosaki T, and Putney JW Jr (2001) Role of the phospholipase C-inositol 1,4,5-trisphosphate pathway in calcium release-activated calcium current and capacitative calcium entry. *J Biol Chem* **276:**15945–15952.
Broad LM, Cannon TR, and Taylor CW (1999) A non-capacitative pathway activated by arachidonic acid is the major Ca^{2+} entry mechanism in rat A7r5 smooth muscle cells stimulated with low concentrations of vasopressin. *J Physiol (Lond)* **517:**121–134.
Bruzzone S, Guida L, Zocchi E, Franco L, and De Flora A (2001) Connexin 43 hemi channels mediate Ca^{2+}-regulated transmembrane NAD+ fluxes in intact cells. *FASEB J* **15:**10–12.
Bulbring E and Tomita T (1969) Suppression of spontaneous spike generation by catecholamines in the smooth muscle of the guinea-pig taenia coli. *Proc R Soc Lond B Biol Sci* **172:**103–119.
Bultynck G, De Smedt H, Parys JB, Callewaert G, and Missiaen L (2002) Washing out of lipophilic compounds induces a transient increase in the passive Ca(2+) leak in permeabilized A7r5 cells. *Cell Calcium* **31:**229–233.
Bultynck G, Rossi D, Callewaert G, Missiaen L, Sorrentino V, Parys JB, and De Smedt H (2001) The conserved sites for the FK506-binding proteins in ryanodine receptors and inositol 1,4,5-trisphosphate receptors are structurally and functionally different. *J Biol Chem* **276:**47715–47724.
Burdyga T, Shmygol A, Eisner DA, and Wray S (2003) A new technique for simultaneous and in situ measurements of Ca(2+) signals in arteriolar smooth muscle and endothelial cells. *Cell Calcium* **34:**27–33.
Burdyga T and Wray S (2002) Sarcoplasmic reticulum function and contractile consequences in ureteric smooth muscles. *Novartis Found Symp* **246:**208–217.
Burdyga TV and Magura IS (1986) The effects of local anesthetics on the electrical and mechanical activity of the guinea pig ureter. *Br J Pharmacol* **88:**523–530.
Burdyga TV, Taggart MJ, Crichton C, Smith GL, and Wray S (1998) The mechanism of Ca^{2+} release from the SR of permeabilised guinea-pig and rat ureteric smooth muscle. *Biochim Biophys Acta* **1402:**109–114.
Buryi V, Morel N, Salomone S, Kerger S, and Godfraind T (1995) Evidence for a direct interaction of thapsigargin with voltage-dependent Ca^{2+} channel. *Naunyn-Schmiedeberg's Arch Pharmacol* **351:**40–45.
Camello C, Lomax R, Petersen OH, and Tepikin AV (2002) Calcium leak from intracellular stores-the enigma of calcium signalling. *Cell Calcium* **32:**355–361.
Campbell AM, Kessler PD, Sagara Y, Inesi G, and Fambrough DM (1991) Nucleotide sequences of avian cardiac and brain SR/ER Ca(2+)-ATPases and functional comparisons with fast twitch Ca(2+)-ATPase. Calcium affinities and inhibitor effects. *J Biol Chem* **266:**16050–16055.
Campbell GR, Uehara Y, Mark G, and Burnstock G (1971) Fine structure of smooth muscle cells grown in tissue culture. *J Cell Biol* **49:**21–34.
Cantilina T, Sagara Y, Inesi G, and Jones LR (1993) Comparative studies of cardiac and skeletal sarcoplasmic reticulum ATPases. Effect of a phospholamban antibody on enzyme activation by Ca^{2+}. *J Biol Chem* **268:**17018–17025.
Carafoli E (1987) Intracellular calcium homeostasis. *Annu Rev Biochem* **56:**395–433.
Carl A, Lee HK, and Sanders KM (1996) Regulation of ion channels in smooth muscles by calcium. *Am J Physiol* **271:**C9–C34.
Carroll S, Skarmeta JG, Yu X, Collins KD, and Inesi G (1991) Interdependence of ryanodine binding, oligomeric receptor interactions and Ca^{2+} release regulation in junctional sarcoplasmic reticulum. *Arch Biochem Biophys* **290:**239–247.
Carrondo MA, Griffith WP, Hall JP, and Skapski AC (1980) X-Ray structure of [Ru3 O2 (NH3)14]6+, cation of the cytological reagent Ruthenium Red. *Biochim Biophys Acta* **627:**332–334.
Cartin L, Lounsbury KM, and Nelson MT (2000) Coupling of Ca(2+) to CREB activation and gene expression in intact cerebral arteries from mouse: roles of ryanodine receptors and voltage-dependent Ca(2+) channels. *Circ Res* **86:**760–767.
Caspersen C and Treiman M (1995) Thapsigargin discriminates strongly between Ca(2+)-ATPase phosphorylated intermediates with different subcellular distributions in bovine adrenal chromaffin cells. *FEBS Lett* **377:**31–36.
Casteels R and Droogmans G (1981) Exchange characteristics of the noradrenaline-sensitive calcium store in vascular smooth muscle cells or rabbit ear artery. *J Physiol (Lond)* **317:**263–279.
Casteels R, Kitamura K, Kuriyama H, and Suzuki H (1977) The membrane properties of the smooth muscle cells of the rabbit main pulmonary artery. *J Physiol (Lond)* **271:**41–61.
Cavallini L, Coassin M, and Alexandre A (1995) Two classes of agonist-sensitive Ca^{2+} stores in platelets, as identified by their differential sensitivity to 2,5-di-(tert-butyl)-1,4-benzohydroquinone and thapsigargin. *Biochem J* **310:**449–452.
Chadwick CC, Saito A, and Fleischer S (1990) Isolation and characterization of the inositol trisphosphate receptor from smooth muscle. *Proc Natl Acad Sci USA* **87:**2132–2136.
Charuk JH, Pirraglia CA, and Reithmeier RA (1990) Interaction of ruthenium red with Ca2(+)-binding proteins. *Anal Biochem* **188:**123–131.
Chaudhary J, Walia M, Matharu J, Escher E, and Grover AK (2001) Caloxin: a novel plasma membrane Ca^{2+} pump inhibitor. *Am J Physiol Cell Physiol* **280:**C1027–C1030.
Cheranov SY and Jaggar JH (2004) Mitochondrial modulation of Ca^{2+} sparks and transient KCa currents in Smooth muscle cells of rat cerebral arteries. *J Physiol (Lond)* **556:**755–771.
Cherednichenko G, Zima AV, Feng W, Schaefer S, Blatter LA, and Pessah IN (2004) NADH oxidase activity of rat cardiac sarcoplasmic reticulum regulates calcium-induced calcium release. *Circ Res* **94:**478–486.
Cheung DW (2003) Modulation of spontaneous transient Ca^{2+}-activated K+ channel currents by cADP-ribose in vascular smooth muscle cells. *Eur J Pharmacol* **458:**57–59.
Christensen SB, Andersen A, and Smitt UW (1997) Sesquiterpenoids from Thapsia species and medicinal chemistry of the thapsigargins. *Fortschr Chem Org Naturst* **71:**129–167.
Christensen SB, Hergenhahn M, Roeser H, and Hecker E (1992) Toxicodynamics of tumour promoters of mouse skin. III. Specific binding of the tumour promoter thapsigargin as measured by the cold-acetone filter assay. *J Cancer Res Clin Oncol* **118:**344–348.
Cibulsky SM and Sather WA (1999) Block by ruthenium red of cloned neuronal voltage-gated calcium channels. *J Pharmacol Exp Ther* **289:**1447–1453.

Cocco L, Martelli AM, Gilmour RS, Rhee SG, and Manzoli FA (2001) Nuclear phospholipase C and signaling. *Biochim Biophys Acta* **1530:**1–14.

Cohen RA, Weisbrod RM, Gericke M, Yaghoubi M, Bierl C, and Bolotina VM (1999) Mechanism of nitric oxide-induced vasodilatation: refilling of intracellular stores by sarcoplasmic reticulum Ca^{2+} ATPase and inhibition of store-operated Ca^{2+} influx. *Circ Res* **84:**210–219.

Collier ML, Ji G, Wang Y, and Kotlikoff MI (2000) Calcium-induced calcium release in smooth muscle: loose coupling between the action potential and calcium release. *J Gen Physiol* **115:**653–662.

Communi D, Vanweyenberg V, and Erneux C (1995) Molecular study and regulation of D-myo-inositol 1,4,5-trisphosphate 3-kinase. *Cell Signal* **7:**643–650.

Connolly TM, Bansal VS, Bross TE, Irvine RF, and Majerus PW (1987) The metabolism of tris- and tetraphosphates of inositol by 5-phosphomonoesterase and 3-kinase enzymes. *J Biol Chem* **262:**2146–2149.

Cooney RA, Honeyman TW, and Scheid CR (1991) Contribution of Na(+)-dependent and ATP-dependent Ca^{2+} transport to smooth muscle calcium homeostasis. *Ann NY Acad Sci* **639:**558–560.

Copello JA, Qi Y, Jeyakumar LH, Ogunbunmi E, and Fleischer S (2001) Lack of effect of cADP-ribose and NAADP on the activity of skeletal muscle and heart ryanodine receptors. *Cell Calcium* **30:**269–284.

Cornwell TL, Pryzwansky KB, Wyatt TA, and Lincoln TM (1991) Regulation of sarcoplasmic reticulum protein phosphorylation by localized cyclic GMP-dependent protein kinase in vascular smooth muscle cells. *Mol Pharmacol* **40:**923–931.

Csordas G and Hajnoczky G (2001) Sorting of calcium signals at the junctions of endoplasmic reticulum and mitochondria. *Cell Calcium* **29:**249–262.

Csordas G and Hajnoczky G (2003) Plasticity of mitochondrial calcium signalling. *J Biol Chem* **278:**42273–42282.

Cui Y, Galione A, and Terrar DA (1999) Effects of photoreleased cADP-ribose on calcium transients and calcium sparks in myocytes isolated from guinea-pig and rat ventricle. *Biochem J* **342:**269–273.

Darby PJ, Kwan CY, and Daniel EE (1996) Selective inhibition of oxalate-stimulated Ca^{2+} transport by cyclopiazonic acid and thapsigargin in smooth muscle microsomes. *Can J Physiol Pharmacol* **74:**182–192.

Daub B and Ganitkevich VY (2000) An estimate of rapid cytoplasmic calcium buffering in a single smooth muscle cell. *Cell Calcium* **27:**3–13.

Davidson GA and Varhol RJ (1995) Kinetics of thapsigargin-Ca(2+)-ATPase (sarcoplasmic reticulum) interaction reveals a two-step binding mechanism and picomolar inhibition. *J Biol Chem* **270:**11731–11734.

Davies-Cox EV, Laffafian I, and Hallett MB (2001) Control of Ca^{2+} influx in human neutrophils by inositol 1,4,5-trisphosphate (IP3) binding: differential effects of micro-injected IP3 receptor antagonists. *Biochem J* **355:**139–143.

de Kort M, Regenbogen AD, Overkleeft HS, John Challiss RA, Iwata Y, Miyamoto S, van der Marel GA, and van Boom JH (2000) Synthesis and biological evaluation of cyclophostin: A 5′,6′′-tethered analog of adenophostin A. *Tetrahedron* **56:**5915–5928.

De Luisi A and Hofer AM (2003) Evidence that Ca(2+) cycling by the plasma membrane Ca(2+)-ATPase increases the 'excitability' of the extracellular Ca(2+)-sensing receptor. *J Cell Sci* **116:**1527–1538.

de Meis L and Inesi G (1992) Functional evidence of a transmembrane channel within the Ca^{2+} transport ATPase of sarcoplasmic reticulum. *FEBS Lett* **299:**33–35.

Desilets M, Driska SP, and Baumgarten CM (1989) Current fluctuations and oscillations in smooth muscle cells from hog carotid artery. Role of the sarcoplasmic reticulum. *Circ Res* **65:**708–722.

De Smedt H, Missiaen L, Parys JB, Henning RH, Sienaert I, Vanlingen S, Gijsens A, Himpens B, and Casteels R (1997) Isoform diversity of the inositol trisphosphate receptor in cell types of mouse origin. *Biochem J* **322:**575–583.

De Smet P, Parys JB, Callewaert G, Weidema AF, Hill E, De Smedt H, Erneux C, Sorrentino V, and Missiaen L (1999) Xestospongin C is an equally potent inhibitor of the inositol 1,4,5-trisphosphate receptor and the endoplasmic reticulum Ca^{2+} pumps. *Cell Calcium* **26:**9–13.

de Toledo FG, Cheng J, Liang M, Chini EN, and Dousa TP (2000) ADP-ribosyl cyclase in rat vascular smooth muscle cells: properties and regulation. *Circ Res* **86:**1153–1159.

Devine CE, Somlyo AV, and Somlyo AP (1972) Sarcoplasmic reticulum and excitation-contraction coupling in mammalian smooth muscles. *J Cell Biol* **52:**690–718.

Dierichs R (1979) Ruthenium red as a stain for electron microscopy. Some new aspects of its application and mode of action. *Histochemistry* **64:**171–187.

Ding J and Kasai M (1996) Analysis of multiple conductance states observed in Ca^{2+} release channel of sarcoplasmic reticulum. *Cell Struct Funct* **21:**7–15.

Dipp M and Evans AM (2001) Cyclic ADP-ribose is the primary trigger for hypoxic pulmonary vasoconstriction in the rat lung in situ. *Cir Res* **89:**77–83.

Dipp M, Nye PCG, and Evans AM (2001) Hypoxic release of calcium from the sarcoplasmic reticulum of pulmonary artery smooth muscle. *Am J Physiol* **281:** L318–L325.

Diver JM, Sage SO, and Rosado JA (2001) The inositol trisphosphate receptor antagonist 2-aminoethoxydiphenylborate (2-APB) blocks Ca^{2+} entry channels in human platelets: cautions for its use in studying Ca^{2+} influx. *Cell Calcium* **30:** 323–329.

Dobrydneva Y and Blackmore P (2001) 2-Aminoethoxydiphenyl borate directly inhibits store-operated calcium entry channels in human platelets. *Mol Pharmacol* **60:**541–552.

Dogan S, White TA, Deshpande DA, Murtaugh MP, Walseth TF, and Kannan MS (2002) Estrogen increases CD38 gene expression and leads to differential regulation of adenosine diphosphate (ADP)-ribosyl cyclase and cyclic ADP-ribose hydrolase activities in rat myometrium. *Biol Reprod* **66:**596–602.

Doi S, Damron DS, Horibe M, and Murray PA (2000) Capacitative Ca(2+) entry and tyrosine kinase activation in canine pulmonary arterial smooth muscle cells. *Am J Physiol Lung Cell Mol Physiol* **278:**L118–L130.

Downes CP, Mussat MC, and Michell RH (1982) The inositol trisphosphate phosphomonoesterase of the human erythrocyte membrane. *Biochem J* **203:**169–177.

Dreja K, Nordstrom I, and Hellstrand P (2001) Rat arterial smooth muscle devoid of ryanodine receptor function: effects on cellular Ca^{2+} handling. *Br J Pharmacol* **132:**1957–1966.

Drummond RM and Tuft RA (1999) Release of Ca^{2+} From the sarcoplasmic reticulum increases mitochondrial [Ca2+] in rat pulmonary artery smooth muscle cells. *J Physiol (Lond)* **516:**139–147.

Duridanova DB, Gagov HS, and Boev KK (1996) Ca(2+)-induced Ca^{2+} release activates K+ currents by a cyclic GMP-dependent mechanism in single gastric smooth muscle cells. *Eur J Pharmacol* **298:**159–163.

Duridanova DB, Nedelcheva MD, and Gagov HS (1997) Oxytocin-induced changes in single cell K+ currents and smooth muscle contraction of guinea-pig gastric antrum. *Eur J Endocrinol* **136:**531–538.

East JM (2000) Sarco(endo)plasmic reticulum calcium pumps: recent advances in our understanding of structure/function and biology (Review). *Mol Membr Biol* **17:**189–200.

Ebashi S and Lipmann F (1962) Adenosine triphosphate-linked concentration of calcium ions in a particulate fraction of rabbit muscle. *J Cell Biol* **14:**389–400.

Eggermont JA, Wuytack F, Verbist J, and Casteels R (1990) Expression of endoplasmic-reticulum Ca2(+)-pump isoforms and of phospholamban in pig smooth-muscle tissues. *Biochem J* **271:**649–653.

Ehrlich BE and Watras J (1988) Inositol 1,4,5-trisphosphate activates a channel from smooth muscle sarcoplasmic reticulum. *Nature (Lond)* **336:**583–586.

Engelender S, Wolosker H, and de Meis L (1995) The Ca(2+)-ATPase isoforms of platelets are located in distinct functional Ca^{2+} pools and are uncoupled by a mechanism different from that of skeletal muscle Ca(2+)-ATPase. *J Biol Chem* **270:**21050–21055.

Ershoff BH (1963) Comparative effects of a purified and stock diet on 2,5-di-tert-butylhydroquinone (DBH) toxicity in the rat. *Proc Soc Exp Biol Med* **112:**362–365.

Ershoff BH (1969) Strain difference in 2,5-di-tert-butylhydroquinone (DBH) toxicity in the mouse. *Proc Soc Exp Biol Med* **131:**776–777.

Ethier MF and Madison JM (2002) LY294002, but not wortmannin, increases intracellular calcium and inhibits calcium transients in bovine and human airway smooth muscle cells. *Cell Calcium* **32:**31–38.

Ethier MF, Yamaguchi H, and Madison JM (2001) Effects of cyclopiazonic acid on cytosolic calcium in bovine airway smooth muscle cells. *Am J Physiol Lung Cell Mol Physiol* **281:**L126–L133.

Etter EF, Minta A, Poenie M, and Fay FS (1996) Near-membrane [Ca2+] transients resolved using the Ca^{2+} indicator FFP18. *Proc Natl Acad Sci USA* **93:**5368–5373.

Fang YI, Adachi M, Kobayashi J, and Ohizumi Y (1993) High affinity binding of 9-[3H]methyl-7-bromoeudistomin D to the caffeine-binding site of skeletal muscle sarcoplasmic reticulum. *J Biol Chem* **268:**18622–18625.

Feinstein MB (1963) Inhibition of caffeine rigor and radiocalcium movements by local anesthetics in frog sartorius muscle. *J Gen Physiol* **47:**151–172.

Felbel J, Trockur B, Ecker T, Landgraf W, and Hofmann F (1988) Regulation of cytosolic calcium by cAMP and cGMP in freshly isolated smooth muscle cells from bovine trachea. *J Biol Chem* **263:**16764–16771.

Ferris CD, Cameron AM, Huganir RL, and Snyder SH (1992) Quantal calcium release by purified reconstituted inositol 1,4,5-trisphosphate receptors. *Nature (Lond)* **356:**350–352.

Flynn ERM, Bradley KN, Muir TC, and McCarron JG (2001) Functionally separate intracellular Ca^{2+} stores in smooth muscle. *J Biol Chem* **276:**36411–36418.

Fohr KJ, Scott J, Ahnert-Hilger G, and Gratzl M (1989) Characterization of the inositol 1,4,5-trisphosphate-induced calcium release from permeabilized endocrine cells and its inhibition by decavanadate and p-hydroxymercuribenzoate. *Biochem J* **262:**83–89.

Forbes MS, Plantholt BA, and Sperelakis N (1977) Cytochemical staining procedures selective for sarcotubular systems of muscle: modifications and applications. *J Ultrastruct Res* **60:**306–327.

Forbes MS, Rennels ML, and Nelson E (1979) Caveolar systems and sarcoplasmic reticulum in coronary smooth muscle cells of the mouse. *J Ultrastruct Res* **67:**325–339.

Foskett JK and Wong D (1992) Calcium oscillations in parotid acinar cells induced by microsomal Ca(2+)-ATPase inhibition. *Am J Physiol* **262:**C656–C663.

Franco L, Bruzzone S, Song P, Guida L, Zocchi E, Walseth TF, Crimi E, Usai C, De Flora A, and Brusasco V (2001) Extracellular cyclic ADP-ribose potentiates ACh-induced contraction in bovine tracheal smooth muscle. *Am J Physiol* **280:**L98–L106.

Fruen BR, Mickelson JR, Shomer NH, Velez P, and Louis CF (1994) Cyclic ADP-ribose does not affect cardiac or skeletal muscle ryanodine receptors. *FEBS Lett* **352:**123–126.

Fujii K, Foster CD, Brading AF, and Parekh AB (1990) Potassium channel blockers and the effects of cromakalim on the smooth muscle of the guinea pig bladder. *Br J Pharmacol* **99:**779–785.

Fujii K, Miyahara H, and Suzuki H (1985) Comparison of the effects of caffeine and procaine on noradrenergic transmission in the guinea-pig mesenteric artery. *Br J Pharmacol* **84:**675–684.

Fujimoto T, Miyawaki A, and Mikoshiba K (1995) Inositol 1,4,5-trisphosphate receptor-like protein in plasmalemmal caveolae is linked to actin filaments. *J Cell Sci* **108:**7–15.

Fujimoto T, Nakade S, Miyawaki A, Mikoshiba K, and Ogawa K (1992) Localization of inositol 1,4,5-trisphosphate receptor-like protein in plasmalemmal caveolae. *J Cell Biol* **119:**1507–1513.

Fujiwara T, Nakada K, Shirakawa H, and Miyazaki S (1993) Development of inositol trisphosphate-induced calcium release mechanism during maturation of hamster oocytes. *Dev Biol* **156:**69–79.

Fukami K (2002) Structure, regulation, and function of phospholipase C isozymes. *J Biochem (Tokyo)* **131:**293–299.

Fukami K, Itagaki M, Komori S, and Ohashi H (1993) Contractile responses to

histamine and GTP gamma S in beta-escin-treated skinned smooth muscle of guinea pig ileum. *Jpn J Pharmacol* **63:**171–179.
Fukuoka M, Shuto S, Minakawa N, Ueno Y, and Matsuda A (1999) Synthetic study on carbocyclic analogs of cyclic ADP-ribose, a novel second messenger: an efficient synthesis of cyclic IDP-carbocyclic-ribose. *Nucleic Acids Symp Ser* **42:**11–12.
Fukuoka M, Shuto S, Minakawa N, Ueno Y, and Matsuda A (2001) Synthesis and biological activities of cyclic ADP-carbocyclic-ribose and its analogs. *Nucleos Nucleot Nucl* **20:**1355–1358.
Fukuta H, Kito Y, and Suzuki H (2002) Spontaneous electrical activity and associated changes in calcium concentration in guinea-pig gastric smooth muscle. *J Physiol (Lond)* **540:**249–260.
Fulceri R, Rossi R, Bottinelli R, Conti A, Intravaia E, Galione A, Benedetti A, Sorrentino V, and Reggiani C (2001) Ca^{2+} release induced by cyclic ADP ribose in mice lacking type 3 ryanodine receptor. *Biochem Biophys Res Commun* **288:**697–702.
Furstenau M, Lohn M, Ried C, Luft FC, Haller H, and Gollasch M (2000) Calcium sparks in human coronary artery smooth muscle cells resolved by confocal imaging. *J Hypertens* **18:**1215–1222.
Furuichi T, Kohda K, Miyawaki A, and Mikoshiba K (1994) Intracellular channels. *Curr Opin Neurobiol* **4:**294–303.
Furuichi T, Yoshikawa S, Miyawaki A, Wada K, Maeda N, and Mikoshiba K (1989) Primary structure and functional expression of the inositol 1,4,5-trisphosphate-binding protein P400. *Nature (Lond)* **342:**32–38.
Fusi F, Gorelli B, Valoti M, Marazova K, and Sgaragli GP (1998) Effects of 2,5-di-*t*-butyl-1,4-benzohydroquinone (BHQ) on rat aorta smooth muscle. *Eur J Pharmacol* **346:**237–243.
Fusi F, Saponara S, Gagov H, and Sgaragli G (2001) 2,5-Di-*t*-butyl-1,4-benzohydroquinone (BHQ) inhibits vascular L-type Ca^{2+} channel via superoxide anion generation. *Br J Pharmacol* **133:**988–996.
Fusi F, Valoti M, Frosini M, and Sgaragli GP (1999) 2,5-Di-*t*-butyl-1,4-benzohydroquinone induces endothelium-dependent relaxation of rat thoracic aorta. *Eur J Pharmacol* **366:**181–187.
Gabella G (1983) Structure of smooth muscles, in *Smooth Muscle: an Assessment of Current Knowledge* (Bulbring E, Brading AF, Jones AW, and Tomita T eds) pp 1–46, University of Texas, Austin, Texas.
Gaburjakova M, Schlossmann J, and Ondrias K (1999) Properties of a new calcium-permeable single channel from tracheal microsomes. *Biochim Biophys Acta* **1417:** 25–31.
Gafni J, Munsch JA, Lam TH, Catlin MC, Costa LG, Molinski TF, and Pessah IN (1997) Xestospongins: potent membrane permeable blockers of the inositol 1,4,5-trisphosphate receptor. *Neuron* **19:**723–733.
Galvan DL, Borrego-Diaz E, Perez PJ, and Mignery GA (1999) Subunit oligomerization and topology of the Inositol 1,4, 5-trisphosphate receptor. *J Biol Chem* **274:** 29483–29492.
Galvan DL and Mignery GA (2002) Carboxyl-terminal sequences critical for inositol 1,4,5-trisphosphate receptor subunit assembly. *J Biol Chem* **277:**48248–48260.
Ganitkevich VY (1996) The amount of acetylcholine mobilisable Ca^{2+} in single smooth muscle cells measured with the exogenous cytoplasmic Ca^{2+} buffer, Indo-1. *Cell Calcium* **20:**483–492.
Ganitkevich VY (1999) Clearance of large Ca^{2+} loads in a single smooth muscle cell: examination of the role of mitochondrial Ca^{2+} uptake and intracellular pH. *Cell Calcium* **25:**29–42.
Ganitkevich VY and Hirche H (1996) High cytoplasmic Ca^{2+} levels reached during Ca(2+)-induced Ca^{2+} release in single smooth muscle cell as reported by a low affinity Ca^{2+} indicator Mag-Indo-1. *Cell Calcium* **19:**391–398.
Ganitkevich VY and Isenberg G (1992) Caffeine-induced release and reuptake of Ca^{2+} by Ca^{2+} stores in myocytes from guinea-pig urinary bladder. *J Physiol (Lond)* **458:**99–117.
Ge ZD, Zhang DX, Chen YF, Yi FX, Zou AP, Campbell WB, and Li PL (2003) Cyclic ADP-ribose contributes to contraction and Ca^{2+} release by M1 muscarinic receptor activation in coronary arterial smooth muscle. *J Vasc Res* **40:**28–36.
Geiger J, Zou AP, Campbell WB, and Li PL (2000) Inhibition of cADP-ribose formation produces vasodilation in bovine coronary arteries. *Hypertension* **35:**397–402.
Geiszt M, Kaldi K, Szeberenyi JB, and Ligeti E (1995) Thapsigargin inhibits Ca^{2+} entry into human neutrophil granulocytes. *Biochem J* **305:**525–528.
Ghosh TK, Eis PS, Mullaney JM, Ebert CL, and Gill DL (1988) Competitive, reversible, and potent antagonism of inositol 1,4,5-trisphosphate-activated calcium release by heparin. *J Biol Chem* **263:**11075–11079.
Giannini G, Clementi E, Ceci R, Marziali G, and Sorrentino V (1992) Expression of a ryanodine receptor-Ca^{2+} channel that is regulated by TGF-beta. *Science (Wash DC)* **257:**91–94.
Gibson A, McFadzean I, Wallace P, and Wayman CP (1998) Capacitative Ca^{2+} entry and the regulation of smooth muscle tone. *Trends Pharmacol Sci* **19:**266–269.
Giulumian AD, Meszaros LG, and Fuchs LC (2000) Endothelin-1-induced contraction of mesenteric small arteries is mediated by ryanodine receptor Ca^{2+} channels and cyclic ADP-ribose. *J Cardiovasc Pharmacol* **36:**758–763.
Goeger DE and Riley RT (1989) Interaction of cyclopiazonic acid with rat skeletal muscle sarcoplasmic reticulum vesicles. Effect on Ca^{2+} binding and Ca^{2+} permeability. *Biochem Pharmacol* **38:**3995–4003.
Goeger DE, Riley RT, Dorner JW, and Cole RJ (1988) Cyclopiazonic acid inhibition of the Ca^{2+}-transport ATPase in rat skeletal muscle sarcoplasmic reticulum vesicles. *Biochem Pharmacol* **37:**978–981.
Gollasch M, Wellman GC, Knot HJ, Jaggar JH, Damon DH, Bonev AD, and Nelson MT (1998) Ontogeny of local sarcoplasmic reticulum Ca^{2+} signals in cerebral arteries: Ca^{2+} sparks as Elementary physiological events. *Circ Res* **83:**1104–1114.
Golovina VA and Blaustein MP (1997) Spatially and functionally distinct Ca^{2+} stores in sarcoplasmic and endoplasmic reticulum. *Science (Wash DC)* **275:**1643–1648.
Gomez MF, Bosc LV, Stevenson AS, Wilkerson MK, Hill-Eubanks DC, and Nelson MT (2003) Constitutively elevated nuclear export activity opposes Ca^{2+}-dependent NFATc3 nuclear accumulation in vascular smooth muscle: role of JNK2 and Crm-1. *J Biol Chem* **278:**46847–46853.
Gomez-Viquez L, Guerrero-Serna G, Garcia U, and Guerrero-Hernandez A (2003) SERCA pump optimizes Ca(2+) release by a mechanism independent of store filling in smooth muscle cells. *Biophys J* **85:**370–380.
Gonzalez De La Fuente P, Savineau JP, and Marthan R (1995) Control of pulmonary vascular smooth muscle tone by sarcoplasmic reticulum Ca^{2+} pump blockers: thapsigargin and cyclopiazonic acid. *Pflugers Arch* **429:**617–624.
Gordienko DV, Greenwood IA, and Bolton TB (2001) Direct visualization of sarcoplasmic reticulum regions discharging Ca(2+) sparks in vascular myocytes. *Cell Calcium* **29:**13–28.
Gordon JA (1991) Use of vanadate as protein-phosphotyrosine phosphatase inhibitor. *Methods Enzymol* **201:**477–482.
Greenberg S, Long JP, and Diecke FP (1973) Differentiation of calcium pools utilized in the contractile response of canine arterial and venous smooth muscle to norepinephrine. *J Pharmacol Exp Ther* **185:**493–504.
Grover AK (1985) Ca-pumps in smooth muscle: one in plasma membrane and another in endoplasmic reticulum. *Cell Calcium* **6:**227–236.
Grover AK and Khan I (1992) Calcium pump isoforms: diversity, selectivity and plasticity. Review article. *Cell Calcium* **13:**9–17.
Grover AK and Samson SE (1986) Pig coronary artery smooth muscle: substrate and pH dependence of the two calcium pumps. *Am J Physiol* **251:**C529–C534.
Grover AK and Samson SE (1997) Peroxide resistance of ER Ca^{2+} pump in endothelium: implications to coronary artery function. *Am J Physiol* **273:**C1250–C1258.
Grover AK, Xu A, Samson SE, and Narayanan N (1996) Sarcoplasmic reticulum Ca^{2+} pump in pig coronary artery smooth muscle is regulated by a novel pathway. *Am J Physiol* **271:**C181–C187.
Guerrero A, Fay FS, and Singer JJ (1994) Caffeine activates a Ca(2+)-permeable, nonselective cation channel in smooth muscle cells. *J Gen Physiol* **104:**375–394.
Guerrero-Hernandez A, Gomez-Viquez L, Guerrero-Serna G, and Rueda A (2002) Ryanodine receptors in smooth muscle. *Front Biosci* **7:**D1676–D1688.
Guibert C, Flemming R, and Beech DJ (2002) Prevention of a hypoxic [Ca2+]i response by SERCA inhibitors in cerebral arterioles. *Br J Pharmacol* **135:**927–934.
Guillemette G, Lamontagne S, Boulay G, and Mouillac B (1989) Differential effects of heparin on inositol 1,4,5-trisphosphate binding, metabolism, and calcium release activity in the bovine adrenal cortex. *Mol Pharmacol* **35:**339–344.
Gunter TE, Buntinas L, Sparagna G, Eliseev R, and Gunter K (2000) Mitochondrial calcium transport: mechanisms and functions. *Cell Calcium* **28:**285–296.
Guo X, Laflamme MA, and Becker PL (1996) Cyclic ADP-ribose does not regulate sarcoplasmic reticulum Ca^{2+} release in intact cardiac myocytes. *Circ Res* **79:**147–151.
Gurney AM, Drummond RM, and Fay FS (2000) Calcium signalling in sarcoplasmic reticulum, cytoplasm and mitochondria during activation of rabbit aorta myocytes. *Cell Calcium* **27:**339–351.
Guse AH (2002) Cyclic ADP-ribose (CADPR) and nicotinic acid adenine dinucleotide phosphate (NAADP): novel regulators of Ca^{2+}-signaling and cell function. *Curr Mol Med* **2:**273–282.
Guse AH, da Silva CP, Weber K, Armah CN, Ashamu GA, Schulze C, Potter BV, Mayr GW, and Hilz H (1997) 1-(5-Phospho-beta-D-ribosyl)2′-phosphoadenosine 5′-phosphate cyclic anhydride induced Ca^{2+} release in human T-cell lines. *Eur J Biochem* **245:**411–417.
Haddock PS, Coetzee WA, Cho E, Porter L, Katoh H, Bers DM, Jafri MS, and Artman M (1999) Subcellular [Ca2+]i gradients during excitation-contraction coupling in newborn rabbit ventricular myocytes. *Circ Res* **85:**415–427.
Haddock RE, Hirst GD, and Hill CE (2002) Voltage independence of vasomotion in isolated irideal arterioles of the rat. *J Physiol (Lond)* **540:**219–229.
Hajnoczky G, Csordas G, Krishnamurthy R, and Szalai G (2000a) Mitochondrial calcium signaling driven by the IP3 receptor. *J Bioenerg Biomembr* **32:**15–25.
Hajnoczky G, Csordas G, Madesh M, and Pacher P (2000b) The machinery of local Ca^{2+} signalling between sarco-endoplasmic reticulum and mitochondria. *J Physiol (Lond)* **529:**69–81.
Hajnoczky G, Csordas G, and Yi M (2002) Old players in a new role: mitochondria-associated membranes, VDAC, and ryanodine receptors as contributors to calcium signal propagation from endoplasmic reticulum to the mitochondria. *Cell Calcium* **32:**363–377.
Haller T, Volkl H, Deetjen P, and Dietl P (1996) The lysosomal Ca^{2+} pool in MDCK cells can be released by Ins(1,4,5)P3-dependent hormones or thapsigargin but does not activate store-operated Ca^{2+} entry. *Biochem J* **319:**909–912.
Hamada K, Miyata T, Mayanagi K, Hirota J, and Mikoshiba K (2002) Two-state conformational changes in inositol 1,4,5-trisphosphate receptor regulated by calcium. *J Biol Chem* **277:**21115–21118.
Hamilton MG and Lundy PM (1995) Effect of ruthenium red on voltage-sensitive Ca^{2+} channels. *J Pharmacol Exp Ther* **273:**940–947.
Hara Y, Kitamura K, and Kuriyama H (1980) Actions of 4-aminopyridine on vascular smooth muscle tissues of the guinea pig. *Br J Pharmacol* **68:**99–106.
Harks EG, Camina JP, Peters PH, Ypey DL, Scheenen WJ, van Zoelen EJ, and Theuvenet AP (2003) Besides affecting intracellular calcium signaling, 2-APB reversibly blocks gap junctional coupling in confluent monolayers, thereby allowing measurement of single-cell membrane currents in undissociated cells. *FASEB J* **17:**941–943.
Hashimoto T, Hirata M, and Ito Y (1985) A role for inositol 1,4,5-trisphosphate in the initiation of agonist-induced contractions of dog tracheal smooth muscle. *Br J Pharmacol* **86:**191–199.
Hawkins C, Xu A, and Narayanan N (1994) Sarcoplasmic reticulum calcium pump in cardiac and slow twitch skeletal muscle but not fast twitch skeletal muscle undergoes phosphorylation by endogenous and exogenous Ca^{2+}/calmodulin-dependent protein kinase. Characterization of optimal conditions for calcium pump phosphorylation. *J Biol Chem* **269:**31198–31206.
Heaps CL, Bowles DK, Sturek M, Laughlin MH, and Parker JL (2000) Enhanced L-type Ca^{2+} channel current density in coronary smooth muscle of exercise-trained pigs is compensated to limit myoplasmic free Ca^{2+} accumulation. *J Physiol (Lond)* **528:**435–445.

Heaps CL, Sturek M, Price EM, Laughlin MH, and Parker JL (2001) Sarcoplasmic reticulum Ca^{2+} uptake is impaired in coronary smooth muscle distal to coronary occlusion. *Am J Physiol* **281:**H223–H231.

Heirwegh KP, Meuwissen JA, Vermeir M, and De Smedt H (1988) Liposomes as carriers of poorly water-soluble substrates: linear modelling of membrane systems with catalytic or binding sites of different facedness. Significance of experimental membrane partition coefficients and of kinetic and equilibrium parameters. *Biochem J* **254:**101–108.

Hermosura MC, Takeuchi H, Fleig A, Riley AM, Potter BV, Hirata M, and Penner R (2000) InsP4 facilitates store-operated calcium influx by inhibition of InsP3 5-phosphatase. *Nature (Lond)* **408:**735–740.

Herrera GM, Heppner TJ, and Nelson MT (2001) Voltage dependence of the coupling of Ca(2+) sparks to BK(Ca) channels in urinary bladder smooth muscle. *Am J Physiol* **280:**C481–C490.

Herrera GM and Nelson MT (2002) Differential regulation of SK and BK channels by Ca^{2+} signals from Ca^{2+} channels and ryanodine receptors in guinea-pig urinary bladder myocytes. *J Physiol (Lond)* **541:**483–492.

Herrmann-Frank A, Darling E, and Meissner G (1991) Functional characterization of the Ca^{2+}-gated Ca^{2+} release channel of vascular smooth muscle sarcoplasmic reticulum. *Pflugers Arch* **418:**353–359.

Higashida H, Hashii M, Yokoyama S, Hoshi N, Chen XL, Egorova A, Noda M, and Zhang JS (2001) Cyclic ADP-ribose as a second messenger revisited from a new aspect of signal transduction from receptors to ADP-ribosyl cyclase. *Pharmacol Ther* **90:**283–296.

Hill-Eubanks DC, Gomez MF, Stevenson AS, and Nelson MT (2003) NFAT regulation in smooth muscle. *Trends Cardiovasc Med* **13:**56–62.

Hirano M, Imaizumi Y, Muraki K, Yamada A, and Watanabe M (1998) Effects of ruthenium red on membrane ionic currents in urinary bladder smooth muscle cells of the guinea-pig. *Pflugers Arch* **435:**645–653.

Hirata M, Watanabe Y, Ishimatsu T, Ikebe T, Kimura Y, Yamaguchi K, Ozaki S, and Koga T (1989) Synthetic inositol trisphosphate analogs and their effects on phosphatase, kinase, and the release of Ca^{2+}. *J Biol Chem* **264:**20303–20308.

Hirata M, Watanabe Y, Yoshida M, Koga T, and Ozaki S (1993) Roles for hydroxyl groups of D-myo-inositol 1,4,5-trisphosphate in the recognition by its receptor and metabolic enzymes. *J Biol Chem* **268:**19260–19266.

Hirose K and Iino M (1994) Heterogeneity of channel density in inositol-1,4,5-trisphosphate-sensitive Ca^{2+} stores. *Nature (Lond)* **372:**791–794.

Hirose K, Kadowaki S, and Iino M (1998) Allosteric regulation by cytoplasmic Ca^{2+} and IP3 of the gating of IP3 receptors in permeabilized guinea-pig vascular smooth muscle cells. *J Physiol (Lond)* **506:**407–414.

Hirota J, Michikawa T, Miyawaki A, Takahashi M, Tanzawa K, Okura I, Furuichi T, and Mikoshiba K (1995) Adenophostin-medicated quantal Ca^{2+} release in the purified and reconstituted inositol 1,4,5-trisphosphate receptor type 1. *FEBS Lett* **368:**248–252.

Hirst GD (1999) A calcium window to the gut. *Nature (Lond)* **399:**16–17.

Hirst GDS, Bramich NJ, Teramoto N, Suzuki H, and Edwards FR (2002) Regenerative component of slow waves in the guinea-pig gastric antrum involves a delayed increase in [Ca2+]i and Cl- channels. *J Physiol (Lond)* **540:**907–919.

Hirst GDS and Edwards FR (2001) Generation of slow waves in the antral region of guinea-pig stomach–a stochastic process. *J Physiol (Lond)* **535:**165–180.

Hoer D, Kwiatkowski A, Seib C, Rosenthal W, Schultz G, and Oberdisse E (1988) Degradation of inositol 1,3,4,5-tetrakisphosphates by porcine brain cytosol yields inositol 1,3,4-trisphosphate and inositol 1,4,5-trisphosphate. *Biochem Biophys Res Commun* **154:**668–675.

Hofer AM and Schulz I (1996) Quantification of intraluminal free [Ca] in the agonist-sensitive internal calcium store using compartmentalized fluorescent indicators: some considerations. *Cell Calcium* **20:**235–242.

Holmes ME, Chaudhary J, and Grover AK (2003) Mechanism of action of the novel plasma membrane Ca(2+)-pump inhibitor caloxin. *Cell Calcium* **33:**241–245.

Holzapfel CW (1968) The isolation and structure of cyclopiazonic acid, a toxic metabolite of Penicillium cyclopium Westling. *Tetrahedron* **24:**2101–2119.

Hoth M and Penner R (1992) Depletion of intracellular calcium stores activates a calcium current in mast cells. *Nature (Lond)* **355:**353–356.

Hoth M and Penner R (1993) Calcium release-activated calcium current in rat mast cells. *J Physiol (Lond)* **465:**359–386.

Hua S, Malak H, Lakowicz JR, and Inesi G (1995) Synthesis and interaction of fluorescent thapsigargin derivatives with the sarcoplasmic reticulum ATPase membrane-bound region. *Biochemistry* **34:**5137–5142.

Huang Y (1995) BaCl2- and 4-aminopyridine-evoked phasic contractions in the rat vas deferens. *Br J Pharmacol* **115:**845–851.

Huang Y and Cheung KK (1997) Endothelium-dependent rhythmic contractions induced by cyclopiazonic acid in rat mesenteric artery. *Eur J Pharmacol* **332:**167–172.

Huang Y, Lau CW, Chan FL, and Yao XQ (1999) Contribution of nitric oxide and K+ channel activation to vasorelaxation of isolated rat aorta induced by procaine. *Eur J Pharmacol* **367:**231–237.

Huang Y, Quayle JM, Worley JF, Standen NB, and Nelson MT (1989) External cadmium and internal calcium block of single calcium channels in smooth muscle cells from rabbit mesenteric artery. *Biophys J* **56:**1023–1028.

Huang Y, Yao X, Lau C, Chan FL, Chan NW, Cheng Y, and Chen Z (2000) Role of endothelium in thapsigargin-induced arterial responses in rat aorta. *Eur J Pharmacol* **392:**51–59.

Hughes AD, Hering S, and Bolton TB (1990) The action of caffeine on inward barium current through voltage-dependent calcium channels in single rabbit ear artery cells. *Pflugers Arch* **416:**462–466.

Hughes G, East JM, and Lee AG (1994) The hydrophilic domain of phospholamban inhibits the Ca^{2+} transport step of the Ca^{2+}-ATPase. *Biochem J* **303:**511–516.

Hughes G, Starling AP, Sharma RP, East JM, and Lee AG (1996) An investigation of the mechanism of inhibition of the Ca(2+)-ATPase by phospholamban. *Biochem J* **318:**973–979.

Hume JR and Leblanc N (1989) Macroscopic K+ currents in single smooth muscle cells of the rabbit portal vein. *J Physiol (Lond)* **413:**49–73.

Hussain A, Garnett C, Klein MG, Tsai W, Schneider MF, and Inesi G (1995) Direct involvement of intracellular Ca^{2+} transport ATPase in the development of thapsigargin resistance by chinese hamster lung fibroblasts. *J Biol Chem* **270:**12140–12146.

Ihara E, Hirano K, Nishimura J, Nawata H, and Kanaide H (1999) Thapsigargin-induced endothelium-dependent triphasic regulation of vascular tone in the porcine renal artery. *Br J Pharmacol* **128:**689–699.

Iino M (1987) Calcium dependent inositol trisphosphate-induced calcium release in the guinea-pig taenia caeci. *Biochem Biophys Res Commun* **142:**47–52.

Iino M (1989) Calcium-induced calcium release mechanism in guinea pig taenia caeci. *J Gen Physiol* **94:**363–383.

Iino M (1990) Biphasic Ca^{2+} dependence of inositol 1,4,5-trisphosphate-induced Ca release in smooth muscle cells of the guinea pig taenia caeci. *J Gen Physiol* **95:**1103–1122.

Iino M (2002) Molecular basis and physiological functions of dynamic Ca^{2+} signalling in smooth muscle cells. *Novartis Found Symp* **246:**142–146.

Iino M and Endo M (1992) Calcium-dependent immediate feedback control of inositol 1,4,5-triphosphate-induced Ca^{2+} release. *Nature (Lond)* **360:**76–78.

Iino S, Cui Y, Galione A, and Terrar DA (1997) Actions of cADP-ribose and its antagonists on contraction in guinea pig isolated ventricular myocytes. Influence of temperature. *Circ Res* **81:**879–884.

Iizuka K, Yoshii A, Dobashi K, Horie T, Mori M, and Nakazawa T (1998) InsP3, but not novel Ca^{2+} releasers, contributes to agonist-initiated contraction in rabbit airway smooth muscle. *J Physiol (Lond)* **511:**915–933.

Imai S, Nakazawa M, Imai H, and Nabata H (1984) Effects of procaine on the isolated dog coronary artery. *Arch Int Pharmacodyn Ther* **271:**98–105.

Imaizumi Y, Henmi S, Uyama Y, Atsuki K, Torii Y, Ohizumi Y, and Watanabe M (1996) Characteristics of Ca^{2+} release for activation of K+ current and contractile system in some smooth muscles. *Am J Physiol* **271:**C772–C782.

Imaizumi Y, Henmi S, Uyama Y, Watanabe M, and Ohizumi Y (1993) Effects of 9-methyl-7-bromoeudistomin D (MBED), a powerful Ca^{2+} releaser, on smooth muscles of the guinea pig. *Ann NY Acad Sci* **707:**546–549.

Imaizumi Y and Watanabe M (1982) Effect of procaine on potassium permeability of canine tracheal smooth muscle. *Pflugers Arch* **394:**144–149.

Inesi G and Hill TL (1983) Calcium and proton dependence of sarcoplasmic reticulum ATPase. *Biophys J* **44:**271–280.

Inesi G and Sagara Y (1992) Thapsigargin, a high affinity and global inhibitor of intracellular Ca^{2+} transport ATPases. *Arch Biochem Biophys* **298:**313–317.

Inesi G and Sagara Y (1994) Specific inhibitors of intracellular Ca^{2+} transport ATPases. *J Membr Biol* **141:**1–6.

Irvine RF, Letcher AJ, Heslop JP, and Berridge MJ (1986) The inositol tris/tetrakisphosphate pathway–demonstration of Ins(1,4,5)P3 3-kinase activity in animal tissues. *Nature (Lond)* **320:**631–634.

Ishihara H and Karaki H (1991) Inhibitory effect of 8-(*N*,*N*-diethylamino)octyl-3,4,5-trimethoxybenzoate (TMB-8) in vascular smooth muscle. *Eur J Pharmacol* **197:**181–186.

Ishii T and Shimo Y (1984) Inhibitory Effects of procaine on the contractile responses of the guinea pig taenia cecum to acetylcholine, substance P and potassium chloride. *Naunyn-Schmiedeberg's Arch Pharmacol* **326:**175–180.

Ito S, Kume H, Honjo H, Katoh H, Kodama I, Yamaki K, and Hayashi H (2000) Capacitative Ca^{2+} entry in guinea pig tracheal smooth muscle. *Environ Med* **44:**101–103.

Ito S, Kume H, Yamaki K, Katoh H, Honjo H, Kodama I, and Hayashi H (2002) Regulation of capacitative and noncapacitative receptor-operated Ca^{2+} entry by Rho-kinase in tracheal smooth muscle. *Am J Respir Cell Mol Biol* **26:**491–498.

Ito Y and Itoh T (1984) The roles of stored calcium in contractions of cat tracheal smooth muscle produced by electrical stimulation, acetylcholine and high K+. *Br J Pharmacol* **83:**667–676.

Ito Y, Suzuki H, and Kuriyama H (1977) Effects of caffeine and procaine on the membrane and mechanical properties of the smooth muscle cells of the rabbit main pulmonary artery. *Jpn J Physiol* **27:**467–481.

Itoh T, Kajiwara M, Kitamura K, and Kuriyama H (1982a) Roles of stored calcium on the mechanical response evoked in smooth muscle cells of the porcine coronary artery. *J Physiol (Lond)* **322:**107–125.

Itoh T, Kuriyama H, and Nanjo T (1982b) Effects of calcium and manganese ions on mechanical properties of intact and skinned muscles from the guinea pig stomach. *J Physiol (Lond)* **333:**555–576.

Itoh T, Kuriyama H, and Suzuki H (1981) Excitation-contraction coupling in smooth muscle cells of the guinea-pig mesenteric artery. *J Physiol (Lond)* **321:**513–535.

Itoh T, Kuriyama H, and Suzuki H (1983) Differences and similarities in the noradrenaline- and caffeine-induced mechanical responses in the rabbit mesenteric artery. *J Physiol (Lond)* **337:**609–629.

Itoh T, Seki N, Suzuki S, Ito S, Kajikuri J, and Kuriyama H (1992) Membrane hyperpolarization inhibits agonist-induced synthesis of inositol 1,4,5-trisphosphate in rabbit mesenteric artery. *J Physiol (Lond)* **451:**307–328.

Jacob R (1990) Agonist-stimulated divalent cation entry into single cultured human umbilical vein endothelial cells. *J Physiol (Lond)* **421:**55–77.

Jacobs A and Kretinge WR (1974) Effects of procaine and lignocaine on electrical and mechanical activity of smooth muscle of sheep carotid arteries. *Br J Pharmacol* **51:**405–411.

Jaggar JH (2001) Intravascular pressure regulates local and global Ca^{2+} signaling in cerebral artery smooth muscle cells. *Am J Physiol* **281:**C439–C448.

Jaggar JH and Nelson MT (2000) Differential regulation of Ca(2+) sparks and Ca(2+) waves by UTP in rat cerebral artery smooth muscle cells. *Am J Physiol Cell Physiol* **279:**C1528–C1539.

Jaggar JH, Porter VA, Lederer WJ, and Nelson MT (2000) Calcium sparks in smooth muscle. *Am J Physiol Cell Physiol* **278:**C235–C256.

James P, Inui M, Tada M, Chiesi M, and Carafoli E (1989) Nature and site of

phospholamban regulation of the Ca^{2+} pump of sarcoplasmic reticulum. *Nature (Lond)* **342:**90–92.
Jan LY and Jan YN (1992) Tracing the roots of ion channels. *Cell* **69:**715–718.
Janiak R, Wilson SM, Montague S, and Hume JR (2001) Heterogeneity of calcium stores and elementary release events in canine pulmonary arterial smooth muscle cells. *Am J Physiol* **280:**C22–C33.
Janssen LJ and Sims SM (1992) Acetylcholine activates non-selective cation and chloride conductances in canine and guinea-pig tracheal myocytes. *J Physiol (Lond)* **453:**197–218.
Janssen LJ and Sims SM (1993) Emptying and refilling of Ca^{2+} store in tracheal myocytes as indicated by ACh-evoked currents and contraction. *Am J Physiol* **265:**C877–C886.
Janssen LJ, Wattie J, Hwa LC, and Tazzeo T (2001) Muscarinic excitation-contraction coupling mechanisms in tracheal and bronchial smooth muscles. *J Appl Physiol* **91:**1142–1151.
Jencks WP (1992) On the mechanism of ATP-driven Ca^{2+} transport by the calcium ATPase of sarcoplasmic reticulum. *Ann NY Acad Sci* **671:**49–56.
Jenkinson S, Challiss RA, and Nahorski SR (1992) Evidence for lithium-sensitive inositol 4,5-bisphosphate accumulation in muscarinic cholinoceptor-stimulated cerebral-cortex slices. *Biochem J* **287:**437–442.
Jeyakumar LH, Ballester L, Cheng DS, McIntyre JO, Chang P, Olivey HE, Rollins-Smith L, Barnett JV, Murray K, Xin HB, et al. (2001) FKBP binding characteristics of cardiac microsomes from diverse vertebrates. *Biochem Biophys Res Commun* **281:**979–986.
Jezior JR, Brady JD, Rosenstein DI, McCammon KA, Miner AS, and Ratz PH (2001) Dependency of detrusor contractions on calcium sensitization and calcium entry through LOE-908-sensitive channels. *Br J Pharmacol* **134:**78–87.
Ji G, Barsotti RJ, Feldman ME, and Kotlikoff MI (2002) Stretch-induced calcium release in smooth muscle. *J Gen Physiol* **119:**533–544.
Jiang QX, Thrower EC, Chester DW, Ehrlich BE, and Sigworth FJ (2002) Three-dimensional structure of the type 1 inositol 1,4,5-trisphosphate receptor at 24 A resolution. *EMBO (Eur Mol Biol Organ) J* **21:**3575–3581.
Joly A (1892) Composés ammoniacaux dérivés du sesquichlorure de ruthénium. *C R Acad Sci* **115**:1299–1301.
Joseph SK, Boehning D, Pierson S, and Nicchitta CV (1997) Membrane insertion, glycosylation, and oligomerization of inositol trisphosphate receptors in a cell-free translation system. *J Biol Chem* **272:**1579–1588.
Juhaszova M, Shimizu H, Borin ML, Yip RK, Santiago EM, Lindenmayer GE, and Blaustein MP (1996) Localization of the Na(+)-Ca^{2+} exchanger in vascular smooth muscle and in neurons and astrocytes. *Ann NY Acad Sci* **779:**318–335.
Kamishima T and McCarron JG (1998) Ca^{2+} removal mechanisms in rat cerebral resistance size arteries. *Biophys J* **75:**1767–1773.
Kamishima T and Quayle JM (2002) Mitochondrial Ca^{2+} uptake is important over low [Ca2+]i range in arterial smooth muscle. *Am J Physiol Heart Circ Physiol* **283:**H2431–H2439.
Kang TM, Park MK, and Uhm DY (2002) Characterization of hypoxia-induced [Ca2+]i rise in rabbit pulmonary arterial smooth muscle cells. *Life Sci* **70:**2321–2333.
Kanmura Y, Raeymaekers L, and Casteels R (1989) Effects of doxorubicin and ruthenium red on intracellular calcium stores in skinned rabbit mesenteric smooth-muscle fibers. *Cell Calcium* **10:**433–439.
Kannan MS, Fenton AM, Prakash YS, and Sieck GC (1996) Cyclic ADP-ribose stimulates sarcoplasmic reticulum calcium release in porcine coronary artery smooth muscle. *Am J Physiol* **270:**H801–H806.
Kannan MS, Prakash YS, Brenner T, Mickelson JR, and Sieck GC (1997) Role of ryanodine receptor channels in Ca^{2+} oscillations of porcine tracheal smooth muscle. *Am J Physiol* **272:**L659–L664.
Karaki H, Ozaki H, Hori M, Mitsui-Saito M, Amano K, Harada K, Miyamoto S, Nakazawa H, Won KJ, and Sato K (1997) Calcium movements, distribution, and functions in smooth muscle. *Pharmacol Rev* **49:**157–230.
Karczewski P, Kelm M, Hartmann M, and Schrader J (1992) Role of phospholamban in NO/EDRF-induced relaxation in rat aorta. *Life Sci* **51:**1205–1210.
Kargacin G and Fay FS (1991) Ca^{2+} Movement in smooth muscle cells studied with one- and two-dimensional diffusion models. *Biophys J* **60:**1088–1100.
Kargacin GJ (1994) Calcium signaling in restricted diffusion spaces. *Biophys J* **67:**262–272.
Kargacin ME and Kargacin GJ (1995) Direct measurement of Ca^{2+} uptake and release by the sarcoplasmic reticulum of saponin permeabilized isolated smooth muscle cells. *J Gen Physiol* **106:**467–484.
Karkanis T, Jiao Y, Hurley BR, Li S, Pickering JG, and Sims SM (2001) Functional receptor-channel coupling compared in contractile and proliferative human vascular smooth muscle. *J Cell Physiol* **187:**244–255.
Karon BS, Mahaney JE, and Thomas DD (1994) Halothane and cyclopiazonic acid modulate Ca-ATPase oligomeric state and function in sarcoplasmic reticulum. *Biochemistry* **33:**13928–13937.
Kawano S, Otsu K, Shoji S, Yamagata K, and Hiraoka M (2003) Ca(2+) oscillations regulated by Na(+)-Ca(2+) exchanger and plasma membrane Ca(2+) pump induce fluctuations of membrane currents and potentials in human mesenchymal stem cells. *Cell Calcium* **34:**145–156.
Kendall JM, Dormer RL, and Campbell AK (1992) Targeting aequorin to the endoplasmic reticulum of living cells. *Biochem Biophys Res Commun* **189:**1008–1016.
Khoo KM, Han MK, Park JB, Chae SW, Kim UH, Lee HC, Bay BH, and Chang CF (2000) Localization of the cyclic ADP-ribose-dependent calcium signaling pathway in hepatocyte nucleus. *J Biol Chem* **275:**24807–24817.
Khoyi MA, Dalziel HH, Zhang L, Bjur RA, Gerthoffer WT, Buxton ILO, and Westfall DP (1993) [Ca2+]i-sensitive, IP3-independent calcium influx in smooth muscle of rat vas deferens revealed by procaine. *Br J Pharmacol* **110:**1353–1358.
Kijima Y, Ogunbunmi E, and Fleischer S (1991) Drug action of thapsigargin on the Ca^{2+} pump protein of sarcoplasmic reticulum. *J Biol Chem* **266:**22912–22918.
Kim CJ, Weir BKA, Macdonald RL, and Zhang H (1998) Erythrocyte lysate releases Ca^{2+} from IP3-sensitive stores and activates Ca^{2+}-dependent K+ channels in rat basilar smooth muscle cells. *Neurol Res* **20:**23–30.
Kiselyov KI, Mamin AG, Semyonova SB, and Mozhayeva GN (1997) Low-conductance high selective inositol (1,4,5)-trisphosphate activated Ca^{2+} channels in plasma membrane of A431 carcinoma cells. *FEBS Lett* **407:**309–312.
Kiselyov KI, Semyonova SB, Mamin AG, and Mozhayeva GN (1999) Miniature Ca^{2+} channels in excised plasma-membrane patches: activation by IP3. *Pflugers Arch* **437:**305–314.
Kobayashi J, Harbour GC, Gilmore J, and Rinehart KL Jr (1984) Eudistomins A, D, G, H, I, J, M, N, O, P and Q, bromo, hydroxy, pyrrolyl and iminoazepino B-carbolines from the antiviral caribbean Tunicate Eudistoma Olivaceum. *J Am Chem Soc* **106:**1526–1528.
Kobayashi J, Ishibashi M, Nagai U, and Ohizumi Y (1989a) 9-Methyl-7-bromoeudistomin D, a potent inducer of calcium release from sarcoplasmic reticulum of skeletal muscle. *Experientia* **45:**782–783.
Kobayashi S, Kitazawa T, Somlyo AV, and Somlyo AP (1989b) Cytosolic heparin inhibits muscarinic and alpha-adrenergic Ca^{2+} release in smooth muscle. Physiological role of inositol 1,4,5-trisphosphate in pharmacomechanical coupling. *J Biol Chem* **264:**17997–18004.
Kobayashi S, Somlyo AV, and Somlyo AP (1988) Heparin inhibits the inositol 1,4,5-trisphosphate-dependent, but not the independent, calcium release induced by guanine nucleotide in vascular smooth muscle. *Biochem Biophys Res Commun* **153:**625–631.
Kong ID, Koh SD, and Sanders KM (2000) Purinergic activation of spontaneous transient outward currents in guinea Pig taenia colonic myocytes. *Am J Physiol* **278:**C352–C362.
Kotlikoff MI and Wang YX (1998) Calcium release and calcium-activated chloride channels in airway smooth muscle cells. *Am J Respir Crit Care Med* **158:**S109–S114.
Kovacs T, Berger G, Corvazier E, Paszty K, Brown A, Bobe R, Papp B, Wuytack F, Cramer EM, and Enouf J (1997) Immunolocalization of the multi-sarco/endoplasmic reticulum Ca^{2+} ATPase system in human platelets. *Br J Haematol* **97:**192–203.
Kuemmerle JF and Makhlouf GM (1995) Agonist-stimulated cyclic ADP ribose. Endogenous modulator of Ca(2+)-induced Ca^{2+} release in intestinal longitudinal muscle. *J Biol Chem* **270:**25488–25494.
Kuemmerle JF, Murthy KS, and Makhlouf GM (1994) Agonist-activated, ryanodine-sensitive, IP3-insensitive Ca^{2+} release channels in longitudinal muscle of intestine. *Am J Physiol* **266:**C1421–C1431.
Kupittayanant S, Luckas MJM, and Wray S (2002) Effect of inhibiting the sarcoplasmic reticulum on spontaneous and oxytocin-induced contractions of human myometrium. *Br J Obstet Gynecol* **109:**289–296.
Kurihara S (1975) The effect of procaine on the mechanical and electrical activities of the smooth muscle cells of the guinea pig urinary bladder. *Jpn J Physiol* **25:**775–788.
Kurihara S and Sakai T (1976a) Inhibitory effects of procaine on the electrical and mechanical activities of the smooth muscle cells of the guinea pig urinary bladder. *Jpn J Physiol* **26:**503–516.
Kurihara S and Sakai T (1976b) Relation between effects of procaine and calcium on spontaneous electrical and mechanical activities of the smooth muscle cells of the guinea pig urinary bladder. *Jpn J Physiol* **26:**487–501.
Kwan CY (1985) Subcellular origin of the oxalate- or inorganic phosphate-stimulated Ca^{2+} transport by smooth muscle microsomes: revisitation of the old problem by a new approach using saponin. *Biochim Biophys Acta* **819:**148–152.
Lagaud GJ, Randriamboavonjy V, Roul G, Stoclet JC, and Andriantsitohaina R (1999) Mechanism of Ca^{2+} release and entry during contraction elicited by norepinephrine in rat resistance arteries. *Am J Physiol* **276:**H300–H308.
Lai FA, Misra M, Xu L, Smith HA, and Meissner G (1989) The ryanodine receptor-Ca^{2+} release channel complex of skeletal muscle sarcoplasmic reticulum. Evidence for a cooperatively coupled, negatively charged homotetramer. *J Biol Chem* **264:**16776–16785.
Lamont C and Wier WG (2004) Different roles of ryanodine receptors and inositol(1,4,5) trisphosphate receptors in adrenergically stimulated contractions of small arteries. *Am J Physiol Heart Circ Physiol* **287:**H617–H625.
Lang RJ, Hashitani H, Keller S, Takano H, Mulholland EL, Fukuta H, and Suzuki H (2002) Modulators of internal Ca^{2+} stores and the spontaneous electrical and contractile activity of the guinea-pig renal pelvis. *Br J Pharmacol* **135:**1363–1374.
Larini F, Menegazzi P, Baricordi O, Zorzato F, and Treves S (1995) A ryanodine receptor-like Ca^{2+} channel is expressed in nonexcitable cells. *Mol Pharmacol* **47:**21–28.
Lee CH, Poburko D, Kuo KH, Seow CY, and van Breemen C (2002a) Ca(2+) oscillations, gradients, and homeostasis in vascular smooth muscle. *Am J Physiol Heart Circ Physiol* **282:**H1571–H1583.
Lee CH, Rahimian R, Szado T, Sandhu J, Poburko D, Behra T, Chan L, and van Breemen C (2002b) Sequential opening of IP(3)-sensitive Ca(2+) channels and SOC during alpha-adrenergic activation of rabbit vena cava. *Am J Physiol Heart Circ Physiol* **282:**H1768–H1777.
Lee HC (1997) Mechanisms of calcium signaling by cyclic ADP-ribose and NAADP (Review). *Physiol Rev* **77:**1133–1164.
Lee HC (2000) NAADP: An emerging calcium signaling molecule. *J Membr Biol* **173:**1–8.
Lee HC (2001) Physiological functions of cyclic ADP-ribose and NAADP as calcium messengers. *Annu Rev Pharmacol Toxicol* **41:**317–345.
Lee HC, Aarhus R, Graeff R, Gurnack ME, and Walseth TF (1994) Cyclic ADP ribose activation of the ryanodine receptor is mediated by calmodulin. *Nature (Lond)* **370:**307–309.
Lee HC, Walseth TF, Bratt GT, Hayes RN, and Clapper DL (1989) Structural determination of a cyclic metabolite of NAD+ with intracellular Ca^{2+}-mobilizing activity. *J Biol Chem* **264:**1608–1615.
Leijten PA and van Breemen C (1984) The effects of caffeine on the noradrenaline-sensitive calcium store in rabbit aorta. *J Physiol (Lond)* **357:**327–339.

Lesh RE, Nixon GF, Fleischer S, Airey JA, Somlyo AP, and Somlyo AV (1998) Localization of ryanodine receptors in smooth muscle. *Circ Res* **82:**175–185.
Li N, Teggatz EG, Li PL, Allaire R, and Zou AP (2000) Formation and actions of cyclic ADP-ribose in renal microvessels. *Microvasc Res* **60:**149–159.
Li P, Zou AP, and Campbell WB (1997) Metabolism and actions of ADP-riboses in coronary arterial smooth muscle. *Adv Exp Med Biol* **419:**437–441.
Li PL, Tang WX, Valdivia HH, Zou AP, and Campbell WB (2001) cADP-ribose activates reconstituted ryanodine receptors from coronary arterial smooth muscle. *Am J Physiol* **280:**H208–H215.
Li W, Llopis J, Whitney M, Zlokarnik G, and Tsien RY (1998) Cell-permeant caged InsP3 ester Shows that Ca^{2+} spike frequency can optimize gene expression. *Nature (Lond)* **392:**936–941.
Lindahl U and Hook M (1978) Glycosaminoglycans and their binding to biological macromolecules. *Annu Rev Biochem* **47:**385–417.
Liu X and Farley JM (1996) Acetylcholine-induced Ca++-dependent chloride current oscillations are mediated by inositol 1,4,5-trisphosphate in tracheal myocytes. *J Pharmacol Exp Ther* **277:**796–804.
Loew LM, Carrington W, Tuft RA, and Fay FS (1994) Physiological cytosolic Ca^{2+} transients evoke concurrent mitochondrial depolarizations. *Proc Natl Acad Sci USA* **91:**12579–12583.
Lohn M, Jessner W, Furstenau M, Wellner M, Sorrentino V, Haller H, Luft FC, and Gollasch M (2001) Regulation of calcium sparks and spontaneous transient outward currents by RyR3 in arterial vascular smooth muscle cells. *Cir Res* **89:**1051–1057.
Loirand G, Pacaud P, Baron A, Mironneau C, and Mironneau J (1991) Large conductance calcium-activated non-selective cation channel in smooth muscle cells isolated from rat portal vein. *J Physiol (Lond)* **437:**461–475.
Lomax RB, Camello C, Van Coppenolle F, Petersen OH, and Tepikin AV (2002) Basal and physiological Ca(2+) leak from the endoplasmic reticulum of pancreatic acinar cells. Second messenger-activated channels and translocons. *J Biol Chem* **277**: 26479–26485.
Lopez JR, Cordovez G, Linares N, and Allen PD (2000) Cyclic ADP-ribose induces a larger than normal calcium release in malignant hyperthermia-susceptible skeletal muscle fibers. *Pflugers Arch* **440:**236–242.
Low AM, Darby PJ, Kwan CY, and Daniel EE (1993) Effects of thapsigargin and ryanodine on vascular contractility: cross-talk between sarcoplasmic reticulum and plasmalemma. *Eur J Pharmacol* **230:**53–62.
Low AM, Kwan CY, and Daniel EE (1992) Evidence for two types of internal Ca^{2+} stores in canine mesenteric artery with different refilling mechanisms. *Am J Physiol* **262:**H31–H37.
Luo D, Nakazawa M, Yoshida Y, Cai J, and Imai S (2000) Effects of three different Ca^{2+} pump ATPase inhibitors on evoked contractions in rabbit aorta and activities of Ca^{2+} pump ATPases in porcine aorta. *Gen Pharmacol* **34:**211–220.
Luo DL, Nakazawa M, Ishibashi T, Kato K, and Imai S (1993) Putative, selective inhibitors of sarcoplasmic reticulum calcium-pump ATPase inhibit relaxation by nitroglycerin and atrial natriuretic factor of the rabbit aorta contracted by phenylephrine. *J Pharmacol Exp Ther* **265:**1187–1192.
Lynn S and Gillespie JI (1995) Basic properties of a novel ryanodine-sensitive, caffeine-insensitive calcium-induced calcium release mechanism in permeabilised human vascular smooth muscle cells. *FEBS Lett* **367:**23–27.
Lynn S, Morgan JM, Gillespie JI, and Greenwell JR (1993) A novel ryanodine sensitive calcium release mechanism in cultured human myometrial smooth-muscle cells. *FEBS Lett* **330:**227–230.
Lynn S, Morgan JM, Lamb HK, Meissner G, and Gillespie JI (1995) Isolation and partial cloning of ryanodine-sensitive Ca^{2+} release channel protein isoforms from human myometrial smooth muscle. *FEBS Lett* **372:**6–12.
Lytton J, Westlin M, Burk SE, Shull GE, and MacLennan DH (1992) Functional comparisons between isoforms of the sarcoplasmic or endoplasmic reticulum family of calcium pumps. *J Biol Chem* **267:**14483–14489.
Lytton J, Westlin M, and Hanley MR (1991) Thapsigargin inhibits the sarcoplasmic or endoplasmic reticulum Ca-ATPase family of calcium pumps. *J Biol Chem* **266:**17067–17071.
Lytton J, Zarain H, Periasamy M, and MacLennan DH (1989) Molecular cloning of the mammalian smooth muscle sarco(endo)plasmic reticulum Ca^{2+}-ATPase. *J Biol Chem* **264:**7059–7065.
Ma H, Zhong L, Inesi G, Fortea I, Soler F, and Fernandez-Belda F (1999) Overlapping effects of S3 stalk segment mutations on the affinity of Ca^{2+}-ATPase (SERCA) for thapsigargin and cyclopiazonic acid. *Biochemistry* **38:**15522–15527.
Mackrill JJ, Wilcox RA, Miyawaki A, Mikoshiba K, Nahorski SR, and Challiss RA (1996) Stable overexpression of the type-1 inositol 1,4,5-trisphosphate receptor in L fibroblasts: subcellular distribution and functional consequences. *Biochem J* **318**:871–878.
Maeda N, Niinobe M, Nakahira K, and Mikoshiba K (1988) Purification and characterization of P400 protein, a glycoprotein characteristic of Purkinje cell, from mouse cerebellum. *J Neurochem* **51:**1724–1730.
Maggi CA, Bevan S, Walpole CSJ, Rang H, and Giuliani S (1993) A comparison of capsazepine and ruthenium red as capsaicin antagonists in the rat isolated urinary bladder and vas deferens. *Br J Pharmacol* **108:**801–805.
Mahaney J, Barlow A, Honaker B, Huffman J, and Muchnok T (1999) Phospholamban reduces cardiac ca-ATPase sensitivity to thapsigargin and cyclopiazonic acid. *Arch Biochem Biophys* **372:**408–413.
Malysz J, Donnelly G, and Huizinga JD (2001) Regulation of slow wave frequency by IP_3-sensitive calcium release in the murine small intestine. *Am J Physiol* **280:** G439–G448.
Marchant JS, Beecroft MD, Riley AM, Jenkins DJ, Marwood RD, Taylor CW, and Potter BVL (1997a) Disaccharide polyphosphates based upon adenophostin A activate hepatic D-myo-inositol 1,4,5-trisphosphate receptors. *Biochemistry* **36:** 12780–12790.
Marchant JS, Chang YT, Chung SK, Irvine RF, and Taylor CW (1997b) Rapid kinetic measurements of $45Ca^{2+}$ mobilization reveal that Ins(2,4,5)P3 is a partial agonist at hepatic $InsP_3$ receptors. *Biochem J* **321**:573–576.
Marklund S and Marklund G (1974) Involvement of the superoxide anion radical in the autoxidation of pyrogallol and a convenient assay for superoxide dismutase. *Eur J Biochem* **47:**469–474.
Marks AR, Tempst P, Chadwick CC, Riviere L, Fleischer S, and Nadal-Ginard B (1990) Smooth muscle and brain inositol 1,4,5-trisphosphate receptors are structurally and functionally similar. *J Biol Chem* **265:**20719–20722.
Martin C, Dacquet C, Mironneau C, and Mironneau J (1989) Caffeine-induced inhibition of calcium channel current in cultured smooth cells from pregnant rat myometrium. *Br J Pharmacol* **98:**493–498.
Martinez-Zaguilan R, Parnami J, and Martinez GM (1998) Mag-Fura-2 (furaptra) exhibits both low (microM) and high (nM) affinity for Ca^{2+}. *Cell Physiol Biochem* **8:**158–174.
Martonosi AN (1996) Structure-function relationships in the Ca(2+)-ATPase of sarcoplasmic reticulum: facts, speculations and questions for the future. *Biochim Biophys Acta* **1275:**111–117.
Maruyama T, Kanaji T, Nakade S, Kanno T, and Mikoshiba K (1997) 2APB, 2-aminoethoxydiphenyl borate, a membrane-penetrable modulator of Ins(1,4,5)P3-induced Ca^{2+} release. *J Biochem (Tokyo)* **122:**498–505.
Marx SO, Gaburjakova J, Gaburjakova M, Henrikson C, Ondrias K, and Marks AR (2001) Coupled gating between cardiac calcium release channels (ryanodine receptors). *Circ Res* **88:**1151–1158.
Mason MJ, Garcia R, and Grinstein S (1991) Coupling between intracellular Ca^{2+} stores and the Ca^{2+} permeability of the plasma membrane. Comparison of the effects of thapsigargin, 2,5-di-(tert-butyl)-1,4-hydroquinone, and cyclopiazonic acid in rat thymic lymphocytes. *J Biol Chem* **266:**20856–20862.
Masuoka H, Ito M, Nakano T, Naka M, and Tanaka T (1990) Effects of ruthenium red on activation of Ca2(+)-dependent cyclic nucleotide phosphodiesterase. *Biochem Biophys Res Commun* **169:**315–322.
Matlib MA, Zhou Z, Knight S, Ahmed S, Choi KM, Krause-Bauer J, Phillips R, Altschuld R, Katsube Y, Sperelakis N, et al. (1998) Oxygen-bridged dinuclear ruthenium amine complex specifically inhibits Ca^{2+} uptake into mitochondria in vitro and in situ in single cardiac myocytes. *J Biol Chem* **273:**10223–10231.
Mauban JR, Lamont C, Balke CW, and Wier WG (2001) Adrenergic stimulation of rat resistance arteries affects Ca(2+) sparks, Ca(2+) waves, and Ca(2+) oscillations. *Am J Physiol Heart Circ Physiol* **280:**H2399–H2405.
Mayrleitner M, Chadwick CC, Timerman AP, Fleischer S, and Schindler H (1991) Purified IP3 receptor from smooth muscle forms an IP3 gated and heparin sensitive calcium channel in planar bilayers. *Cell Calcium* **12:**505–514.
Mayrleitner M, Schaefer R, and Fleischer S (1995) IP_3 receptor purified from liver plasma membrane is an (1,4,5)IP3 activated and (1,3,4,5)IP4 inhibited calcium permeable ion channel. *Cell Calcium* **17:**141–153.
McCarron JG, Craig JW, Bradley KN, and Muir TC (2002) Agonist-induced phasic and tonic responses in smooth muscle are mediated by InsP(3). *J Cell Sci* **115:** 2207–2218.
McCarron JG and Muir TC (1999) Mitochondrial regulation of the cytosolic Ca^{2+} concentration and the InsP3-sensitive Ca^{2+} store in guinea-pig colonic smooth muscle. *J Physiol (Lond)* **516:**149–161.
McDaniel NL, Rembold CM, Richard HM, and Murphy RA (1991) Cyclic AMP relaxes swine arterial smooth muscle predominantly by decreasing cell Ca^{2+} concentration. *J Physiol (Lond)* **439:**147–160.
McFadzean I and Gibson A (2002) The developing relationship between receptor-operated and store-operated calcium channels in smooth muscle. *Br J Pharmacol* **135:**1–13.
McGrogan I, Lu S, Hipworth S, Sormaz L, Eng R, Preocanin D, and Daniel EE (1995) Mechanisms of cyclic nucleotide-induced relaxation in canine tracheal smooth muscle. *Am J Physiol* **268:**L407–L413.
McLaughlin S (1973) Salicylates and phospholipid bilayer membranes. *Nature (Lond)* 234–236.
Mehlmann LM, Mikoshiba K, and Kline D (1996) Redistribution and increase in cortical inositol 1,4,5-trisphosphate receptors after meiotic maturation of the mouse oocyte. *Dev Biol* **180:**489–498.
Meissner G (1994) Ryanodine receptor/Ca^{2+} release channels and their regulation by endogenous effectors. *Annu Rev Physiol* **56:**485–508.
Meldolesi J and Pozzan T (1998) The endoplasmic reticulum Ca^{2+} store: a view from the lumen. *Trends Biochem Sci* **23:**10–14.
Meszaros LG, Bak J, and Chu A (1993) Cyclic ADP-ribose as an endogenous regulator of the non-skeletal type ryanodine receptor Ca^{2+} channel. *Nature (Lond)* **364:**76–79.
Meszaros LG and Ikemoto N (1985) Ruthenium red and caffeine affect the Ca^{2+}-ATPase of the sarcoplasmic reticulum. *Biochem Biophys Res Commun* **127:**836–842.
Michelangeli F, Mezna M, Tovey S, and Sayers LG (1995) Pharmacological modulators of the inositol 1,4,5-trisphosphate receptor. *Neuropharmacology* **34:**1111–1122.
Michikawa T, Miyawaki A, Furuichi T, and Mikoshiba K (1996) Inositol 1,4,5-trisphosphate receptors and calcium signaling. *Crit Rev Neurobiol* **10:**39–55.
Mironneau J, Coussin F, Jeyakumar LH, Fleischer S, Mironneau C, and Macrez N (2001) Contribution of ryanodine receptor subtype 3 to Ca^{2+} responses in Ca^{2+}-overloaded cultured rat portal vein myocytes. *J Biol Chem* **276:**11257–11264.
Mironneau J, Macrez N, Morel JL, Sorrentino V, and Mironneau C (2002) Identification and function of ryanodine receptor subtype 3 in non-pregnant mouse myometrial cells. *J Physiol (Lond)* **538:**707–716.
Missiaen L, Callewaert G, De Smedt H, and Parys JB (2001a) 2-Aminoethoxydiphenyl borate affects the inositol 1,4,5-trisphosphate receptor, the intracellular Ca^{2+} pump and the non-specific Ca^{2+} leak from the non-mitochondrial Ca^{2+} stores in permeabilized A7r5 Cells. *Cell Calcium* **29:**111–116.
Missiaen L, De Smedt H, Droogmans G, and Casteels R (1992a) 2,5-Di-(Tert-Butyl)-1,4-benzohydroquinone and cyclopiazonic acid decrease the Ca^{2+} permeability of endoplasmic reticulum. *Eur J Pharmacol* **227:**391–394.
Missiaen L, De Smedt H, Droogmans G, Himpens B, and Casteels R (1992b) Calcium ion homeostasis in smooth muscle. *Pharmacol Ther* **56:**191–231.

Missiaen L, De Smedt H, Droogmans G, Wuytack F, Raeymaekers L, and Casteels R (1990) Ruthenium red and compound 48/80 inhibit the smooth-muscle plasma-membrane calcium pump via interaction with associated polyphosphoinositides. *Biochim Biophys Acta* **1023:**449–454.
Missiaen L, De Smedt H, Parys JB, Raeymaekers L, Droogmans G, Van Den Bosch L, and Casteels R (1996) kinetics of the non-specific calcium leak from non-mitochondrial calcium stores in permeabilized A7r5 cells. *Biochem J* **317**:849–853.
Missiaen L, Parys JB, De Smedt H, Himpens B, and Casteels R (1994) Inhibition of inositol trisphosphate-induced calcium release by caffeine is prevented by ATP. *Biochem J* **300**:81–84.
Missiaen L, Taylor CW, and Berridge MJ (1992c) Luminal Ca^{2+} promoting spontaneous Ca^{2+} release from Inositol trisphosphate-sensitive stores in rat hepatocytes. *J Physiol (Lond)* **455:**623–640.
Missiaen L, Van Acker K, Parys JB, De Smedt H, Van Baelen K, Weidema AF, Vanoevelen J, Raeymaekers L, Renders J, Callewaert G, et al. (2001b) Baseline cytosolic Ca^{2+} oscillations derived from a non-endoplasmic reticulum Ca^{2+} store. *J Biol Chem* **276:**39161–39170.
Missiaen L, Vanoevelen J, Parys JB, Raeymaekers L, De Smedt H, Callewaert G, Erneux C, and Wuytack F (2002) Ca^{2+} uptake and release properties of a thapsigargin-insensitive nonmitochondrial Ca^{2+} store in A7r5 and 16HBE14o- cells. *J Biol Chem* **277:**6898–6902.
Missiaen L, Wuytack F, De Smedt H, Vrolix M, and Casteels R (1988) AlF4-reversibly inhibits 'P'-type cation-transport ATPases, possibly by interacting with the phosphate-binding site of the ATPase. *Biochem J* **253:**827–833.
Mitchell CA, Gurung R, Kong AM, Dyson JM, Tan A, and Ooms LM (2002) Inositol polyphosphate 5-phosphatases: lipid phosphatases with flair. *IUBMB Life* **53:**25–36.
Mitchell RW, Halayko AJ, Kahraman S, Solway J, and Wylam ME (2000) Selective restoration of calcium coupling to muscarinic M3 receptors in contractile cultured airway myocytes. *Am J Physiol* **278:**L1091–L1100.
Miyazaki S and Shirakawa H (1993) Ca^{2+}-induced Ca^{2+} release mediated by the IP_3 receptor is responsible for Ca^{2+} waves and Ca^{2+} oscillations at fertilization of mammalian eggs. *Biomed Res* **14:**35–38.
Miyazaki S, Yuzaki M, Nakada K, Shirakawa H, Nakanishi S, Nakade S, and Mikoshiba K (1992) Block of calcium wave and Ca^{2+} oscillation by antibody to the inositol 1,4,5-triphosphate receptor in fertilized hamster eggs. *Science (Wash DC)* **257:**251–255.
Molimard M, Martin CA, Naline E, Hirsch A, and Advenier C (1994) Contractile effects of bradykinin on the isolated human small bronchus. *Am J Respir Crit Care Med* **149:**123–127.
Moller JV, Juul B, and le Maire (1996) Structural organization, ion transport, and energy transduction of P-type ATPases. *Biochim Biophys Acta* **1286:**1–51.
Molnar M and Hertelendy F (1995) Signal transduction in rat myometrial cells: comparison of the actions of endothelin-1, oxytocin and prostaglandin F2 alpha. *Eur J Endocrinol* **133:**467–474.
Montell C (1997) New light on TRP and TRPL. *Mol Pharmacol* **52:**755–763.
Moore CL (1971) Specific inhibition of mitochondrial Ca++ transport by ruthenium red. *Biochem Biophys Res Commun* **42:**298–305.
Moore GA, McConkey DJ, Kass GE, Brien PJ, and Orrenius S (1987) 2,5-di(tert-butyl)-1,4-benzohydroquinone–a novel inhibitor of liver microsomal Ca^{2+} sequestration. *FEBS Lett* **224:**331–336.
Morgan JM and Gillespie JI (1995) The modulation and characterisation of the Ca(2+)-induced Ca^{2+} release mechanism in cultured human myometrial smooth muscle cells. *FEBS Lett* **369:**295–300.
Morio Y and McMurtry IF (2002) Ca^{2+} release from ryanodine-sensitive store contributes to mechanism of hypoxic vasoconstriction in rat lungs. *J Appl Physiol* **92:**527–534.
Morrissette J, Heisermann G, Cleary J, Ruoho A, and Coronado R (1993) Cyclic ADP-ribose induced Ca^{2+} release in rabbit skeletal muscle sarcoplasmic reticulum. *FEBS Lett* **330:**270–274.
Mourey RJ, Verma A, Supattapone S, and Snyder SH (1990) Purification and characterization of the inositol 1,4,5-trisphosphate receptor protein from rat vas deferens. *Biochem J* **272:**383–389.
Murphy CT, Riley AM, Lindley CJ, Jenkins DJ, Westwick J, and Potter BVL (1997) Structural analogs of D-myo-inositol-1,4,5-trisphosphate and adenophostin A: recognition by cerebellar and platelet inositol-1,4,5-trisphosphate receptors. *Mol Pharmacol* **52:**741–748.
Murthy KS (2001) cAMP inhibits IP(3)-dependent Ca(2+) release by preferential activation of cGMP-primed PKG. *Am J Physiol Gastrointest Liver Physiol* **281:** G1238–G1245.
Murthy KS and Zhou H (2003) Selective phosphorylation of the IP3R-I in vivo by cGMP-dependent protein kinase in smooth muscle. *Am J Physiol Gastrointest Liver Physiol* **284:**G221–G230.
Nahorski SR and Potter BV (1989) Molecular recognition of inositol polyphosphates by intracellular receptors and metabolic enzymes. *Trends Pharmacol Sci* **10:**139–144.
Nakade S, Maeda N, and Mikoshiba K (1991) Involvement of the C-terminus of the inositol 1,4,5-trisphosphate receptor in calcium release analyzed using region-specific monoclonal antibodies. *Biochem J* **277:**125–131.
Nakade S, Rhee SK, Hamanaka H, and Mikoshiba K (1994) Cyclic AMP-dependent phosphorylation of an immunoaffinity-purified homotetrameric inositol 1,4,5-trisphosphate receptor (type I) increases Ca^{2+} flux in reconstituted lipid vesicles. *J Biol Chem* **269:**6735–6742.
Nakagawa M, Endo M, Tanaka N, and Lee GP (1984) Structures of Xestospongin A, B, C, and D, novel vasodilative compounds from marine sponge, Xestospongia exigua. *Tetrahedron Lett* **25:**3227–3230.
Nakahara T, Yunoki M, Moriuchi H, Sakamato K, and Ishii K (2000) Lidocaine potentiates the relaxant effects of cAMP-elevating agents in bovine tracheal smooth muscle. *Naunyn-Schmiedeberg's Arch Pharmacol* **361:**605–609.
Nakamura F, Naka M, and Tanaka T (1992a) Inhibition of actin-activated myosin magnesium-ATPase in smooth muscle by ruthenium red. *FEBS Lett* **314:**93–96.
Nakamura H, Nakasaki Y, Matsuda N, and Shigekawa M (1992b) Inhibition of sarcoplasmic reticulum Ca(2+)-ATPase by 2,5-di(tert-butyl)-1,4-benzohydroquinone. *J Biochem (Tokyo)* **112:**750–755.
Nakamura Y, Kobayashi J, Gilmore J, Mascal M, Rinehart KL Jr, Nakamura H, and Ohizumi Y (1986) Bromo-eudistomin D, a novel inducer of calcium release from fragmented sarcoplasmic reticulum that causes contractions of skinned muscle fibers. *J Biol Chem* **261:**4139–4142.
Nakanishi S, Maeda N, and Mikoshiba K (1991) Immunohistochemical localization of an inositol 1,4,5-trisphosphate receptor, P400, in neural tissue: studies in developing and adult mouse brain. *J Neurosci* **11:**2075–2086.
Nakasaki Y, Iwamoto T, Hanada H, Imagawa T, and Shigekawa M (1993) Cloning of the rat aortic smooth muscle $Na+/Ca^{2+}$ exchanger and tissue-specific expression of isoforms. *J Biochem (Tokyo)* **114:**528–534.
Nanjo T (1984) Effects of noradrenaline and acetylcholine on electro-mechanical properties of the guinea-pig portal vein. *Br J Pharmacol* **81:**427–440.
Nasu T, Oosako H, and Shibata H (1996) Dantrolene blocks the tonic contraction and calcium influx evoked by K+ in ileal longitudinal smooth muscle. *Gen Pharmacol* **27:**513–517.
Nazer MA and van Breemen C (1998) A role for the sarcoplasmic reticulum in Ca^{2+} extrusion from rabbit inferior vena cava smooth muscle. *Am J Physiol* **274:**H123–H131.
Nelson EJ, Li CC, Bangalore R, Benson T, Kass RS, and Hinkle PM (1994) Inhibition of L-type calcium-channel activity by thapsigargin and 2,5-*t*-butylhydroquinone, but not by cyclopiazonic acid. *Biochem J* **302:**147–154.
Nelson MT, Cheng H, Rubart M, Santana LF, Bonev AD, Knot HJ, and Lederer WJ (1995) Relaxation of arterial smooth muscle by calcium sparks. *Science (Wash DC)* **270:**633–637.
Nelson MT and Quayle JM (1995) Physiological roles and properties of potassium channels in arterial smooth muscle. *Am J Physiol* **268:**C799–C822.
Neusser M, Golinski P, Zhu Z, Zidek W, and Tepel M (1999) Thapsigargin-insensitive calcium pools in vascular smooth muscle cells. *Clin Exp Hypertens* **21:**395–405.
Neusser M, Tepel M, Golinski P, Zhu Z, Rahn KH, Spieker C, and Zidek W (1993) Protein kinase C and calcium distribution in vascular smooth muscle cells from spontaneously hypertensive rats. *J Hypertens* **11 (Suppl 5):**S114–S115.
Newton CL, Mignery GA, and Sudhof TC (1994) Co-expression in vertebrate tissues and cell lines of multiple inositol 1,4,5-trisphosphate (InsP3) receptors with distinct affinities for InsP3. *J Biol Chem* **269:**28613–28619.
Neylon CB, Nickashin A, Little PJ, Tkachuk VA, and Bobik A (1992) Thrombin-induced Ca^{2+} mobilization in vascular smooth muscle utilizes a slowly ribosylating pertussis toxin-sensitive G protein. Evidence for the involvement of a G protein in inositol trisphosphate-dependent Ca^{2+} release. *J Biol Chem* **267:**7295–7302.
Nielsen MS, Olsen CE, Dich J, Christensen SB, and Grunnet N (1994) Metabolism of thapsigargin in rat hepatocytes. *Drug Metab Dispos* **22:**433–437.
Nielsen SF, Thastrup O, Pedersen R, Olsen CE, and Christensen SB (1995) Structure-activity relationships of analogues of thapsigargin modified at O-11 and O-12. *J Med Chem* **38:**272–276.
Nilius B (2003) From TRPs to SOCs, CCEs and CRACs: consensus and controversies. *Cell Calcium* **33:**293–298.
Nixon GF, Mignery GA, and Somlyo AV (1994) Immunogold localization of inositol 1,4,5-trisphosphate receptors and characterization of ultrastructural features of the sarcoplasmic reticulum in phasic and tonic smooth muscle. *J Muscle Res Cell Motil* **15:**682–700.
Nobe K, Sutliff RL, Kranias EG, and Paul RJ (2001) Phospholamban regulation of bladder contractility: evidence from gene-altered mouse models. *J Physiol (Lond)* **535:**867–878.
Nomura Y and Asano M (2000) Ca^{2+} Uptake function of sarcoplasmic reticulum during contraction of rat arterial smooth muscles. *Eur J Pharmacol* **404:**315–326.
Nomura Y, Asano M, Ito K, Uyama Y, Imaizumi Y, and Watanabe M (1997) Potent vasoconstrictor actions of cyclopiazonic acid and thapsigargin on femoral arteries from spontaneously hypertensive rats. *Br J Pharmacol* **120:**65–73.
Norred WP, Morrissey RE, Riley RT, Cole RJ, and Dorner JW (1985) Distribution, excretion and skeletal muscle effects of the mycotoxin [14C]cyclopiazonic acid in rats. *Food Chem Toxicol* **23:**1069–1076.
Norregaard A, Vilsen B, and Andersen JP (1993) Chimeric Ca(2+)-ATPase/Na+,K(+)-ATPase molecules. Their phosphoenzyme intermediates and sensitivity to Ca^{2+} and thapsigargin. *FEBS Lett* **336:**248–254.
Norregaard A, Vilsen B, and Andersen JP (1994) Transmembrane segment M3 is essential to thapsigargin sensitivity of the sarcoplasmic reticulum Ca(2+)-ATPase. *J Biol Chem* **269:**26598–26601.
Ohi Y, Atsuki K, Torii Y, Ohizumi Y, Watanabe M, and Imaizumi Y (2001a) Imaging of Ca^{2+} release by caffeine and 9-methyl-7-bromoeudistomin D and the associated activation of large conductance Ca^{2+}-dependent K+ channels in urinary bladder smooth muscle cells of the guinea pig. *Jpn J Pharmacol* **85:**382–390.
Ohi Y, Yamamura H, Nagano N, Ohya S, Muraki K, Watanabe M, and Imaizumi Y (2001b) Local Ca^{2+} transients and distribution of BK channels and ryanodine receptors in smooth muscle cells of guinea-pig vas deferens and urinary Bladder. *J Physiol (Lond)* **534:**313–326.
Ohta T, Kawai K, Ito S, and Nakazato Y (1995) Ca^{2+} entry activated by emptying of intracellular Ca2+ stores in ileal smooth muscle of the rat. *Br J Pharmacol* **114:**1165–1170.
Ohya Y, Kitamura K, and Kuriyama H (1987) Cellular calcium regulates outward currents in rabbit intestinal smooth muscle cell. *Am J Physiol* **252:**C401–C410.
Okumura F and Denborough MA (1980) Effects of anesthetics on guinea pig tracheal smooth muscle. *Br J Anaesth* **52:**199–204.
Ozaki H, Hori M, Kim YS, Kwon SC, Ahn DS, Nakazawa H, Kobayashi M, and Karaki H (2002) Inhibitory mechanism of xestospongin-C on contraction and ion channels in the intestinal smooth muscle. *Br J Pharmacol* **137:**1207–1212.
Ozaki H, Kasai H, Hori M, Sato K, Ishihara H, and Karaki H (1990) Direct inhibition of chicken gizzard smooth muscle contractile apparatus by caffeine. *Naunyn-Schmiedeberg's Arch Pharmacol* **341:**262–267.
Ozturk Y, Altinkurt O, Yildizoglu-Ari N, and Altan VM (1990) Evaluation of con-

traction time and recovery period as a parameter in the calcium antagonistic action on the potassium-depolarized rat deodenum. *J Pharm Pharmacol* **42:**874–877.
Pabelick CM, Prakash YS, Kannan MS, Warner DO, and Sieck GC (2001a) Effects of halothane on sarcoplasmic reticulum calcium release channels in porcine airway smooth muscle cells. *Anesthesiology* **95:**207–215.
Pabelick CM, Sieck GC, and Prakash YS (2001b) Invited review: significance of spatial and temporal heterogeneity of calcium transients in smooth muscle. *J Appl Physiol* **91:**488–496.
Pacaud P and Bolton TB (1991a) Calcium entry into guinea-pig jejunum cells after calcium stores depletion. *Z Kardiol* **80 (Suppl 7):**69–72.
Pacaud P and Bolton TB (1991b) Relation between muscarinic receptor cationic current and internal calcium in guinea-pig jejunal smooth muscle cells. *J Physiol (Lond)* **441:**477–499.
Pacaud P, Loirand G, Gregoire G, Mironneau C, and Mironneau J (1993) Noradrenaline-activated heparin-sensitive Ca^{2+} entry after depletion of intracellular Ca2+ store in portal vein smooth muscle cells. *J Biol Chem* **268:**3866–3872.
Pacher P, Csordas P, Schneider T, and Hajnoczky G (2000) Quantification of calcium signal transmission from sarco-endoplasmic reticulum to the mitochondria. *J Physiol (Lond)* **529:**553–564.
Papp B, Enyedi A, Kovacs T, Sarkadi B, Wuytack F, Thastrup O, Gardos G, Bredoux R, Levy T, and Enouf J (1991) Demonstration of two forms of calcium pumps by thapsigargin inhibition and radioimmunoblotting in platelet membrane vesicles. *J Biol Chem* **266:**14593–14596.
Papp B, Enyedi A, Paszty K, Kovacs T, Sarkadi B, Gardos G, Magnier C, Wuytack F, and Enouf J (1992) Simultaneous presence of two distinct endoplasmic-reticulum-type calcium-pump isoforms in human cells. Characterization by radioimmunoblotting and inhibition by 2,5-di-(*t*-butyl)-1,4-benzohydroquinone. *Biochem J* **288:**297–302.
Papp B, Paszty K, Kovacs T, Sarkadi B, Gardos G, Enouf J, and Enyedi A (1993) Characterization of the inositol trisphosphate-sensitive and insensitive calcium stores by selective inhibition of the endoplasmic reticulum-type calcium pump isoforms in isolated platelet membrane vesicles. *Cell Calcium* **14:**531–538.
Parekh AB (2003) Store-operated Ca^{2+} entry: dynamic interplay between endoplasmic reticulum, mitochondria, and plasma membrane. *J Physiol (Lond)* **547:**333–348.
Patel S, Joseph SK, and Thomas AP (1999) Molecular properties of inositol 1,4,5-trisphosphate receptors. *Cell Calcium* **25:**247–264.
Pauwels PJ, Leysen JE, and Laduron PM (1986) [^{3}H]Batrachotoxinin A 20-alpha-benzoate binding to sodium channels in rat brain: characterization and pharmacological significance. *Eur J Pharmacol* **124:**291–298.
Peng H, Matchkov V, Ivarsen A, Aalkjaer C, and Nilsson H (2001) Hypothesis for the initiation of vasomotion. *Circ Res* **88:**810–815.
Perez CF, Marengo JJ, Bull R, and Hidalgo C (1998) Cyclic ADP-ribose activates caffeine-sensitive calcium channels from sea urchin egg microsomes. *Am J Physiol* **274:**C430–C439.
Perez GJ, Bonev AD, Patlak JB, and Nelson MT (1999) Functional coupling of ryanodine receptors to KCa channels in smooth muscle cells from rat cerebral arteries. *J Gen Physiol* **113:**229–238.
Pesco J, Salmon JM, Vigo J, and Viallet P (2001) Mag-indo1 affinity for Ca(2+), compartmentalization and binding to proteins: the challenge of measuring Mg(2+) concentrations in living cells. *Anal Biochem* **290:**221–231.
Pessah IN, Stambuk RA, and Casida JE (1987) Ca^{2+}-activated ryanodine binding: mechanisms of sensitivity and intensity modulation by Mg^{2+}, caffeine, and adenine nucleotides. *Mol Pharmacol* **31:**232–238.
Pessah IN and Zimanyi I (1991) Characterization of multiple [^{3}H]ryanodine binding sites on the Ca^{2+} release channel of sarcoplasmic reticulum from skeletal and cardiac muscle: evidence for a sequential mechanism in ryanodine action. *Mol Pharmacol* **39:**679–689.
Pesty A, Avazeri N, and Lefevre B (1998) Nuclear calcium release by $InsP_3$-receptor channels plays a role in meiosis reinitiation in the mouse oocyte. *Cell Calcium* **24:**239–251.
Petkov GV and Boev KK (1996) The role of sarcoplasmic reticulum and sarcoplasmic reticulum Ca^{2+}-ATPase in the smooth muscle tone of the cat gastric fundus. *Pflugers Arch* **431:**928–935.
Phillippe M and Basa A (1996) The Effects of ruthenium red, an inhibitor of calcium-induced calcium release, on phasic myometrial contractions. *Biochem Biophys Res Commun* **221:**656–661.
Plenge-Tellechea F, Soler F, and Fernandez B (1997) On the inhibition mechanism of sarcoplasmic or endoplasmic reticulum Ca^{2+}-ATPases by cyclopiazonic acid. *J Biol Chem* **272:**2794–2800.
Poburko D, Kuo KH, Dai J, Lee CH, and van Breemen C (2004) Organellar junctions promote targeted Ca^{2+} signaling in smooth muscle: why two membranes are better than one. *Trends Pharmacol Sci* **25:**8–15.
Poch G and Umfahrer W (1976) Differentiation of intestinal smooth muscle relaxation caused by drugs that inhibit phosphodiesterase. *Naunyn-Schmiedeberg's Arch Pharmacol* **293:**257–268.
Pollock NS, Kargacin ME, and Kargacin GJ (1998) Chloride channel blockers inhibit Ca^{2+} uptake by the smooth muscle sarcoplasmic reticulum. *Biophys J* **75:**1759–1766.
Popescu LM and Diculescu I (1975) Calcium in smooth muscle sarcoplasmic reticulum in situ. Conventional and X-ray analytical electron microscopy. *J Cell Biol* **67:**911–918.
Popescu LM, Hinescu ME, Spiru L, Popescu M, and Diculescu I (1987) The effect of procaine on calcium-magnesium-ATPase of erythrocyte membrane. *Rev Roum Biochim* **24:**119–124.
Potocnik SJ and Hill MA (2001) Pharmacological evidence for capacitative Ca^{2+} entry in cannulated and pressurized skeletal muscle arterioles. *Br J Pharmacol* **134:**247–256.
Povstyan OV, Gordienko DV, Harhun MI, and Bolton TB (2003) Identification of interstitial cells of cajal in the rabbit portal vein. *Cell Calcium* **33:**223–239.
Pozo MJ, Perez GJ, Nelson MT, and Mawe GM (2002) Ca^{2+} sparks and BK currents in gallbladder myocytes: role in CCK-induced response. *Am J Physiol* **282:**G165–G174.
Pozzan T, Rizzuto R, Volpe P, and Meldolesi J (1994) Molecular and cellular physiology of intracellular calcium stores. *Physiol Rev* **74:**595–636.
Prakash YS, Kannan MS, Walseth TF, and Sieck GC (1998) Role of cyclic ADP-ribose in the regulation of [Ca^{2+}]i in porcine tracheal smooth muscle. *Am J Physiol* **274:**C1653–C1660.
Prakriya M and Lewis RS (2001) Potentiation and inhibition of Ca^{2+} release-activated Ca^{2+} channels by 2-aminoethyldiphenyl borate (2-APB) occurs independently of IP_3 receptors. *J Physiol (Lond)* **536:**3–19.
Pratusevich VR and Balke CW (1996) Factors shaping the confocal image of the calcium spark in cardiac muscle cells. *Biophys J* **71:**2942–2957.
Procida K, Caspersen C, Kromann H, Christensen SB, and Treiman M (1998) ACTA, a fluorescent analogue of thapsigargin, is a potent inhibitor and a conformational probe of skeletal muscle Ca^{2+}-ATPase. *FEBS Lett* **439:**127–132.
Prozialeck WC, Wallace TL, and Weiss B (1987) Differential inhibition of calmodulin-sensitive phosphodiesterase and Ca++-adenosine triphosphatase by chlorpromazine-linked calmodulin. *J Pharmacol Exp Ther* **243:**171–179.
Pucovsky V, Gordienko DV, and Bolton TB (2002) Effect of nitric oxide donors and noradrenaline on Ca^{2+} release sites and global intracellular Ca^{2+} in myocytes from guinea-pig small mesenteric arteries. *J Physiol (Lond)* **539:**25–39.
Putney JW Jr (1986) A model for receptor-regulated calcium entry. *Cell Calcium* **7:**1–12.
Putney JW Jr, Broad LM, Braun FJ, Lievremont JP, and Bird GS (2001) Mechanisms of capacitative calcium entry. *J Cell Sci* **114:**2223–2229.
Qazi S and Trimmer BA (1999) The role of inositol 1,4,5-trisphosphate 5-phosphatase in inositol signaling in the CNS of larval manduca sexta. *Insect Biochem Mol Biol* **29:**161–175.
Raeymaekers L (1982) The sarcoplasmic reticulum of smooth muscle fibers. *Z Naturforsch Sect C Biosci* **37:**481–488.
Raeymaekers L, Hofmann F, and Casteels R (1988) Cyclic GMP-dependent protein kinase phosphorylates phospholamban in isolated sarcoplasmic reticulum from cardiac and smooth muscle. *Biochem J* **252:**269–273.
Raeymaekers L and Jones LR (1986) Evidence for the presence of phospholamban in the endoplasmic reticulum of smooth muscle. *Biochim Biophys Acta* **882:**258–265.
Raeymaekers L and Wuytack F (1993) Ca^{2+} pumps in smooth muscle cells. *J Muscle Res Cell Motil* **14:**141–157.
Ramos-Franco J, Galvan D, Mignery GA, and Fill M (1999) Location of the permeation pathway in the recombinant type 1 inositol 1,4,5-trisphosphate receptor. *J Gen Physiol* **114:**243–250.
Rasmussen U, Christensen SB, and Sandberg F (1981) Phytochemistry of the genus Thapsia. *Planta Med* **43:**336–341.
Rebecchi MJ and Pentyala SN (2000) Structure, function, and control of phosphoinositide-specific phospholipase C. *Physiol Rev* **80:**1291–1335.
Rembold CM, van Riper DA, and Chen XL (1995) Focal [Ca2+]i increases detected by aequorin but not by fura-2 in histamine- and caffeine-stimulated swine carotid artery. *J Physiol (Lond)* **488:**549–564.
Rettig SJ and Trotter J (1976) Crystal and molecular structure of *B,B*-Bis(*p*-tolyl)boroxazolidine and the orthorhombic form of *B,B*-diphenylboroxazolidine. *Can J Chem* **54:**3130–3141.
Rhee SG (2001) Regulation of phosphoinositide-specific phospholipase C. *Annu Rev Biochem* **70:**281–312.
Ritov VB, Men'shikova EV, and Kozlov YP (1985) Heparin induces Ca^{2+} release from the terminal cisterns of skeletal muscle sarcoplasmic reticulum. *FEBS Lett* **188:**77–80.
Rosado JA, Brownlow SL, and Sage SO (2002) Endogenously expressed Trp1 is involved in store-mediated Ca^{2+} entry by conformational coupling in human platelets. *J Biol Chem* **277:**42157–42163.
Rosado JA and Sage SO (2000) Coupling between inositol 1,4,5-trisphosphate receptors and human transient receptor potential channel 1 when intracellular Ca^{2+} stores are depleted. *Biochem J* **350:**631–635.
Ross CA, Danoff SK, Schell MJ, Snyder SH, and Ullrich A (1992) Three additional inositol 1,4,5-trisphosphate receptors: molecular cloning and differential localization in brain and peripheral tissues. *Proc Natl Acad Sci USA* **89:**4265–4269.
Ross R and Klebanoff SJ (1971) The smooth muscle cell. I. In vivo synthesis of connective tissue proteins. *J Cell Biol* **50:**159–171.
Rossi D and Sorrentino V (2002) Molecular genetics of ryanodine receptors Ca(2+)-release channels. *Cell Calcium* **32:**307–319.
Rossi FM and Kao JP (1997) Nmoc-DBHQ, a new caged molecule for modulating sarcoplasmic/endoplasmic reticulum Ca^{2+} ATPase activity with light flashes. *J Biol Chem* **272:**3266–3271.
Rossier MF, Python CP, Burnay MM, Schlegel W, Vallotton MB, and Capponi AM (1993) Thapsigargin inhibits voltage-activated calcium channels in adrenal glomerulosa cells. *Biochem J* **296:**309–312.
Rousseau E, Ladine J, Liu QY, and Meissner G (1988) Activation of the Ca^{2+} release channel of skeletal muscle sarcoplasmic reticulum by caffeine and related compounds. *Arch Biochem Biophys* **267:**75–86.
Rousseau E and Meissner G (1989) Single cardiac sarcoplasmic reticulum Ca^{2+}-release channel: activation by caffeine. *Am J Physiol* **256:**H328–H333.
Rousseau E, Smith JS, and Meissner G (1987) Ryanodine modifies conductance and gating behavior of single Ca^{2+} release channel. *Am J Physiol* **253:**C364–C368.
Rubio C, Moreno A, Briones A, Ivorra MD, D'Ocon P, and Vila E (2002) Alterations by age of calcium handling in rat resistance arteries. *J Cardiovasc Pharmacol* **40:**832–840.
Rueda A, Garcia L, and Guerrero-Hernandez A (2002a) Luminal Ca^{2+} and the activity of sarcoplasmic reticulum Ca2+ pumps modulate histamine-induced all-or-none Ca2+ release in smooth muscle cells. *Cell Signal* **14:**517–527.
Rueda A, Garcia L, Soria-Jasso LE, Arias-Montano JA, and Guerrero-Hernandez A (2002b) The initial inositol 1,4,5-trisphosphate response induced by histamine is

strongly amplified by Ca(2+) release from internal stores in smooth muscle. *Cell Calcium* **31:**161–173.
Ruehlmann DO, Lee CH, Poburko D, and van Breemen C (2000) Asynchronous Ca2+ waves in intact venous smooth muscle. *Cir Res* **86:**E72–E79.
Safrany ST, Wojcikiewicz RJ, Strupish J, Nahorski SR, Dubreuil D, Cleophax J, Gero SD, and Potter BV (1991) Interaction of synthetic D-6-deoxy-myo-inositol 1,4,5-trisphosphate with the Ca2(+)-releasing D-myo-inositol 1,4,5-trisphosphate receptor and the metabolic enzymes 5-phosphatase and 3-kinase. *FEBS Lett* **278:**252–256.
Sagara Y, Fernandez-Belda F, de Meis L, and Inesi G (1992) Characterization of the inhibition of intracellular Ca2+ transport ATPases by thapsigargin. *J Biol Chem* **267:**12606–12613.
Sagara Y and Inesi G (1991) Inhibition of the sarcoplasmic reticulum Ca2+ transport ATPase by thapsigargin at subnanomolar concentrations. *J Biol Chem* **266:** 13503–13506.
Saino T, Matsuura M, and Satoh YI (2002) Comparison of the effect of ATP on intracellular calcium ion dynamics between rat testicular and cerebral arteriole smooth muscle cells. *Cell Calcium* **32:**153–163.
Sanders KM (2001) Mechanisms of calcium handling in smooth muscles. *J Appl Physiol* **91:**1438–1449.
Sanz CM, Cortijo J, Ortiz JL, Perpina M, Sarria B, Esplugues J, and Morcillo EJ (1990) Effect of dantrolene sodium in isolated guinea-pig trachea. *Eur J Pharmacol* **176:**177–185.
Sasaki T, Inui M, Kimura Y, Kuzuya T, and Tada M (1992a) Molecular mechanism of regulation of Ca2+ pump ATPase by phospholamban in cardiac sarcoplasmic reticulum. Effects of synthetic phospholamban peptides on Ca2+ pump ATPase. *J Biol Chem* **267:**1674–1679.
Sasaki T, Naka M, Nakamura F, and Tanaka T (1992b) Ruthenium red inhibits the binding of calcium to calmodulin required for enzyme activation. *J Biol Chem* **267:**21518–21523.
Sato K, Ozaki H, and Karaki H (1988) Multiple effects of caffeine on contraction and cytosolic free Ca2+ levels in vascular smooth muscle of rat aorta. *Naunyn-Schmiedeberg's Arch Pharmacol* **338:**443–448.
Satoh K, Ohta T, Ito S, and Nakazato Y (1994) Inhibitory effects of dantrolene on contractile responses in gastric smooth muscle of the rat. *J Vet Med Sci* **56:**275–279.
Savineau JP (1988) Caffeine does not contract skinned uterine fibers with a functional Ca store. *Eur J Pharmacol* **149:**187–190.
Savineau JP and Mironneau J (1990) Caffeine acting on pregnant rat myometrium: analysis of its relaxant action and its failure to release Ca2+ from intracellular stores. *Br J Pharmacol* **99:**261–266.
Savineau JP, Mironneau J, and Mironneau C (1988) Contractile properties of chemically skinned fibers from pregnant rat myometrium: existence of an internal Ca-store. *Pflugers Arch* **411:**296–303.
Sawynok J and Yaksh TL (1993) Caffeine as an analgesic adjuvant: a review of pharmacology and mechanisms of action. *Pharmacol Rev* **45:**43–85.
Scamps F, Vigues S, Restituito S, Campo B, Roig A, Charnet P, and Valmier J (2000) Sarco-endoplasmic ATPase blocker 2,5-di(tert-butyl)-1, 4-benzohydroquinone inhibits N-, P- and Q- but not T-, L-, or R-type calcium currents in central and peripheral neurons. *Mol Pharmacol* **58:**18–26.
Seidler NW, Jona I, Vegh M, and Martonosi A (1989) Cyclopiazonic acid is a specific inhibitor of the Ca2+-ATPase of sarcoplasmic reticulum. *J Biol Chem* **264:**17816–17823.
Seino A, Kobayashi M, Kobayashi J, Fang YI, Ishibashi M, Nakamura H, Momose K, and Ohizumi Y (1991) 9-Methyl-7-bromoeudistomin D, a powerful radio-labelable Ca++ releaser having caffeine-like properties, acts on Ca(++)-induced Ca++ release channels of sarcoplasmic reticulum. *J Pharmacol Exp Ther* **256:**861–867.
Semenova SB, Kiselev KI, and Mozhaeva GN (1999) Low-conductivity calcium channels in the macrophage plasma membrane: activation by inositol-1,4,5-triphosphate. *Neurosci Behav Physiol* **29:**339–345.
Serysheva II, Bare DJ, Ludtke SJ, Kettlun CS, Chiu W, and Mignery GA (2003) Structure of the type 1 inositol 1,4,5-trisphosphate receptor revealed by electron cryomicroscopy. *J Biol Chem* **278:**21319–21322.
Sethi JK, Empson RM, Bailey VC, Potter BV, and Galione A (1997) 7-Deaza-8-bromo-cyclic ADP-ribose, the first membrane-permeant, hydrolysis-resistant cyclic ADP-ribose antagonist. *J Biol Chem* **272:**16358–16363.
Sharma NR and Davis MJ (1996) Calcium entry activated by store depletion in coronary endothelium is promoted by tyrosine phosphorylation. *Am J Physiol* **270:**H267–H274.
Shears SB (1989) Metabolism of the inositol phosphates produced upon receptor activation. *Biochem J* **260:**313–324.
Shears SB (1998) The versatility of inositol phosphates as cellular signals. *Biochim Biophys Acta* **1436:**49–67.
Shen JZ, Zheng XF, Wei EQ, and Kwan CY (2001) Evidence against inhibition of sarcoplasmic reticulum Ca2+-pump as mechanism of H2O2-induced contraction of rat aorta. *Acta Pharmacol Sin* **22:**498–504.
Shi XZ and Sarna SK (2000) Impairment of Ca2+ mobilization in circular muscle cells of the inflamed colon. *Am J Physiol* **278:**G234–G242.
Shim JO, Shin CY, Lee TS, Yang SJ, An JY, Song HJ, Kim TH, Huh IH, and Sohn UD (2002) Signal transduction mechanism via adenosine A1 receptor in the cat esophageal smooth muscle cells. *Cell Signal* **14:**365–372.
Shimamoto H, Majarais IL, Shimamoto Y, Kwan CY, and Daniel EE (1992) Role of sarcoplasmic reticulum in the contractile function of vascular smooth muscle as studied by 2,5-di-(tert-butyl)-1,4-benzohydroquinone. *Biol Signals* **1:**182–193.
Shinlova OP, Kosterin SA, and Veklich TA (1996) Ruthenium red inhibits energy-dependent and passive Ca2+ transport in permeabilized smooth muscle cells. *Biokhimiia* **61:**1440–1447.
Shirakawa H and Miyazaki S (1995) Evidence for inositol tetrakisphosphate-activated Ca2+ influx pathway refilling inositol trisphosphate-sensitive Ca2+ stores in hamster eggs. *Cell Calcium* **17:**1–13.
Shmigol AV, Eisner DA, and Wray S (1999) The role of the sarcoplasmic reticulum as a Ca2+ sink in rat uterine smooth muscle cells. *J Physiol (Lond)* **520:**153–163.
Shmigol AV, Eisner DA, and Wray S (2001) Simultaneous measurements of changes in sarcoplasmic reticulum and cytosolic [Ca2+] in rat uterine smooth muscle cells. *J Physiol (Lond)* **531:**707–713.
Shoenberg CF (1958) An electron microscopic study of smooth muscle in pregnant uterus of the rabbit. *Biophys Biochem Cytol* **4:**609–614.
Shuto S, Fukuoka M, Manikowsky A, Ueno Y, Nakano T, Kuroda R, Kuroda H, and Matsuda A (2001) Total synthesis of cyclic ADP-carbocyclic-ribose, a stable mimic of Ca2+-mobilizing second messenger cyclic ADP-ribose. *J Am Chem Soc* **123:** 8750–8759.
Shuto S, Tatani K, Ueno Y, and Matsuda A (1998) Synthesis of adenophostin analogs lacking the adenine moiety as novel potent IP3 receptor ligands: some structural requirements for the significant activity of adenophostin A. *J Org Chem* **63:**8815–8824.
Shuttleworth TJ (1999) What drives calcium entry during [Ca2+]i oscillations?–Challenging the capacitative model. *Cell Calcium* **25:**237–246.
Sims SM (1992) Cholinergic Activation of a non-selective cation current in canine gastric smooth muscle is associated with contraction. *J Physiol (Lond)* **449:**377–398.
Sims SM, Jiao Y, and Preiksaitis HG (1997) Regulation of intracellular calcium in human esophageal smooth muscles. *Am J Physiol* **273:**C1679–C1689.
Sitsapesan R, McGarry SJ, and Williams AJ (1994) Cyclic ADP-ribose competes with ATP for the adenine nucleotide binding site on the cardiac ryanodine receptor Ca(2+)-release channel. *Circ Res* **75:**596–600.
Sitsapesan R, Montgomery RA, MacLeod KT, and Williams AJ (1991) Sheep cardiac sarcoplasmic reticulum calcium-release channels: modification of conductance and gating by temperature. *J Physiol (Lond)* **434:**469–488.
Sitsapesan R and Williams AJ (1990) Mechanisms of caffeine activation of single calcium-release channels of sheep cardiac sarcoplasmic reticulum. *J Physiol (Lond)* **423:**425–439.
Sitsapesan R and Williams AJ (1995) Cyclic ADP-ribose and related compounds activate sheep skeletal sarcoplasmic reticulum Ca2+ release channel. *Am J Physiol* **268:**C1235–C1240.
Smani T, Iwabuchi S, Lopez-Barneo J, and Urena J (2001) Differential segmental activation of Ca2+ -dependent CI-and K+ channels in pulmonary arterial myocytes. *Cell Calcium* **29:**369–377.
Sohn UD, Harnett KM, De Petris G, Behar J, and Biancani P (1993) Distinct muscarinic receptors, G proteins and phospholipases in esophageal and lower esophageal sphincter circular muscle. *J Pharmacol Exp Ther* **267:**1205–1214.
Soler F, Plenge-Tellechea F, Fortea I, and Fernandez-Belda F (1998) Cyclopiazonic acid effect on Ca2+-dependent conformational states of the sarcoplasmic reticulum ATPase. Implication for the enzyme turnover. *Biochemistry* **37:**4266–4274.
Somlyo AP (1975) Ultrastructure and function of vascular smooth muscle, in *The Smooth Muscle of the Artery* (Wolf S and Werthessen NT eds) Plenum Publishing Corporation, New York.
Somlyo AV (1980) Ultrastructure of vascular smooth muscle, in *Section 2: The Cardiovascular System* (Bohr DF, Somlyo AP, and Sparks HV eds) American Physiological Society, Bethesda, Maryland.
Somlyo AV, Bond M, Somlyo AP, and Scarpa A (1985) Inositol trisphosphate-induced calcium release and contraction in vascular smooth muscle. *Proc Natl Acad Sci USA* **82:**5231–5235.
Somlyo AV and Franzini-Armstrong C (1985) New views of smooth muscle structure using freezing, deep-etching and rotary shadowing. *Experientia* **41:**841–856.
Somlyo AV, Horiuti K, Trentham DR, Kitazawa T, and Somlyo AP (1992) Kinetics of calcium release and contraction induced by photolysis of caged D-myo-inositol 1,4,5-trisphosphate in smooth muscle. The effects of heparin, procaine, and adenine nucleotides. *J Biol Chem* **267:**22316–22322.
Somlyo AV and Somlyo AP (1971) Strontium accumulation by sarcoplasmic reticulum and mitochondria in vascular smooth muscle. *Science (Wash DC)* **174:**955–958.
Sonnleitner A, Conti A, Bertocchini F, Schindler H, and Sorrentino V (1998) Functional properties of the ryanodine receptor type 3 (RyR3) Ca2+ release channel. *EMBO (Eur Mol Biol Organ) J* **17:**2790–2798.
Sorin A, Rosas G, and Rao R (1997) PMR1, a Ca2+-ATPase in yeast Golgi, has properties distinct from sarco/endoplasmic reticulum and plasma membrane calcium pumps. *J Biol Chem* **272:**9895–9901.
Sorrentino V and Rizzuto R (2001) Molecular genetics of Ca(2+) stores and intracellular Ca(2+) signalling. *Trends Pharmacol Sci* **22:**459–464.
Spedding M and Berg C (1985) Antagonism of calcium-induced contractions of potassium-depolarized smooth muscle by local anesthetics. *Eur J Pharmacol* **108:** 143–150.
Steenbergen JM and Fay FS (1996) The quantal nature of calcium release to caffeine in single smooth muscle cells results from activation of the sarcoplasmic reticulum Ca(2+)-ATPase. *J Biol Chem* **271:**1821–1824.
Stehno-Bittel L, Luckhoff A, and Clapham DE (1995) Calcium release from the nucleus by InsP3 receptor channels. *Neuron* **14:**163–167.
Stehno-Bittel L and Sturek M (1992) Spontaneous sarcoplasmic reticulum calcium release and extrusion from bovine, not porcine, coronary artery smooth muscle. *J Physiol (Lond)* **451:**49–78.
Stout MA (1991) Calcium transport by sarcoplasmic reticulum of vascular smooth muscle: I. MgATP-dependent and MgATP-independent calcium uptake. *J Cell Physiol* **149:**383–395.
Stout MA, Raeymaekers L, De Smedt H, and Casteels R (2002) Characterization of Ca^{2+} release from heterogeneous Ca^{2+} stores in sarcoplasmic reticulum isolated from arterial and gastric smooth muscle. *Can J Physiol Pharmacol* **80:**588–603.
Strang CJ, Henson E, Okamoto Y, Paz MA, and Gallop PM (1989) Separation and determination of alpha-amino acids by boroxazolidone formation. *Anal Biochem* **178:**276–286.
Strupish J, Wojcikiewicz RJ, Challiss RA, Safrany ST, Willcocks AL, Potter BV, and

Nahorski SR (1991) Is decavanadate a specific inositol 1,4,5-trisphosphate receptor antagonist? *Biochem J* **277:**294.
Sugiyama T and Goldman WF (1995) Measurement of SR free Ca^{2+} and Mg^{2+} in permeabilized smooth Muscle cells with use of furaptra. *Am J Physiol* **269:**C698–C705.
Sugiyama T, Matsuda Y, and Mikoshiba K (2000) Inositol 1,4,5-trisphosphate receptor associated with focal contact cytoskeletal proteins. *FEBS Lett* **466:**29–34.
Sullivan KMC, Lin DD, Agnew W, and Wilson KL (1995) Inhibition of nuclear vesicle fusion by antibodies that block activation of inositol 1,4,5-trisphosphate receptors. *Proc Natl Acad Sci USA* **92:**8611–8615.
Surroca A and Wolff D (2000) Inositol 1,4,5-trisphosphate but not ryanodine-receptor agonists induces calcium release from rat liver Golgi apparatus membrane vesicles. *J Membr Biol* **177:**243–249.
Sutko JL, Airey JA, Welch W, and Ruest L (1997) The pharmacology of ryanodine and related compounds. *Pharmacol Rev* **49:**53–98.
Sutko JL, Robinson E, Lattanzio FA Jr, Schlatterer RG, Deslongchamps P, and Ruest L (1990) Pharmacology of the *Ryania* alkaloids: The ester A, a ryanodine analog that only increases sarcoplasmic reticulum calcium permeability, in *Transduction in Biological Systems* (Hidalgo C, Bacigalupo J, Jaimovich E, and Vergara J eds) pp 465–473, Plenum Publishing Corporation, New York.
Suzuki M, Muraki K, Imaizumi Y, and Watanabe M (1992) Cyclopiazonic acid, an inhibitor of the sarcoplasmic reticulum Ca(2+)-pump, reduces Ca(2+)-dependent K+ currents in guinea-pig smooth muscle cells. *Br J Pharmacol* **107:**134–140.
Szado T, Kuo KH, Bernard-Helary K, Poburko D, Lee CH, Seow C, Ruegg UT, and van Breemen C (2003) Agonist-induced mitochondrial Ca^{2+} transients in smooth muscle. *FASEB J* **17:**28–37.
Szado T, McLarnon M, Wang X, and van Breemen C (2001) Role of sarcoplasmic reticulum in regulation of tonic contraction of rabbit basilar artery. *Am J Physiol* **281:**H1481–H1489.
Szalai G, Csordas G, Hantash BM, Thomas AP, and Hajnoczky G (2000) Calcium signal transmission between ryanodine receptors and mitochondria. *J Biol Chem* **275:**15305–15313.
Tada M (1992) Molecular structure and function of phospholamban in regulating the calcium pump from sarcoplasmic reticulum. *Ann NY Acad Sci* **671:**92–102.
Takahashi A, Camacho P, Lechleiter JD, and Herman B (1999) Measurement of intracellular calcium. *Physiol Rev* **79:**1089–1125.
Takahashi M, Kagasaki T, Hosoya T, and Takahashi S (1993) Adenophostins A and B: potent agonists of inositol-1,4,5-trisphosphate receptor produced by Penicillium brevicompactum. Taxonomy, fermentation, isolation, physicochemical and biological properties. *J Antibiot* **46:**1643–1647.
Takahashi M, Tanazawa K, and Takahashi S (1994) Adenophostins, newly discovered metabolites of penicillium brevicompactum, act as potent agonists of the inositol 1,4,5-trisphosphate receptor. *J Biol Chem* **269:**369–372.
Takahashi N, Aizawa H, Fukuyama S, Inoue H, Nishima S, and Hara N (2000) Thapsigargin, a Ca^{2+}-ATPase inhibitor, relaxes guinea pig tracheal smooth muscle by producing epithelium-dependent relaxing factors. *Eur J Pharmacol* **410:**61–68.
Takahashi Y, Furukawa K, Ishibashi M, Kozutsumi D, Ishiyama H, Kobayashi J, and Ohizumi Y (1995) Structure-activity relationship of bromoeudistomin D, a powerful Ca^{2+} releaser in skeletal muscle sarcoplasmic reticulum. *Eur J Pharmacol* **288:**285–293.
Takasawa S, Ishida A, Nata K, Nakagawa K, Noguchi N, Tohgo A, Kato I, Yonekura H, Fujisawa H, and Okamoto H (1995) Requirement of calmodulin-dependent protein kinase II in cyclic ADP-ribose-mediated intracellular Ca^{2+} mobilization. *J Biol Chem* **270:**30257–30259.
Takeshima H, Komazaki S, Hirose K, Nishi M, Noda T, and Iino M (1998) Embryonic lethality and abnormal cardiac myocytes in mice lacking ryanodine receptor type 2. *EMBO (Eur Mol Biol Organ) J* **17:**3309–3316.
Tanaka Y and Tashjian AH (1993) Functional identification and quantitation of three intracellular calcium pools in GH4C1 cells: evidence that the caffeine-responsive pool is coupled to a thapsigargin-resistant, ATP-dependent process. *Biochemistry* **32:**12062–12073.
Tanaka Y and Tashjian AH Jr (1995) Calmodulin is a selective Mediator of Ca(2+)-induced Ca^{2+} release via the ryanodine receptor-like Ca^{2+} channel triggered by cyclic ADP-ribose. *Proc Natl Acad Sci USA* **92:**3244–3248.
Tang WX, Chen YF, Zou AP, Campbell WB, and Li PL (2002) Role of FKBP12.6 in cADPR-induced activation of reconstituted ryanodine receptors from arterial smooth muscle. *Am J Physiol* **282:**H1304–H1310.
Tao L, Huang Y, and Bourreau JP (2000) Control of the mode of excitation-contraction coupling by Ca(2+) stores in bovine trachealis muscle. *Am J Physiol Lung Cell Mol Physiol* **279:**L722–L732.
Tapia R, Arias C, and Morales E (1985) Binding of lanthanum ions and ruthenium red to synaptosomes and its effects on neurotransmitter release. *J Neurochem* **45:**1464–1470.
Tapia R and Velasco I (1996) Ruthenium red as a tool to study calcium channels, neuronal death and the function of neural pathways. *Neurochem Int* **30:**137–147.
Tasker PN, Taylor CW, and Nixon GF (2000) Expression and distribution of InsP(3) receptor subtypes in proliferating vascular smooth muscle cells. *Biochem Biophys Res Commun* **273:**907–912.
Taylor CW (1998) Inositol trisphosphate receptors: Ca^{2+}-modulated intracellular Ca^{2+} channels. *Biochim Biophys Acta* **1436:**19–33.
Thastrup O, Cullen PJ, Drobak BK, Hanley MR, and Dawson AP (1990) Thapsigargin, a tumor promoter, discharges intracellular Ca^{2+} stores by specific inhibition of the endoplasmic reticulum Ca2(+)-ATPase. *Proc Natl Acad Sci USA* **87:**2466–2470.
Thastrup O, Dawson AP, Scharff O, Foder B, Cullen PJ, Drobak BK, Bjerrum PJ, Christensen SB, and Hanley MR (1989) Thapsigargin, a novel molecular probe for studying intracellular calcium release and storage. *Agents Actions* **27:**17–23.
Thomas JM, Masgrau R, Churchill GC, and Galione A (2001) Pharmacological characterization of the putative cADP-ribose receptor. *Biochem J* **359:**451–457.
Timerman AP, Onoue H, Xin HB, Barg S, Copello J, Wiederrecht G, and Fleischer S (1996) Selective binding of FKBP12.6 by the cardiac ryanodine receptor. *J Biol Chem* **271:**20385–20391.
Tokutomi Y, Tokutomi N, and Nishi K (2001) The properties of ryanodine-sensitive Ca^{2+} release in mouse gastric smooth muscle cells. *Br J Pharmacol* **133:**125–137.
Tosun M, Paul RJ, and Rapoport RM (1998) Coupling of store-operated Ca++ entry to contraction in rat aorta. *J Pharmacol Exp Ther* **285:**759–766.
Tovey SC, Dyer JL, Godfrey RE, Khan SZ, Bilmen JG, Mezna M, and Michelangeli F (2000) Subtype identification and functional properties of inositol 1,4,5-triphosphate receptors in heart and aorta. *Pharmacol Res* **42:**581–590.
Toyofuku T, Curotto KK, Narayanan N, and MacLennan DH (1994) Identification of Ser38 as the site in cardiac sarcoplasmic reticulum Ca(2+)-ATPase that is phosphorylated by Ca^{2+}/calmodulin-dependent protein kinase. *J Biol Chem* **269:**26492–26496.
Treiman M, Caspersen C, and Christensen SB (1998) A tool coming of age: thapsigargin as an inhibitor of sarco-endoplasmic reticulum Ca^{2+}-ATPases. *Trends Pharmacol Sci* **19:**131–135.
Trepakova ES, Csutora P, Hunton DL, Marchase RB, Cohen RA, and Bolotina VM (2000) Calcium influx factor directly activates store-operated cation channels in vascular smooth muscle cells. *J Biol Chem* **275:**26158–26163.
Tsien RW and Tsien RY (1990) Calcium channels, stores, and oscillations. *Annu Rev Cell Biol* **6:**715–760.
Twort CH and van Breemen C (1989) Human airway smooth muscle in cell culture: control of the intracellular calcium store. *Pulm Pharmacol* **2:**45–53.
Ueno H, Sumimoto K, Hashimoto T, Hirata M, and Kuriyama H (1987) Effects of procaine on pharmaco-mechanical coupling mechanisms activated by acetylcholine in smooth muscle cells of porcine coronary artery. *Circ Res* **60:**356–366.
Ueno S and Shimada K (2001) Pharmacology of heparin. *BIO Clinica* **16:**273–277.
Uyama Y, Imaizumi Y, and Watanabe M (1992) Effects of cyclopiazonic acid, a novel Ca(2+)-ATPase inhibitor, on contractile responses in skinned ileal smooth muscle. *Br J Pharmacol* **106:**208–214.
Uyama Y, Imaizumi Y, and Watanabe M (1993) Cyclopiazonic acid, an inhibitor of Ca(2+)-ATPase in sarcoplasmic reticulum, increases excitability in ileal smooth muscle. *Br J Pharmacol* **110:**565–572.
Vaca L and Kunze DL (1995) IP3-Activated Ca^{2+} channels in the plasma membrane of cultured vascular endothelial cells. *Am J Physiol* **269:**C733–C738.
Vallot O, Combettes L, and Lompre AM (2001) Functional coupling between the caffeine/ryanodine-sensitive Ca^{2+} store and mitochondria in rat aortic smooth muscle cells. *Biochem J* **357:**363–371.
van Breemen C, Chen Q, and Laher I (1995) Superficial buffer barrier function of smooth muscle sarcoplasmic reticulum. *Trends Pharmacol Sci* **16:**98–105.
Van Helden DF, Imtiaz MS, Nurgaliyeva K, von der Weid P, and Dosen PJ (2000) Role of calcium stores and membrane voltage in the generation of slow wave action potentials in guinea-pig gastric pylorus. *J Physiol (Lond)* **524:**245–265.
Varadi A and Rutter GA (2002) Dynamic imaging of endoplasmic reticulum Ca^{2+} concentration in insulin-secreting MIN6 cells using recombinant targeted cameleons: roles of sarco(endo)plasmic reticulum Ca^{2+}-ATPase (SERCA)-2 and ryanodine receptors. *Diabetes* **51 (Suppl 1):**S190–S201.
Varney MA, Rivera J, Lopez BA, and Watson SP (1990) Are there subtypes of the inositol 1,4,5-trisphosphate receptor? *Biochem J* **269:**211–216.
Vassas A, Bourdy G, Paillard JJ, Lavayre J, Pais M, Quirion JC, and Debitus C (1996) Naturally occurring somatostatin and vasoactive intestinal peptide inhibitors. Isolation of alkaloids from two marine sponges. *Planta Med* **62:**28–30.
Vennekens R, Voets T, Bindels RJ, Droogmans G, and Nilius B (2002) Current understanding of mammalian TRP homologues. *Cell Calcium* **31:**253–264.
Veratti E (1902) Ricerche sulla fine strutturra della fibra muscolarae striata. *Mem Ist Lomb Classe Sci Nat* **19:**87–103.
Verboomen H, Wuytack F, De Smedt H, Himpens B, and Casteels R (1992) Functional difference between SERCA2a and SERCA2b Ca^{2+} pumps and their modulation by phospholamban. *Biochem J* **286:**591–595.
Verjans B, Moreau C, and Erneux C (1994) The control of intracellular signal molecules at the level of their hydrolysis: the example of inositol 1,4,5-trisphosphate 5-phosphatase. *Mol Cell Endocrinol* **98:**167–171.
Villa A, Podini P, Panzeri MC, Soling HD, Volpe P, and Meldolesi J (1993) The endoplasmic-sarcoplasmic reticulum of smooth muscle: immunocytochemistry of vas deferens fibers reveals specialized subcompartments differently equipped for the control of Ca^{2+} homeostasis. *J Cell Biol* **121:**1041–1051.
Virji AS, Puffer HW, and McKenzie RG (1969) Historical development of procaine from cocaine. *N Z Dent J* **65:**107–114.
Voelker D and Smejtek P (1996) Adsorption of ruthenium red to phospholipid membranes. *Biophys J* **70:**818–830.
Vu CQ, Lu PJ, Chen CS, and Jacobson MK (1996) 2′-Phospho-cyclic ADP-ribose, a calcium-mobilizing agent derived from NADP. *J Biol Chem* **271:**4747–4754.
Wagenknecht T and Samso M (2002) Three-dimensional reconstruction of ryanodine receptors. *Front Biosci* **7:**d1464–d1474.
Waldron RT, Short AD, and Gill DL (1995) Thapsigargin-resistant intracellular calcium pumps. Role in calcium pool function and growth of thapsigargin-resistant cells. *J Biol Chem* **270:**11955–11961.
Walia M, Samson SE, Schmidt T, Best K, Kwan CY, and Grover AK (2003) Effects of peroxynitrite on pig coronary artery smooth muscle. *Cell Calcium* **34:**69–74.
Walker JW, Somlyo AV, Goldman YE, Somlyo AP, and Trentham DR (1987) Kinetics of smooth and skeletal muscle activation by laser pulse photolysis of caged inositol 1,4,5-trisphosphate. *Nature (Lond)* **327:**249–252.
Walseth TF, Aarhus R, Gurnack ME, Wong L, Breitinger HG, Gee KR, and Lee HC (1997) Preparation of cyclic ADP-ribose antagonists and caged cyclic ADP-ribose. *Methods Enzymol* **280:**294–305.
Walseth TF and Lee HC (1993) Synthesis and characterization of antagonists of cyclic-ADP-ribose-induced Ca^{2+} release. *Biochim Biophys Acta* **1178:**235–242.
Walsh MP (1994) Calmodulin and the regulation of smooth muscle contraction. *Mol Cell Biochem* **135:**21–41.
Walter M, Tepel M, Nofer JR, Neusser M, Assmann G, and Zidek W (2000) Involve-

ment of phospholipase D in store-operated calcium influx in vascular smooth muscle cells. *FEBS Lett* **479:**51–56.
Wang HW and Jackson RT (1988) Effects of lidocaine and procaine on canine nasal blood vessels. *Ann Otol Rhinol Laryngol* **97:**409–413.
Wang JP, Needleman DH, and Hamilton SL (1993) Relationship of low affinity [3H]ryanodine binding sites to high affinity sites on the skeletal muscle Ca^{2+} release channel. *J Biol Chem* **268:**20974–20982.
Wang YX and Kotlikoff MI (1997) Muscarinic signaling pathway for calcium release and calcium-activated chloride current in smooth muscle. *Am J Physiol* **273:**C509–C519.
Waniishi Y, Inoue R, Morita H, Teramoto N, Abe K, and Ito Y (1998) Cyclic GMP-dependent but G-kinase-independent inhibition of Ca^{2+}-dependent Cl- currents by NO donors in cat tracheal smooth muscle. *J Physiol (Lond)* **511:**719–731.
Watanabe J, Karibe A, Horiguchi S, Keitoku M, Satoh S, Takishima T, and Shirato K (1993) Modification of myogenic intrinsic tone and [Ca2+]i of rat isolated arterioles by ryanodine and cyclopiazonic acid. *Circ Res* **73:**465–472.
Watras J (1988) Regulation of calcium uptake in bovine aortic sarcoplasmic reticulum by cyclic AMP-dependent protein kinase. *J Mol Cell Cardiol* **20:**711–723.
Watson EL, Vincenzi FF, and Davis PW (1971) Ca^{2+}-activated membrane ATPase: selective inhibition by ruthenium red. *Biochim Biophys Acta* **249:**606–610.
Wayman CP, Gibson A, and McFadzean I (1998) Depletion of either ryanodine- or IP3-sensitive calcium stores activates capacitative calcium entry in mouse anococcygeus smooth muscle cells. *Pflugers Arch* **435:**231–239.
Wayman CP, McFadzean I, Gibson A, and Tucker JF (1997) Cellular mechanisms underlying carbachol-induced oscillations of calcium-dependent membrane current in smooth muscle cells from mouse anococcygeus. *Br J Pharmacol* **121:**1301–1308.
Weidelt T and Isenberg G (2000) Augmentation of SR Ca^{2+} release by rapamycin and FK506 causes K+-channel activation and membrane hyperpolarization in bladder smooth muscle. *Br J Pharmacol* **129:**1293–1300.
Weirich J, Seiler L, Hug MJ, and Fleckenstein-Grun G (2001) Ca(2+) entry into primary cultured pig coronary smooth muscle cells after previous store depletion by repetitive P2Y purinoceptor stimulation. *Cell Calcium* **29:**359–367.
Welch W, Ahmad S, Airey JA, Gerzon K, Humerickhouse RA, Besch HR Jr, Ruest L, Deslongchamps P, and Sutko JL (1994) Structural determinants of high-affinity binding of ryanoids to the vertebrate skeletal muscle ryanodine receptor: a comparative molecular field analysis. *Biochemistry* **33:**6074–6085.
Welch W, Williams AJ, Tinker A, Mitchell KE, Deslongchamps P, Lamothe J, Gerzon K, Bidasee KR, Besch HR Jr, Airey JA, et al. (1997) Structural components of ryanodine responsible for modulation of sarcoplasmic reticulum calcium channel function. *Biochemistry* **36:**2939–2950.
Wellman GC and Nelson MT (2003) Signaling between SR and plasmalemma in smooth muscle: sparks and the activation of Ca^{2+}-sensitive ion channels. *Cell Calcium* **34:**211–229.
Wellman GC, Santana LF, Bonev AD, and Nelson MT (2001) Role of phospholamban in the modulation of arterial Ca^{2+} sparks and Ca^{2+}-activated K+ channels by cAMP. *Am J Physiol* **281:**C1029–C1037.
Westerblad H and Allen DG (1994) The role of sarcoplasmic reticulum in relaxation of mouse muscle; effects of 2,5-di(tert-butyl)-1,4-benzohydroquinone. *J Physiol (Lond)* **474:**291–301.
Westerduin P, Willems HA, and van Boeckel CA (1992) Synthesis of analogues of myo-inositol 1,4,5-trisphosphate that contain sulfonamide, sulfate, methylphosphonate, and carboxymethyl groups. *Carbohydr Res* **234:**131–140.
Whisstock JC, Wiradjaja F, Waters JE, and Gurung R (2002) The structure and function of catalytic domains within inositol polyphosphate 5-phosphatases. *IUBMB Life* **53:**15–23.
White C and McGeown G (2002) Imaging of changes in sarcoplasmic reticulum [Ca(2+)] using Oregon Green BAPTA 5N and confocal laser scanning microscopy. *Cell Calcium* **31:**151–159.
White C and McGeown JG (2000) Regulation of basal intracellular calcium concentration by the sarcoplasmic reticulum in myocytes from the rat gastric antrum. *J Physiol (Lond)* **529:**395–404.
White C and McGeown JG (2003) Inositol 1,4,5-trisphosphate receptors modulate Ca^{2+}-sparks and Ca^{2+}-store content in vas deferens myocytes. *Am J Physiol Cell Physiol* **285:**C195–C204.
White TA, Johnson S, Walseth TF, Lee HC, Graeff RM, Munshi CB, Prakash YS, Sieck GC, and Kannan MS (2000) Subcellular localization of cyclic ADP-ribosyl cyclase and cyclic ADP-ribose hydrolase activities in porcine airway smooth muscle. *Biochim Biophys Acta* **1498:**64–71.
White TA, Walseth TF, and Kannan MS (2002) Nitric oxide inhibits ADP-ribosyl cyclase through a cGMP-independent pathway in airway smooth muscle. *Am J Physiol Lung Cell Mol Physiol* **283:**L1065–L1071.
Wibo M and Godfraind T (1994) Comparative localization of inositol 1,4,5-trisphosphate and ryanodine receptors in intestinal smooth muscle: an analytical subfractionation study. *Biochem J* **297:**415–423.
Wier WG and Morgan KG (2003) Alpha1-adrenergic signaling mechanisms in contraction of resistance arteries. *Rev Physiol Biochem Pharmacol* **150:**91–139.
Wijetunge S, Aalkjaer C, Schachter M, and Hughes AD (1992) Tyrosine kinase inhibitors block calcium channel currents in vascular smooth muscle cells. *Biochem Biophys Res Commun* **189:**1620–1623.
Wilcox RA, Challiss RA, Liu C, Potter BV, and Nahorski SR (1993) Inositol-1,3,4,5-tetrakisphosphate induces calcium mobilization via the inositol-1,4,5-trisphosphate receptor in SH-SY5Y neuroblastoma cells. *Mol Pharmacol* **44:**810–817.
Wilcox RA, Challiss RA, Traynor JR, Fauq AH, Ognayanov VI, Kozikowski AP, and Nahorski SR (1994a) Molecular recognition at the myo-inositol 1,4,5-trisphosphate receptor. 3-position substituted myo-inositol 1,4,5-trisphosphate analogues reveal the binding and Ca^{2+} release requirements for high affinity interaction with the myo-inositol 1,4,5-trisphosphate receptor. *J Biol Chem* **269:**26815–26821.
Wilcox RA, Erneux C, Primrose WU, Gigg R, and Nahorski SR (1995) 2-Hydroxyethyl-alpha-D-glucopyranoside-2,3′,4′-trisphosphate, a novel, metabolically resistant, adenophostin A and myo-inositol-1,4,5-trisphosphate analog, potently interacts with the myo-inositol-1,4,5-trisphosphate receptor. *Mol Pharmacol* **47:**1204–1211.
Wilcox RA, Fauq A, Kozikowski AP, and Nahorski SR (1997) Defining the minimal structural requirements for partial agonism at the type I myo-inositol 1,4,5-trisphosphate receptor. *FEBS Lett* **402:**241–245.
Wilcox RA, Primrose WU, Nahorski SR, and Challiss RA (1998) New developments in the molecular pharmacology of the myo-inositol 1,4,5-trisphosphate receptor. *Trends Pharmacol Sci* **19:**467–475.
Wilcox RA, Safrany ST, Lampe D, Mills SJ, Nahorski SR, and Potter BV (1994b) Modification at C2 of myo-inositol 1,4,5-trisphosphate produces inositol trisphosphates and tetrakisphosphates with potent biological activities. *Eur J Biochem* **223:**115–124.
Willcocks AL, Strupish J, Irvine RF, and Nahorski SR (1989) Inositol 1:2-cyclic,4,5-trisphosphate is only a weak agonist at inositol 1,4,5-trisphosphate receptors. *Biochem J* **257:**297–300.
Wilson HL, Dipp M, Thomas JM, Lad C, Galione A, and Evans AM (2001) ADP-ribosyl cyclase and cyclic ADP-ribose hydrolase act as a redox sensor. a primary role for cyclic ADP-ribose in hypoxic pulmonary Vasoconstriction. *J Biol Chem* **276:**11180–11188.
Wilson RH and Poley GW (1960) Toxicity studies on dibutyl- and diamyl-hydroquinone. *Proc Soc Exp Biol Med* **104:**29–31.
Wojcikiewicz RJ (1995) Type I, II, and III inositol 1,4,5-trisphosphate receptors are unequally susceptible to down-regulation and are expressed in markedly different proportions in different cell types. *J Biol Chem* **270:**11678–11683.
Wojcikiewicz RJ and Luo SG (1998a) Differences among type I, II, and III inositol-1,4,5-trisphosphate receptors in ligand-binding affinity influence the sensitivity of calcium stores to inositol-1,4,5-trisphosphate. *Mol Pharmacol* **53:**656–662.
Wojcikiewicz RJ and Luo SG (1998b) Phosphorylation of inositol 1,4,5-trisphosphate receptors by cAMP-dependent protein kinase. Type I, II, and III receptors are differentially susceptible to phosphorylation and are phosphorylated in intact cells. *J Biol Chem* **273:**5670–5677.
Wong L, Aarhus R, Lee HC, and Walseth TF (1999) Cyclic 3-deaza-adenosine diphosphoribose: a potent and stable analog of cyclic ADP-ribose. *Biochim Biophys Acta* **1472:**555–564.
Worley PF, Baraban JM, Supattapone S, Wilson VS, and Snyder SH (1987) Characterization of inositol trisphosphate receptor binding in brain. Regulation by PH and calcium. *J Biol Chem* **262:**12132–12136.
Wu C, Sui G, and Fry CH (2002) The role of the L-type Ca^{2+} channel in refilling functional intracellular Ca^{2+} stores in guinea-pig detrusor smooth muscle. *J Physiol (Lond)* **538:**357–369.
Wu KD, Bungard D, and Lytton J (2001) Regulation of SERCA Ca^{2+} pump expression by cytoplasmic [Ca2+] in vascular smooth muscle cells. *Am J Physiol* **280:**C843–C851.
Wu KD and Lytton J (1993) Molecular cloning and quantification of sarcoplasmic reticulum Ca(2+)-ATPase isoforms in rat muscles. *Am J Physiol* **264:**C333–C341.
Wuytack F, Eggermont JA, Raeymaekers L, Plessers L, and Casteels R (1989) Antibodies against the non-muscle isoform of the endoplasmic reticulum Ca2(+)-transport ATPase. *Biochem J* **264:**765–769.
Wuytack F, Raeymaekers L, and Missiaen L (2002) Molecular physiology of the SERCA and SPCA pumps. *Cell Calcium* **32:**279–305.
Wuytack F, Raeymaekers L, and Missiaen L (2003) PMR1/SPCA Ca^{2+} pumps and the role of the Golgi apparatus as a Ca^{2+} store. *Pflugers Arch* **446:**148–153.
Xiong ZL, Kitamura K, and Kuriyama H (1992) Evidence for contribution of Ca^{2+} storage sites on unitary K+ channel currents in inside-out membrane of rabbit portal vein. *Pflugers Arch* **420:**112–114.
Xu A, Hawkins C, and Narayanan N (1993) Phosphorylation and activation of the Ca(2+)-pumping ATPase of cardiac sarcoplasmic reticulum by Ca^{2+}/calmodulin-dependent protein kinase. *J Biol Chem* **268:**8394–8397.
Xu Z, Kopf GS, and Schultz RM (1994) Involvement of inositol 1,4,5-trisphosphate-mediated Ca^{2+} release in early and late events of mouse egg activation. *Development* **120:**1851–1859.
Yagi S, Matsumura N, and Endo M (1985) Effects of inhibitors of calcium-induced calcium release on receptor-mediated responses of smooth muscles and platelets. *Proc Jpn Acad Ser B* **61:**399–402.
Yamada A, Ohya S, Hirano M, Watanabe M, Walsh MP, and Imaizumi Y (1999) Ca^{2+} sensitization of smooth muscle contractility induced by ruthenium red. *Am J Physiol* **276:**C566–C575.
Yamada A, Sato O, Watanabe M, Walsh MP, Ogawa Y, and Imaizumi Y (2000) Inhibition of smooth-muscle myosin-light-chain phosphatase by ruthenium red. *Biochem J* **349:**797–804.
Yamaguchi N and Kasai M (1997) Potentiation of depolarization-induced calcium release from skeletal muscle triads by cyclic ADP-ribose and inositol 1,4,5-trisphosphate. *Biochem Biophys Res Commun* **240:**772–777.
Yamamoto H, Kanaide H, and Nakamura M (1990) Heparin specifically inhibits the inositol 1,4,5-trisphosphate-induced Ca^{2+} release from skinned rat aortic smooth muscle cells in primary culture. *Naunyn-Schmiedeberg's Arch Pharmacol* **341:**273–278.
Yamamoto H, Kanaide H, and Nakamura M (1991) Dextran sulfate inhibits the inositol 1,4,5-trisphosphate-induced Ca^{2+} release from skinned and cultured smooth muscle cells. *Eur J Pharmacol* **206:**175–179.
Yamazawa T, Takeshima H, Sakurai T, Endo M, and Iino M (1996) Subtype specificity of the ryanodine receptor for Ca^{2+} signal amplification in excitation-contraction coupling. *EMBO (Eur Mol Biol Organ) J* **15:**6172–6177.
Yashiro Y and Duling BR (2003) Participation of intracellular Ca^{2+} stores in arteriolar conducted responses. *Am J Physiol Heart Circ Physiol* **285:**H65–H73.
Yoshida M, Aizawa H, Inoue H, Koto H, Nakano H, Komori M, Fukuyama S, and Hara N (2002) Ozone exposure may enhance airway smooth muscle contraction by

increasing Ca^{2+} refilling of sarcoplasmic reticulum in guinea pig. *Pulm Pharmacol Ther* **15:**111–119.
Yoshida M, Sensui N, Inoue T, Morisawa M, and Mikoshiba K (1998) Role of two series of Ca^{2+} oscillations in activation of ascidian eggs. *Dev Biol* **203:**122–133.
Yoshida Y and Imai S (1997) Structure and function of inositol 1,4,5-trisphosphate receptor. *Jpn J Pharmacol* **74:**125–137.
Young RC, Schumann R, and Zhang P (2001) Nifedipine block of capacitative calcium entry in cultured human uterine smooth-muscle cells. *J Soc Gynecol Investig* **8:**210–215.
Yu JZ, Zhang DX, Zou AP, Campbell WB, and Li PL (2000) Nitric oxide inhibits Ca(2+) mobilization through cADP-ribose signaling in coronary arterial smooth muscle cells. *Am J Physiol Heart Circ Physiol* **279:**H873–H881.
Yu P, Chen Q, Xiao Z, Harnett K, Biancani P, and Behar J (1998) Signal transduction pathways mediating CCK-induced gallbladder muscle contraction. *Am J Physiol* **275:**G203–G211.
Yule DI (2001) Subtype-specific regulation of inositol 1,4,5-trisphosphate receptors: controlling calcium signals in time and space. *J Gen Physiol* **117:**431–434.
Yusufi ANK, Cheng J, Thompson MA, Burnett JC, and Grande JP (2002) Differential mechanisms of Ca(2+) release from vascular smooth muscle cell microsomes. *Exp Biol Med (Maywood)* **227:**36–44.
Zahradnikova A and Palade P (1993) Procaine effects on single sarcoplasmic reticulum Ca^{2+} release channels. *Biophys J* **64:**991–1003.
Zang WJ, Balke CW, and Wier WG (2001) Graded alpha1-adrenoceptor activation of arteries involves recruitment of smooth muscle cells to produce 'all or none' Ca(2+) signals. *Cell Calcium* **29:**327–334.
Zhang L, Bradley ME, and Buxton IL (1995) Inositolpolyphosphate binding sites and their likely role in calcium regulation in smooth muscle. *Int J Biochem Cell Biol* **27:**1231–1248.
Zhang WM, Yip KP, Lin MJ, Shimoda LA, Li WH, and Sham JS (2003) ET-1 activates Ca^{2+} sparks in PASMC: local Ca^{2+} signaling between inositol trisphosphate and ryanodine receptors. *Am J Physiol Lung Cell Mol Physiol* **285:**L680–L690.
Zholos AV, Baidan LV, and Shuba MF (1991) The inhibitory action of caffeine on calcium currents in isolated intestinal smooth muscle cells. *Pflugers Arch* **419:**267–273.
Zhong L and Inesi G (1998) Role of the S3 stalk segment in the thapsigargin concentration dependence of sarco-endoplasmic reticulum Ca^{2+} ATPase inhibition. *J Biol Chem* **273:**12994–12998.
Zhu X and Birnbaumer L (1998) Calcium channels formed by mammalian Trp homologues. *News Physiol Sci* **13:**211–217.
ZhuGe R, Fogarty KE, Tuft RA, Lifshitz LM, Sayar K, and Walsh JV Jr (2000) Dynamics of signaling between Ca(2+) sparks and Ca(2+)-activated K(+) channels studied with a novel image-based method for direct intracellular measurement of ryanodine receptor Ca(2+) current. *J Gen Physiol* **116:**845–864.
ZhuGe R, Fogarty KE, Tuft RA, and Walsh JV Jr (2002) Spontaneous transient outward currents arise from microdomains where BK channels Are exposed to a mean Ca(2+) concentration on the order of 10 microM during a Ca(2+) spark. *J Gen Physiol* **120:**15–27.
Ziganshin AU, Hoyle CH, Ziganshina LE, and Burnstock G (1994) Effects of cyclopiazonic acid on contractility and ecto-ATPase activity in guinea-pig urinary bladder and vas deferens. *Br J Pharmacol* **113:**669–674.
Zocchi E, Usai C, Guida L, Franco L, Bruzzone S, Passalacqua M, and De Flora A (1999) Ligand-induced internalization of CD38 results in intracellular Ca2+ mobilization: role of NAD+ transport across cell membranes. *FASEB J* **13:**273–283.
Zucchi R and Ronca-Testoni S (1997) The sarcoplasmic reticulum Ca2+ channel/ryanodine receptor: modulation by endogenous effectors, drugs and disease states. *Pharmacol Rev* **49:**1–51.